



The
University
Of
Sheffield.



A FRET biosensor for measuring the effectiveness of remediation of heavy metals contaminated soils

THESIS

Submitted to the University of Sheffield in partial fulfillment
of the requirements for the Degree of Doctor of Philosophy

by

Bastian Saputra

August 2021

Department of Civil and Structural Engineering
The University of Sheffield

Abstract

The application of biochar as an amendment to contaminated soils can reduce the bioavailability of the metals to microorganisms, by adsorption and other chemical mechanisms. This can potentially decrease heavy metal toxicity, thus improving soil function and productivity. To assess the performance of biochar for the remediation of heavy metal-contaminated soil, a bacterial biosensor was developed in this study to monitor metal bioavailability at the cellular level. In contrast to chemical extraction methods, which measure heavy metal concentrations in operationally defined soil phases, biosensors can produce signals to measure the biologically-relevant impact of heavy metals on cell physiology.

A FRET (Förster Resonance Energy Transfer) biosensor was constructed to measure the bioavailability of heavy metals in contaminated soil amended with biochar and compost. This is an attractive approach for the quantification of free heavy metals within living cells. The biosensor consists of a metallothionein protein (which binds Pb^{2+} , Cd^{2+} and Zn^{2+}), inserted between cyan (eCFP) and yellow (Venus) fluorescent proteins expressed in bacteria cell. *In vitro* tests of fluorescence emission ratio (VenusFP/eCFP) indicated that the addition of metals to the purified biosensor enhanced FRET between the two fluorescent proteins. The sensitivity of the biosensor was greater for Pb^{2+} followed by Cd^{2+} and Zn^{2+} . The FRET biosensor has been expressed in *Escherichia coli* and *Pseudomonas putida*, showing its ability to measure heavy metal concentrations in the cytoplasm. The analysis of K_a and FRET ratio maximum parameters revealed that the metal concentrations inside the cells were not the same as those outside (in metal solution), indicating the measurement of bioavailability.

This research has demonstrated the use of a FRET biosensor inside *P.putida* to measure the bioavailable heavy metals in contaminated soil samples. *In situ* measurement of the biosensor showed a reduction in heavy metal bioavailability in the biochar-amended soil. The reduction was enhanced in soil amended with a mixture of biochar and compost. The results from the biosensors were supported by a decrease in soluble metals (estimated by chemical extraction) and an increase in soil respiration, suggesting an improvement in soil quality, following the addition of the organic amendments. The research has demonstrated that the FRET biosensor can be used as a complementary tool to assess the remediation performance of biochar more precisely.

Author's Declaration

I, the author, confirm that the Thesis is my own work. I am aware of the University's Guidance on the Use of Unfair Means (www.sheffield.ac.uk/ssid/unfair-means). This work has not been previously been presented for an award at this, or any other, university.

August 2021

Bastian Saputra

Acknowledgements

The completion of this study could not have possible without the extensive financial, academic, and emotional support from a number of people.

This PhD was supported by Marie Skłodowska-Curie Innovative Training Networks project funded by the European Union's Horizon 2020 research and innovation programme.

First, I would like to extend my gratitude to supervisors, Professor Steve F. Thornton and Dr. Stephen A. Rolfe, who played a substantial role in my scientific development and supported me throughout the PhD.

I would like to thank the people working in GPRG research group, C45 Laboratory, and Plant Biotic Interactions research group in the Department of Animal and Plant Science, for their support and help in using essential equipment for conducting the experiments.

Table of Contents

1. General Introduction.....	1
1.1 Background.....	1
1.2 Thesis aim.....	5
2. Literature Review.....	7
2.1. Heavy metal contamination of soils.....	7
2.1.1 Heavy metal interactions in soil.....	8
I.2 Heavy metal interactions with soil organisms.....	9
1.2.1 Interactions with plants.....	9
1.2.2 Interaction with microorganisms.....	12
I.3 Microbial response to metals.....	13
1.4 Metallothionein.....	14
2.2. Remediation of contaminated soils.....	15
2.2.1 Remediation methods.....	15
2.2.2 Soil amendment with biochar.....	16
2.3. Measurement of Metal Bioavailability.....	18
2.3.1 Chemical-based extraction.....	19
2.3.2 Biological approach.....	21
2.4.1 Inducible biosensors.....	22
2.4.2 FRET biosensors.....	25
2.4.3 Application of FRET biosensors.....	27
2.4.4 FRET Biosensor for measuring heavy metal bioavailability.....	29
2.4.5 Application to soil samples.....	32
2.4.6 Biosensors for the assessment of remediation performance.....	34
3. Construction and characterization of the FRET biosensor for measuring heavy metals in <i>E.coli</i>	36
3.1 Introduction.....	36
3.1.1 Construction of the FRET biosensor.....	36
3.2 Aim and objectives.....	40
3. 3 Methods.....	41
3.3.1 CMT Gene amplification.....	41
3.3.2 Vector construct.....	42
3.3.4 Transformation of pGWF1-CMT and protein expression.....	44

3.3.5 Protein extraction and purification	45
3.3.6 SDS-PAGE	46
3.3.7 <i>In vitro</i> characterisation	47
3.3.8 <i>In vivo</i> characterisation	48
3.4 Results	50
3.4.1 Vector construct.....	50
3.4.2 Protein expression.....	53
3.4.3 Heavy metal binding <i>in vitro</i>	55
3.4.4 Heavy metal binding <i>in vivo</i>	58
3.5 Discussion	61
3.5.1 In-vitro binding.....	61
3.5.2 In vivo binding.....	62
3.5.3 Comparison of heavy metal binding <i>in vitro</i> and <i>in vivo</i>	63
3.5.4 Comparison with other FRET-based metal biosensors	64
3.6 Conclusion.....	66
4. Development of FRET Biosensor for measuring heavy metals using <i>Pseudomonas putida</i>	67
4.1 Introduction	67
4.1.1 <i>Pseudomonas putida</i> KT2440	67
4.1.2 FRET measurement using a confocal microscopy	68
4.2 Aim and objectives.....	70
4.3 Methods.....	71
4.3.1 Primer design.....	72
4.3.2 <i>eCFP-CMT-Venus</i> gene amplification	72
4.3.3 Ligation.....	75
4.3.4 pEBP18-CMT Transformation into <i>P. putida</i> host cell.....	75
4.3.5 Protein expression.....	76
4.3.6 Heavy metals in <i>P. putida</i>	76
4.3.7 FRET Measurement using a confocal microscopy.....	77
4.3.8 Image Processing using Fiji and statistical analysis	78
4.3 Results	79
4.4.1 Creation of pEBP18-CMT	79
4.4.2 Electroporation and Protein expression.....	81
4.4.3 Metal-induced FRET signals inside <i>P. putida</i> (spectrofluorimeter).....	81
4.4.4 Analysis of FRET emission ratio image.....	84
.....	85

4.5. Discussion.....	93
4.5.1 Metal-induced FRET signals in <i>P. putida</i>	93
4.5.2 Potential application of FRET biosensor in <i>P. putida</i>	94
4.5.3 Future development of the FRET biosensor	95
4.6 Conclusion	97
5. A FRET biosensor for measuring the bioavailability of heavy metals in biochar-amended soil	98
5.1. Introduction.....	98
5.2. Aim and objectives	99
5.3 Methods.....	101
5.3.1 Experiment of Soil amendment with biochar and compost	101
5.3.2. Biosensor Test (Initial test : soil exposure with cell separation).....	106
5.3.3 Biosensor test: <i>In situ</i> soil measurement	108
5.3.4 Estimation of bioavailable metal concentrations	108
5.3.5. <i>In situ</i> biochar test	109
5.3.6 Statistical analysis	110
5.3.7. Analysis of soil respiration and PLFAs.....	111
5.4. Results.....	113
5.4.1 Physicochemical parameters of soil samples	113
5.4.2. Biosensor function in soil-water extracts	116
5.4.3. <i>In situ</i> soil measurement.....	118
5.4.4 Comparison of <i>in situ</i> biosensor measurement with soluble metal based on NH ₄ NO ₃ extraction.....	122
5.4.5. <i>In situ</i> biochar test	124
5.4.6. Measurement of soil respiration in biochar-amended soil	126
5.5. Discussion.....	130
5.5.1 Direct application of the FRET biosensor in the soil.....	130
5.5.2 <i>In situ</i> measurement	131
5.5.3 Comparison of bioavailable metal measured by the biosensor and NH ₄ NO ₃ extraction.....	132
5.5.4 Improvement of soil microbial activities in biochar-amended soil.....	135
5.6. Conclusion	137
6. Synthesis, future research, and conclusion.....	138
6.1 Synthesis	138
6.1.1 Development of the FRET biosensor	138

6.1.2 FRET biosensor in <i>P.putida</i>	139
6.1.3 Application of FRET biosensor in soil remediation.....	139
6.2 Future research	141
6.3 Conclusion.....	143
7. References.....	144
8. Appendices.....	162

1. General Introduction

1.1 Background

This research was hosted within the INSPIRATION project (managing soil and groundwater impacts from agriculture for sustainable intensification), a multi-site Marie Skłodowska-Curie Innovative Training Network coordinated by the University of Sheffield. This research described in this thesis focused on the development of biosensor assays to detect specific pollutants as an indicator of environmental stress. The biosensor developed is intended to be used as a tool to evaluate restoration measures for soil contaminated with heavy metals using low-cost organic amendments.

Contamination of soil by heavy metals is a challenging issue, with significant threats to the environment and human health. Mining activities are a common source of metal contamination in soils. Deposition of mine tailings wastes usually produces harsh conditions such as acidic pH, high metal concentrations, low water retention and limited nutrients availability in the soils (Misra *et al*, 2009). Different remediation strategies have been employed to address this soil contamination, including soil washing, soil vapor extraction, soil flushing etc (Zhou and Song, 2004; Anawar *et al*, 2015; Prasad and Nakbanpote, 2015). However, they are relatively expensive and may result in soil erosion and loss of soil function.

Remediation of contaminated sites using soil amendments, which immobilise heavy metals, has been considered as a promising and cost-effective method. Research on biochar as a soil amendment has increased because of its production from various biomass sources and effectiveness for metal immobilization (Park *et al*, 2011, Bandara *et al*, 2017). Soil amendment with biochar supports the use of remediation measures such as natural attenuation, which is viewed as a more environmentally sustainable method. A recent study by Soria *et al*, 2020 proposed plant-based biochars derived from herbaceous feedstock as a good candidate for remediation of soil polluted with lead, cadmium, and zinc. Soil remediation with biochar also improves soil physical, chemical, and biological properties, providing a favorable environment for microbial activity (Yuan *et al*, 2011). The application of biochar is often combined with other high organic content materials such as compost. This combination has been shown to be an efficient approach for reducing heavy metal bioavailability in contaminated soils (Beesley *et al*, 2014; Medynska-Juraszek *et al*, 2020).

The measurement of total heavy metal concentrations indicates the metal saturation level as a first impression of soil contamination status. However, this provides uncertain information regarding metal mobility and availability to soil organisms. A measure of metal bioavailability is more meaningful because it can be related to both mobility and potential toxicity. Mobility means that these metals are present as freely available and can be transported from the surrounding of the organism inhabits to enter the cellular system. Once inside the cell, these metals can interact with cellular components and may adversely impact the cellular processes (Semple *et al.*, 2002). Fractions of metals that are active in organisms need to be predicted accurately depending on the organism considered and the properties of soils in which the target organism is exposed. Therefore, there is no standard definition and method to determine bioavailability (Harmsen, 2007).

According to Kim *et al.* (2015), the most frequently used methods to predict bioavailable metals still rely on chemical extraction, in which the metals are grouped, based on soil fractions. The fractions are often operationally defined, for example, as exchangeable, oxide-bound, organic matter-bound, carbonate-bound, residual, as a basis to assess the environmental behaviour and availability of the metals within them. These methods require sample digestion with strong acids or weak salts to extract metals from soil particles, followed by chemical analysis to quantify the concentrations. The main limitation of this approach is understanding the environmental risk associated with the metal contamination and predicting its biological relevance.

Chemical extractions are useful to determine the form of heavy metals present and the extent of contamination level, but they do not provide relevant information on the heavy metals bioavailability and associated risks to soil microorganisms. Assessment of toxic effect requires a model organism that can take up the contaminant. This can be obtained by deploying the Biosensors which can measure the biologically relevant impact of heavy metals on cell physiology. The FRET biosensor in this research utilized a metal-binding protein in *P.putida* cells that mimic the response of soil microorganisms to heavy metal bioavailability. Therefore, results from the biosensors can be used as an indicator of heavy metals toxicity to living organisms.

Soil microorganisms have important functions in soil health, such as nutrient cycling, decomposing organic materials and forming symbiotic mutualisms with plants (Hoorman, 2011). These microbes are more susceptible to the toxic impacts of heavy metal contamination than higher organisms in soil. Microbiological indicators such as microbial biomass, counts of total bacteria, and enzyme activities are often included as the main basis to assess soil health and as

an early forecast to predict the restoration of contaminated soil (Cardoso *et al*, 2013). For this reason, studies on the remediation of contaminated soils should consider the impact of metal toxicity at a microbial level.

Research on the engineering of microbial cells for sensing chemicals, or so-called microbial biosensors, has been increasing in the last 30 years (King *et.al*, 1990). The use of microbial biosensors is mainly motivated by the need for information on pollutant bioavailability, to assess the risk of toxicity. Biosensors are usually preferred over chemical methods because biosensors give a measurement of biological response (Branco *et al*, 2013). Results from biosensors define bioavailable metals as freely ionic metals that cross a cellular membrane from the surrounding environment (Harms *et al*, 2006). The type of results from biosensor measurement is the signals that correspond to the concentration of metals that are present inside the cell. If the signals are high, it means that the metal concentration inside the cell is high. The signals can go higher and reach saturation or reduction level. This indicates that the concentration of accumulated metal has caused a toxic impact and disrupted the cellular process.

The development of bacteria-based biosensors is expanding, with construction mainly by fusing a pollutant-responsive promoter to a reporter gene (transcription-inducible). A signal is produced as the transcription of the reporter gene is induced by the presence of a specific target pollutant inside the host cell, thus providing an indirect measurement. Despite the different transcription-inducible bacteria biosensors available for various metals, only a few have been used to analyse environmental samples and even fewer for direct application in contaminated soil remediation. This provides the opportunity for further improvement, involving the biosensor construct, signal measurement and optimisation strategies for real applications.

This research investigated the function of a FRET biosensor for heavy metal sensing and subsequent deployment as a biological tool to measure the bioavailability of heavy metals in contaminated soils. The main feature of the FRET biosensor constructed in this study is a fusion of a metal-binding protein (metallothionein) between two fluorescent proteins (FPs) which are capable of absorbing and emitting light (Fehr *et al*, 2002; Rajamani *et al*, 2014). Changes in emission spectra between the two FPs can be calculated according to the amount of metal binding on the metallothionein. This approach offers a rapid and direct signal measurement compared to transcription-inducible biosensors. Another advantage is that the FRET biosensor can be produced in different host cells, ranging from eukaryote to prokaryote.

Therefore, this FRET biosensor was developed in a bacteria host cell typically found in a contaminated soil environment to simulate the response of soil microbes to heavy metal bioavailability. A fundamental understanding of the FRET biosensor response to heavy metals in bacteria host cells was explored in the research. The biosensor was expected to give a robust measurement of heavy metal bioavailability in contaminated soil samples. Furthermore, the practical application of this biosensor was evaluated together with soil chemical parameters to assess the remediation performance of biochar in order to achieve soil restoration.

This is the first FRET Biosensor that has been developed inside *Pseudomonas putida* and applied for measuring the bioavailability of heavy metals in a real environmental sample (polluted soil). The FRET Biosensor brings a new approach in a way that the metals can be measured directly and allows for *in-situ* application with minimum soil preparation. Existing biosensors technology for heavy metals mostly relies on transcription-inducible based which have some limitations in terms of soil application. The limitations are the soil preparation (soil-water extract) which is destructive to the sample and issues with signals interference produced from soil particles which can underestimate the measurement of bioavailable heavy metals. These biosensors measure bioavailable metals indirectly in which the metals must bind to regulatory protein inside the cell and induce the transcription and translation of reporter proteins to produce signals.

Unlike the transcription-inducible biosensors, the concept of FRET biosensor relies on the direct binding of bioavailable metals onto the receptor protein (part of the FRET biosensor component) inside the cells and the signals can be produced rapidly without involving cellular transcription/translation. The FRET biosensor can simply be deployed onto soil samples and the signals can be measured under a confocal microscope. *In-situ* measurement can provide a more accurate and representative analysis of metals that are available to soil microbes

The FRET biosensor can be used as a complementary tool meaning that the results from biosensor measurement can be used together in combination with chemical extraction to assess the remediation performance. Chemical extractions or biosensor alone are not sufficient to give a comprehensive monitoring of remediation. Assessment of soil remediation requires a combination of measurement involving chemical/sequential extraction to determine the metal speciation, mobility and transport in the soil, and biosensor to determine the changes in biological toxicity and how this can affect the biological response of soil microbes. Both are useful to determine whether the soil restoration due to the remediation applied has been achieved.

1.2 Thesis aim

This research aims to develop a heavy-metal-based biosensor and use it to assess the remediation performance of biochar in reducing bioavailable heavy metals. The function of the biosensor will be put into context with other parameters to measure the effectiveness of biochar amendment to improve soil health.

The structure of this thesis consisted of introduction, literature reviews, experimental works (which was divided into three chapters), and synthesis, including future research and conclusion:

Chapter 1. Introduction

This chapter introduces the concept of metal bioavailability in contaminated soils and its importance as part of risk assessment in the remediation of biochar-amended soil. The biosensor was discussed as the main approach to measure bioavailable heavy metals, which needs to be put into context to monitor soil remediation performance.

Chapter 2. Literature Reviews

The review covers a fundamental understanding of heavy metals contamination, bioavailability, and the impacts on soil organisms, particularly microbes. The importance of biosensor was seen as a tool to measure heavy metals bioavailability that complements chemical methods. Literature on existing bacteria biosensor for heavy metal sensing and its limitation were reviewed. This was addressed as the main drawback of FRET biosensor development and application in soil remediation.

Chapter 3. Construction and characterization of the FRET Biosensor for measuring heavy metals in *E.coli*

This chapter describes the component of the FRET Biosensor, cloning approach, and protein expression in a bacteria host cell. Initial testing of the biosensor performance was investigated as the sensor was outside and inside the cell. This will provide information on the sensitivity and measurement range to heavy metals.

Chapter 4. Development of FRET Biosensor for measuring heavy metals in *P.putida*

The FRET biosensor construct in Chapter 3 was developed in a soil bacteria considered as a robust host cell for contaminated soil application. The focus of this chapter is mainly on the cloning approach and protein expression inside the new host cell, including heavy metals

testing. This chapter also investigated the use of confocal microscopy to measure the signals of the FRET biosensor due to heavy metals binding at a cellular level.

Chapter 5. A FRET Biosensor for Measuring the Bioavailability of Heavy Metals in Biochar-Amended Soil

The biosensor developed in chapter 4 was applied to measure the bioavailability of heavy metals in contaminated soil samples. The approaches for a direct biosensor application were explored together with their capability to monitor the changes in bioavailable metal concentrations due to the biochar amendment effect. In the end, the results from the biosensor were combined with other soil physicochemical parameters to assess the effectiveness of remediation performance.

Chapter 6. Thesis Synthesis, Future Research, and Conclusion

Results from all experimental chapters were discussed and summarised in a broader context. The needs of future research as identified from the experiments were also described. The final conclusion of the study was presented at the end of the thesis.

2. Literature Review

2.1. Heavy metal contamination of soils

Heavy metals exist naturally in soil from the weathering process of parent rock materials, which are regarded as trace level (<1000 mg/kg) and rarely toxic (Wuana and Okieimen, 2011). Soils may become contaminated due to anthropogenic activities such as mine tailings, expanding industrial areas, waste disposal, fertilizer application, and pesticides usage. This leads to heavy metals accumulation above soil background values and alteration in metal species' chemical states, which may cause risk to the ecosystem. Heavy metals are non-biodegradable and remain persistent in the environment or can be accumulated inside organisms and end up in the food chains (Guo *et.al*, 2006). Heavy metals can be transformed into different oxidation states which govern their toxicological properties depending on metal species and soil physicochemical conditions (EPA, 1992). Transformation of heavy metals through complexation or immobilization may lead to changes in metal toxicity and mobility, therefore, it is a suitable approach for soil remediation.

Most commonly found heavy metals at contaminated sites are lead (Pb), cadmium (Cd), arsenic (As), zinc (Zn), copper (Cu), mercury (Hg), and nickel (Ni) (United States Environmental Protection Agency, 1996). Pb, Cd, and Zn are widely distributed in lithosphere and considered as some of the largest heavy metal emission from mining or refining processes. Pb is typically found in ores containing Zn, which can be extracted as a co-product of this metal (Cheng and Hu, 2010). Cd can also be found as a by-product of Zn and Pb refining (Wuana and Okieimen, 2011). Therefore, Cd, Zn, and Pb are generally distributed together in contaminated soil in the form of various composites; cases of single-metal contamination are rarely found (Yun and Yu, 2015).

Lead and cadmium are considered highly toxic metals for living organisms (Mahar *et al.*, 2015). This metal is naturally found as a mineral combined with other elements, for example, sulphur (PbS and PbSO₄). The normal concentration of lead in the surface soil worldwide ranges from 10 to 67 mg/kg. Some regulations set the maximum allowed concentration of lead in soils should be less than 600 mg/kg (NJDEP, 1996; Kabata, 2001). Cadmium has a lesser toxicological effect than lead, but it is known as highly bio-persistent. The regulatory limit for the safe concentration of cadmium in soils is typically below 100 mg/kg. Zinc is one of the essential metals that are

required as micronutrient by cells. This metal naturally occurs in soils with the normal concentration of 150 mg/kg with a regulation limit concentration for less than 1500 mg/kg (Riley *et.al*, 1991; NJDEP 1996).

2.1.1 Heavy metal interactions in soil

Heavy metals are present in the soil as separate entities or in combination with other soil components controlled by adsorption/desorption, precipitation/dissolution, complexation/dissociation, and diffusion. These processes lead to various forms of metal interactions such as the sorption of exchangeable ions on the surface of inorganic solids, free metal ions in the soil solution, a metal complex of organic materials, and metal attached to silicate minerals (Kim *et al.*, 2015).

Heavy metal interactions with soil organisms are influenced by many factors, mainly coming from the soil properties and biological receptors in the soil. Heavy metals mobility or movement is controlled by the properties of soil pH, cation exchange capacity, clay, organic matter content, presence of oxides, and soil textures (Jung *et.al*, 2008). Soil pH is the main factor affecting metal bioavailability. Availability of Cd and Zn to plants decreased with an increase in soil pH (Wang *et. al*, 2006). Semple *et.al*, 2002 reported that heavy metals that are physically removed from soil adsorption sites due to changes in soil properties can become bioavailable. Biological receptors of heavy metals in soils are plants and microorganisms. Heavy metals can diffuse and accumulate into plant roots depending on the cell wall structures and the release of exudates. In the case of microbes, the presence of extracellular polymeric substances (EPS) plays an important role in the sorption of metals from their surrounding environment (Gupta and Diwan, 2017). The term bioavailability is widely used to describe the release of chemicals from a particular medium onto biological receptors. In terms of heavy metal contamination in soils, bioavailability is defined as the fraction of metal accessible to soil organisms (Misra *et al.*, 2009). This metal may cause toxic effects depending on several factors such as pH, the presence of water and organic matters, and soil structures (Chibuike and Obiora, 2014). In acidic soil pH, heavy metals mainly exist in ionic form with high mobility and become readily available (Wang *et al.*, 2006). Organic matters have been known to reduce heavy metals bioavailability through immobilization process, thus making the metals to be less mobile (Bernal *et al*, 2007). Sharma and Raju (2013) reported the positive correlation between the high water holding capacity and moisture content with increased metal bioavailability.

I.2 Heavy metal interactions with soil organisms

Heavy metal contamination may cause a detrimental impact on soil organisms, leading to the change in soil biological processes. High metal concentrations can reduce the number of beneficial soil microorganisms which play important roles in the decomposition of organic matters and nutrient cycles. This lead to a decline in soil nutrients needed by plants or soil microbiota (Chibuike and Obiora 2014). Furthermore, Friedlova (2010) reported the contamination of metal caused a reduction in soil biological processes particularly basal respiration and enzymatic activities such as dehydrogenase, arylsulphatase, and urease.

Therefore, monitoring of biological properties such as plant growth, microbial activities, etc., can be used to evaluate the toxicity of metal bioavailability accurately and are more sensitive than analysis of soil physical and chemical properties alone (Chibuike and Obiora, 2014).

1.2.1 Interactions with plants

Heavy metals become available for plant uptake when they are present as soluble components in soil pore water or solubilized by root exudates (Blaylock and Huang, 2000; Chibuike and Obiora, 2014). Plants can maintain physiological concentrations of essential and nonessential metals to achieve ionic homeostatic. However, exposure to high concentrations or toxic heavy metals can trigger stress responses and adaptation mechanisms at structural and physiological levels (Ovečka and Takáč, 2014). According to Amari *et.al*, (2017), the toxic impact of heavy metals on plants can be grouped as direct and indirect effects. Direct effect includes the changes of cell envelopes, inhibition of enzyme activities, and disruption in DNA synthesis. Indirect effects can be observed from the disruption of photosynthesis, tissue dehydration, and induction of stress oxidative species. These can lead to a decline in plant growth, yield reduction, chlorosis, and eventually, plant death (Figure 2.1).

Dhalaria *et al.*, (2020) reported the interaction between heavy metals with arbuscular mycorrhizal fungi (AMF) and plants. AMFs have been known to reduce heavy metal stress on plants by immobilization or sequestration in its hyphae structure and precipitation and chelation in the rhizosphere. Intracellular functions of arbuscular mycorrhizal fungi and rhizosphere bacteria may transform heavy metals near the vicinity of plant roots; hence changing the metal mobility and solubility (Gadd, 2010).

Root exudates containing organic acids, amino acids, and phytochelatins play a significant role in changing metal bioavailability through acidification, precipitation, chelation, and

complexation around plant roots. They can reduce the pH in the rhizosphere, which enhances metal bioavailability (Ma *et al.*, 2016) (Figure 2.1).

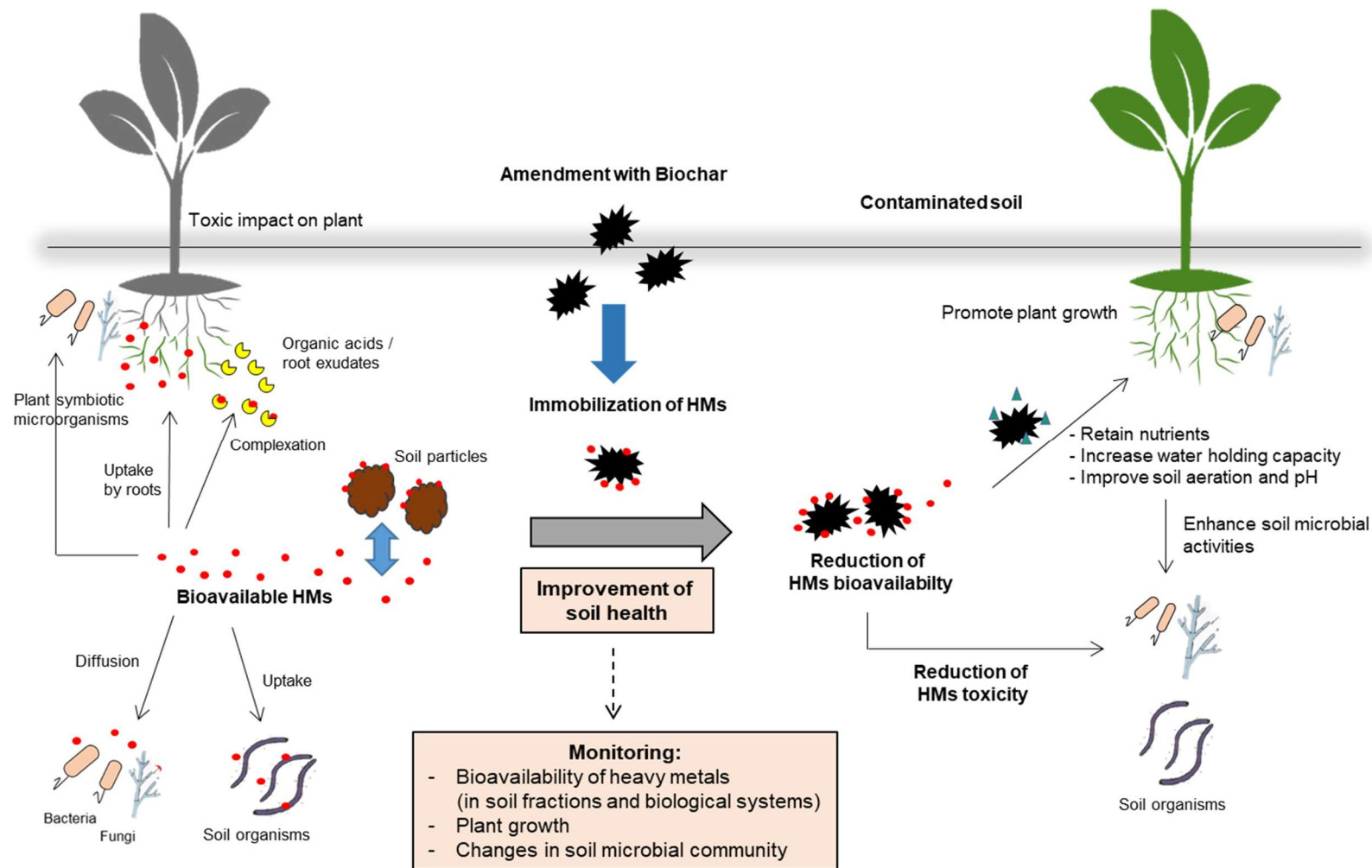


Figure 2. 1 Interaction of bioavailable heavy metals with soil biological systems such as plant roots, soil microorganisms, etc. Soil amendment with biochar can immobilize heavy metals leading to the reduction of bioavailability. This can improve the soil health to sustain the live of organisms. Therefore, soil health monitoring should consider the heavy metal interactions with soil organisms, analysis of plant growth and soil microbial community to assess remediation performance more precisely.

1.2.2 Interaction with microorganisms

Soil microorganisms are very diverse; they play essential roles in soil functions, particularly for organic matter decomposition, nutrient cycles, structural formation, and plant interactions (Harris, 2009). Hence, the study of soil microorganisms is an important part of soil monitoring. Soil microbial biomass and respiration have been widely used as the primary indicator of soil health (Bastida *et al*, 2008). Heavy metal stress may cause changes in the metabolic status of soil microbes, thus leading to disruption of cellular respiration.

Heavy metal contamination can cause harmful impacts on microorganisms which affect particular functions in the soil. One of the significant impacts of metal toxicity is to decrease microbial diversity, particularly the species richness of microbes that lack metal tolerance, whereas microbes that tolerate metals survive well (Giller *et.al*, 2009). Microbes in heavy metal-polluted soils synthesize less biomass due to the stress caused by the heavy metals. They use most of their energy to survive in this unfavorable environment (Šmejkalová *et.al*, 2003). Microbes that are unable to survive will eventually die and thus change the diversity of soil microbial groups. For example, heavy metals can reduce the growth and activity of symbiotic soil microbes in the rhizosphere of plants. Arora *et al.*, 2010 reported the reduction of enzymes for nitrogen metabolism (nitrite & nitrate reduction, nitrogenase, hydrogenase) in rhizobial strains due to heavy metal stress. A study carried out by Younis (2007) showed that the concentrations of heavy metals (Cd, Zn, Co, Cu) above 50 mg/kg affected the growth, nodulation, and nitrogenase activities of plant symbiotic microbes in the soil. Cd, Zn, As, and Cu have been reported to inhibit the growth and activities of *Rhizobium* sp. and *Bradyrhizobium* sp. (Vigna) and *Sinorhizobium* (Bianucci et al., 2011). In this case, the soil lost its ability to maintain nitrogen cycles, which can decrease the nutrient availability to support plant growth.

I.3 Microbial response to metals

Soil microorganisms can interact with heavy metals in many ways. They can utilize Zn in the cellular redox process, osmoregulation, or act as a cofactor for some enzymes (Silver and Phung, 2005). Cd and Pb have no essential function for living microorganisms. These metals can disrupt cellular functions by damaging cell membranes, DNA, and proteins, leading to cell death. Toxicity of Cd can occur through the displacement of essential metals from native binding sites, which results in the alteration of protein conformational structure (Bruins *et.al*, 2000).

Metal detoxification mechanisms in microbial cells confer the ability to survive under heavy metal stress (Figure 2.2). In general, these mechanisms can be grouped as follows: 1) expulsion by permeability barrier, 2) intracellular sequestration by binding to protein, 3). extracellular sequestration, 4) expulsion by active metal transport out of the cell, and 5) transformation or enzymatic detoxification (Hu, *et.al*, 2005; Prabhakaran, Ashraf and Aqma, 2016).

Active transport is the most widespread metal resistance mechanism in microorganisms (Leedj r v *et al*, 2008). According to Hynninen (2010), three major types of active transporters or efflux protein families are known: 1) Ptype-ATPase that utilizes the energy from ATP hydrolysis to pump out metals from the cells, 2) CBA Transporter which involves three trans-envelope pump proteins as a chemiosmosis antiporter, and 3) Cation diffusion facilitator (CDF) that exploits the proton motive force to drive metals out of the cytoplasm.

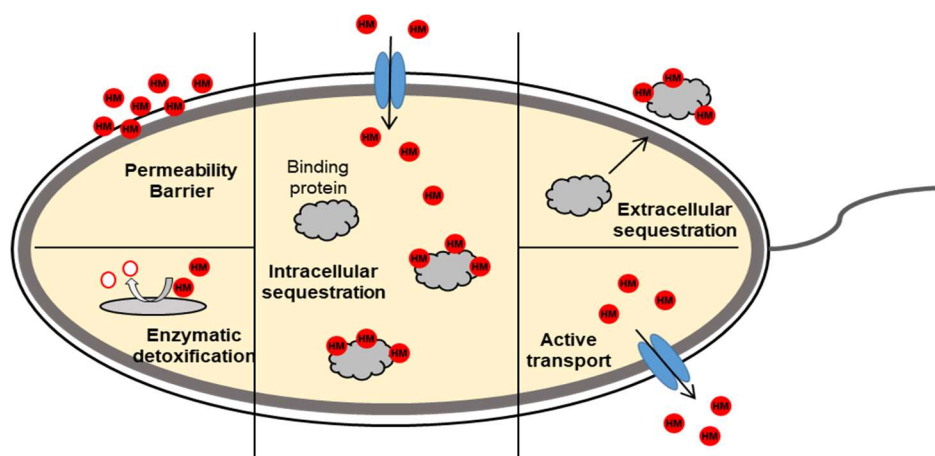


Figure 2. 2 Overview of general metal resistance mechanisms in microbial cells (heavy metals are shown as red circles). These mechanisms are important to avoid metal toxicity (adapted from Hu, *et.al*, 2005; Prabhakaran, Ashraf and Aqma, 2016)

1.4 Metallothionein

Metallothionein (MT) is a cytoplasmic metal-binding protein commonly found in prokaryotes and eukaryotes. This highly cysteine-rich protein plays an important role in the detoxifying of nonessential metals and controlling the intracellular concentration of essential metals (Saydam *et al.*, 2002). Living cells utilize MTs in the homeostasis of essential trace metals, e.g zinc, or sequestration of toxic metals such as cadmium and lead. They have been found in *Synechococcus elongates* PC 7942 known as SmtA (Blindauer, *et.al*, 2001), in *Pseudomonas putida* known as pseudothionein (Higham, *et.al*, 1986), or in *Mycobacterium tuberculosis* H37Rv known as mymT (Gold, *et.al*, 2008). Metallothionein plays important roles in *M.tuberculosis* for chelation, intracellular distribution, storage and detoxification of metals and defence against oxidative stress (Gold *et.al*, 2008). Some host organisms utilised macrophage phagosome to uptake and kill *M.tuberculosis* infection. The killing of this bacterium inside macrophages involves various mechanisms including an excess release of zinc and copper into the microbial environment. The presence of metallothionein in *M.tuberculosis* provides a detoxification system against these metals and allows the bacterium to thrive inside the macrophage cell. This will make the bacterium survive and manifest toxic effects to the host organism (Neyrolles, *et.al*, 2013). Various types of MTs also have been identified in *Gallus gallus* (Wei and Andrews, 1988) and humans (Thirumoorthy *et al.*, 2011).

MTs are genetically encoded and synthesized as polypeptides with approximately 20 conserved cysteine residues (Cobbett and Goldsbrough, 2002). The binding of metals to MT is due to the interaction of thiolate sulphur ligands within cysteine residues (Figure 2.3). (Kagi, 1991; Rajamani *et al.*, 2014). In the absence of metals, MT has a random-coil structure. This structure changes into a compact dumbbell-shaped upon binding to metal ions (Romero-Isart and Vasak, 2002). Studies about structural changes of MT due to metal binding complex have provided information about the binding specificity and affinity to some metals.

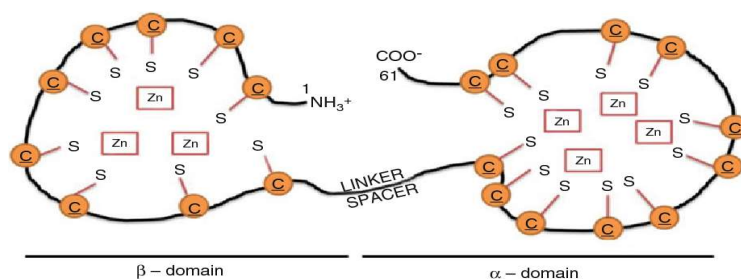


Figure 2. 3 Binding sites of metal ions in a metallothionein molecule. The α and β domains are capable of binding of up to three or four metal ions such as Zn, Cd, and Pb. The cysteine sulphurs bind to the metals as thiolates resulting in a metal induced folding of the protein structure (Adapted from Nielsen, *et.al*, 2007)

2.2. Remediation of contaminated soils

2.2.1 Remediation methods

Heavy metal contamination can reduce soil health and degrade its function to sustain life. Healthy soils have the capacity to function as a living ecosystem that supports plants, animals, and humans. This is characterized by the good physical structures (tilth, well aggregated, and dark with organic matter) and the ability to maintain nutrient cycles, support plant growth, and microbial communities. Soil tilth indicates a physical characteristic of soil that is suitable for crop production. Good tilth is shown by crumbly and well structures with no large and hard clods. Well aggregated soil refers to the presence of mineral and organic particles clumping together. This soil is full of a diverse community of living organisms and makes them more resistant to adverse conditions such as erosion by wind and rain, extreme drought, disease outbreak, and other degrading influences. Organic matters together with clay are the main component of soils. High organic matter contributes to a good soil structure, water and ionic nutrient holding capacity, and exchange capacity (Moebius-Clune, *et.al*, 2017). These characteristics may provide a habitable environment for a large and diverse population of organisms to decompose organic matters or toxic chemicals (Natural Resources Conservation Services -USDA, 2012; Moebius-Clune, *et.al*, 2016). Therefore, remediation of heavy metal-contaminated soils is required to protect and restore soil health.

Selection and assessment of remediation methods should include three components; protection of sources, break the pathway, and protection of the receptors to minimise the risk (Vik *et al.*, 2001). Some remediation options available based on these components can be categorised as isolation of contaminated sites (e.g, soil capping and subsurface barriers), immobilization of contaminants (e.g, amendment with organic or inorganic materials and solidification), reduction of contaminant mobility or toxicity (e.g biological treatment, phytoremediation), and contaminant separation or extraction (e.g soil washing, electrokinetic treatment) (Wuana and Okieimen, 2011)

Remediation technologies, such as soil washing, phytoremediation, and immobilization techniques, are the most commonly used for heavy metal-contaminated soils. Immobilization technique is fast, easy applicability, and relatively unexpensive operation among other technologies. This technique often uses organic or inorganic amendment to reduce metal mobility and toxicity in soils. The purpose of immobilizing heavy metals is to alter the metal

contamination to more stable phases via sorption, precipitation, and complexation process (Wuana and Okieimen, 2011)

2.2.2 Soil amendment with biochar

Biochar is porous, low-density carbon material produced by pyrolysis of plant and animal-based biomass (Ahmad *et al.*, 2014). It has a large surface area with high porosity and functional groups on its surface (Tang *et al.*, 2013). These characteristics make biochar a good sorbent material for heavy metals and can potentially be applied as a soil remediation tool in various contaminated sites (Anawar *et al.*, 2015).

Immobilization of heavy metals on biochar surface is as a result of organometallic interaction, sorption via electron donor-acceptor interaction, and pore diffusion (Bandara *et al.*, 2017). Heavy metals can interact with some functional groups (carboxylic, hydroxyl, or alcohol) on the biochar surface to form a complex structure. The oxygen and nitrogen atoms within those functional groups act as ligands which tend to donate their electron pairs to the metals with electron deficiency. This process leads to the formation of organometallic complexes. The presence of aromatic groups on the biochar surface can also stimulate the sorption of metals. These aromatic groups contain double bonds, creating electron pools that will be easily donated to the metal ions, leading to the formation of donor-acceptor interactions. Ahmad *et al.* (2014) summarized the interactions between biochar and heavy metals, as shown in Figure.2.4. These interactions involve the ion exchange of metals, anionic or cationic metal attractions, and metal precipitation on the biochar surface.

Biochar is an emerging relatively low-cost material for the remediation of metal contamination in soils. The ability to adsorb metals on its surface has led to biochar application as a soil amendment to decrease metal mobility (Tang *et al.*, 2013). This principle has been widely used to reduce metal bioavailability in contaminated soil (Park *et al.*, 2011; Beesley *et al.*, 2014).

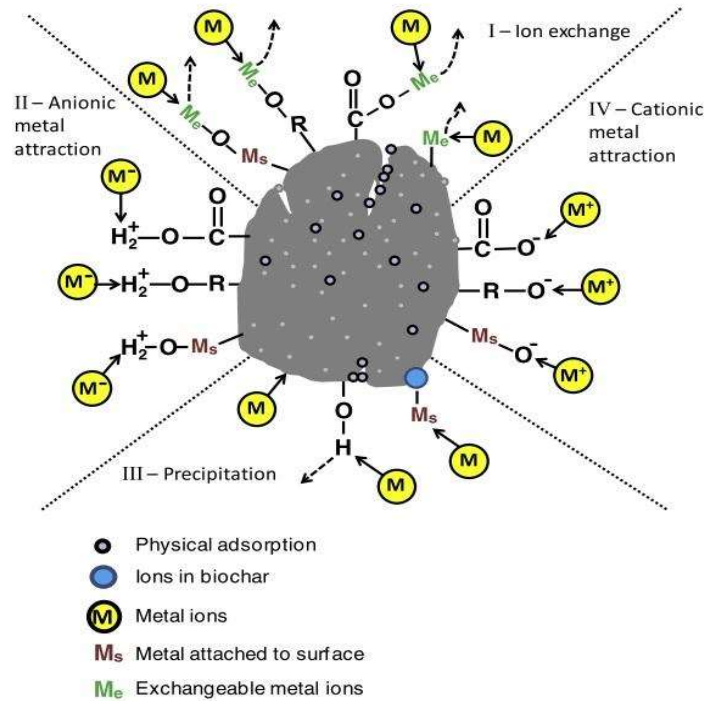


Figure 2. 4 Mechanisms of biochar interactions with heavy metals (Ahmad et al. 2014). The binding of metals on biochar surface is facilitated by ion exchange, anionic metal attraction, precipitation, and cationic metal attraction.

Another advantage is that biochar can improve soil moisture, pH, texture, and nutrient retention (Anawar *et al.*, 2015) that influences soil microorganisms during the remediation process (Figure 1). The pore structure of biochar provides a habitable environment for microbial attachment (Zhu *et al.*, 2017). Amendment with biochar changes soil properties, bulk density, improvement for aeration and liming effect to neutralize pH, which are favourable conditions for microbial activities (Yuan, Xu and Zhang, 2011). The large and negative surface area of biochar can retain nutrients required for soil microbes (Lehmann, 2007).

Despite these advantages, some studies reported the negative effects of biochar due to the increase of application rate and source of feedstocks used in biochar production. Application of biochar higher than 50 ton/ha in temperate soils leads to a significant effect on yields (Jeffery, *et al.*, 2017). The negative yield is mostly observed under alkaline conditions which can potentially limit the Phosphorous (P) supply to plants (Lorenz *et al.* 2018). Excessive application of biochar can potentially immobilize pesticides, which leads to a reduction in treatment efficiency against plant pathogens. Depending on pore sizes, biochar with size ranges from 60 to 6000 μm are almost inaccessible for nematodes and amoebae causing a decrease in its abundance. This could bring to a shortage of food resources for soil microbiota and may disturb the soil food web (Liu, *et al.* 2020). Biochar from sewage sludge may contain a high concentration of potentially toxic

heavy metals. Biochar produced from *Miscanthus sacchariflorus* plant with steam activation can induce acute toxicity due to the high amount of aromatic compounds (Beesley *et al.*, 2011; Shim *et al.*, 2015).

The implication of biochar interactions with heavy metals and organisms in the soils is not completely understood. This may vary depending on biochar properties and soil characteristics. Therefore, further study and investigation are required to assess the biochar application in reducing heavy metal bioavailability in the remediation of contaminated soils.

2.3. Measurement of Metal Bioavailability

Many regulatory authorities have established guideline values of heavy metals for assessing and remediating contaminated soil (US EPA 2002, EA. 2004). These guidelines are mostly based on the soil's total metal content, which may overestimate the potential risk, causing unnecessary or expensive remediation efforts. The use of total metal content is limited; it is normally used to indicate metal saturation concentration and as a first impression of soil contamination status (Kim *et al.*, 2015).

Frameworks for the assessment of contaminated soil remediation performance take into account a risk-based approach that considers contaminant bioavailability (Kim *et al.*, 2015). There is still much debate on the definition and methods for measuring heavy metal bioavailability because of the complexity of metal interactions in soils. Heavy metals behave in numerous ways. Therefore, the approach for measuring bioavailability should consider metal-soil physicochemical interactions (e.g pH and organic matters), and the biological endpoints (plant uptake across roots, bioaccumulation in soil microbes, etc). According to NRC Committee (2003), no single method can be universally used to measure bioavailability, and an appropriate method can be selected based on the site-specific conditions.

Kim *et al.*, (2015) described some conceptual steps that can be used as a guideline for selecting methods to assess the bioavailability of contaminants in soils. The concept emphasized that heavy metals bioavailability is a dynamic process that comprises three steps: (1) *Environmental availability*, determined by measuring the potentially available amount in the soil matrix (mineral surface) and pore water. This stage depends on soil physicochemical conditions (texture, pH, organic content) and metal properties. Chemical extraction methods can be used to analyse heavy metals in this stage. (2) *Environmental bioavailability*, the metal fraction dissolved in the pore water that can be taken up by soil organisms. This bioavailability is controlled by the

physiological process or uptake mechanisms of the organisms, for example, metals present near the vicinity of plant roots can be taken up through the root cell membrane by passive diffusion and active process (Morel, 1997; Weiss *et.al*, 2005). (3) *Toxicological bioavailability* is the biological effect of metal accumulation inside organism which depends on the cellular process. This can be determined by measuring the metal accumulation in organisms, e.g, bioaccumulation of metals plant roots and bacteria-based bioassays. Understanding all these processes of metal interaction is essential to assess the overall bioavailability (Harmsen, 2007; ISO 17402, 2008).

2.3.1 Chemical-based extraction

Conventional methods to determine the bioavailability of metals in contaminated soils are single-step extraction and sequential extraction technique (Park *et al.*, 2011; Bandara *et al.*, 2017). According to the Standard Measurement & Testing program (SM&T) of the European Commission, a single-step procedure using EDTA and acetic acid is the most suitable approach to characterize the bioavailable fraction of metal in a soil sample (Quevauviller *et.al*, 1997; Zemberyova *et.al*, 2007). The use of EDTA or NH_4NO_3 as chelating agents extracts readily available metals in soils forming soluble complexes. The number of chelated metals in the solution during the extraction process can be interpreted as a function of metal ions activity in the soil (intensity factor) and the soil's ability to replenish these ions (capacity factor). Acetic acid extracts ion-exchangeable forms of metals and metals bound to carbonates. These metals are easily mobile and potentially available for plant uptake (Sahuquillo *et.al*, 2003).

Sequential extraction facilitates the fractionation of metals as exchangeable, carbonate bound, hydrous-oxide bound, organic matter bound, and residual (lattice material components) (Maiz *et al.*, 2000). These procedures utilise a series of extractant solutions (MgCl_2 , NaOAc , HNO_3 , HCl , etc) designed to dissolve fractions of the associated metals (Bandara *et al.*, 2017). The concept of sequential extraction is; the most mobile heavy metals are extracted in the first fraction and continue in the order of decreasing mobility.

Following the extraction process, the metal concentrations are measured by analytical instruments such as Atomic Absorption Spectroscopy (AAS) or Inductively Coupled Plasma Mass Spectrometry (ICP-MS) (Dean, 2010). This procedure can exhibit high sensitivity and accuracy; however, it requires sophisticated instrumentation, pre-treatment of samples, and a long measuring period (Turdean, 2011). Limitations in sequential extraction procedures such as

the non-selectivity of the reagents used, handling of soil samples prior to extraction, soil-reagent ratio, and length of extraction may lead to inconsistent results.

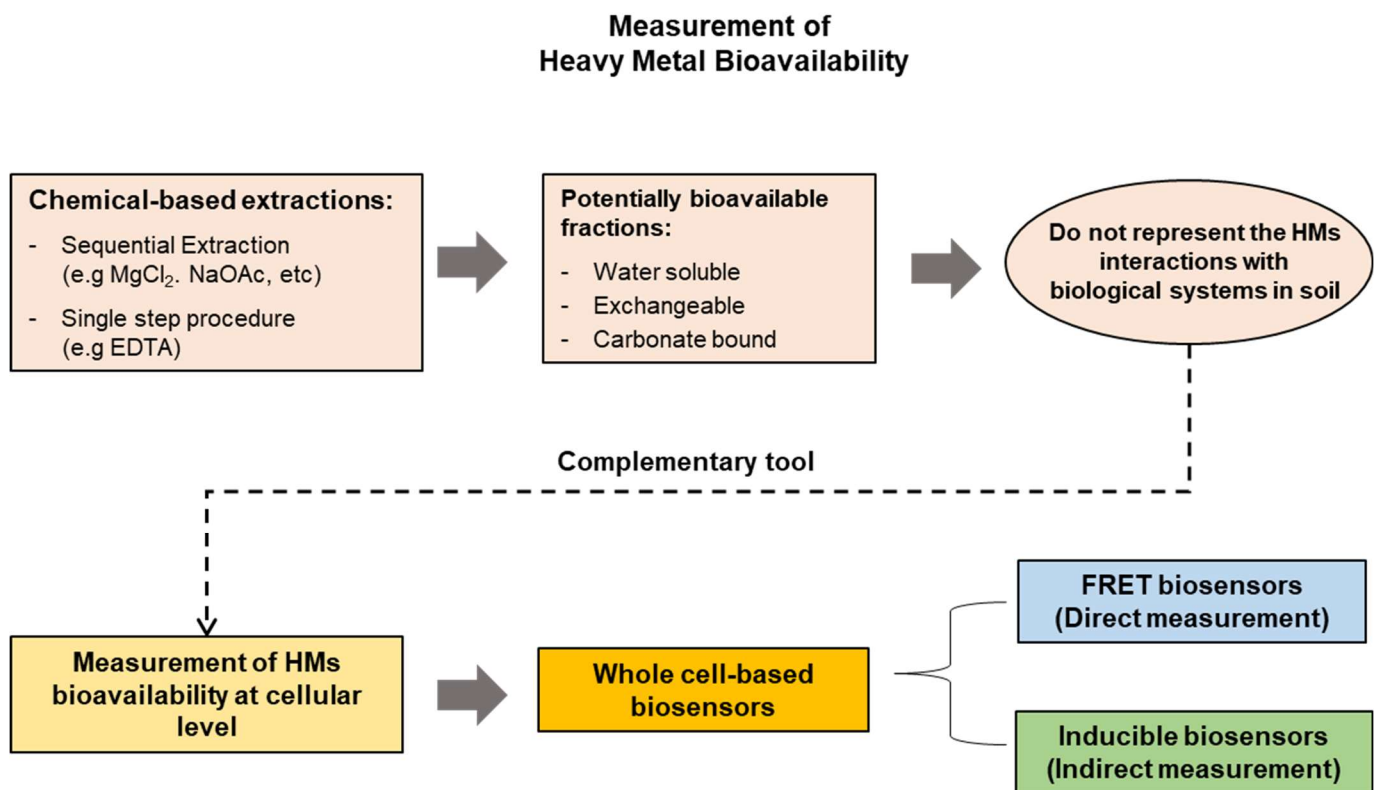


Figure 2. 5 Concept of biosensor approach for measuring the bioavailability of heavy metals as a complementary tool to chemical-based extraction methods. Sequential extractions or single-step procedures only rely on the extraction of metals from soil fractions using chemical solutions. This doesn't represent the complex interaction of heavy metals with soil biological properties. Whole-cell biosensors can be used to mimic the cellular response (in the form of signals) due to the presence of bioavailable heavy metals. Signal generation can be obtained directly with FRET biosensors or indirectly with inducible biosensors.

The main drawback from the use of chemical-based extraction is how interpret the transfer of the results obtained on non-biological systems to biological ones (Ivask *et.al*, 2002). This method only assumes a specific form of metal present in the soil and its bioavailability, which has little relation to the form of metal taken up by plants or soil microorganisms. The results cannot represent the complex interaction of metals with biological systems in the soil (Figure 2.1 and 2.5). Therefore, analysis using bioassays, biomarkers, and biosensors has gained much attention as a tool that integrates the important aspects of metal bioavailability such as exposure, accumulation, and toxic impact at the receptor level (Olaniran *et.al* , 2013).

2.3.2 Biological approach

The impact of metals on soil microorganisms has been considered as a toxicological assessment of soil remediation. Many studies concerning heavy metal effects on soil microbes only look at the changes in the microbial community (genetic variation) and functional diversity (Xie *et al.*, 2016; Ding *et al.*, 2017). These approaches only provide information on how metal toxicity affects different types of microorganisms and soil processes without measuring the direct response at the cellular level. These methods also require high-throughput sequencing instruments and complex computational data analysis (Shakya *et.al*, 2019).

Various biological indicators have been widely used to study the effect of metal toxicity on soil microorganisms such as microbial biomass, soil respiration, counts of N-fixing bacteria, and enzyme activities (Šmejkalová *et.al*, 2003). These methods are relatively easy indicators to monitor microbial activity in polluted soils. The results can represent the size of the microbial community, including the number of living cells and substrate utilization (a process of C and N cycles). However, they cannot provide information about the mechanisms of metal toxicity and its physiological effects.

Methods for measuring the heavy metal toxicity should represent the impact on microbes found in the naturally contaminated soil environment. Some studies have employed genetically modified bacteria biosensors that can respond to metal contamination. Signals generated from the cells were used to determine the metals that crossed biological membranes and caused harmful effects to the cells (Hynninen *et al*, 2010; Bereza-malcolm *et.al*, 2015). Responses from the model organisms can be linked to actual toxicity in the field that may explain the soil's biological processes.

Bacteria-based biosensors are a reliable tool to measure the negative impact of heavy metals on a population of test soil microorganisms. The use of bacteria for environmental sensing offers some advantages compared to higher organisms: rapid responses, a large and homogenous population with a short generation time, and relative ease of application for soil monitoring (Renella and Giagnoni, 2016). This can be achieved by exploiting a model organism that mimics the response of living cells to heavy metal exposure in a real polluted environment.

2.4. Biosensors

A biosensor is defined as the combination of biological recognition systems with a transducer (Castillo *et al.*, 2004). Biological recognition systems act as receptors that interact with target

chemicals to produce a response, whereas the transducer converts this response into a measurable signal. Some devices for signal transduction, such as spectroscopy and microscopy instruments, can transfer the biological responses into the electrical domain to generate signals proportional to the concentration of chemicals (Thévenot *et al.*, 2001).

The most commonly used biological recognition elements are enzymes, antibodies, genes, and whole cells (Turdean, 2011). The use of whole cells is more attractive than other recognition elements because the cells can be modified at a certain level to produce signals when the target chemicals are present. Most whole-cell biosensors can produce responses after the target chemicals have diffused into the intracellular components (Renella and Giagnoni, 2016).

2.4.1 Inducible biosensors

According to the regulation of gene expression, whole-cell biosensors can be classified as inducible or constitutive (Renella and Giagnoni, 2016). Inducible biosensors have become of great interest for environmental applications since the development of molecular biology techniques has enabled scientists to engineer various heavy metal response genes in microbial host cells. This approach relies on the host cells emitting luminescence or fluorescence signals controlled by a promoter induced in the presence of intracellular heavy metals (He *et al.*, 2016). The gene construct involves the fusion of a reporter gene (luciferase/*lux* or green fluorescence protein/*gfp*), with an inducible promoter from a metal responsive gene. When metals are present inside the cell, they will activate the regulatory protein, which induces the promoter-reporter gene construct. Induction of this promoter will initiate the expression of reporter proteins as signals (Figure 2.6) (Xu *et al.*, 2013; He *et al.*, 2016).

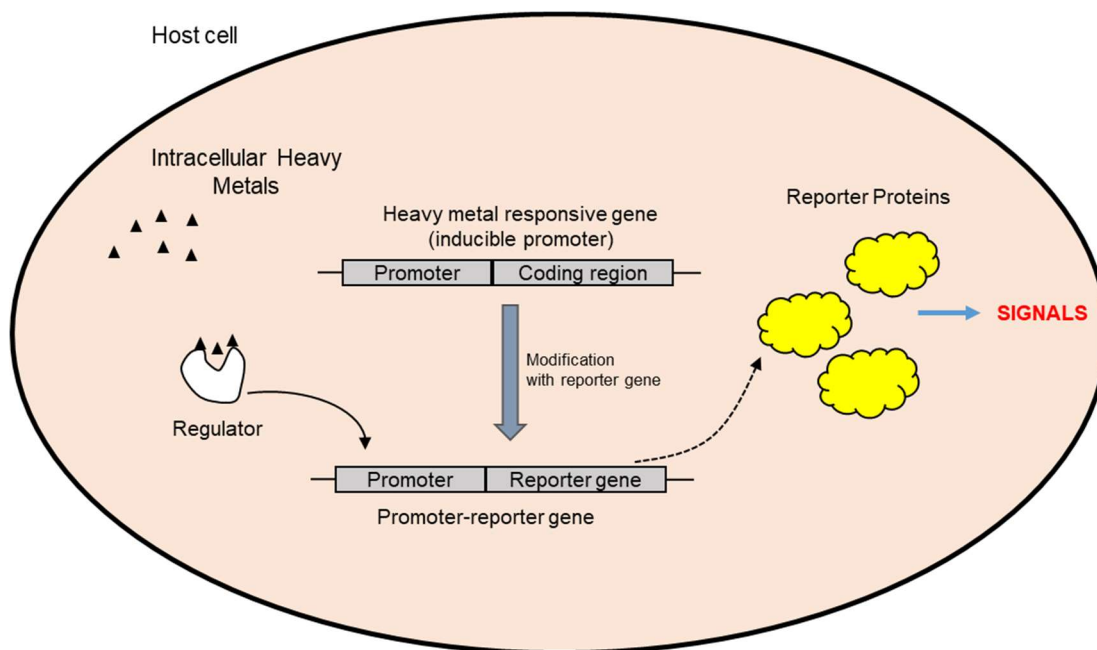


Figure 2. 6 The principle of inducible biosensors. The gene encoding a response to heavy metal is modified to construct the promoter-reporter gene inside the host cell. The metal binding with regulatory proteins will activate the promoter and induce the production of reporter proteins as signals. (Adapted from Xu et al., 2013; He et al., 2016).

Inducible biosensors can be made for specific and non-specific detection of heavy metals. Bereza-malcolm *et.al*, (2015) developed an *E.coli* biosensor specifically for Pb^{2+} by inserting a promoterless *gfp* gene into the promoter region of gene encoding Pb regulatory protein (PbR). The GFP can be expressed due to the presence of intracellular Pb^{2+} . Hynninen *et.al*, (2010) developed an inducible biosensor by constructing a promoter fusion from metal transporter gene (*czc1*) with a *lux* gene in *Pseudomonas putida* host cell. This biosensor can produce luminescence signals due to the presence of intracellular Zn^{2+} , Cd^{2+} , and Pb^{2+} . More examples of inducible biosensors for heavy metals in a variety of bacteria host cells, including their performance, are provided in Table 1 below.

Table 2.1. Inducible biosensors for detection of Cd, Zn, and Pb.

Host cell	Target Heavy metals	Metal responsive-reporter gene construct	Responsive time	Detection limit	References
<i>Pseudomonas putida</i> KT2440	Zn, Cd, Pb	<i>pDNPczc1-lux</i>	3 hours	0.16 μ M (Cd), 1.12 μ M (Cd), 0.9 μ M (Pb)	Hynninen, 2010

<i>E.coli</i> XL1-Blue	Cu & Zn	<i>cusC-RFP</i>	4-6 hours	13 mg/L (Zn), 11.4 mg/L (Zn)	Ravikumar <i>et al.</i> , 2012
<i>Pseudomonas fluorescens</i> OS8	Cd, Zn, Pb	<i>pbrR PpbrAlux</i>	2 hours	0.8-500 μ M (Cd), 40 μ M-10 Mm (Zn), 0.9 μ M-1 mM (Pb)	Ivask <i>et.al</i> , 2009
<i>P.putida</i> X4	Zn	<i>czcR3-gfp</i>	2-5 hours	5-55 μ mol/L	Liu, Huang and Chen, 2012
<i>E.coli</i> DH5 α	Cr(IV)	<i>pCHR-GFP1</i>	3-5 hours	100 nM	Branco, Cristóvão and Morais, 2013
<i>Synechococcus sp.</i> PCC 7942	Zn, Cd, Cu	<i>smtAB-luxCDABE</i>	3-6 hours	0.97-2.04 μ M (Zn), 1.54-5.35 μ M (Cd), 0.027-0.05 μ M (Cu)	Martin-Betancor <i>et al.</i> , 2015
<i>P.aeruginosa</i> PAO1, <i>E.coli</i> DH5 α , <i>Enterobacter</i> sp.LCR17	Pb	<i>pbrR-gfp</i>	1.5- 2 hours	0.2-1 μ g/mL	Bereza-Malcolm, Aracic and Franks, 2016
<i>E.coli</i> DH5 α <i>Acinetobacter baylyi</i> Tox2	Cd, Zn Zn, Cd, Cu	<i>zntAP-gfp</i> <i>Ptet-luxCDABE</i>	3 hours 8 hours	1-5 mg/L 70-72 mg/L (Zn), 37-50 mg/L (Cd)	Yoon <i>et al.</i> , 2016b Cui <i>et al.</i> , 2018
<i>E.coli</i> MG1655	Cd	<i>ZntA-gfp</i>	3.5-6 hours	5-100 ug/L	Elcin and Öktem, 2020

The main limitations of inducible biosensors are the indirect measurement and the time required to produce signals. The signal production is a result of transcription regulation processes. The induction time from some inducible biosensors can vary from 2 hours up to 12 hours after exposure to heavy metals (Magrisso *et.al*, 2008; Yoon, *et al.*, 2016b). The time for measuring the signals depends on the level of intracellular metal concentration that can induce the promoter activation, cellular mechanisms to carry out the transcription of reporter proteins, and the amount of reporter proteins that can give a readable measurement (Table 2.1).

2.4.2 FRET biosensors

Forster resonance energy transfer (FRET) is a phenomenon in which direct non-radiation energy transfer occurs from a donor fluorophore in its excited state to an acceptor fluorophore. This process can cause the acceptor fluorophore to emit its characteristic fluorescence (Bajar *et al.*, 2016). FRET can occur between a donor and acceptor if the donor emission spectrum overlaps with the absorption spectrum of the acceptor (Figure 2.7). This approach has been exploited for monitoring various biochemical activities (Abraham, *et al.*, 2014), intracellular ion concentrations (Carter, *et al.*, 2014), and protein-protein interactions (Day and Davidson, 2012).

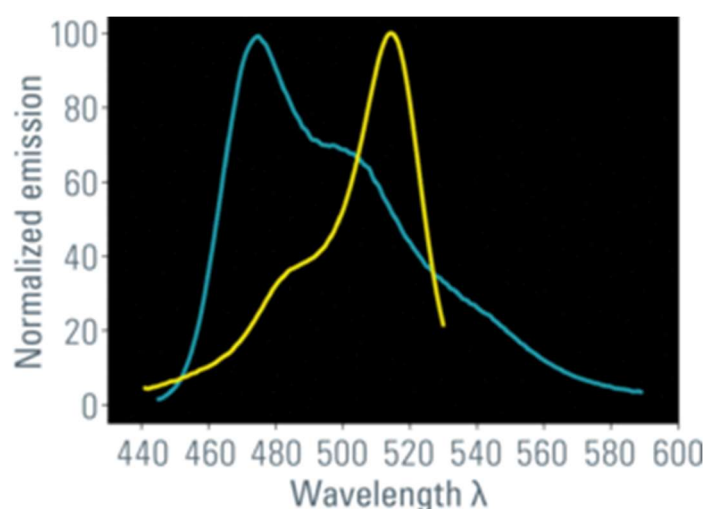


Figure 2. 7 Emission spectra of donor fluorophore (e.g Cyan Fluorescence Protein/CFP, blue line) overlaps with excitation spectra of acceptor fluorophore (Yellow Fluorescence Protein/YFP, yellow line). This shows that both FPs are in compatible energy levels, which is required for FRET to occur.

FRET-based biosensors are composed of a receptor protein as the sensing domain fused with two donor-acceptor fluorescent proteins (FPs) capable of absorbing and emitting light (Miyawaki *et al.*, 1997; Fehr *et al.*, 2002). The binding of a chemical to the receptor protein can change the molecular distance between the two FPs (Figure 2.8). If the donor FP is excited, energy is transferred from the donor to the acceptor leading to excitation of the acceptor FP (Tsien, 1998; Carter *et al.*, 2014). The percent of energy transfer from donor to acceptor FPs at a particular state is described as FRET Efficiency. FRET Efficiency for a given FPs pair is proportional to the inverse sixth power ($1/d^6$) of the distance between two FPs. This distance is restricted to an upper limit of ~ 10 nm (Chatterjee *et al.*, 2011; Bajar *et al.*, 2016).

According to Bajar *et al.* (2016), there are two methods for measuring the FRET change: 1) direct, which directly calculates the change of fluorescence intensity (sensitized emission FRET) or polarization to the FRET change (prFRET), and 2) indirectly, which involves the measurement

of FRET Efficiency at different states through spectral imaging (siFRET), acceptor photo bleaching FRET (apFRET), and fluorescence lifetime imaging FRET (FLIM-FRET). Direct measurement with sensitized emission (seFRET) is the most applied method because it is easy to use, less expensive, and offers fast imaging times. The Ratio metric analysis (ratio: emission acceptor/emission donor) is commonly used to calculate sensitized emission of FRET biosensor. The implementation of ratio metric analysis is simple and can be correlated directly to the concentration of target molecules inside the cell.

A FRET biosensor can be used to study protein interaction with the target heavy metals under live-cell physiological conditions. The development of light microscopy techniques enables the FRET events to be visualized, which provides the two-dimensional spatial distribution of protein-chemical interactions inside the cells (Periasamy., 2001; Rizza *et al.*, 2017). The FRET biosensor offers a non-invasive technique to report metal concentration with a high resolution and requires only light inputs once the protein sensor is expressed *in vivo*.

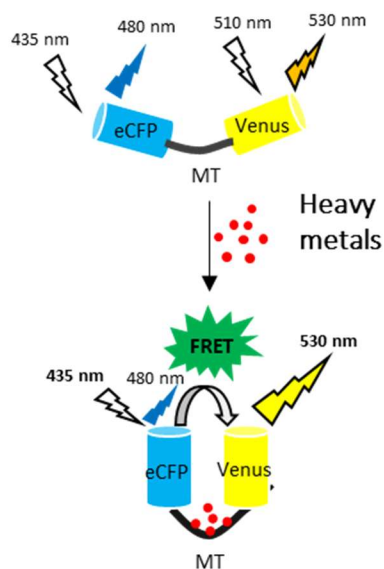


Figure 2. 8 A model of FRET biosensor for detecting heavy metals. The biosensor is a fusion of metal binding protein (MT) between two fluorescence proteins (eCFP and Venus) as donor and acceptor fluorophores, respectively. Heavy metals binding onto MT cause a conformational of the FRET biosensor. In this case, energy transfer occurs from the excited eCFP to Venus, leading to the change in FRET.

2.4.3 Application of FRET biosensors

FRET biosensors have been applied to measure ligand concentrations, distribution and monitor cellular activities in various organisms (Table 2.2). Chiu and Yang (2012) and Yang *et al.*, 2020 reported the development of FRET biosensor (lead binding protein (PbrR) fused between eCFP and Venus) as a diagnostic tool to measure lead toxicity inside mammalian, plant, and animal cells. Rajamani *et al.* (2014) have developed FRET-based heavy metal biosensors inside the microalgae *Chlamydomonas reinhardtii*. This biosensor consists of chicken metallothionein inserted between eCFP and YFP. Their results revealed the ability of this biosensor to quantify intracellular Cd, Pb, and Zn.

FRET biosensors have been utilized to measure a variety of ligands inside living plants. FRET-gibberellin biosensor was developed by Rizza *et al.*, (2017), which composed of Cerulean (donor) and Aphrodite (acceptor) fused with gibberellin binding proteins (GAI and GID1). This sensor has enabled the monitoring of gibberellin concentration and distribution across plant cells and tissues. Assuncao *et al.*, (2020) used the FRET biosensors (fusion of Phosphate binding protein (PiBP) with CFP and YFP) for measuring the phosphate level inside *Arabidopsis thaliana*. The sensor has provided information about phosphate transport and homeostasis in living plant cells.

FRET biosensors can be used as a tool to visualize a variety of biochemical events or redox status in living cells. Ibraheem *et al.*, 2011 developed H3K27-trymethylation FRET biosensor for the detection of methylation of lysine 27 (histone H3) in *E.coli*. The biosensor comprises a donor mTFP1, a domain that binds to methylated lysine residues, and an acceptor mCitrine. Abraham *et al.*, (2014) reported the use of FRET biosensor to monitor intracellular redox status in bacteria cells. They utilized a pair of Citrine and Cerullean fluorescence proteins fused with Biotinylation domain of transcarboxylase. This biosensor provides a vital information about the physiological status of the cells due to exposure to oxidizing and reducing agents.

Based on the response time of FRET biosensors (Table 2.2) and inducible biosensors (Table 2.1), FRET biosensor offers a measurement of intracellular heavy metals in a rapid manner. The FRET biosensor can be produced inside the host cells before heavy metal exposure. Direct binding of intracellular metals with the FRET biosensor will generate signals that can be measured in proportion to the heavy metal concentrations.

Moreover, the application of FRET biosensors can visualize and quantify target chemical pools in different cell locations (Carter, Young and Palmer, 2014; Rizza *et al.*, 2017). Unlike inducible

biosensors, the FRET biosensor can be engineered for the expression in specific target compartments within the host cell. FRET biosensors expressed within the cytoplasm can detect the presence of metals that have passed through the cell wall, therefore, may provide information about the metal distribution within the cell.

Table 2.2 FRET biosensor in various host cells and its applications for monitoring intracellular ligands and biological processes.

Host cells	Target Detection	FRET Constructs	Responsive time	Detection limit	References
Human embryonic kidney cell (<i>HEK239</i>)	Pb	<i>eCFP-Pb binding protein (PbrR)-Venus</i>	2-3 minutes	0.1-50 μ M	Chiu and Yang, 2012, Yang <i>et al.</i> , 2020
Microalgae <i>Chlamydomonas reinhardtii</i>	Cd, Zn, Pb	<i>eCFP-chicken metallothionein-Venus</i>	1-3 minutes	24-1500 μ M (Cd)	Rajamani <i>et al.</i> , 2014
<i>E.coli</i> , <i>Saccharomyces cerevisiae</i> (yeast), and Human embryonic kidney cell (<i>HEK239</i>)	Hg	<i>eCFP-mercury binding protein(MerFS)-Venus</i>	2 minutes (<i>E.coli</i>), 8 (yeast), 8-10 minutes (<i>HEK239</i>)	0.210 – 1.196 μ M	Soleja <i>et al.</i> , 2019
Human embryonic kidney cell (<i>HEK239</i>)	Cd	<i>eCFP-Cd binding protein (CadR)- Venus</i>	60 minutes	1-100 μ M	Chiu <i>et al.</i> , 2013
Plant <i>Arabidopsis thaliana</i>	Gibberellin	<i>Cerulean- Gibberellin Perception Sensor 1(GPS1)-Aphrodite</i>	20 minutes	0.01-10 μ M	Rizza <i>et al.</i> , 2017
Plant <i>Arabidopsis thaliana</i>	Abscisic acid (ABA)	<i>mTurquoise- ABA receptors(PYRI&ABII)- Venus</i>	2-24 minutes	0.1 – 0.6 μ M	Waadt <i>et al.</i> , 2014
Root cells of <i>Arabidopsis thaliana</i>	Phosphate	<i>eCFP-Phosphate binding protein (PiBP)-eYFP</i>	10-20 minutes	25-200 mM	Assuncao <i>et al.</i> , 2020
<i>E.coli</i> K-12 and <i>Saccharomyces cerevisiae</i>	Glutathione	<i>CFP- glutathione binding protein (YliB)-YFP</i>	5-10 minutes	50 μ M – 5 mM	Ahmad <i>et al.</i> , 2020
<i>E.coli</i> BL21-DE3	Pentose and Disaccharide	<i>eCFP-maltose binding protein (malE)-Eyfp</i>	2-7 minutes	0.1-100 mM	Kaper <i>et al.</i> , 2008
<i>E.coli</i> BL21-DE3 and <i>S.cerevisiae</i>	Lysine flux	<i>CFP-lysine binding periplasmic protein-YFP</i>	2-4 minutes	2-1500 μ M	Ameen <i>et al.</i> , 2016
<i>E.coli</i> BL21-DE3	Monitoring intracellular redox status	<i>Cerulean- Biotinylation domain of</i>	50-100 minutes	0.01-10 mM (Reducing	Abraham <i>et al.</i> , 2014

<i>transcarboxylase- Citrine</i>	agent DTT), 1 mM (Oxidizing agent H ₂ O ₂)
--------------------------------------	--

2.4.4 FRET Biosensor for measuring heavy metal bioavailability

In this research, a bacterial biosensor was used to simulate the response of soil microorganisms to bioavailable Pb²⁺, Cd²⁺, and Zn²⁺ (Figure 2.9). The response is reported through the activity of FRET biosensor bound with heavy metals inside the cells. This can be achieved by engineering the host cell of interest to produce the biosensor construct; a fusion of a metal-binding protein (metallothionein) with two fluorescence proteins. The interaction of the FRET biosensor with heavy metals is stable, well maintained, simplified, and packaged within the cell as its natural environment. The properties of this FRET biosensor are discussed in more detail as follows:

1) Host cells

FRET biosensors offer a flexibility to be applied in different host cells (prokaryote and eukaryote). Soleja *et al.*, (2019) developed a FRET-mercury biosensor (MerFS) that was used to measure Hg²⁺ concentrations within *E.coli*, yeast, and human embryonic kidney cells (Table 2.2). This can be done by sub-cloning the chimeric sequence of FRET-mercury biosensor into different expression vectors suitable for particular host cells. Chimeric sequence means a DNA sequence originating from two or more parent DNA sequences joined together. In this case, the FRET-mercury biosensor was encoded as the join of multiple parent DNA sequences from eCFP, merP (mercury binding protein), and Venus Fluorescent protein (Soleja, *et.al* 2019). FRET biosensor developed by Rajamani *et al.*, (2014) was proved to quantify intracellular Cd, Zn, and Pb in microalgae. This sensor may be developed in soil bacteria which can potentially be used to measure bioavailable heavy metals in contaminated soils.

The choice of host cell should consider these aspects: flexibility for genetic manipulation, ease of growth, inexpensive culture preparation, and safety or non-pathogen. It is important to use a host cell in which the protein expression mechanisms have been well studied. *E.coli* has been widely used as a host cell for cloning and protein recombinants (Rosano and

Ceccarelli, 2014). This host cell is suitable for the construction of genes encoding the FRET biosensor and studying the function of protein sensors.

Biosensors for measuring heavy metals in environmental samples should utilize a robust host cell. This could be obtained by selecting a microorganism that naturally exists in a polluted environment. For this reason, *Pseudomonas putida* might be a good candidate host cell. This bacterium can survive in a toxic environment due to the presence of metal resistance mechanisms. The genetic properties of *P.putida* strain KT2440T7 have been well characterized and certified as a safe microorganism for various applications (Nelson *et al.*, 2002; Troeschel *et al.*, 2012).

2) Reporter proteins

Fluorescent proteins are genetically encoded and can easily be introduced into the host cells through plasmid transformation and expressed without affecting intracellular stability (Bajar *et al.*, 2016). The generation of fluorescent protein mutants with distinct excitation and emission spectra can serve as FRET donor/acceptor pairs. GFP mutants, green and blue fluorescent protein (GFP and BFP), were first used for early FRET biosensor applications (Miyawaki *et al.*, 1997). However, it was found that BFP produced less brightness and was more likely to suffer from photobleaching than other GFP mutants.

Photobleaching is a process where fluorophore molecules lose their ability to emit fluorescence signals over several absorption and emission events (Kalies *et.al*, 2011). This often occurs due to the high intensity of light exposure when using a confocal microscopy. This light exposure can cause the fluorophore in excited state and undergoes a permanent structural change by reacting with another species (e.g oxygen) (Bernas, *et.al* 2004). The loss of fluorescence decreases the signal-to-noise ratio and prevents the acquisition of image resolution data during repeated scanning. This will reduce the quality of images obtained by confocal microscopy. Photobleaching can be minimized by removing oxygen with oxidase and catalase (Tanhuanpaa *et.al* 2000), antioxidants (phenyldiamine, mercaptoethanol, DABCO, cysteine, ascorbic acid, nitroxide free radicals), or by shielding the fluorophore with a bound antibody (Abuknesha *et.al.*, 1992; Bernas, *et.al* 2004).

The most commonly used FRET pairs consist of cyan and yellow fluorescent protein mutants (eCFP and eYFP) (Kremers *et al.*, 2006; Bajar, *et al* 2016). Utilising eCFP as a donor produces a high quantum yield with a long fluorescence lifetime. Venus is a mutant of YFP, which is a very bright and fast-maturing variant. The first YFP was very sensitive to H⁺

and Cl⁻ ions, resulting in the production of artifact signals during intracellular FRET application. Therefore, this fluorescent protein was engineered by introducing a specific mutation (F46L) to generate a Venus FP (Kremers *et al.*, 2006). As a result, the issues with artifact signals can be avoided with an improved photostability (Zaccolo, 2004). Venus FP is less sensitive to pH, chloride and more photostable.

3) Sensing domain

One of the challenges in developing FRET biosensors for heavy metals is to find a suitable sensing domain. Metal-binding protein that can perform conformational changes upon metal binding is a good candidate for FRET pair. Depending on the purpose of the application, FRET biosensor can be made specifically for a single species or group of metals. Chiu and Yang, (2012) developed the FRET biosensor that exploited the role of PbrR from *Cupriavidus metallidurans* (CH34) as a specific binding domain for Pb²⁺. The performance of this sensor was proven to measure different levels of Pb²⁺ poisoning in human kidney cells suggesting its application for biomedical purposes.

The unique folding properties of MT have become a particular interest in biosensor development. The first utilisation of MT as one of the components in FRET biosensor was demonstrated by Pearce *et al.*, 2000 by studying the function of human MT in metal transfer and interaction with redox partners and ligands. The MT was inserted between two fluorescent proteins, thus allowing for monitoring of metal binding and nitrous oxide signalling in animal tissues. Rajamani *et al.*, (2014) incorporated the chicken metallothionein (CMT) as a binding domain in the FRET biosensor for detecting a group of metals; Cd, Pb, and Zn. This sensor showed the half-maximal metal saturation concentration for Cd, Pb, and Zn are 225, 205, and 310 μM respectively with a large range of detection limit (0.1-5000 μM for Cd, 0.1-500 μM for Pb, and 0.01-1000 μM for Zn). The function and structure of metallothionein from chicken and birds (avian) have been studied by Andrews *et al.*, (1996). Analysis of CMT gene showed that MT gene family from avian family is very simple. The 63 amino acids of avian MT share extensive structural homology (74.2%) with the consensus sequence of mammalian MT, in which each MT molecule can bind to 7 atoms of Zn or Cd. Considering the binding affinity of CMT for Cd, Pb, and Zn and its well-studied protein structure, this research focused on the exploitation of CMT as a binding domain for the FRET biosensor development.

2.4.5 Application to soil samples

FRET biosensor application in contaminated soil has not been reported in the literature. Most biosensors for measuring the bioavailability of Cd^{2+} , Pb^{2+} , and Zn^{2+} still rely on the principle of metal responsive genes induced by intracellular heavy metals. Hynninen *et al.*, (2010) reported the measurement of bioavailable Zn^{2+} in artificially contaminated soils using an inducible biosensor (*P. putida* KT2440.2431(pDNPczc1lux)). The results showed that soil containing 20-65 mg/kg of Zn could induce the luminescence signal production. This signal was used to estimate the safe level of metals in soils according to regulation. Yoon,*et al.*, (2016a) investigated the applicability of *E.coli* harbouring As-inducible promoter fused with a *gfp* gene for measuring bioavailable Arsenic in contaminated soils. They reported the percentage of bioavailable arsenic was in the range of 0.6%-1.09% of the total concentration.

One of the limitations of inducible biosensors is the potential interference of the soil matrix (e.g, turbidity, nutrients, minerals) that may change the physiological state of the host cell and affect the expression of reporter proteins (Bereza-malcolm *et al.*, 2015). Another concern in utilizing inducible biosensors is the possibility of basal-level expression from leaky promoters that may produce false-positive signals (Jia *et al.*, 2019). Leaky promoters mean that the promoter has leakage expression of the target protein. In this case, the transcription occurs even when the repressor is present, and the inducer is absent (Penumetcha, *et al.*, 2010). Leaky promoters can take place in some inducible-transcription biosensors for example; the interaction of mer promoter and MerR regulator system was initially regulated the Hg induction response, however, Ivask *et al.* (2009) reported that this system can also be induced by Cd^{2+} and Zn^{2+} . This indicates that the biosensors using mer promoter and MerR regulator do not exclusively respond to a specific target of heavy metals and reduce the accuracy of reporter protein expression. Therefore, the interpretation of inducible-transcription biosensors response in the complex metal environment must be undertaken with caution (Zhang, *et al.* 2016).

This issue may be overcome by employing the FRET biosensor; the change of FRET signals occurs only through the binding of heavy metals with the sensing domain inside the host cell.

Measurement of bioavailable metals using biosensor was mainly carried out by exposing the host cells to soil-water extract (particle-free supernatant formed after centrifugation of the suspension) or soil-water suspensions (obtained by mixing the soil with water) (Hynninen and Virta, 2010; Xu *et al.*, 2013). Ivask *et al.*, (2004) reported the contaminated soils tested with luc-based inducible biosensors (*Bacillus subtilis* BR151 (pTOO24) and *S. aureus* RN4220 (pTOO24)) showed that 115-fold more Cd and 40-fold more Pb were bioavailable in soil

suspensions than in soil-water extracts. Biosensor analysis from soil-water suspensions have become a particular interest because the host cells are in direct contact with soil particles. This allows for a measurement of bioavailable metals both in soluble fraction as well as the metals absorbed in the soil samples.

The main challenge to applying biosensor is the opacity of the soil, including the presence of organic matters, minerals, and organisms that may interfere with signal measurement. Some attempts have been made to improve the applicability of biosensors in soil. Biosensor cells can be encapsulated into alginate beads to enhance stability in the soil environment (Bae *et al.*, 2020). Exposure of the alginate beads containing biosensors cells with soil particles may be beneficial for *in situ* soil measurement. Hurdebise *et al.*, (2015) applied a density gradient centrifugation to recover the biosensor cells from the soil matrix. A highly soluble, non-ionic, and non-toxic agent (*Nycodenz*) was mixed into the soil biosensor suspensions. Following the centrifugation, the biosensor cells were accumulated at the culture media interface forming a visible halo. The cells can be easily separated, and the signals can be further analysed by using a fluorescence spectroscopy instrument (Hurdebise *et.al.*, 2015)

2.4.6 Biosensors for the assessment of remediation performance

Monitoring the level of bioavailable heavy metals can be used as one of the parameters in assessing the effectiveness of biochar application. Development of FRET-heavy metal biosensor inside *P.putida* (Figure 2.9) can potentially be employed as a robust biosensor with direct measurement of bioavailable heavy metals in soil samples. Reduction of heavy metal bioavailability due to biochar application will be observed based on the changes of FRET signals. The results are expected to give reliable information about the concentration of biologically relevant heavy metals.

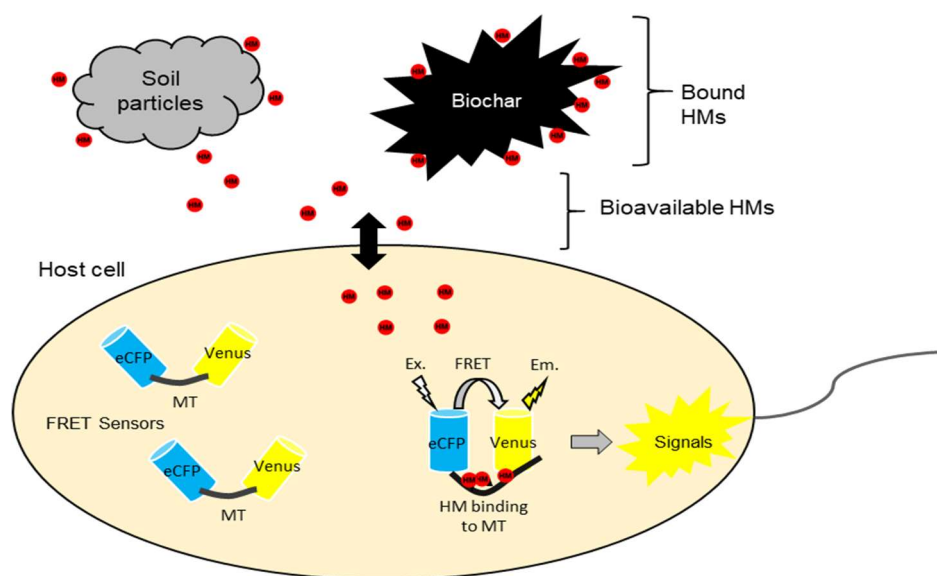


Figure 2. 9 FRET biosensors inside a bacterial host cell. Bioavailable heavy metals from soil amendment with biochar can potentially be measured directly by exposing the cells to soil samples.

Incorporating biosensors into ecological risk-based criteria will provide a better understanding of the level of heavy metals contamination which potentially cause damaging effect to soil microorganisms. The response of biosensor can be interpreted in correspond to the concentrations of bioavailable heavy metals in the tested soil. Furthermore, the comparison of biosensor response with higher organisms' response can be made to evaluate their relative merits in soil ecotoxicity testing (Trott, *et.al*, 2006).

The combination of biosensor application with parameters of chemical analysis, plant growth, and soil biological process will provide useful information concerning the reduction of heavy metal toxicity and a comprehensive understanding of the changes in bioavailable metals during soil remediation. The correlation of these parameters can be used to consider the potential capacity of soil function and productivity to achieve soil restoration. It also enables the

rehabilitation of degraded (metal-contaminated) land back into productive use as an asset, according to the reduction in risk achieved and suitability for different land uses.

3. Construction and characterization of the FRET biosensor for measuring heavy metals in *E.coli*

3.1 Introduction

A number of studies have demonstrated the use of FRET biosensors to measure the concentrations of heavy metals at a cellular level (Chiu and Yang, 2012; Chiu *et al.*, 2013; Rajamani *et al.*, 2014). FRET biosensors offer a direct and rapid measurement of heavy metal concentrations inside the living host cells and provide a more rapid response compared to transcriptionally-induced reporter fusions. A previous study of a FRET-heavy metal biosensor in microalgae *Chlamydomonas reinhardtii* showed how the sensor could measure heavy metal accumulation within a time scale of minutes (Rajamani *et al.*, 2014). This FRET biosensor utilised a chicken metallothionein (CMT) as the sensing domain, which is very sensitive to Pb^{2+} , Cd^{2+} , and Zn^{2+} . Therefore, this CMT was exploited as a component of a FRET biosensor in prokaryotic host cells and the biosensor then applied to measure the toxicity of heavy metal-polluted soils.

In this research, the FRET biosensor consists of a metal binding protein (CMT) as the sensing domain inserted between two fluorescence protein (eCFP and Venus). The properties of CMT and reporter proteins (eCFP and Venus) have been explained in Chapter II, section 3.4. All these components are fused in a single polypeptide chain and expressed inside bacteria cells. Binding of metals to CMT brings about a change in the conformation of the protein which can be detected by measuring the emission ratio of eCFP and Venus. Measuring the changes in the ratio of donor-acceptor FPs is a straightforward and versatile method which can be applied on a wide variety of equipment such as spectro-fluorimeter and fluorescence microscopes (Hochreiter *et.al*, 2015). This method is non-destructive and suitable for the application on live cells.

3.1.1 Construction of the FRET biosensor

FRET biosensors are genetically encoded and relatively easy to construct using standard molecular biology techniques. The gene construct encoding a FRET biosensor can be introduced into the host cells and the protein sensors are expressed using the host's cellular transcriptional and translational systems.

1. Vector system

Gene construction requires a vector system that can express the target protein in bacterial host cells at a high level. A standard expression vector must contain at least a promoter, antibiotic marker, replication site, multiple cloning sites, and fusion protein tag. The gene encoding a FRET biosensor can be cloned downstream of a strong promoter, for example, the T7 promoter system which is recognized by the T7 RNA polymerase that can be produced under the control of a specific inducer. This system is commonly used for recombinant protein production and can express the target protein in large amounts (Graumann and Premstaller, 2006).

To study FRET and heavy metal binding *in vitro*, the recombinant protein needs to be pure, soluble and in an active form. Therefore, the vectors typically include peptide tags at the N-or C terminal end of the recombinant protein for purification purposes. Additional amino acid residues or tags can be engineered on the N or C terminal end of the recombinant protein during the cloning step. These tags are used to improve the solubility and affinity purification of the target protein. Peptide tags consisted of six consecutive histidine residues (also called 6x His-tag) is one of the simplest and most widely used for protein purification. These residues can readily coordinate with nickel ions immobilised on beads or a resin for purification. This approach typically has high binding capacities (5-40 mg of His-tagged protein/mL of media) with a relatively low cost (Malhotra, 2009)

A N-terminal poly-Histidine tag was chosen because small peptide tags are less likely to interfere with sensor function. The His-tagged protein can be recovered by immobilized nickel affinity chromatography (Rosano and Ceccarelli, 2014). Antibiotic resistance genes are included in the vector backbone and used to prevent the growth of vector-free cells.

2. Recombinational cloning the FRET biosensor

Gateway recombination is a universal cloning method that provides a highly specific and efficient way to move DNA sequences into multiple vector systems (Hartley *et al.*, 2000). In the FRET biosensor development, Gateway Recombination offers flexibility to clone multiple gene fragments (CMT and FPs gene) into a single construct. The main advantage of this method is that the orientation of the gene construct and reading frame can be maintained throughout the cloning process.

This method is based on a bacteriophage lambda (λ) site-specific recombination system which mediates the lambda integration into *E.coli* chromosome during lytic and lysogenic pathways (Landy, 1989). The basis of this recombination constitutes two steps of reactions, BP and LR reactions (Figure 3.1). The BP reaction facilitates the recombination of *attB*-PCR product with

attP sites in the donor vector to generate *attL* sites (entry clone). This reaction is mediated by BP clonase enzyme mixture (λ Integrase, Integration Host Factor (IHF) proteins). The LR reaction facilitates the recombination of *attL* sites (entry clone) with *attR* sites in the destination vector to generate *attB* sites (expression vector). This reaction is mediated by the LR clonase enzyme mixture (λ Integrase, Integration Host Factor (IHF) proteins, and Excisionase).

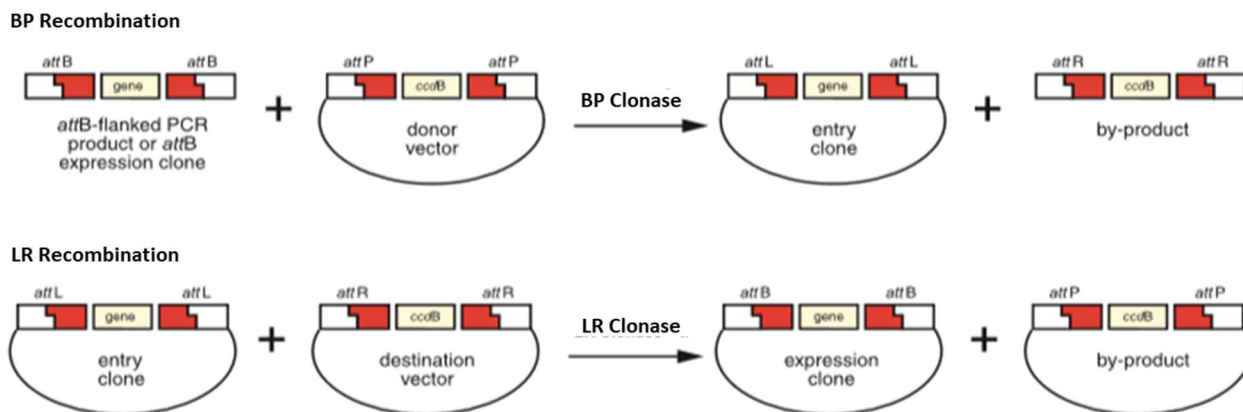


Fig 3.1. Two recombination reactions in Gateway cloning (BP and LR recombination) (Landy, 1989; Invitrogen). In BP recombination, a target gene flanked between *attB* sites can be cloned into a donor vector containing *attP* sites. The target in the entry vector can be cloned into a destination vector containing *attB* sites. This results in the insertion of target gene into the expression vector.

This research utilised the Gateway recombination to construct the FRET biosensor which involves the amplification of DNA sequence by using customised *attB* PCR Primers, followed by the BP recombination (reaction of *attB*-PCR product with a donor vector to generate an entry clone) and LR recombination (reaction of the entry clone with a destination vector to generate an expression vector). The resulting expression vector will be transformed into the target host cell and used for protein expression.

3. Choice of host cell

In this research, *E. coli* strains were used as the host cells for cloning of the gene encoding the FRET biosensor (*E. coli* OmniMAX™ 2-T1R) and initial study of FRET response to intracellular heavy metals (*E. coli* BL21 Rosetta 2(DE3)). Some advantages of using *E. coli* strains as the host organism are: (i) they can grow rapidly, with a doubling time of approximately 20 minutes under optimal environmental conditions, (ii) high cell density cultures can be easily achieved, which is useful to boost the recombinant protein production, (iii) various types of inexpensive and readily available media can be used to grow the cells, and (iv) preparation of competent cells and transformation with vectors can be performed easily and quickly (Rosano and Ceccarelli, 2014).

The mechanism of protein expression in *E.coli* has been well studied, which makes it suitable for protein recombinant experiment (Rosano and Ceccarelli, 2014). The use of an inducible T7 promoter system in *E.coli* BL21 Rosetta 2DE3 can minimize the possibility of alteration of native cellular processes, thus allowing for FRET biosensor production without disturbing the endogenous systems of the host cells (VanEngelenburg and Palmer, 2008). A combination of an inducible T7 promoter with λ DE3 lysogen is the most popular induction system to produce a high level of protein (Studier and Moffatt, 1986; Structural Genomics Consortium, 2008). λ DE3 lysogen expresses T7 RNA polymerase from the genome under the control of *lacUV5 promoter*, which is induced by the addition of Isopropyl β - d-1-thiogalactopyranoside (IPTG). The presence of T7 RNA polymerase will transcribe the gene of interest from a T7 promoter on the vector and translated into protein.

The concept of the FRET biosensor development is shown in Figure 3.2 below. A commercial strain *E.coli* BL21 Rosetta 2(DE3) containing a chromosomal copy of T7 RNA Polymerase with basic IPTG-inducible system was used. The CMT gene was fused between eCFP and Venus genes under the T7 promoter in an expression vector. In the presence of IPTG, T7 RNA polymerase is produced and induce the expression of FRET biosensor protein from the expression vector.

In the absence of heavy metals, the two fluorescent proteins are widely separated but become closer to each other when metals are bound to CMT. When the eCFP is excited, energy transfer occurs from donor (eCFP) to acceptor (Venus FPs) leading to the changes in emission spectra. This allows the heavy metal concentration within the host cell to be quantified as the change of emission signals.

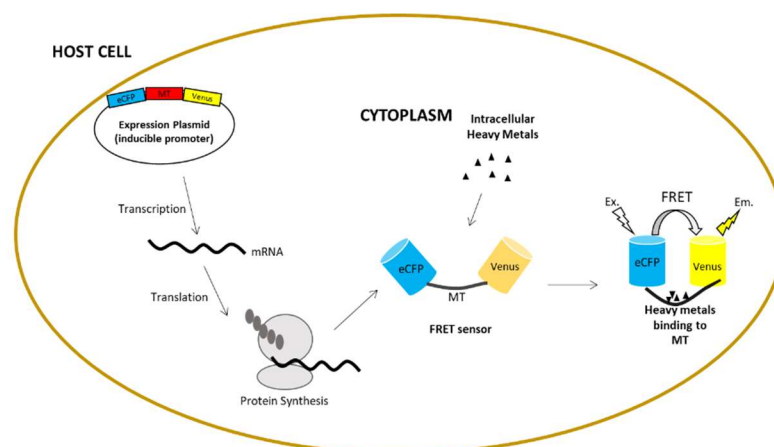


Fig 3.2. Concept of FRET biosensor development inside a bacterial cell. An expression vector encoding the *eCFP-CMT-Venus* gene is transformed into the host cell. The FRET biosensor is produced following

induction with IPTG and undergoes conformational change when bound with heavy metals, which results in a change in fluorescence emission spectrum.

3.2 Aim and objectives

The aim of this chapter is to develop a FRET-heavy metal biosensor. It utilises a CMT in which the codon usage has been optimised for protein expression in bacterial cells. Binding studies using the purified sensor were performed to demonstrate the proof of concept and to determine the specificity and sensitivity of the biosensor. The ability of the FRET biosensor to measure intracellular heavy metals was studied by exposing the host cell with different concentrations of heavy metals.

The achievement of this aim requires the following objectives to be completed:

1. To construct the gene encoding FRET biosensor (*eCFP-CMT-Venus*) in a vector for protein expression in *E.coli* host cell
2. To extract the FRET biosensor from the host cell and characterise the FRET signals due to binding with Pb^{2+} , Cd^{2+} , and Zn^{2+} *in vitro*
3. To characterise the FRET signals (*in vivo*) within *E.coli* host cells in the presence of Pb^{2+} , Cd^{2+} , and Zn^{2+} .

3.3 Methods

3.3.1 CMT Gene amplification

The sequence of the CMT gene (Rajamani *et al.*, 2014) was codon optimized for bacteria cell expression. The CMT was originated from *Gallus gallus*, therefore, the expression of this eukaryotic protein in bacteria cell e.g *E.coli* may produce insoluble aggregates proteins. As a result, the protein will be misfolded and present as biologically inactive form (Khalili, *et.al*, 2015). In this research, the codon optimisation of CMT for prokaryotic expression was performed using a web tool that converts the DNA sequence from *eukaryote* for expression in *prokaryote* cells (bacteria). There are 64 different codons in which 61 of them encode the 20 standard amino acids, while another 3 functions as stop codons. A single amino acid can be encoded by more than one codon, particularly if the number of codons is greater relative to the number of amino acids they coded.

The tool provides the best sequence option through screening and filtering sequences to lower complexity and minimize secondary protein structures. The codon optimization was written using a codon sampling strategy in which the reading frame is recorded according to the frequencies of each codon's usage in bacteria cells. This alteration of codon usage can improve the efficiency of heterogeneous expression of CMT in the bacteria host cell.

The codon optimised sequence was synthesized *de novo* (ThermoFisher) including the *attB* recombination sites at both ends (Figure 3.4). This construct was designated as *attB1-CMT-attB2*.

The *attB1-CMT-attB2* gene was amplified using primers:

forward(5'-3'):

GGGGACAAGTTTGTACAAAAAAGCAGGCTTCGATCCGCAGGATTGTACCTGT

reverse(3'-5'):

GGGGACCACTTTGTACAAGAAAGCTGGGTTCACCTTTTGCTGCTGCATGAC

attB primer sequences are underlined.

The PCR mixture consisted of 5 μ L (1X) of 10 X amplification buffer (ThermoFisher), 1 μ L (1mM) of 50 mM MgSO₄, 1.5 μ L (0.3 mM) of 10 mM dNTP mixture, 1.5 μ L (0.3 mM) of 10 mM primer reverse and forward, 1 μ L (10 ng) of *attB-CMT-attB* template, 0.4 μ L DNA polymerase (Platinum® Pfx DNA Polymerase, ThermoFisher), and 33.1 μ L of distilled water giving a total reaction volume of 50 μ L. A PCR reaction without *attB-CMT-attB* template was

used as the negative control. The PCR conditions were; initial denaturation at 94°C for 5 minutes, followed by denaturation at 94°C for 15 seconds, annealing at 72°C for 30 seconds, extension at 68°C for 20 seconds (30 cycles) and final extension at 68°C for 5 minutes, and maintained at 4°C, with a total of 30 cycles.

The PCR product was purified using a QIAquick Purification Kit (Qiagen) to remove primers, unincorporated dNTPs, enzymes, and salts from the reaction mixture. The purified PCR product was loaded into gel electrophoresis (1.5% agarose) to verify the size of *attB1-CMT-attB2* fragments.

3.3.2 Vector construct

A vector containing the FRET biosensor was constructed using Gateway Recombination (Landy, 1989, Invitrogen) as this allows elements of the construct to be changed easily. BP and LR recombination was performed to fuse the CMT between eCFP and Venus gene (Figure 3.3).

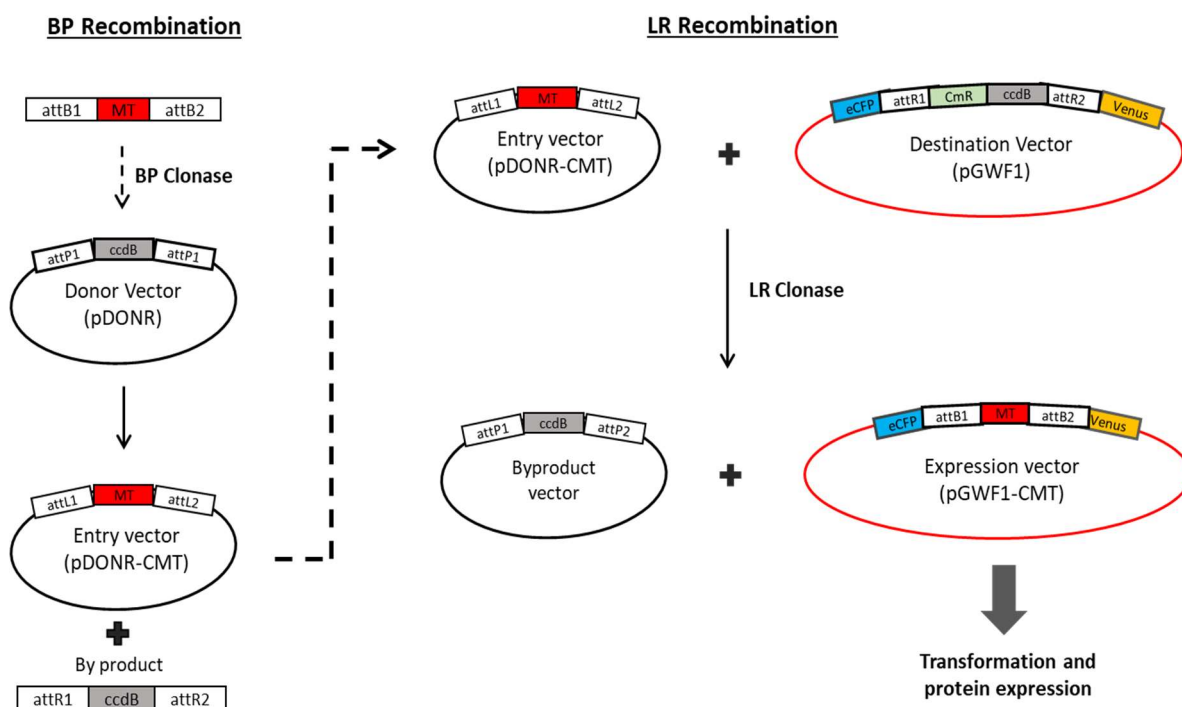


Fig.3.3 LR and BP recombinase reactions for the construction of vector (pGWF1-CMT) for the expression of FRET biosensor. MT gene including *attB1* and *attB2* sites were synthesized and cloned into a donor vector (pDONOR) catalysed by BP clonase. The resultant entry vector (pDONOR-CMT) contains MT gene flanked by *attL1* and *attL2* genes which are responsible as cloning sites with *attR1* and *attR2* in the destination vector (pGWF1-CMT). The CMT gene (in pDONOR-CMT) was cloned into

pGWF1 in framed between eCFP and Venus gene catalysed by LR Clonase. The final construct pGWF1-CMT contains the gene encoding the FRET biosensor (eCFP-CMT-Venus) which can be transformed and expressed inside *E.coli* BL21 Rosetta 2(DE3) host cells.

BP Recombination

The *attB1-CMT-attB2* gene was cloned into a donor vector (pDNOR, see appendices I-a for the construct map) catalysed by BP clonase to generate an entry vector (pDONR-CMT) (Figure 3.3). pDONR contains a kanamycin-chloramphenicol resistant gene and *ccdB* gene flanked by two *attR* sites. The entry vector was transformed into *E.coli* OmniMAX™ 2 T1R competent cell (Invitrogen).

The compositions of the BP reaction mixture was 2 µL of 40 fmol *attB1-CMT-attB2* PCR product, 1 µL (15 ng) of 150 ng pDONR (Invitrogen), 2 µL BP Clonase enzyme mix (Invitrogen), and 5 µL of TE Buffer pH 8. The reaction mixture was incubated at 25°C for 16 hours. 1 µL of Proteinase K solution (2 µg/µL) (Invitrogen) was added into the mixture followed by incubation 37°C for 10 minutes. The mixture was then prepared for a heat shock transformation.

The transformation was carried out by adding 1 µL of BP reaction mixture into a tube containing 50 µL of competent cells followed by incubation on ice for 30 minutes. The cells were heat-shocked for 30 seconds at 42°C without shaking in a water bath and immediately placed onto ice. 450 µL of (Super Optimal Broth) S.O.C. medium (ThermoFisher) was added to the cells at room temperature and shaken at 37°C for 1 hour. 20 µL and 100 µL of the transformation reaction were spread on selective LB plates containing 50 µg/mL of Kanamycin (Thermofisher). The plates were incubated overnight at 37°C to grow the transformant colonies. Five cell colonies were selected from the agar and each of them was grown in a selective LB liquid (50 µg/mL of Kanamycin) overnight at 37°C for vector (pDONR-CMT) purification. Bacteria glycerol stocks (15% v/v) were prepared from the overnight culture and stored at 80°C.

pDONR-CMT was isolated and purified from host cells by using QIA Spin Miniprep Kit (Qiagen). The purified vectors were prepared for restriction enzyme digestion with *ApaI* (ThermoFisher) and *EcoRV* (ThermoFisher). The digestion mixture consisted of 10 µL (1 µg) of vector, 2 µL of 10X digestion buffer, 0.5 µL of *ApaI*, 0.5 µL of *EcoRI*, and 7 µL of distilled water. The mixture was incubated at 37°C for 45 minutes followed by enzyme inactivation at 65°C for 5 minutes. The mixture was subject to gel electrophoresis (through 1% (w/v) agarose in 1X of Tris-acetate EDTA buffer) to verify the correct size of pDONR-CMT.

LR Recombination

The CMT insert from pDONR-CMT was cloned into a destination vector (pGWF1, see appendices I-b for detail construct) using LR Recombination. pGWF1 contains attR recombination sites flanked between eCFP and Venus gene. LR clonase catalyses the insertion of CMT between eCFP and Venus gene to produce an expression vector (pGWF1-CMT) (Figure 3.3).

The LR reaction mixture consisted of 5 μ L (50 ng) of purified pDONR-CMT, 2 μ L (300 ng) of pGWF1 (Addgene), 4 μ L of 5x LR Clonase reaction buffer (Invitrogen), and 4 μ L LR Clonase enzyme mix (Invitrogen). The mixture was incubated at 25°C for 16 hours. Proteinase K solution (2 μ g/ μ L) (Invitrogen) was added into the mixture followed by incubation for 10 minutes at 37°C. The mixture was then prepared for transformation. Transformation of LR mixture was carried out similar to BP reaction, except 100 μ g/mL of Ampicillin (ThermoFisher) was added into the agar to select the transformant colonies bearing pGWF1-CMT.

pGWF1-CMT was isolated and purified from host cells by using QIA Spin Miniprep Kit (Qiagen). The purified vectors were prepared for restriction enzyme digestion with XbaI and HindIII (ThermoFisher). The digestion mixture consists of 5 μ L (1 μ g) of vector, 2 μ L of 10X digestion buffer, 1 μ L of XbaI, 1 μ L of HindIII, and 11 μ L of distilled water. The mixture was incubated at 37°C for 45 minutes followed by enzyme inactivation at 65°C for 5 minutes. The mixture was then loaded into the gel electrophoresis (1% agarose) to verify the correct size of pGWF1-CMT.

A sample of pGWF1-CMT was sent for sequencing with T7 primers (reverse and forward). The sequencing data were analysed using MEGA7 and SnapGene Viewer software to verify the correct sequence of CMT.

3.3.4 Transformation of pGWF1-CMT and protein expression

The pGWF1-CMT was transformed into *E.coli* BL21 Rosetta 2(DE3) (Merck) for initial expression of the FRET biosensor. The transformation was performed by adding 1 μ L (10 ng) of pGWF1-CMT into 50 μ L of competent cells, then incubation on ice for 10 minutes. The cells were heat-shocked for 30 seconds at 42°C without shaking and immediately placed onto ice. 250 μ L of LB medium was added into the cells and shaken at 37°C for 1 hour. 20 μ L and 100 μ L from each transformation reaction were spread on agar plates containing 100 μ g/mL of Ampicillin (ThermoFisher) and 25 μ g/mL of Chloramphenicol (Sigma Aldrich). The agar plates were incubated overnight at 37°C. Five cell colonies were selected from the agar and grown in

selective LB liquid (100 µg/mL of Ampicillin and 25 µg/mL of Chloramphenicol) overnight at 27°C for inoculation prior to protein expression. Bacteria glycerol stocks (15%) were prepared for cell preservation at -80°C.

The overnight culture was transferred (10% v/v) into a fresh LB liquid supplemented with 100 µg/mL of Ampicillin and 25 µg/mL of Chloramphenicol. Protein expression was induced by adding isopropyl thiogalactoside (IPTG) (0.1 mM final concentration) (Sigma Aldrich). The cells were grown for 24 hours while shaking at 27°C in the dark and then incubated at 4°C for 16 hours to ensure appropriate folding of the fluorophores (Kaper, et.al, 2008). The expression of eCFP and Venus FP inside the host cells was observed using the fluorescence microscope Nikon Eclipse LV 100.

Monitoring of FRET biosensor expression was carried out by sampling the cells at 4 and 20 hours following the IPTG addition. Selection of incubation hours for protein expression was carried out based on the growth curve of *E.coli* in LB media (Mukherjee *et.al*, 2018). 4 hours is a typical condition where the cells were in an early exponential phase, whilst 20 hours is in stationary phase assuming that the most of nutrients have been consumed and target proteins have been produced.

3.3.5 Protein extraction and purification

Cells expressing the FRET biosensor were harvested by centrifugation and resuspended in sonication buffer consisting of 50 mM Tris-HCl pH 8, 500 mM NaCl, and 15% v/v glycerol, 1 mM phenyl methyl sulfonyl fluoride (PMSF) and 1 mg/L of lysozyme (Sigma-Aldrich). Samples were placed on ice, and the sonicator probe (Soniprep 150, MSE) was inserted. Exposure was 7 microns amplitude for 30 seconds with 5 sonication cycles separated by 30 seconds of cooling. Following the sonication process, 0.1 mg/L DNase (Sigma-Aldrich) and 1 mM MgCl₂ were added into the cells and incubated for 30 minutes, followed by centrifuged at 13000 x g for 30 minutes at 4°C.

The FRET biosensor was purified from the cell lysate by using 6xHis-Tag Ni-NTA purification kit (Qiagen). The composition of the binding buffer (NPI-10), wash buffer (NPI-20), and elution buffer (NPI-500) is shown in Appendices II. An Ni-NTA spin column was equilibrated with 600 µL of buffer NPI-10 and centrifuged at 890 x g. The cell lysate was loaded onto the pre-equilibrated Ni-NTA spin column and centrifuged for 5 minutes at 270 x g. The spin column was washed twice with 600 µL buffer NPI-20 and centrifuged for 2 minutes at 890 x

g. The protein was eluted with 300 μ L of buffer NPI-500 and centrifuged for 2 minutes 890 x g. The eluate containing the purified protein was collected and analysed with SDS-Page.

The purified protein was incubated with 15 mM 2-mercaptoethanol (Sigma-Aldrich) for 16 hours at 4°C to produce the reducing conditions needed for metallothionein function. All solutions were degassed with nitrogen to remove dissolved oxygen. The presence of oxygen in the solution can oxidize the metallothionein, resulting in the formation of disulphide bonds, and reduce its binding affinity to metals (Rajamani *et al.*, 2014). Samples were loaded onto a Sephadex G-25 size-exclusion column (Sigma-Aldrich) in 30mM of Tris buffer (pH 8), and the excluded volume containing reduced FRET biosensor was collected for *in vitro* characterisation. The protein concentration was determined by measuring the absorbance at 280 nm using UV-Visible 2600 Spectrophotometer (Shimadzu) (Green and Sambrook, 2012). The measurement was performed using a spectrophotometer with quartz cuvettes (volume of 1 mL).

3.3.6 SDS-PAGE

SDS-PAGE (sodium dodecyl sulphate–polyacrylamide gel electrophoresis) was performed to observe the expression of FRET biosensor by looking at the molecular weight. This section describes the preparation and running of SDS-PAGE gels, followed by staining to detect proteins using Coomassie Brilliant Blue (Green and Sambrook, 2012).

3.3.6.1 SDS-Polyacrylamide gels

The SDS Page gels include 8 ml of resolving gel (10%) and 5 mL of stacking gel (5%) assembled on a glass plate. The components of resolving gel were 2.6 mL of Acrylamide (30%) (Sigma), 2 mL of Lower Tris (1.5 M, pH 8.8), 0.08 mL of SDS (10%), 0.1 mL of Ammonium persulfate (10%) (Biorad), 0.012 TEMED (Biorad), and 3.2 mL of deionised water. The components of stacking gel were 0.67 mL of Acrylamide (30%) (Sigma), 1.25 mL of Upper Tris (1.5 M, pH 6.8), 0.05 mL of SDS (10%), 0.07 mL of Ammonium persulfate (10%) (Biorad), 0.007 TEMED (Biorad), and 3 mL of deionised water. After polymerization was complete, the gel plate was installed in the electrophoresis apparatus. The electrophoresis buffer (Tris-glycine 1X, Appendices III) was added to the top and bottom of the reservoir.

A 40 μ L volume of cell lysate was mixed with 10 μ L of SDS gel loading buffer (5x) (see Appendices III for the composition) and heated for 7 minutes in an 95°C heat block to denature the proteins. The mixture was centrifuged at 12000 x g for 1 minute and the 20 μ L supernatant

was loaded. A voltage of 90 V was applied to the gel for 90 minutes or until the bromphenol blue reached the bottom of resolving gel.

3.3.6.2 Staining and De-staining

The gel was immersed into 50 mL of Coomassie Brilliant Blue stain solution (see Appendix III for the composition) and incubated for 4 hours at room temperature on a rotating platform. The stain solution was removed, and the gel was rinsed with deionised H₂O. The gel was soaked into a 50 mL of destain solution (Appendices II) for 6-8 hours on a rotating platform (the destained solution was changed three times to remove the remaining stain solution). The gel was visualized by using transillumination light and images captured.

3.3.7 *In vitro* characterisation

In vitro characterisation was carried out by measuring the changes in fluorescence signals due to heavy metals binding to the CMT FRET sensor. The metal salts used were obtained from Fisher Scientific: CdCl₂, ZnSO₄, Pb(NO₃)₂, MgCl₂, NaCl and KCl salts (Fisher Scientific) were used as control. Each was prepared as a 0.1M stock solution. Heavy metal binding tests were carried out immediately after the removal of mercaptoethanol from the purified protein solution by a Sephadex G-25 size-exclusion column (Sigma-Aldrich). The fluorescence intensity of FRET biosensor protein in the absence of metals was measured using a spectrofluorometer (Horiba Jobin Yvon - FluoroMax-4, Edinburgh Instruments) as the background signal. In order to check the expression of eCFP and Venus FP, the protein was excited (λ_{ex}) at 435 nm and 510 nm, respectively (Kaper *et al.*, 2008).

Metal solutions were added to the purified FRET sensor protein in a 3mL-cuvette. The final concentration of metals were: 0.1 μ M, 1 μ M, 5 μ M, 10 μ M, 50 μ M, 100 μ M, 500 μ M, 1000 μ M, and 5000 μ M. All experiments were performed in triplicate. The fluorescence intensity was measured immediately by exciting the eCFP (λ_{ex} 435 nm). The emission peaks of eCFP and Venus were determined at 475 and 525 nm, respectively, to calculate the FRET ratio. The ratios (Venus / eCFP) from each heavy metal tested were normalized against purified protein without heavy metal addition. The ratio data were plotted against metal concentration and fitted to a simple binding affinity model (Equation 1) (Sutherland *et al.*, 2012).

$$R = \frac{[M].FRET\ max}{K_a [M]} \quad (1)$$

Where, R is the FRET ratio of biosensor, $FRET_{max}$ is the FRET ratio maximum at saturating metal concentration, M is the heavy metal concentration (μM), and K_a is the half-maximum concentration of metal-binding affinity (μM).

3.3.8 *In vivo* characterisation

E.coli BL21 Rosetta DE3 bearing pGWF1-CMT was recovered from frozen glycerol stocks. The cells were grown in a selective LB liquid (100 $\mu\text{g}/\text{mL}$ of Ampicillin and 25 $\mu\text{g}/\text{mL}$ of Chloramphenicol) (Sigma-Aldrich) overnight at 27°C. The overnight culture was transferred (10% v/v) into a fresh LB liquid supplemented with 100 $\mu\text{g}/\text{mL}$ of Ampicillin and 25 $\mu\text{g}/\text{mL}$ of Chloramphenicol. Protein expression was induced by adding IPTG (0.1 mM final concentration). The cells were grown for 24 hours while shaking at 27°C in the dark and then incubated at 4°C for 16 hours.

Cells expressing the FRET biosensors were harvested by centrifugation and re-suspended with Heavy Metal MOPS medium (HMM). This medium was formulated by Larossa *et al* , 1995 which consists of 5 mM MOPS (3-(N-morpholino) propanesulfonic acid) (Sigma-Aldrich), 50 mM KCl, 10 mM NH_3Cl , 0.5 mM MgSO_4 , 0.4% glucose, and 1 mM glycerol-2-phosphate (Sigma-Aldrich). The pH of medium was adjusted to 7 using NaOH.

In vivo tests were carried out by adding different concentrations of metal solution into a cell suspension of optical density (OD) 0.5 in a 3 mL cuvette. OD 0.5 was selected because the fluorescence emission from OD cells of 1 and 2 showed a high background noise signal in which the emission peak of eCFP and Venus FP cannot be distinguished clearly (data not shown). Fluorescence intensity measurement with high OD cells (above 1) can potentially reduce the accuracy of measurement. Therefore, all *in vivo* experiment was carried out by diluting the cell suspension to lower OD prior to heavy metals addition.

The OD was measured using a spectrophotometer (wavelength: 600nm) in a 3 mL-cuvette. The final-OD of host cells suspension in HMM media was set to 0.5. This was carried out by measuring the original OD prior to centrifugation and using this OD value to calculate the dilution volume. Following the centrifugation, the cell pellets were resuspended with a proportion volume of HMM media to achieve the final OD 0.5.

The final concentrations of metal were as follows: 1 μM , 10 μM , 100 μM , and 1000 μM . The cells were excited at 435 nm and the fluorescence emission was measured after 2 hours incubation using a spectrofluorometer (Horiba Jobin Yvon - FluoroMax-4, Edinburgh Instruments). All experiments were performed in triplicate.

Data analysis and graphing of the emission spectra were carried out using Origin (OriginLab Corporation). The FRET ratio was calculated by dividing the emission peak of Venus FP by eCFP (525/475 nm). A significant reduction in FRET ratio signal at particular concentration was calculated Student t-test, with a p value < 0.05.

Analysis and graphing of metal-induced FRET signal was calculated using R version 3.52 (R core Team 2018). The FRET ratios were normalized against values from host cells without heavy metal addition, plotted against metal concentrations and fitted to a simple binding affinity model (Equation 1). Parameters of apparent K_a (half maximum metal binding affinity) and apparent FRET maximum were derived from the fitted model to determine host cell response to metal exposure. Comparison between metal-induced FRET signals *in-vitro* and *in-vivo* was made in which the difference was calculated using a One-way ANOVA with a significant level $p < 0.05$.

Analysis using the ANOVA test can determine the influence that independent variables (test condition of the FRET biosensor) have on the dependent variable (heavy metals Cd, Pb, and Zn). In this case, the mean value of FRET signals from two groups of measurements (*in-vitro* and *in-vivo*) from each heavy metal was tested to see if there was a difference between them. ANOVA can test more than one treatment is a major advantage over other statistical analyses such as t-test. ANOVA opens many testing capabilities such as the analysis of variance and treatment conditions (factor). F-ratio is used as its significance statistic which is variance because it is impossible to calculate the sample means difference with more than two samples. Furthermore, this enables us to see how effective two different types of test conditions are and how durable they are. ANOVA test assumes that the population sample must be normal, the observations must be independent in each sample, and the samples have homogeneity of variance.

3.4 Results

3.4.1 Vector construct

CMT gene

The chicken metallothionein gene was synthesised with the recombination sites *attB1* and *attB2* at each end, giving a DNA sequence of 254 bp (204 bp CMT and 2 x 25 bp *att* sites) (Figure 3.4). The gene was amplified in a PCR reaction using primers complementary to the *attB1* and *attB2* sites with the addition of 4 G residues at their 5' end. Figure 3.5 shows the amplification product of *attB1*-CMT-*attB2* gene. The bands in lane 1 and 2 were of the expected size. Lanes 3 and 4 are negative amplification controls.

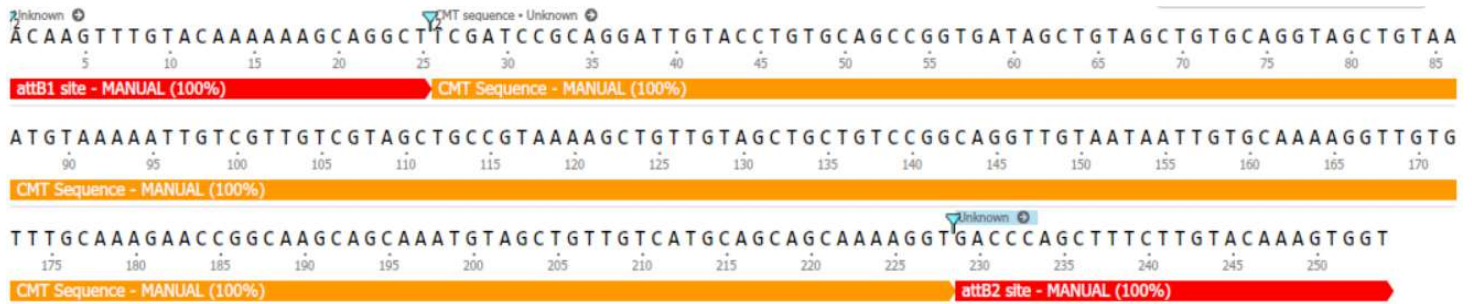


Fig. 3.4 Sequence of *attB1* -CMT-*attB2* (254 bp). CMT sequence is shown in yellow colour flanked by two *attB* sites (red).

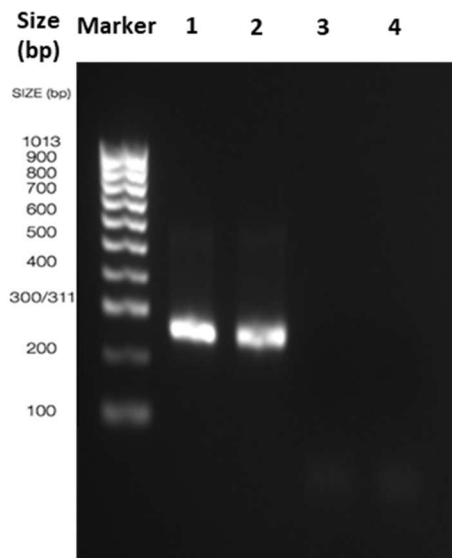


Fig. 3.5 Agarose gel (1.5%) of PCR amplification product using *attB*-primers. Lane 1 and 2: *attB1*-CMT-*attB2* (254 bp); lane 3 and 4: control negative

Entry vector and expression vector

The PCR fragment *AttB1-CMT-attB2* was cloned by BP recombination into the donor vector pDONR (Appendices I). The resulting vector (pDONR-CMT) contained an *attL1-CMT-attL2* insert allowing recombination of CMT fragment into a destination vector (Figure 3.6).

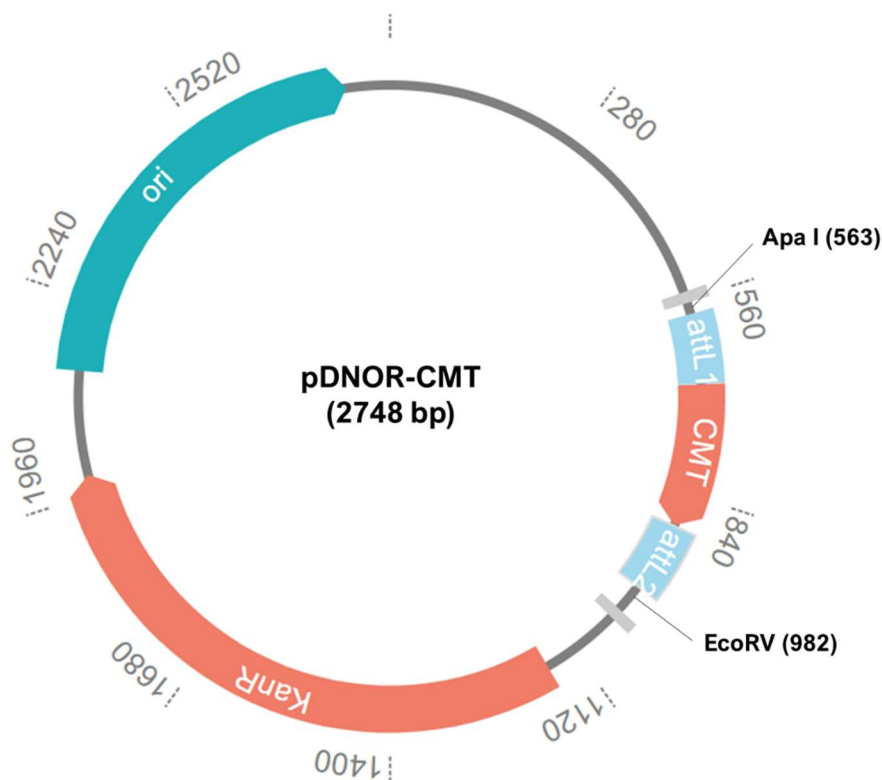


Fig. 3.6 The map of pDONR-CMT encoding *attL1-CMT-attL2* gene as an insert generated from BP recombination. *KanR* is a gene encoding kanamycin resistance for selection of transformant colonies. *Ori* is a gene for plasmid replication.

The pDONR-CMT construct was verified by restriction enzyme digestion with *Apa*I and *Eco*RV producing fragments (Figure 3.7) of approximately 2300 bp and 410 bp as expected. pDONR-CMT was used as an entry vector for cloning the *CMT* insert into the destination vector (pGWF1) (see Figure 3.3 for detailed steps).

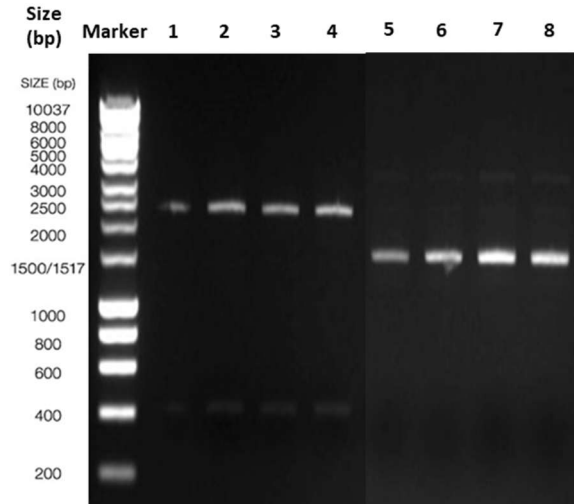


Fig. 3.7 Agarose gel (1%) of pDONR-CMT (2753 bp) digested with *Apa*I and *Eco*RV. Lane 1-4: approximately 2330 bp fragments and 410 bp fragments, lane 5-8: control negative (without the restriction enzyme).

The *CMT* was cloned into pGWF1, generating the expression vector pGWF1-CMT. This construct was verified by restriction enzyme digestion with *Xba*I and *Hind*III located at 224 and 3499 bp, respectively (Figure 3.9). Restriction fragments of the expected size were observed by gel electrophoresis (1827 bp and 2712 bp) (Figure 3.8). pGWF1-CMT without restriction enzyme digestion showed bands indicating the presence of supercoiled, nicked, or open circle vectors.

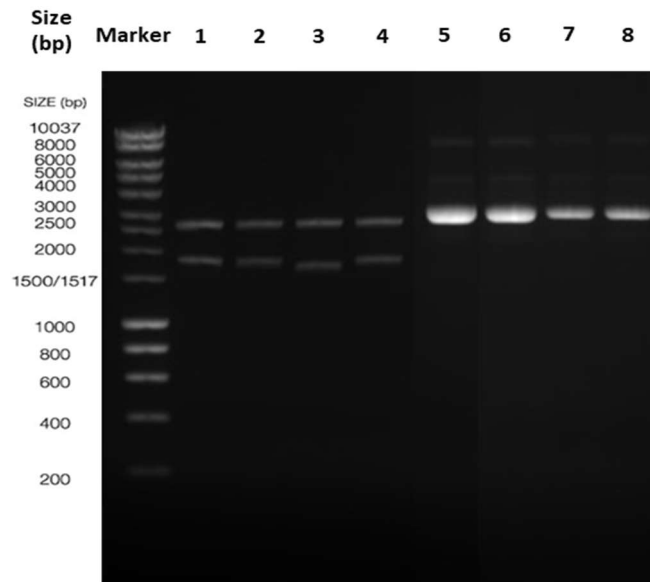


Fig. 3.8 Agarose gel (1%) of pGWF1-CMT (4540 bp) digested with *Xba*I and *Hind*III. Lane 1-4: 2712 bp and 1827 bp, lane 5-8: control negative (without addition of restriction enzyme).

The genetic map of expression vector pGWF1-CMT is shown in Figure 3.9. This vector allows high levels of IPTG-inducible gene expression from the T7 RNA polymerase promoter. The inclusion of a 6xHis-Tag on the N-terminus allows purification of the expressed protein by Nickel affinity chromatography. *eCFP-CMT-Venus* gene encodes the FRET biosensor as a fusion of metallothionein/CMT with eCFP and Venus FP. A T7 terminator sequence is located downstream of *eCFP-CMT-Venus* gene which marks the end of gene transcription. Ampicillin resistance gene is used as a selection marker. Sequencing showed the CMT gene was in-frame between eCFP and Venus genes and oriented correctly.

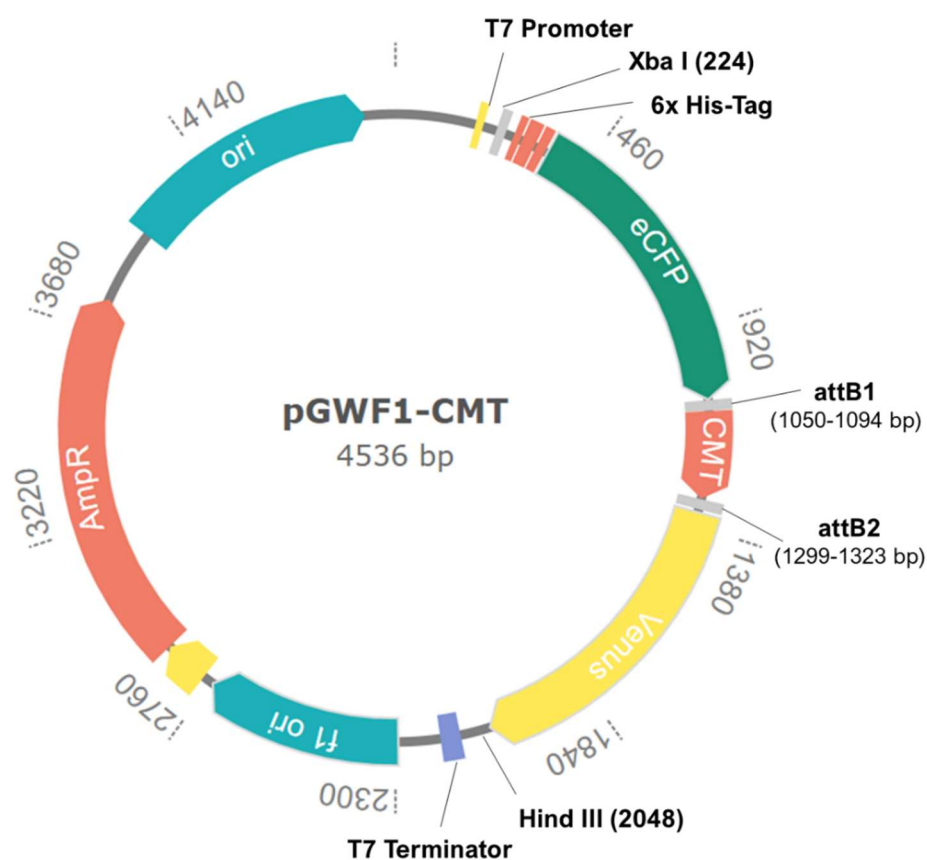


Fig. 3.9 The map of pGWF1-CMT encoding *eCFP-CMT-Venus* gene to produce the FRET biosensor. Important features for protein expression in *E.coli* host cell are: *T7 promoter* as a binding site for RNA polymerase located upstream of the insert, *T7 terminator* as the end of transcription site, *ori* for plasmid replication, and *AmpR* gene encodes ampicillin resistance gene for selection of cells bearing this plasmid.

3.4.2 Protein expression

The codon-optimised CMT sequence was translated to its corresponding amino acid sequence (Figure 3.10). It contains 20 cysteines (C) residues responsible for heavy metal binding via thiolate sulphur ligand interaction.

```
>EMBOSS_CMT_+3
DPQDCTCAAGDSCSCAGSCKCKNCRCSRKSCCSCPAGCNCNCAKGCVCKEPASSKSCCHAAAKG
```

Fig. 3.10 Amino acid sequence encoded by the CMT gene. The cysteine (C) residues are highlighted in yellow.

When the CMT-FRET sensor was extracted from the host cells, the cysteine residues were oxidized, leading to the formation of disulphide bonds, which reduced the affinity for metals. Therefore, the protein were incubated with 15 mM of mercaptoethanol to reduce the Cys residues and improve the affinity for metals (Suzuki and Maitani, 1981 and Rajamani *et al.*, 2014). This replicates the reducing conditions inside the host cell.

The expression of *eCFP-CMT-Venus* gene in *E.coli* BL21 Rosetta DE3 host cell was examined 4 and 20 hours after IPTG addition. The proteins were extracted by sonication followed by HisTag purification and applied to an SDS-PAGE gel. The molecular weight of recombinant protein of the FRET biosensor was expected at 61 kD. SDS page results showed the molecular weight was observed at molecular weight ~62 kD (Figure 3.11). Level of expression at 20 hours were higher than 4 hours. Therefore, the host cells were harvested 20 hours after IPTG addition.

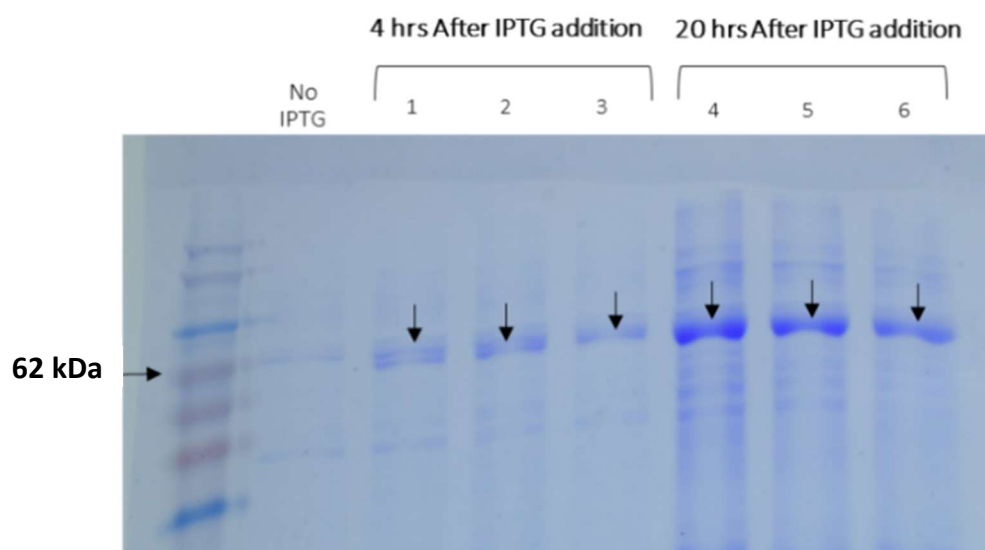


Fig.3.11 SDS PAGE analysis of proteins expressed from pGWF1-CMT vector in *E.coli* BL21 Rosetta 2(DE3) host cell (after HisTag purification). The molecular size of FRET biosensor protein is approximately 61 kDa as shown in the figure. The level of expression is higher at 20 hours after IPTG addition.

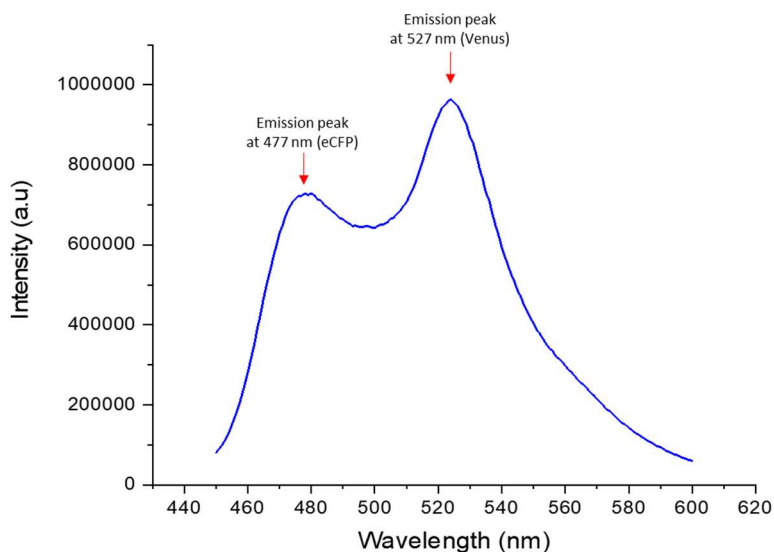


Fig.3.12 Emission spectra of the purified FRET biosensor in reducing conditions (protein concentration: 575 nM) with eCFP excitation at 435 nm.

The fluorescence emission spectrum of the purified FRET biosensor in reducing condition is shown in Figure 3.12. Excitation at 435 nm was chosen to study the energy transfer between eCFP and Venus with the least possible direct excitation of Venus while maintaining high eCFP excitation efficiency. Two emission peaks at 475 and 525 nm were observed, corresponding to emission signals of eCFP and Venus (Kaper *et al.*, 2008).

3.4.3 Heavy metal binding *in vitro*

To characterize the response of FRET biosensors to heavy metals, the purified sensors were tested with various concentrations of Pb^{2+} , Cd^{2+} , and Zn^{2+} . eCFP was excited at 435 nm immediately following the heavy metal addition. The emission spectra of eCFP and Venus for each metal concentration tested are shown in Figure 3.13 (A, B, C) below. Changes in the emission spectra of eCFP and Venus were observed after heavy metal exposure. There was a concentration-dependent increase in FRET ratio (525 nm / 425 nm). The increase in FRET ratio was observed over the concentration range 0.1 – 100 μM for Pb^{2+} , 1-1000 μM for Cd^{2+} , and 1 – 1000 μM for Zn^{2+} .

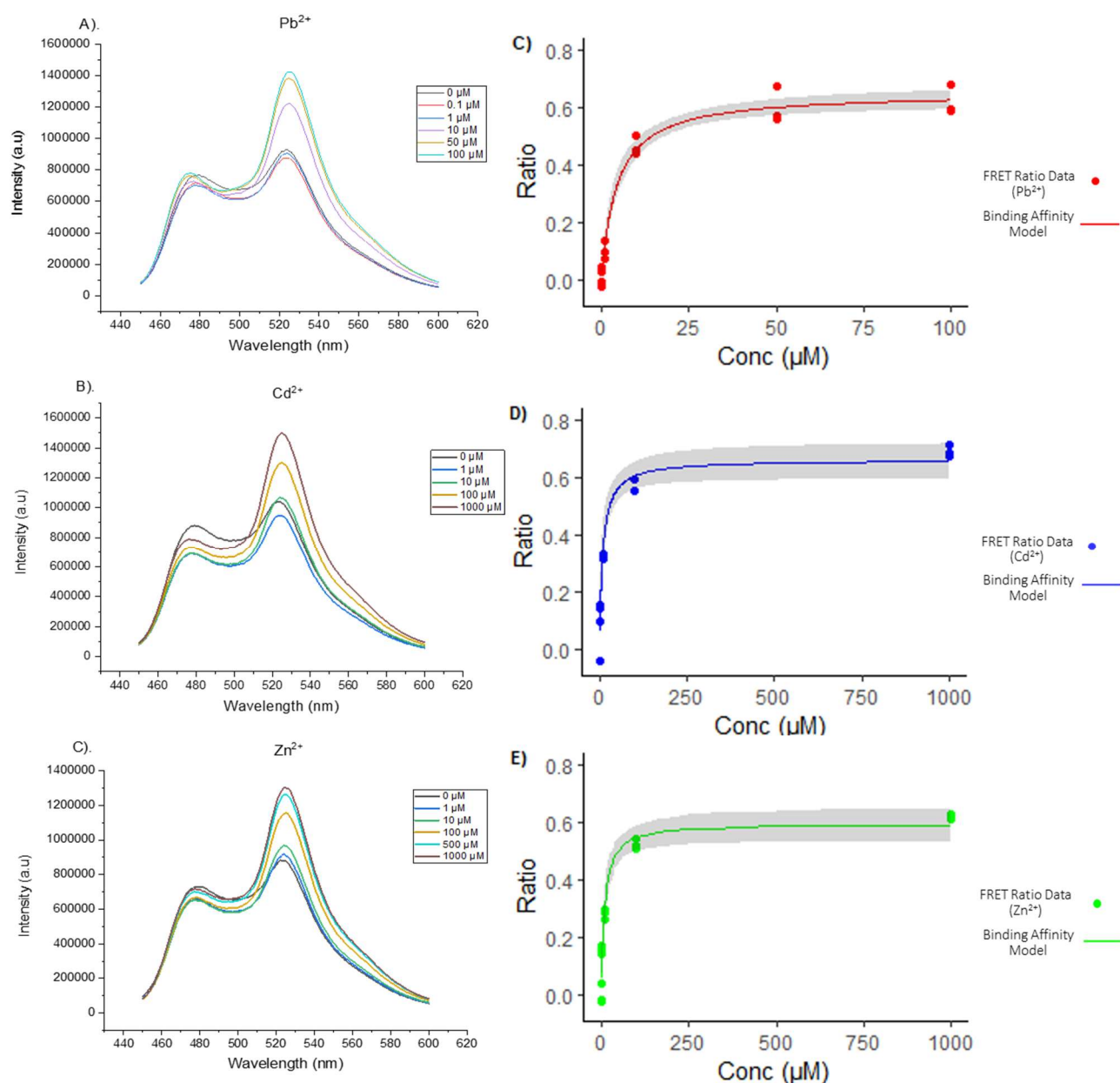


Fig. 3.13 Changes in emission spectra of the FRET biosensors (*in vitro*) after the addition of Pb^{2+} (A), Cd^{2+} (B), and Zn^{2+} (C). Ratio of Venus/eCFP (525 nm/425 nm) against heavy metal concentration, fitted to a simple binding affinity curve based on Equation 1 (C, D, E). The FRET ratio data were normalized to 0 by subtracting the mean value in the absence of heavy metals. Measurements were made in triplicate (n=3).

The plot of FRET ratio against heavy metal concentrations was fitted to a simple binding affinity model (Equation 1) and followed a rectangular hyperbola curve (Figure 13 C, D, and E). The curve fitting assumed that the binding of metals occurred in a non-cooperative manner, in which the parameters describing the half-maximum binding concentration (K_a) and FRET maximum values were estimated (Table 3.1). The K_a values for Pb^{2+} , Cd^{2+} , and Zn^{2+} are $4.55 \pm 0.78 \mu M$, $9.44 \pm 2.4 \mu M$, and $9.47 \pm 2.14 \mu M$, respectively (Table 1). The values are different

because the CMT has different affinities to each metal. These results show that the binding concentration in metal solution was higher for Pb^{2+} , followed by Cd^{2+} , and Zn^{2+} (i.e. $\text{Pb} > \text{Cd} > \text{Zn}$). The maximum FRET ratio was obtained at the following saturating concentrations: 0.6 ± 0.01 at $50 \mu\text{M}$ for Pb^{2+} , 0.66 ± 0.02 at $1000 \mu\text{M}$ for Cd^{2+} , and 9.47 ± 2.14 at $1000 \mu\text{M}$ for Zn^{2+} . The maximum FRET ratio of Pb^{2+} was achieved at a lower saturating concentration than Cd^{2+} and Zn^{2+} , suggesting a greater sensitivity to Pb^{2+} .

The FRET biosensor was tested with other ions not known to bind with CMT, as a negative control. Figure 3.14 shows the emission spectra of FRET biosensors after the exposure to Na^+ , Mg^{2+} , and K^+ . Changes in the emission signals at 475 nm (eCFP) and 525 nm (Venus) were not apparent, indicating that the FRET biosensor was not responsive to these ions.

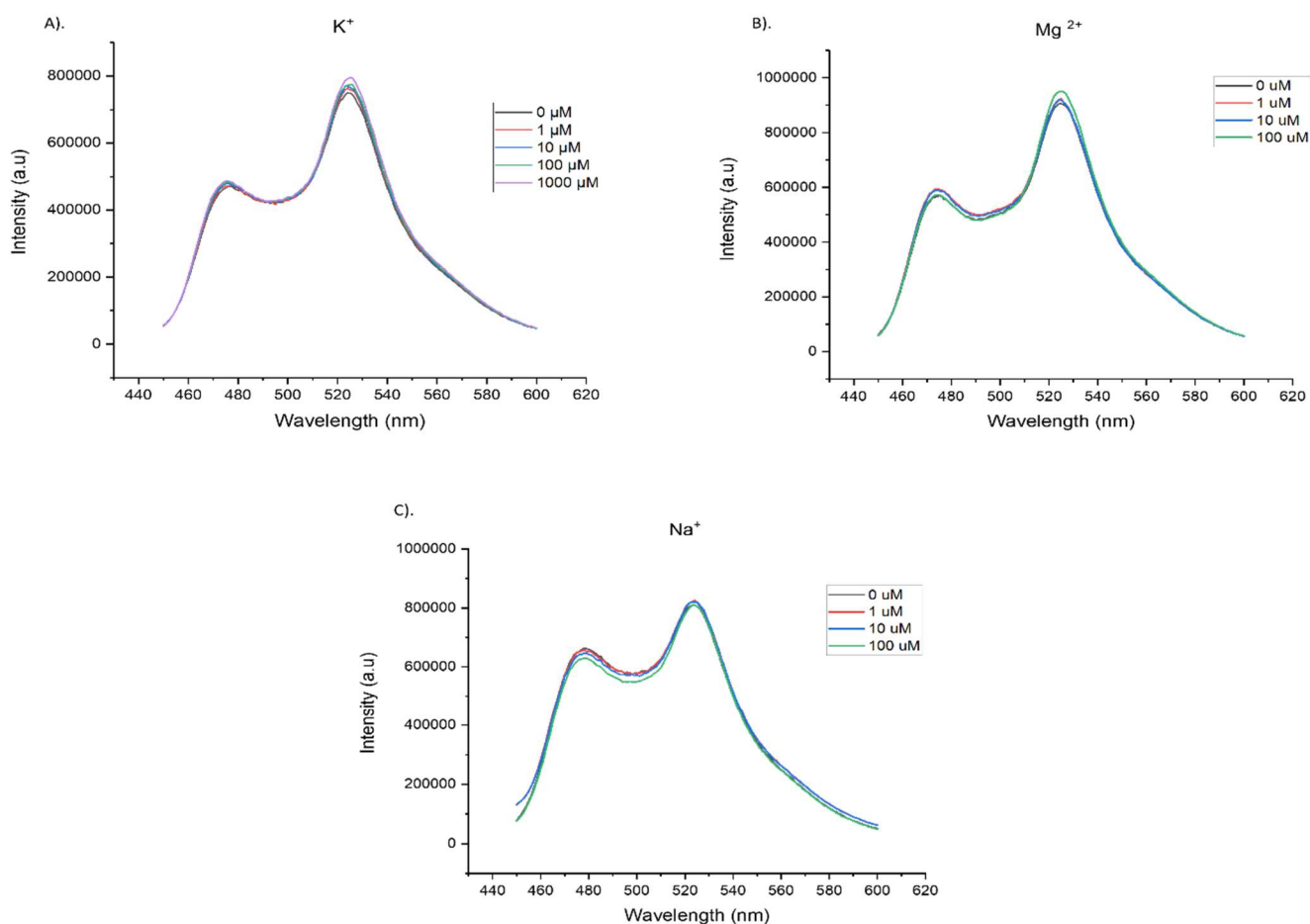


Fig. 3.14 Emission spectra of the FRET biosensors (*in vitro*) after exposure to K^+ (KCl salt) (A), Mg^{2+} (MgSO_4) (B), and Na^+ (NaCl) (C). The FRET biosensors showed no response to these ions.

3.4.4 Heavy metal binding *in vivo*

In vivo tests were carried out by adding heavy metals to *E.coli* BL21 Rosetta 2(DE3) cells expressing the FRET biosensor and the emission spectra measured at intervals. Changes in eCFP and Venus FP emission spectra inside the cells were observed in response to heavy metals (Figure 3.15). The ratio of Venus/eCFP (525/475 nm) was calculated and plotted against the metal concentration (Figure 3.15.B).

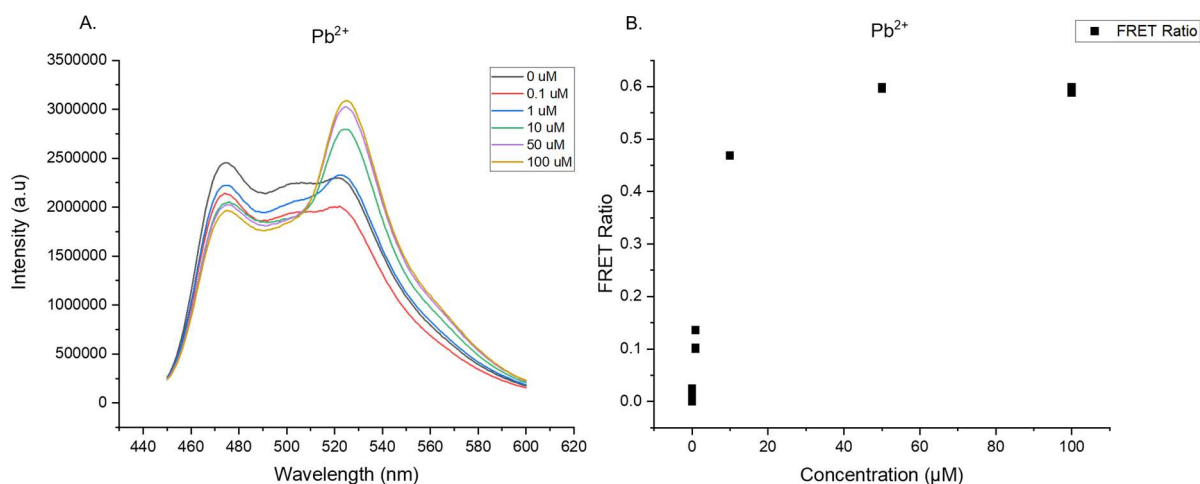


Fig 3.15. Changes in emission spectra of the FRET biosensor inside *E.coli* BL21 Rosetta 2(DE3) cells exposed to different concentrations of metal (Pb^{2+}). Emission peaks at 475 nm and 525 nm indicate the signals of eCFP and Venus FP, which can be calculated to measure the FRET ratio in response to metals (B). The ratio of Venus FP/eCFP were plotted against metal concentration. A reduction in FRET signal was observed at 100 μM . The measurement was carried out using a spectrofluorimeter with 3 replication ($n=3$).

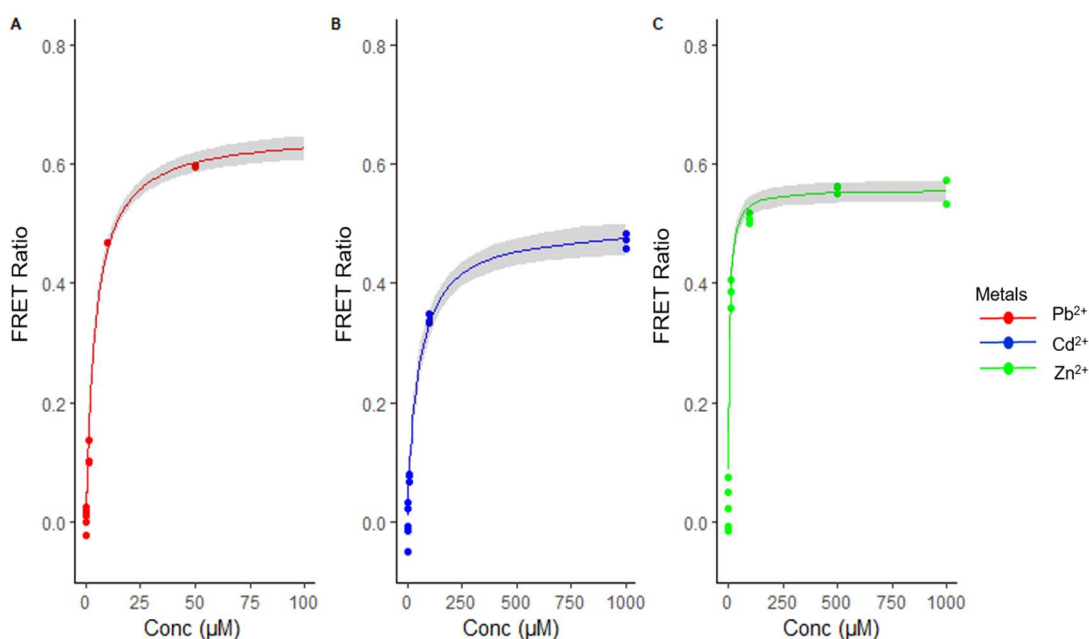


Fig. 3.16 Ratio of Venus/eCFP (525 nm/425 nm) in response to heavy metal binding inside *E.coli* BL21 Rosetta 2(DE3) cells. The FRET ratio plot against metal concentrations fitted a simple binding affinity curve based on Equation 1. The FRET ratio data were normalized to 0 by subtracting the mean value in the absence of heavy metals. Measurements were made in triplicate ($n=3$). Note the different concentration scales for the metals.

Similar to the *in-vitro* FRET analysis, the parameters describing the apparent K_a and FRET maximum values inside the cells were estimated by curve fitting (Figure 3.16) using the simple binding affinity model (Eq.1). The apparent K_a for Pb^{2+} , Cd^{2+} and Zn^{2+} are $4.27 \pm 0.30 \mu M$, $50.56 \pm 6.55 \mu M$, and $5.41 \pm 0.53 \mu M$, respectively (Table 3.1). These values indicate that the range of binding concentrations inside the host cell were lower for Pb^{2+} , followed by Zn^{2+} , and Cd^{2+} . The FRET max ratio was achieved in response to Pb^{2+} at $50 \mu M$, whereas Cd^{2+} and Zn^{2+} exhibited the max ratio at $1000 \mu M$. This suggests that the concentration of Pb^{2+} inside the cell was much lower than Cd^{2+} and Zn^{2+} , which was possibly caused by the different cellular responses to these metals.

Comparison of *in vitro* and *in vivo* binding

Figure 3.17 compares the metal-induced FRET signals *in vitro* and *in vivo*. The results showed that the binding model for Cd^{2+} and Zn^{2+} inside the cell were significantly different to the outside (ANOVA, $p < 0.05$), except for Pb^{2+} ($p > 0.05$). The value of K_a defines the range of binding concentrations, in which the concentration of Pb^{2+} was not significantly different inside and outside the cell. The K_a value for Cd^{2+} was higher inside the cell compared to outside. In contrast, the value for Zn^{2+} was lower inside the cell than outside. These results showed that the FRET biosensors detected different concentrations of heavy metals when the sensors were present inside the cell (*in-vivo*) and outside the cell (*in-vitro*). This difference was potentially caused by the mechanisms of host cell to regulate metal uptake from the outside and passed through the cell membrane to enter the cytoplasm. As a result, the number of metals inside the cell will always be lower than outside the cell.

The values of FRET max for Cd^{2+} and Zn^{2+} were lower inside the cell compared to outside. This revealed that the metal concentration that went into the cell and detected by the FRET biosensor was not the same as that outside, indicating the measurement of metals bioavailability.

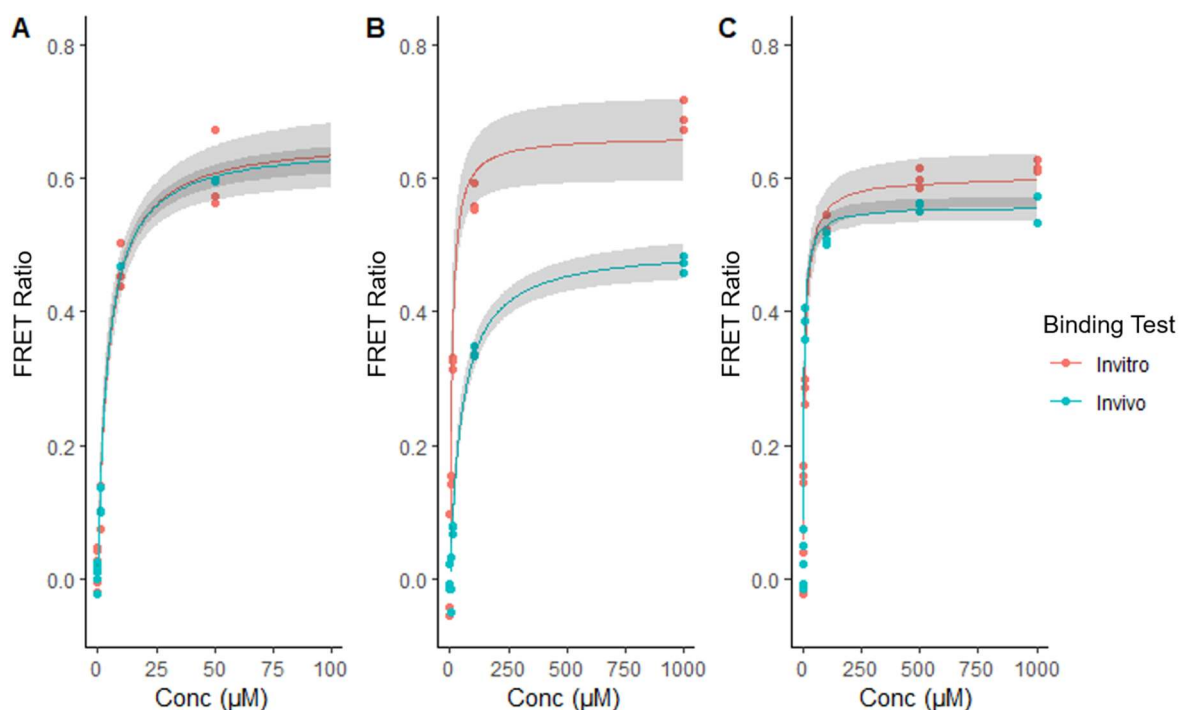


Fig 3.17. Comparison of *in vitro* and *in vivo* binding to Pb²⁺ (A), Cd²⁺(B), and Zn²⁺(C). The dots represent the FRET ratio data obtained from each metal concentration; the straight line shows the curve fitting based on a simple binding affinity model.

Table 3.1. The parameters of apparent K_a and FRET maximum estimated from the curve fitting describing the binding sensitivity of the FRET biosensor to *In-vitro* and *In-vivo* inside *E.coli* BL21 Rosetta 2(DE3). FRET measurement was carried out using a spectrofluorimeter. Differences in the binding affinity model of metals with CMT between *in-vitro* and *in-vivo* tests were calculated using One-way ANOVA (significant level was quoted as 95% confidence level ($p < 0.05$)).

Heavy Metals	Parameters	Estimate \pm Std.Error		Difference in the binding model for each metal between <i>In-vitro</i> and <i>In-vivo</i>
		<i>In-vitro</i>	<i>In-vivo</i>	
Pb	K_a	4.55 ± 0.78	4.27 ± 0.30	$p > 0.05$
	FRET max	0.66 ± 0.02	0.65 ± 0.01	
Cd	K_a	9.44 ± 2.41	50.56 ± 6.55	$p < 0.05$
	FRET max	0.66 ± 0.02	0.49 ± 0.01	
Zn	K_a	9.47 ± 2.14	5.41 ± 0.53	$p < 0.05$
	FRET max	0.60 ± 0.01	0.55 ± 0.008	

3.5 Discussion

A FRET-based heavy metal biosensor has been developed from an expression vector compatible with protein production in the *E.coli* BL21 Rosetta 2(DE3). The vector construction was facilitated by phage λ (Gateway) recombination, which efficiently transferred the *CMT* gene in framed between eCFP and Venus FP genes. Induction with IPTG enabled a high expression of the biosensor, which can be used to characterise the FRET signals in response to the heavy metal binding inside and outside the cell.

3.5.1 In-vitro binding

Direct exposure of the purified protein sensors to Pb^{2+} , Cd^{2+} , and Zn^{2+} resulted in decreased eCFP emission and increased Venus FP emission compared to the absence of these metals (Figure 3.13). This indicates the energy transfer occurred from the eCFP (donor) to Venus FP (acceptor) due to the binding of metals on the CMT. The increase in FRET ratio depended on the metal concentrations in the solutions, which can be interpreted using a simple binding affinity model (Equation 1) to estimate the binding affinity of the FRET biosensor. CMT as a sensing domain of the FRET biosensor contains 20 Cys residues responsible for binding with metals. Under a free metal condition, the CMT forms a disordered structure. In a condition where metals are bound, the thiols from each Cys residue coordinate the metal binding, resulting in CMT rearrangement to be a well-defined protein fold structure (Romero-Isart and Vasak, 2002). This conformational change caused the distance between eCFP and Venus in close proximity and enhanced the energy transfer from donor to acceptor protein.

The analysis of half-maximum binding affinity (K_a) and FRET maximum values (Table 3.1) revealed the sensitivity of the FRET biosensor was the highest for Pb^{2+} , followed by Cd^{2+} and Zn^{2+} ($\text{Pb}^{2+} > \text{Cd}^{2+} > \text{Zn}^{2+}$). This trend is consistent with the finding from Rajamani *et al.* (2014), in which the sensitivity of the FRET biosensor using the similar CMT was greatest to Pb^{2+} and Cd^{2+} , but lower to Zn^{2+} .

Initial sequence of CMT was produced based on eukaryotic expression system (Rajamani *et al.* 2014), however; in the current experiment, the CMT sequence have been optimised for bacteria cell expression. The results have shown that the optimised CMT did not change the order of sensitivity (Pb^{2+} , Cd^{2+} , and Zn^{2+}), and the function of the FRET biosensor was consistent between these metals regardless the difference in host cell expression systems (*E.coli* and microalgae). FRET biosensor constructed by Rajamani *et al.*, 2014 utilised the CFP and YFP as acceptor and donor fluorescent proteins, respectively. In the current experiment, eCFP and Venus FP were used as acceptor and donor fluorescent proteins. eCFP is a mutant version of

CFP (Ser 66), whilst Venus FP is a mutant of YFP (Phe 46). The combination of eCFP and Venus FP as FRET offers some benefits such as longer fluorescence lifetime, less sensitivity to changes in pH or salts, and more photostable (Zaccolo, 2004; Kremers *et al.*, 2006; Bajar, *et al* 2016).

3.5.2 In vivo binding

This research has demonstrated the use of FRET biosensor to measure Pb^{2+} , Cd^{2+} , and Zn^{2+} inside *E.coli* BL21 Rosetta 2DE3. The emission ratio of Venus/eCFP within the host cells increased following exposure to the heavy metals. The apparent K_a and FRET maximum values (Table 3.1) revealed that the binding concentration inside the host cell was lower for Pb^{2+} compared to Cd^{2+} and Zn^{2+} . Likewise, the apparent FRET maximum values indicated that a lower saturating concentration for Pb^{2+} (50 μ M) than Cd^{2+} and Zn^{2+} (1000 μ M). Pb^{2+} is considered as a toxic metal even at low concentration. This metal can bind to various biomolecules ranging from proteins, enzymes, and DNA. Pb^{2+} can interact with cellular proteins by mimicking the physiological effects of divalent metals such as Zn^{2+} in zinc finger proteins. The replacement of Zn^{2+} with Pb^{2+} in a protein or enzyme will diminish the protein function and disturb the cellular process (Cangelosi *et.al*, 2014).

The apparent FRET maximum values indicated that the saturating concentrations for Cd^{2+} and Zn^{2+} are much higher (20-times) than Pb^{2+} (Figure 16, Table 3.1). Metal concentrations above the max values are attributed as toxic levels, in which the host cell can no longer maintain cytoplasmic metal concentrations. In this condition, the metals did not meet physiological requirements and potentially caused cellular damage.

Cadmium is considered a highly toxic and non-essential metal (Silver and Phung, 2005); however, the *E.coli* cell in this study showed the maximum FRET signals in the exposure to 1000 μ M of Cd^{2+} . This might result from cellular mechanisms through the role of efflux transporter ATPases (Binet and Poole, 2000) and potentially the function of cadmium adsorption protein. According to Qin *et al.* (2017) the *E.coli* BL21 (DE3) strain contained a fragment of cadmium resistant gene (*capB*) located at the lambda phage DE3 region in its genome. The overexpression of *capB* protein occurred due to exposure of the cell to 50 μ M of Cd(II). This protein plays an important role in absorbing and removing intracellular Cd^{2+} .

The FRET signals inside the cell reached saturation in the exposure to 1000 μ M of Zn^{2+} . Zinc homeostatic in *E.coli* is regulated by the uptake and efflux transporters across the cell membrane. Extracellular zinc ions are accumulated into the cytoplasm through the ZnuABC transporter (Patzner and Hantke, 1998). When the saturated Zn^{2+} was reached inside the cell, the

excessive Zn^{2+} will activate a regulatory protein (Zur) to repress the transcription of *znuABC* gene to stop the metal accumulation. Conversely, another regulatory protein (ZntR) can induce the expression of ZntA efflux transporter to remove Zn^{2+} from the cytoplasm. Brocklehurst *et al.* (1999) reported the ZntA protein was highly expressed in *E.coli* TG1 strain due to Zn(II) exposure at 500 – 1000 μ M. This mechanism may have happened in *E.coli* host cell in the current experiment, which enabled the cell to survive in 1000 μ M of Zn^{2+} exposure.

3.5.3 Comparison of heavy metal binding *in vitro* and *in vivo*

The range of metal concentrations bound to the FRET biosensor inside the cell were not the same as it was outside in metal solution. The evidence of this can be seen in Figure 4.17 showing the curve of *in vivo* shaped rectangular hyperbolic similar to *in vitro* measurement. This means that the FRET biosensor behaved the same in terms of binding heavy metals in a non-cooperative manner. The same curve patterns can be evidence that the FRET biosensor measured metal doses inside the cell depending on the metal concentrations outside in which the cells are being exposed. The signals of the FRET biosensor when present inside the cell (*in vivo*-blue line) are lower than signals when the sensors were present outside the cell (*in vitro*). This indicates the concentration of metals detected inside the cell was lower than outside the cell as expected.

There are several possible reasons for the reduced intracellular metal concentrations relative to the external concentrations. These are: (1) The outer membrane material of the host cell may sequester some fractions of metals. The extracellular surface of gram negative bacteria cells contains negatively charged functional groups such as carboxyl, hydroxyl, sulfhydryl, and phosphate, which provide binding sites for cations at neutral pH (Diep *et.al*, 2018). Only some metals that passed through the outer and inner membrane can accumulate in the cell. (2) Once inside the cytoplasm, these heavy metals could form complexes with cellular components, such as organic molecules or proteins containing cysteine residues. This can potentially influence the amount of metal that is sensed by the FRET biosensors.

In the case of Pb^{2+} , it seems that the cell membrane barrier did not significantly affect the concentration of metal uptake from the solution into the cytoplasm; hence the metal can be easily detected by the FRET biosensor. Pb^{2+} may enter bacteria cells by various mechanisms, including diffusion through cell membrane or passing through the uptake and transport pathways of essential metal ions, particularly Zn^{2+} and Ca^{2+} (Martinez-Finley *et al.*, 2012).

Unlike Pb^{2+} , the mechanisms of Cd^{2+} and Zn^{2+} uptake are different and have been well characterised. *E.coli* has developed resistance mechanisms to these metals, particularly at the

cell membrane level. An ABC-type transporter, ZnuABC, and ZntA and periplasmic protein ZraP have been known responsible for Zn²⁺ uptake and efflux (Noll, et al, 1998; Binet and Poole, 2000). Two P-type ATPases (CadA1 and CadA2) are responsible for the Cd²⁺ transport system on *E.coli* cell membrane (Hynninen, 2010). These systems may explain the reason why the FRET biosensors detected lower concentrations of Cd²⁺ and Zn²⁺ inside the cell compared to outside the cell.

3.5.4 Comparison with other FRET-based metal biosensors

Results in this study showed the detection limit of the FRET biosensor using a CMT sensing domain were 4.55 µM for Pb²⁺, 9.44 µM for Cd²⁺, and 9.47 µM for Zn²⁺. Other studies have developed two different types of FRET biosensors: for Pb sensing ; Met-lead 1.59 (Chiu and Yang, 2012), and Cd sensing; Met-cad 1.57 (Chiu *et al.*, (2013)). These two FRET biosensors exhibited a lower detection limit compared to FRET Biosensor using CMT in the current research. A Met-lead 1.59 FRET biosensor is a fusion of Pb binding protein (pbrR) from *Cupriavidus metallidurans* between eCFP and Venus. *In vitro* properties of this biosensor indicated that the affinity for Pb²⁺ was 69 nM, which is 60-fold more sensitive than results (4.55 µM) found in the current study. Another FRET biosensor (Met-cad 1.57) which contains a fusion of Cd-binding protein (CadR) with a pair of eCFP and Venus, showed an apparent affinity of 250 nM for Cd²⁺, which is also 40-fold more sensitive than the value (9.44 µM) in the current research. The differences in detection limit can be attributed to the metal binding affinity of the sensing domains.

Unlike CMT, the protein structure of pbrR and CadR contain fewer Cys residues. Single metallothionein from vertebrates, such as CMT contains 20 Cys residues which can provide binding sites for seven metals (Sutherland, *et.al*, 2012), whereas one pbrR or cadR molecule contains 3 Cys residues which are responsible for binding one metal (Lee, *et al*, 2001; Chen *et al.*, 2007). pbrR and CadR are originally protein regulators that can be activated due to binding with Pb²⁺ and Cd²⁺, respectively. These proteins control the transcription of metal resistance genes in prokaryotic cells. In contrast, CMT functions in storing and detoxifying metals within animal cells and bind to a larger amount of heavy metals than pbrR or cadR.

However, the application of pbrR and CadR as a component of FRET Biosensor is limited in terms of the specificity. These FRET biosensors can only be used for detecting specific metal such as for measuring the toxic effect of either Pb or Cd only in the host cells (Chiu and Yang, 2012). Their selectivity is limited to a single metal species; therefore, they are inconvenient for the application in an environment where multiple metal ion species are present. The use of

metallothionein as a sensing domain in the FRET biosensor enables the measurement of toxicity effects from a group of metals (Pb, Cd, and Zn).

3.6 Conclusion

The *eCFP-CMT-Venus* gene encoding the FRET biosensor has been constructed in an expression vector (pGWF1-CMT), which is compatible for expressing the sensor protein in *E.coli*. The FRET biosensor consists of CMT as a sensing domain fused between eCFP (donor) and Venus FP (acceptor). Excitation of eCFP at 435 nm resulted in the emission peak of eCFP at 475 nm and Venus FP at 525 nm, which can be used to calculate the FRET ratio corresponding to metal concentrations. *In vitro* characterisation of the purified biosensor showed the changes in FRET ratio due to heavy metal binding on CMT. Estimates of half-maximum binding (K_a) and FRET maximum values suggested that the sensitivity of the FRET biosensor was higher for Pb^{2+} than by Cd^{2+} and Zn^{2+} . The FRET biosensor was unresponsive to other ions such as K^+ , Mg^{2+} , and Na^+ .

In vivo characterisation inside living *E.coli* BL21 Rosetta 2DE3 cells revealed that the FRET biosensor can sense cytoplasmic Pb^{2+} , Cd^{2+} , and Zn^{2+} . The FRET signals revealed the metals concentration outside the cell were not the same as inside, indicating a measurement of bioavailability. This can be explained by the native metal resistance mechanisms of the host cell, which may influence the concentration of metals uptake that the FRET biosensor can detect.

The FRET biosensor employing CMT has been proven to measure heavy metals inside the bacterial host cell. The biosensor can potentially be developed in a different type of bacteria, typically found in soil environments contaminated with heavy metals. Therefore, a subsequent study (in the next Chapter 4) focused on developing a FRET biosensor inside a *P.putida* strain using the same gene construct (*eCFP-CMT-Venus*) to express the biosensor.

4. Development of FRET Biosensor for measuring heavy metals using *Pseudomonas putida*

4.1 Introduction

In the previous chapter a FRET biosensor based on Chicken Metallothionein was used to measure heavy metal concentrations inside *E.coli* BL21 Rosetta 2(DE3). This host cell is a genetically well-characterized strain that has been developed for use in a laboratory environment as a host for plasmid vectors and protein over-expression (Rosano and Ceccarelli, 2014). However, its application in polluted soil is less relevant because it could be negatively affected by the toxicity of pollutants, extreme pH or low nutrient availability, etc. Therefore, the aim of this chapter was to test the FRET biosensor for measuring metal toxicity using *Pseudomonas putida* KT2440T7, a strain that was isolated from polluted soils. This approach has not been described in the literature. Existing bacterial biosensors for sensing Pb^{2+} , Cd^{2+} , and Zn^{2+} rely mostly on metal-inducible transcription to produce signals. The application of FRET sensors in actual environmental samples is still rare (Hynninen *et al.*, 2010; Elcin and Öktem, 2020), mainly because of the limitation of spectroscopic measurements where there is signal interference from soil particles (Song *et al.*, 2014; Yoon *et al.*, 2016a,b).

4.1.1 *Pseudomonas putida* KT2440

P. putida is a gram-negative bacteria isolated in 1960 from a soil field in Japan (Nakazawa, 2002). Early studies of this isolate have shown its potential for biodegradation of aromatic compounds in soils and high colonization of plant rhizosphere (Ramos-Gonzales, *et.al*, 2005). This bacterium can survive and function in a contaminated environment due to its capability to adapt to various physicochemical conditions, such as extremes of pH and oxidative stress. *P. putida* has been used as a model organism in many environmental applications, particularly in the remediation of recalcitrant compounds such as hydrocarbons (Fernandez *et al.*, 2012) and pesticides (Zuo *et al.*, 2015; Gong *et al.*, 2016). *P. putida* can colonize the rhizosphere of plants, which may facilitate the development of rhizoremediation systems for soil decontamination (Espinosa-Urgel *et al.*, 2002; Gong *et al.*, 2016). Heavy metal resistance mechanisms in *P. putida* have been well characterized (Cánovas *et al.*, 2003; Leedjävär *et al.*, 2008). Heavy metal homeostasis is maintained mainly through efflux transporters, sequestration, chelation, and enzymatic reduction.

P. putida strain KT2440 is a restriction-negative and plasmid-free derivative of a toluene-degrading bacterium. The normal restriction system against DNA uptake is defective in this strain, making it a suitable recipient for gene transfer (Bagdasarian *et al.*, 1981). This strain has been used for genetic manipulation and biotechnology because it is highly competent for plasmid transformation and is considered a safe host strain (Nelson *et al.*, 2002).

Troeschel *et al.* (2012) have developed the T7 RNA polymerase-dependent expression strain *P. putida* KT2440T7. A gene encoding T7 RNA polymerase under the control of an inducible lacUV5 promoter was introduced into the chromosome of *P. putida* KT2440. This system allows for the expression of a recombinant protein by IPTG induction. Considering all these properties, *P. putida* KT2440T7 was selected as a model organism suitable for FRET biosensor application in contaminated soil.

An efficient host-vector system is required for the production of the FRET biosensor in *P. putida*. Promoter strength, plasmid DNA replication, post-transcriptional and post-translational modifications, and unwanted protein degradation mechanisms can potentially influence the target protein expression (Francis and Page, 2010; Troeschel *et al.*, 2012). Therefore, pEBP18 was selected (Figure 4.2) as an alternative prokaryotic expression vector that carries an inducible T7 promoter, multiple cloning sites, antibiotic resistance genes and origin of replication specifically for *P. putida* KT2440T7 (Troeschel *et al.*, 2012). The gene encoding the FRET biosensor can be easily cloned into this vector and expressed in the host cell for the study of metal-induced FRET signal.

4.1.2 FRET measurement using a confocal microscopy

Measurement of FRET signals using a spectrofluorimeter does not provide spatial information on the distribution of heavy metals within samples. Metals must be separated from soil particles before measurement, removing many of the advantages of an *in vivo* biosensor (Song *et al.*, 2014; Yoon *et al.*, 2016a,b).

In this research, laser scanning confocal microscopy was used to measure the FRET signals in *P. putida* cells. This method overcomes the limitations of standard fluorescence microscopy. Standard fluorescence microscopy illuminates the entire sample specimen and detects the resulting fluorescence which often includes a collection of out-of-focus light above and below the focal plane (Figure 4.1). A focal plane is the plane of a specimen object that is perpendicular to the axis of lens and passes through the focal point. Signals from above and below the focal plane cause blurriness and image degradation.

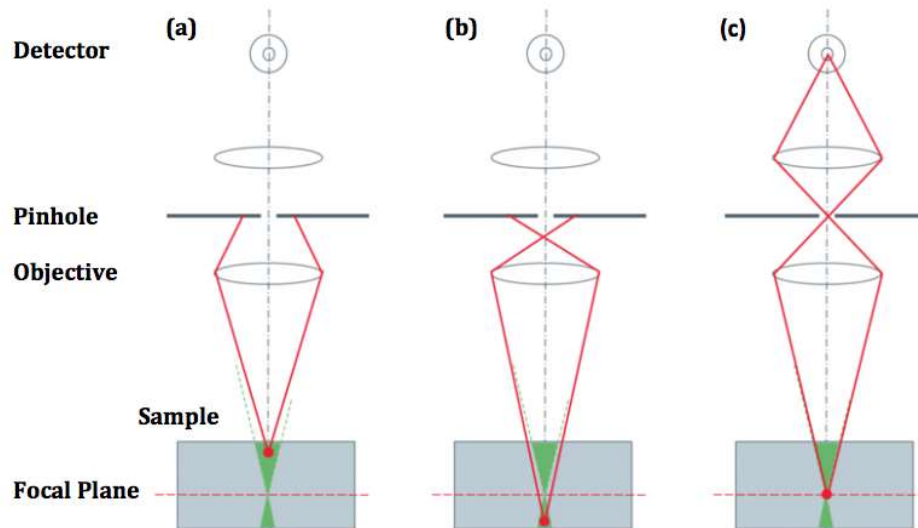


Figure 4.1 The main feature of confocal microscopy is the pinhole to block out-of-focus light. Light from above (a) and below (b) the focal plane of sample specimen is blocked by the pinhole aperture. Therefore, only light from the main focal plane (c) passes the pinhole to the detector which can improve the image resolution (Image adapted from Leica-Teledyne Photometrics, 2021)

The main goal of confocal microscopy is to reject out-of-focus light from the image which can be achieved with a pinhole aperture (Sanderson, *et.al*, 2014). This ensures that light reaching the detector comes only from the equivalent confocal point in the specimen where the excitation light was focused (Figure 4.1). An image can be compiled pixel by pixel by recording the fluorescence intensity, known as laser scanning, at each position across the specimen. This results in a greater image resolution, higher contrast, and noise reduction (Sekar and Periasamy, 2001; Lemasters *et al.*, 2001). However, some limitations of confocal microscopy are the use of an intense laser line, which can potentially cause photobleaching of the fluorophore and the requirement to use fluorophores which are excited by common laser emission lines.

4.2 Aim and objectives

The aim of this chapter is to express the FRET biosensor (a fusion of CMT between eCFP and Venus) inside *P. putida* KT2440T7 and study the sensor's function for measuring heavy metals inside the host cell. Initial heavy metals tests were carried out using a spectrofluorimeter to characterise the emission spectra of FPs inside the host cell. A confocal microscope was used to measure the FRET signals due to binding with metals inside the cells. The FRET signals and corresponding heavy metal concentrations were analysed to determine the response of the host cell.

To address the aim above, the objectives of this chapter are:

1. To clone the gene encoding the FRET biosensor (*eCFP-CMT-Venus*) into an expression vector pEBP18.
2. To express the biosensor and characterise the emission signals *in vivo* within *P. putida* in the presence of Pb^{2+} , Cd^{2+} and Zn^{2+} .
3. To visualize the changes in FRET signals inside living *P. putida* cells using confocal microscopy and use this information to determine the response curve of the host cell to heavy metal exposure.

4.3 Methods

The cloning process is summarised in Figure 4.2 below. The *eCFP-CMT-Venus* gene along with the T7 promoter, ribosomal binding site and T7 terminator sequence were amplified from the expression vector pGWF1-CMT (Chapter III, see Figure 3.9) as an insert and cloned into pEBP18 obtained from Troeschel *et al.*, 2012 (Figure 4.4) to produce an expression vector pEBP18-CMT for transformation into *P. putida* cells. NotI and HpaI sites were added at the end of the target gene, allowing for ligation into a linearised pEBP18 with compatible restriction sites.

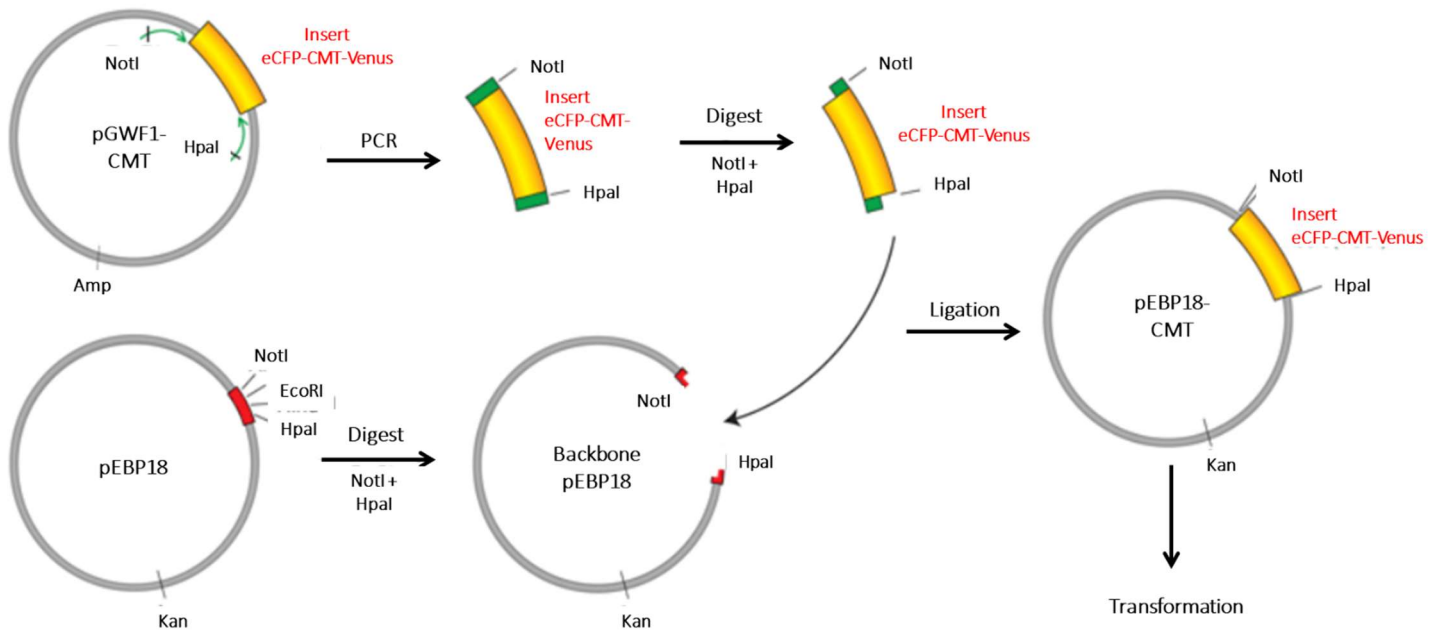


Fig. 4.2 The cloning process to construct pEBP18-CMT for the expression of the FRET biosensor in *P. putida* KT2440T7. A gene encoding the FRET biosensor (*eCFP-CMT-Venus*) was amplified from pGWF1-CMT, followed by digestion with NotI and HpaI. The recipient vector pEBP18 was linearized by digestion with NotI and HpaI. The insert *eCFP-CMT-Venus* was cloned into the backbone pEBP18 to produce pEBP18-CMT, which was transformed into *P. putida* cells.

In chapter 3, Gateway Cloning was used to construct the gene sequence encoding *eCFP*, *CMT*, and *Venus FP* as the components of FRET Biosensor. This construct was developed in a Gateway plasmid compatible for protein expression in *E.coli* host cell. However, Gateway plasmid for protein expression in *P.putida* has not been developed. Therefore, the *eCFP-CMT-Venus FP* gene construct was cloned directly into an existing plasmid (pEBP18) which contains a specific origin of replication and T7 promoter expression system suitable for *P.putida* host cell.

4.3.1 Primer design

The PCR primers consisted of leader sequence (3-6 bp on the 5' end of the primer to assist the restriction enzyme digestion), restriction sites (NotI and HpaI) and region sequence of the primer that binds to the target sequence (Figure 4.3). The primers were designed using the software Genome Compiler™. The principle of designing these primers was based on some considerations such as; the length of 20-30 bases, G/C content of 40-60%, start and end with 1-2 G/C pairs, melting temperature (T_m) of 50-60°C, including restriction sites with an addition of 3-6 base pair clamp upstream the region for the enzyme to cleave efficiently.

NotI and HpaI were selected because they do not cut within the *eCFP-CMT-Venus* sequence and are present in the multiple cloning sites of recipient vector pEBP18 (Figure 4.4). They also cut the *gfp* gene sequence in pEBP18 so the GFP expression can be avoided. To maintain the correct orientation of the *eCFP-CMT-Venus* sequence within the pEBP18 cloning sites, the location of the forward primer was determined at the upstream restriction site (NotI) and the reverse primer at the downstream restriction site (HpaI) (Figure 4.2)

The forward and reverse primers were designed to amplify the 100-2190 bp region covering a T7 promoter, ribosome binding site, *eCPF-CMT-Venus* gene and T7 Terminator sequence. NotI and HpaI sites were added to the primer sequence (Figure 4.2), so the amplification product contains the same restriction sites as in pEBP18.

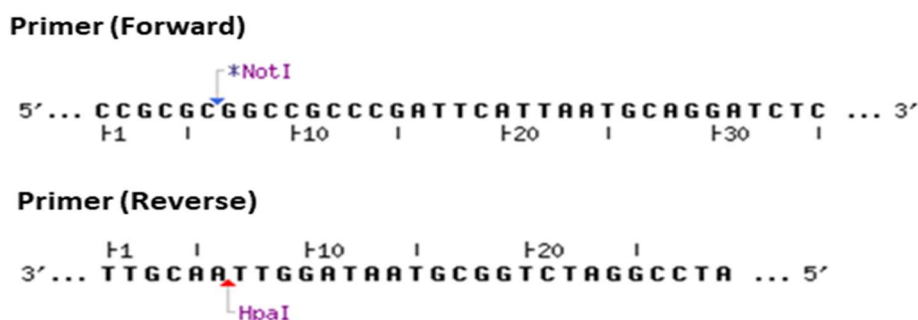


Fig 4.3. Primers design (reverse and forward) for amplification of *eCFP-CMT-Venus* from pGWF1-CMT. NotI and HpaI sites were added to the primers providing restriction sites for cloning into pEBP18.

4.3.2 *eCFP-CMT-Venus* gene amplification

The PCR reaction (50 μ L) consisted of 0.2 μ L of 10 μ M primer reverse and forward, 0.2 μ L (20 ng) of pGWF1-CMT template, 0.5 μ L DNA HiFi polymerase (PCR Bio), 10 μ L (1X) of amplification buffer (PCR Bio) containing 15 mM MgCl₂ and 5 mM dNTPs (PCR Bio), and 38.9 μ L of distilled water. One set of PCR reactions without the pGWF1-CMT template was

used as the negative control. The PCR reactions were carried out using PCR Thermal Cycle (Prime-Cole Palmer, UK) with the following conditions: initial denaturation at 95°C for 1 minute, denaturation at 95°C for 15 seconds, annealing at gradient temperature of 53, 56, 60°C for 15 seconds, extension at 72°C for 90 seconds (30 cycles), final extension at 72°C for 5 minutes, and maintained at 4°C.

The PCR product was purified by QIAquick Purification Kit (Qiagen) to remove primers, unincorporated dNTPs, enzymes and salts from the reaction mixture. The purified PCR product was loaded into gel electrophoresis (0.6% agarose, 100 Volt, 60 minutes) to verify the insert size.

Digestion of DNA insert and recipient vector

The purified PCR product and vector pEBP18 (Figure 4.4) were digested separately with NotI and HpaI (NEB UK). The first digestion mixture consisted of 5 µL (1 µg) of DNA, 1 µL of HpaI, 5 µL of 10X NEB Cut Smart digestion buffer, and 39 µL of distilled water. The mixture was incubated at 37°C for 60 minutes, followed by purification with QIAquick Purification Kit (Qiagen). The purified DNA was set up for the second digestion, which consisted of 5 µL (1 µg) of DNA, 1 µL of NotI, 5 µL of 10X NEB 3.1 digestion buffer and 39 µL of distilled water. The mixture was incubated at 37°C for 30 minutes and subjected to gel electrophoresis (0.6% agarose, 90 Volt, 40 minutes).

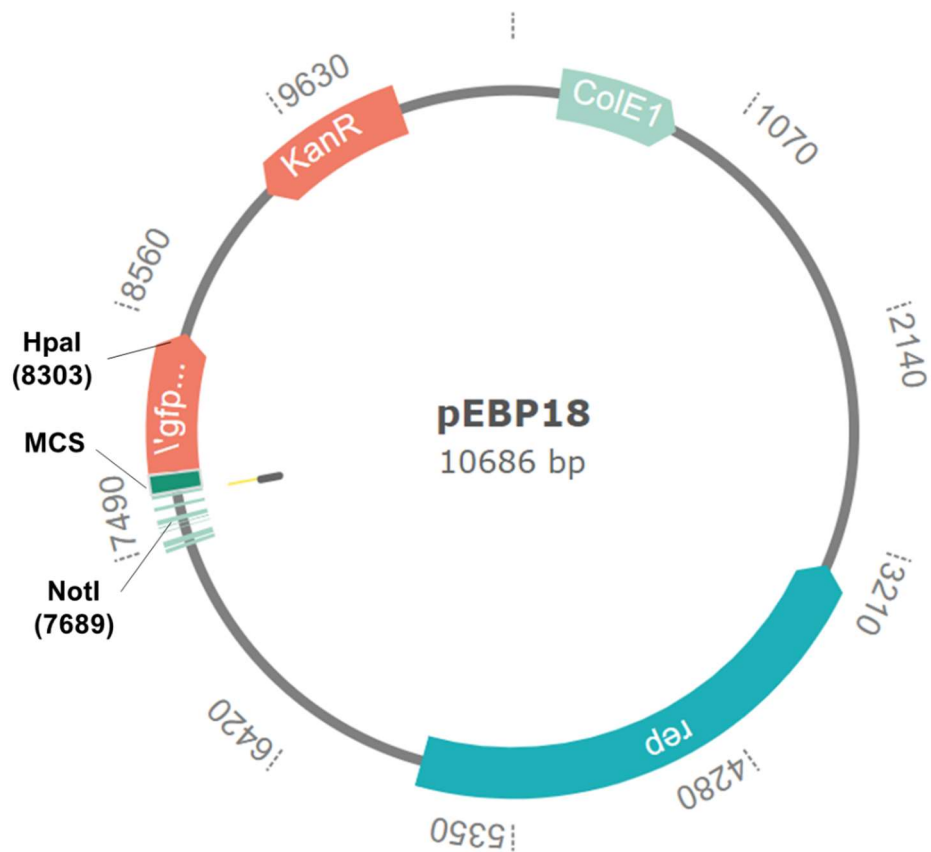


Fig. 4.4 A map of pEBP18 as the shuttle vector for the *P. putida* host cell. Necessary features are the origin of replication (*rep*) for plasmid replication in *P. putida* and kanamycin resistance (*KanR*). The vector was digested with Not I (7689) and Hpa I (8303) to remove the *gfp* sequence and generate a backbone for cloning the *eCFP-CMT-Venus* insert.

PCR product extraction and desalting

The gel was visualized under UV light and the band of interest excised using a scalpel. The gel slice was transferred to a 1.5 mL centrifuged tube and weighed. A 300 μ L volume of gel dissolving buffer (Qiagen) was added to the tube containing the gel slice (100 mg). The mixture was incubated at 50°C for 15 minutes and vortexed periodically until the gel was completely dissolved. A 150 μ L volume of isopropanol was added to the sample. The final mixture was transferred to a spin column (Qiagen) in a 2 ml collection tube and centrifuged at 17.900 x g for 1 minute. A 750 μ L volume of buffer PE (Qiagen) was added to the column and centrifuged at 17.900 x g for 1 minute. The flow-through was discharged and the column was placed into a microcentrifuge tube. A 50 μ L volume of distilled water was added to the column and centrifuged for 1 minute to elute the DNA.

The DNA was desalted using Microcon DNA Fast Flow Filter (Merck Millipore). A 50 μ L volume of DNA was diluted with distilled water to a volume of 500 μ L and put into the filter

in a Microcon tube assembly. The sample was centrifuged at 500 x g for 20 minutes. The filter device was removed from the assembly and placed into a recovery tube, followed by centrifugation at 1000 x g for 3 minutes. The purified DNA was collected in a recovery tube and stored at -20°C.

4.3.3 Ligation

The ligation reaction was carried out at a molar ratio of 3:1 (insert: vector). The ligation mixture (50 µL) consisted of 2 µL (10X) of T4 Ligation buffer (NEB UK), 7 µL (50 ng) of linearized vector pEBP18 (10092 bp), 3.8 µL (31 ng) of insert (2051 bp), 1 µL of T4 DNA ligase (NEB UK) and 6.1 µL of nuclease-free water. Samples without the addition of insert were used as the negative control. The mixture was incubated at 16°C overnight.

The transformation was carried out by adding 5 µL of ligation reaction mixture to a tube containing 50 µL of *E.coli* OmniMAX™ competent cell (Invitrogen) followed by incubation on ice for 30 minutes. The cells were heat-shocked for 30 seconds at 42°C without shaking in a water bath and immediately placed onto the ice. A 450 µL volume of Super Optimal Broth medium (S.O.C) (ThermoFisher) medium was added to the cells at room temperature and shaken at 37°C for 1 hour. A 100 µL volume of the transformation reaction were spread on selective LB plates containing 50 µg/mL of Kanamycin (Thermofisher) and incubated overnight at 37°C. Five cell colonies were selected and grown in selective LB medium (50 µg/mL of Kanamycin) overnight at 37°C for vector (pEBP18-CMT) purification. Bacteria glycerol stocks (15%) were prepared from the overnight culture and stored at -80°C.

Verification of pEBP18-CMT construct

pEBP18-CMT was isolated and purified from the host cells by using QIA Spin Miniprep Kit (Qiagen). The purified plasmid was digested with HpaI and NotI as described above. Following the digestion, the samples subjected to gel electrophoresis (1% agarose, 90 Volts, 45 minutes).

The plasmid pEBP18-CMT was sequenced using T7 primers (reverse and forward) to verify the *eCFP-CMT-Venus* construct and orientation. Following this, pEBP18-CMT was prepared for transformation and protein expression in *P. putida* KT2440T7.

4.3.4 pEBP18-CMT Transformation into *P. putida* host cell

P. putida KT2440T7 was obtained from Troeschel *et al.*, 2012 and maintained on LB agar containing 10 µg/mL of Gentamicin. Preparation of *P. putida* KT2440T7 competent cells was carried out by inoculating a single colony from an agar plate into 20 mL of LB and incubated

overnight at 28 °C with constant shaking (120 rpm). 6 x 2 mL of the overnight culture was transferred into 2 mL centrifuge tube and the cells were harvested by centrifugation at 16,000 x g (room temperature) for 2 minutes. The pellets were washed twice with 2 mL of 0.3 M sterile sucrose solution and re-suspended in 500 µL of 0.3 M sucrose solution. The competent cells were stored on ice before the transformation.

The transformation of pEBP18-CMT into *P. putida* KT2440T7 was carried out by electroporation using the Gene Pulser electroporation apparatus (Bio-Rad). A 50 µL volume of competent cells was mixed with 2 µL (500 ng) of pEBP18-CMT and transferred into electroporation cuvettes (2 mm gap) (Bio-Rad). Competent cells mixed with 1 µL (250 ng) of pEBP18 was used as positive control. The competent cells without vector mixture was used as a negative control. The electroporation was performed using program EC2 (2.5 Kv, 5.8 ms). Following this, the cuvette was immediately placed on ice and the cells were re-suspended in 1 mL of LB. The suspension was transferred into a test tube and incubated at 28°C for 2 hours. A 100 µL volume of cells was spread onto LB agar containing 10 µg/mL of Gentamicin and 20 µg/mL of Kanamycin. The agar plates were incubated overnight at 28°C. Five cell colonies were selected from the agar and grown in selective LB liquid (10 µg/mL of Gentamicin and 20 µg/mL of Kanamycin) overnight at 28°C for protein expression. Bacteria glycerol stocks (15%) were prepared for cell preservation at -80°C.

4.3.5 Protein expression

The overnight culture was transferred (10% v/v) into a fresh LB liquid supplemented with 10 µg/mL of Gentamicin and 20 µg/mL of Kanamycin (ThermoFisher). Protein expression was induced by adding isopropyl thiogalactoside (IPTG) (0.125 mM final concentration). The cells were grown for 20 hours while shaking at 27°C. The expression of eCFP and Venus inside the host cells was measured using a spectrofluorimeter (Horiba Jobin Yvon - FluoroMax-4, Edinburgh Instruments).

4.3.6 Heavy metals in *P. putida*

P. putida KT2440T7 expressing the FRET biosensor was harvested by centrifugation and suspended with Heavy Metal MOPS medium (HMM), pH 7. The medium composition and preparation are described in Chapter III, section III.3.8.

The *in vivo* binding test was carried out by adding different concentrations of metal salt solutions (Pb(NO₃)₂, CdCl₂, ZnSO₄) to a cell suspension of final OD of 0.5 in a 3 ml cuvette. The final concentrations of each metal were: 0.1, 1, 10, 50, 100 µM for Pb(II); 1, 10, 100, 500,

1000 μM for Cd(II) and Zn(II). Metal concentrations were selected based on results reported by Rajamani et al 2014 in which the sensitivity of detection for Pb^{2+} was lower than Cd^{2+} and Zn^{2+} . The initial trial in the current study showed that the exposure of Pb^{2+} above 100 μM caused precipitation of protein and cell samples which eventually interfered with the fluorescence reading. Therefore, 100 μM was selected as the maximum concentration that can be tested. In terms of Cd^{2+} and Zn^{2+} , 1000 μM was selected as the maximum concentration which did not cause precipitation of the samples. MgSO_4 with a final concentration of 1000 μM was used as the negative control. FRET measurements of cells in suspension were performed using a spectrofluorimeter. The cells were excited at 435 nm and the fluorescence emission recorded after 2 h incubation at room temperature. All experiments were performed in triplicate. The emission peak from eCFP and Venus were identified, and the FRET ratio (525/475 nm) calculated.

Data were analysed using R version 3.52 (R core Team 2018). A plot of FRET ratio against metal concentration was fitted to a simple binding affinity model (Equation 1). The data was corrected using the FRET signal of the cells in the absence of metal. The difference in metal induced FRET signals inside *P. putida* was compared to *E. coli* using One-way Anova.

4.3.7 FRET Measurement using a confocal microscopy

The FRET signals of living *P. putida* KT2440T7 cells were measured using a confocal laser microscope (Zeiss LSM Airyscan). Before microscopic observation the cells bearing FRET biosensors were exposed to different concentrations of metals, as described above. After 3 h incubation with metals, the cells were vacuum filtered through a dark 0.2 μm membrane (Whatman® Cyclopore® polycarbonate and polyester membranes, Merck). ProLong Live Antifade reagent (Thermofisher) with a ratio of 1:100 was added to the cells on the filter membrane. The filter membrane was placed on the microscope slide and covered with a coverslip.

The slide was assembled on the microscope stage and a 63x oil-immersion objective lens used for image acquisition. Cells were excited at 458 nm using an argon laser filter. Detectors were set at 469-491 nm to collect signals from eCFP (Channel 1) and 500 – 561 nm for Venus FP (Channel 2). The laser power was set to 10 and the pinhole was 1 airy unit (AU). The gain was adjusted to 775 for CFP emission (Channel 1) and 750 for Venus emission (Channel 2), and kept the same for all experiments. Z-stacks were acquired with a step size of 5.87 μM . Images

were acquired immediately at 512 x 512 pixels and a resolution of 12-bit pixel depth for quantitative measurements.

4.3.8 Image Processing using Fiji and statistical analysis

ImageJ (Fiji) was used to process the images of the FRET emission ratios in *P. putida* KT2440T7. Image stacks from the confocal (czi. format) were opened in Fiji (ImageJ) as a hyper-stack and Z projection image calculated based on maximum intensity. Cells were identified by creating a mask from channel 1 (eCFP emission), thresholded and converted to binary. A 32-bit floating point FRET ratio image was calculated by dividing the Venus emission image by the eCFP emission image. The mask was subtracted so that only cells were present in the image. Cells were identified as objects >2 pixels in size and the mean value for each cell extracted from each channel. The mean value for each cell in the FRET ratio image was copied and transferred into an excel file in csv format for graphing and statistical analysis using R version 3.52 (R core Team 2018).

The distribution of FRET ratio signals from cells in one image was displayed in a box plot. Three images were obtained (n=3) for each heavy metal concentration. Statistical differences in the FRET signal at a particular concentration was determined using a one-way ANOVA. The average of FRET signals from the three images was plotted against metal concentration and fitted to a simple binding affinity model (Equation 1, Chapter III). The data were corrected using the signals in the absence of metal (0 μ M). Parameters of apparent K_a (half maximum metal binding affinity) and apparent FRET maximum were derived from the fitted model to determine host cell response to metal exposure.

4.3 Results

4.4.1 Creation of pEBP18-CMT

The region encoding the FRET biosensor from pGWF1-CMT was amplified by PCR and cloned into pEBP18 to generate an expression vector (pEBP18-CMT). The size of the *eCFP-CMT-Venus* insert after digestion with NotI and HpaI was approximately 2109 bp, as expected. Digestion of pEBP18 with NotI and HpaI generated two linearized vector fragments (10.092 bp and 614 bp). The fragment with size of 10.092 bp was selected as the backbone vector for ligation.

Ligation

The presence of salts may inhibit the ligation reaction. Therefore, the extracted DNA (insert and backbone vector) were purified with Microcon (Merck Millipore) to remove carried over salts and organic compounds from the gel extraction process. NotI and HpaI digestion generated four-based 5' overhangs and blunt ends for both the insert and backbone vector sequence (Figure 4.5). These ends are complementary to each other, allowing the ligase to work catalysed by T4 DNA ligase. The insert and backbone vector molecules can only join in one orientation and are prevented from self-ligation.

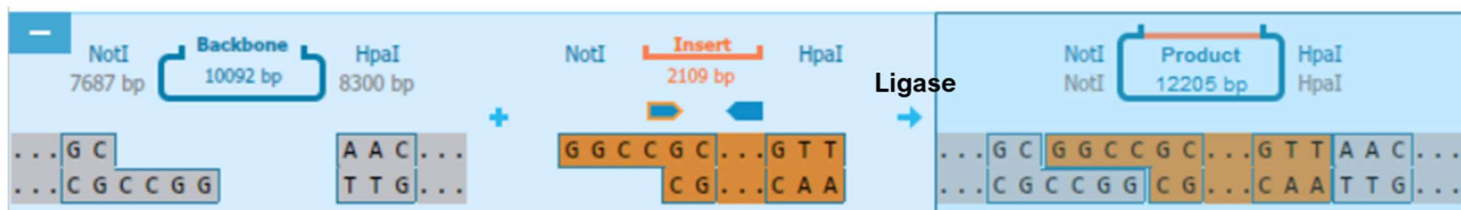


Fig 4.5. Four-based 5' overhang and blunt ends on backbone vector and insert sequence generated from NotI and HpaI digestion. These ends are compatible for ligation between the insert and vector molecule.

The 3:1 insert to vector molar ratio was sufficient for the ligation reaction, resulting in the new vector construct of pEBP18-CMT. Transformation of the ligation mixture into *E.coli* OmniMAX™ was carried out to select and replicate the pEBP18-CMT.

The construct pEBP18-CMT was verified by digestion with NotI (7688) and HpaI (9807), and sequencing. Lanes 1-5 in Figure 4.6 show the digestion products indicated by the presence of two linearized DNA at 10,0092 and 2118 bp, as expected. Sequencing results with T7 primers showed the correct sequence of *eCFP-CMT-Venus*, with orientation for both reverse and forward directions.

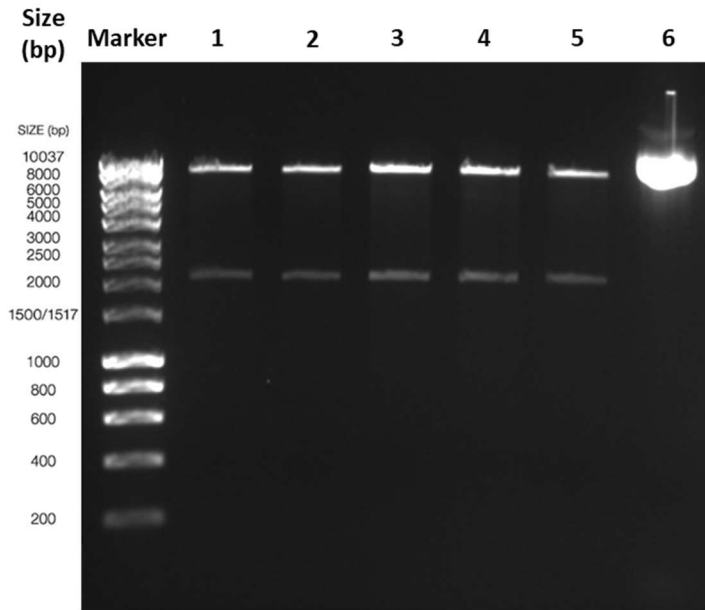


Fig 4.6. Agarose gel (1%) of pEBP18-CMT digestion using NotI & HpaI. Lane 1-5: linearized vector (10092 bp + 2118 bp), lane 6: control negative (vector only)

The genetic map of pEBP18-CMT is shown in Figure 4.7. This vector allows for protein expression from the T7 RNA polymerase promoter located upstream of the *eCFP-CMT-Venus* sequence. *P. putida* KT2440 T7 harbours an IPTG inducible T7 RNA polymerase in its genome and therefore induction with IPTG will activate the T7 RNA polymerase and express the FRET biosensor. The T7 terminator sequence is located downstream of *eCFP-CMT-Venus*, which marks the end of gene transcription. A kanamycin resistance gene is used as a selection marker of the host cell bearing pEBP18-CMT.

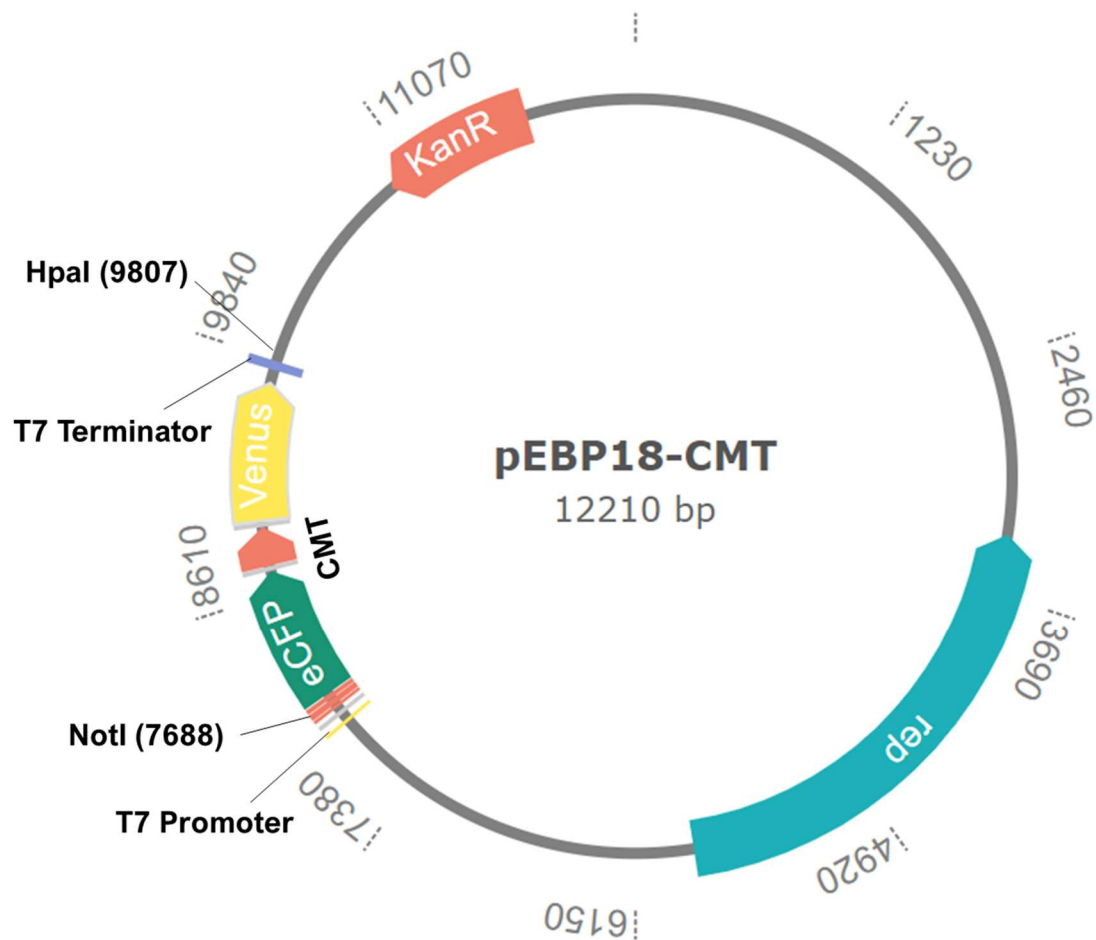


Fig. 4.7 A map of pEBP18-CMT encoding the *eCFP-CMT-Venus* sequence for FRET biosensor production in *P. putida*. Important features are the T7 promoter as transcription start site located upstream of the *eCFP-CMT-Venus* gene, *rep* gene which is responsible for plasmid replication, KanR which encodes the kanamycin resistance gene, and T7 terminator as the termination site for the transcription process located downstream of the insert.

4.4.2 Electroporation and Protein expression

pEBP18-CMT was transformed into *P. putida* KT2440T7 host cell by electroporation. Following the incubation at 28°C, cell colonies were found on LB + Kanamycin + Gentamycin agar, indicating the *P. putida* cells bearing the pEBP18-CMT. No colony was found on agar with untransformed cells.

Following the IPTG addition, the expression of the FRET biosensor was detected using a spectrofluorimeter. Figure 4.8 shows the spectra emission of the *P. putida*-bearing FRET biosensor indicating the presence of eCFP (peak at 475 nm) and Venus FP (peak at 525 nm).

4.4.3 Metal-induced FRET signals inside *P. putida* (spectrofluorimeter)

A preliminary study of metal-induced FRET in *P. putida* KT2440T7 was carried out using a spectrofluorimeter. Changes in eCFP and Venus FP can be observed due to metal binding with the

FRET biosensor inside the cell (Figure 4.7). A change in FRET ratio occurred in response to exposure to Pb^{2+} at 100 μM (Figure 4.10B).

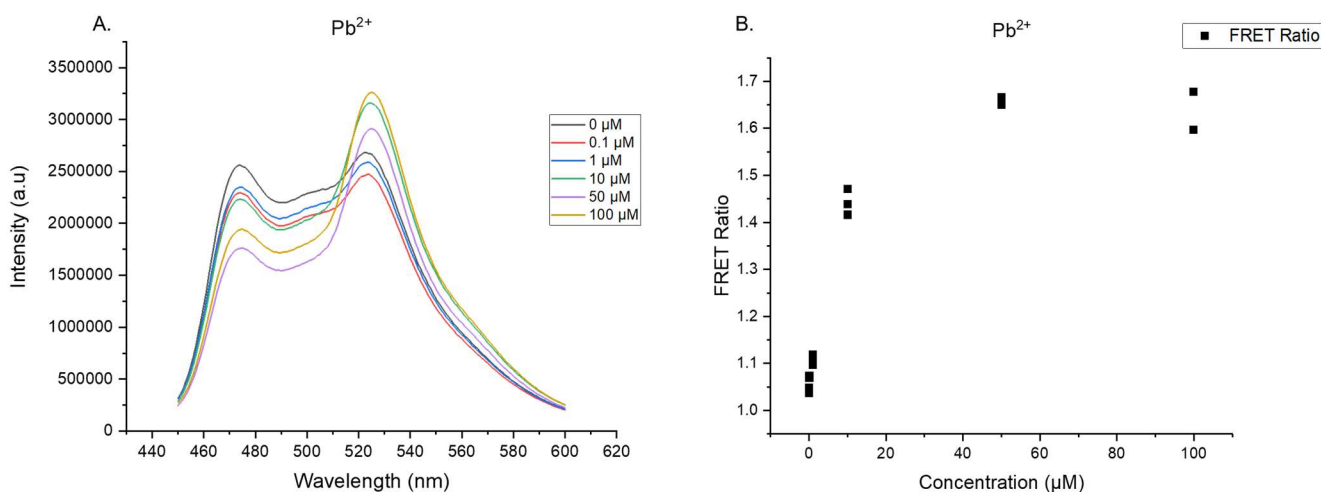


Fig 4.8 Changes in emission spectra of the FRET biosensor inside *P. putida* KT2440T7 cells exposed to different concentrations of metal (Pb^{2+}). Emission peaks at 475 nm and 525 nm indicate the signals of eCFP and Venus FP, which can be calculated to measure the FRET ratio in response to metals (B). The ratio of Venus FP/eCFP was plotted against metal concentration. A reduction in the FRET signal was observed at 100 μM . The measurement was carried out using a spectrofluorimeter with 3 replicates ($n=3$).

The FRET ratio versus metal concentration was fitted to a simple affinity model (Equation 1, Chapter III), from which the parameters of apparent K_a and FRET maximum were obtained (Figure 4.9). The apparent K_a defines the range of concentrations in which the metals bind to CMT inside the host cell. The apparent K_a due binding with Pb^{2+} ($6.67 \pm 0.96 \mu\text{M}$) was the lowest, compared to Cd^{2+} ($73.25 \pm 14.67 \mu\text{M}$) and Zn^{2+} ($35.40 \pm 6.3 \mu\text{M}$) (Table 4.1). This suggest that the smallest binding concentration was exhibited by Pb^{2+} , then followed by Zn^{2+} and Cd^{2+}

The comparison of binding affinity models inside *P. putida* and *E.coli* is shown in Figure 4.9 and summarised in Table 4.1. The binding model inside *P.putida* were statistically different with *E.coli* ($p<0.05$), except for Cd^{2+} ($p>0.05$). The values of apparent K_a inside *P. putida* were higher than *E.coli*, particularly for Zn^{2+} , in which the K_a value was 6.5-fold higher (Table 4.1). Likewise, the maximum values in *P.putida* were also higher than in *E.coli*. These results showed that a higher metal concentration inside *P.putida* compared to *E.coli*. The binding of metals within both host cells should be the same, the alteration of apparent K_a and FRET maximum values were due to the difference in cellular metal regulations which affected the amount of metal available for the detection by the FRET biosensor.

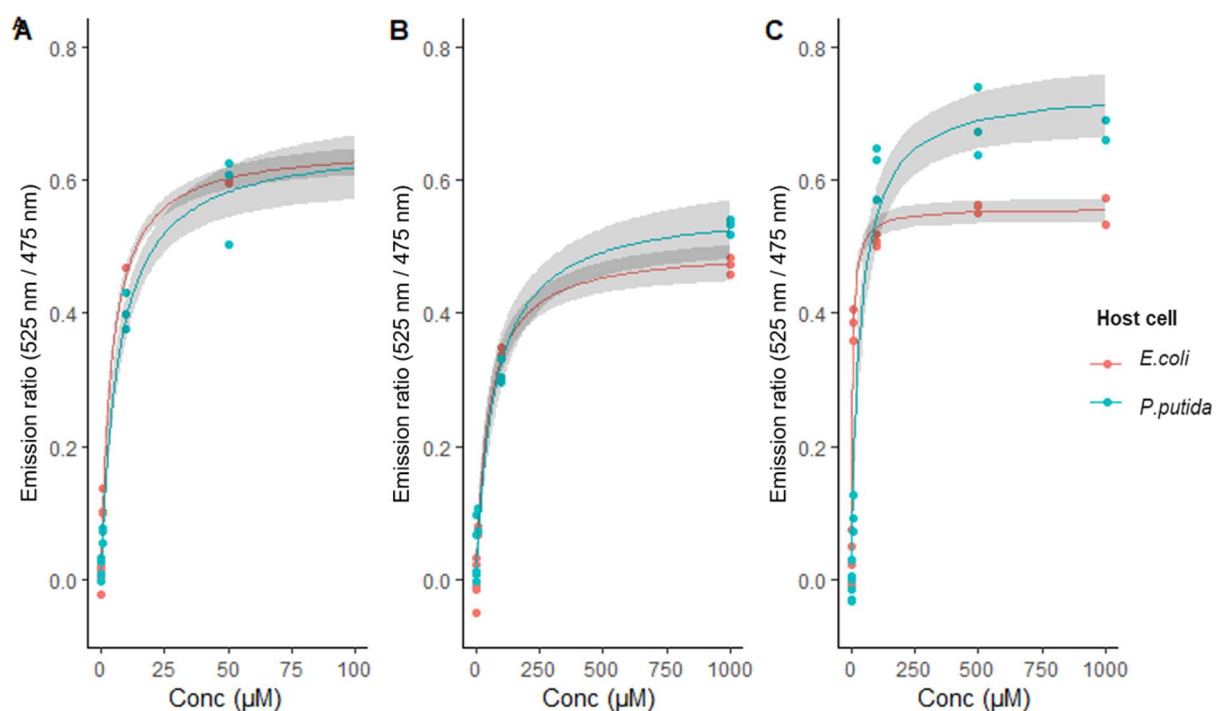


Fig. 4.9 Changes in FRET emission ratio inside *P. putida* KT2440T7 (blue) and *E.coli* BL21 DE3 (red) in response to Pb^{2+} (A), Cd^{2+} (B), and Zn^{2+} (C). Measurement was carried out using a spectrofluorimeter in three replications ($n=3$). Dots represent the FRET ratio data and a rectangular hyperbolic curve fitted based on simple binding affinity model (Equation 1).

Table 4.1. Apparent K_a and FRET maximum parameters estimated from the curve fitting describing the binding sensitivity of the FRET biosensor to Pb, Cd, and Zn inside *P. putida* KT2440T7 and *E.coli* BL21 DE3 cells. FRET measurement was carried out using a spectrofluorimeter. Difference in the binding model between inside *E.coli* and *P. putida* were calculated using One-way ANOVA (significant level was quoted as 95% confidence level ($p < 0.05$)).

Heavy metals	Parameters	Estimate \pm standard error		Difference in the binding model between <i>E.coli</i> and <i>P. putida</i>
		<i>E.coli</i>	<i>P. putida</i>	
Pb	Apparent K_a	4.27 ± 0.30	6.67 ± 0.96	$p < 0.05$
	Apparent FRET max	0.65 ± 0.01	0.65 ± 0.019	
Cd	Apparent K_a	50.56 ± 6.55	73.25 ± 14.67	$p = 0.069$
	Apparent FRET max	0.49 ± 0.01	0.56 ± 0.027	
Zn	Apparent K_a	5.41 ± 0.53	35.40 ± 6.3	$p < 0.05$
	Apparent FRET max	0.55 ± 0.008	0.73 ± 0.025	

4.4.4 Analysis of FRET emission ratio image

Live cell imaging of *P. putida* bearing the FRET biosensors and its response to heavy metal binding was performed using confocal microscopy. The specimen slide preparation involved retaining the host cells on the surface of a black polycarbonate membrane to provide a contrast and low background fluorescence so they could be viewed clearly under the microscope.

At the beginning of this experiment, photobleaching of eCFP and Venus FP was observed during the image acquisition (Figure 4.10). Therefore, an antifade reagent (Prolong Live, Thermofisher) was added to the samples to reduce the photobleaching effect. Figure 4.10 and 4.11 show that the photobleaching effect was minimized after the addition of the antifade reagent. The difference can be seen clearly in image 3, in which the mean value of eCFP signal was 1069 due the antifade effect, whereas the value was 667 in the absence of antifade. Overall, the eCFP signals were reduced significantly ($p < 0.05$) from the mean value of 1310 (Image 1) to 438 (Image 5) in the absence of antifade. In the presence of antifade (1:100), the median value of the eCFP signal was reduced ($p < 0.05$) from 1242 (Image 1) to 1069 (Image 5).

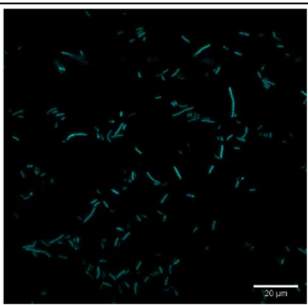
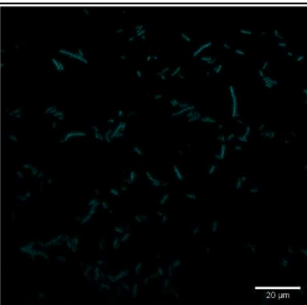
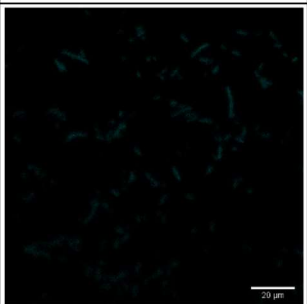
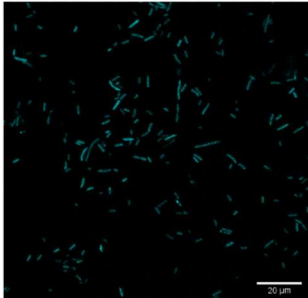
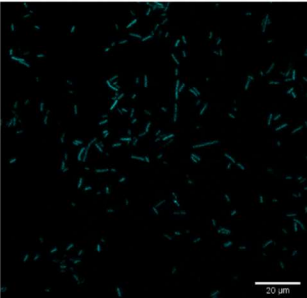
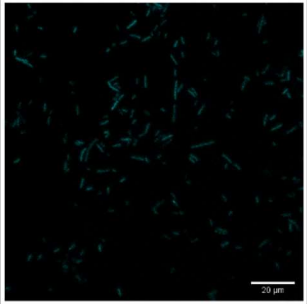
Treatment	Image number taken at 5 sec interval (eCFP channel)		
	1	3	5
No Antifade			
Antifade (1:100)			

Figure 4.10 Representative images of photobleaching (eCFP Channel) inside the cells (without and with the addition of antifade). In the absence of antifade, the effect of photobleaching can be observed clearly on images 3 and 5 (blur image), whilst the addition of antifade minimised the effect of photobleaching on images 3 and 5. The measurement was carried out using confocal microscopy under argon-laser (458). The image was taken 5 times with a 5-second interval. Scale bar: 20 µm. The value of the emission signals for each cell is shown in Figure 4.10 below.

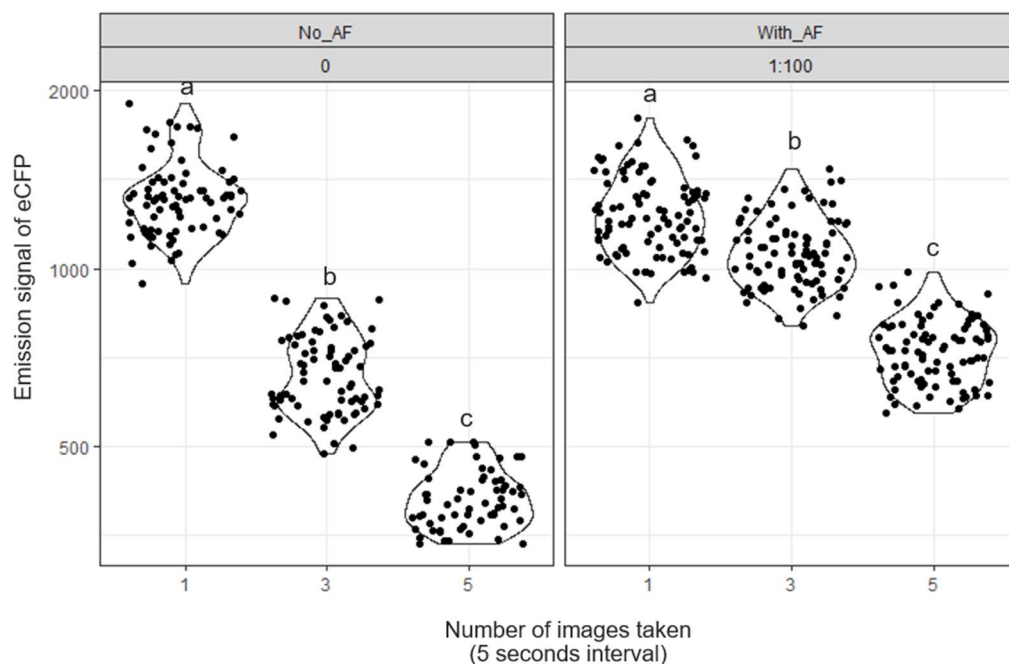


Figure 4.11. Emission signal of host cells following exposure under laser 458 nm to excite the eCFP. Each dot represents the emission signal from a single cell. The eCFP signals were reduced significantly ($p < 0.05$) from the mean value of 1310 (Image 1) to 438 (Image 5) in the absence of antifade. In the presence of antifade (1:100), the mean value of the eCFP signal was reduced ($p < 0.05$) from 1242 (Image 1) to 1069. The difference in signals between images in each treatment was calculated using Two-way ANOVA, followed by Tukey's test. Different letters indicate significant difference between images. Significant level was determined as 95% confidence level ($p < 0.05$).

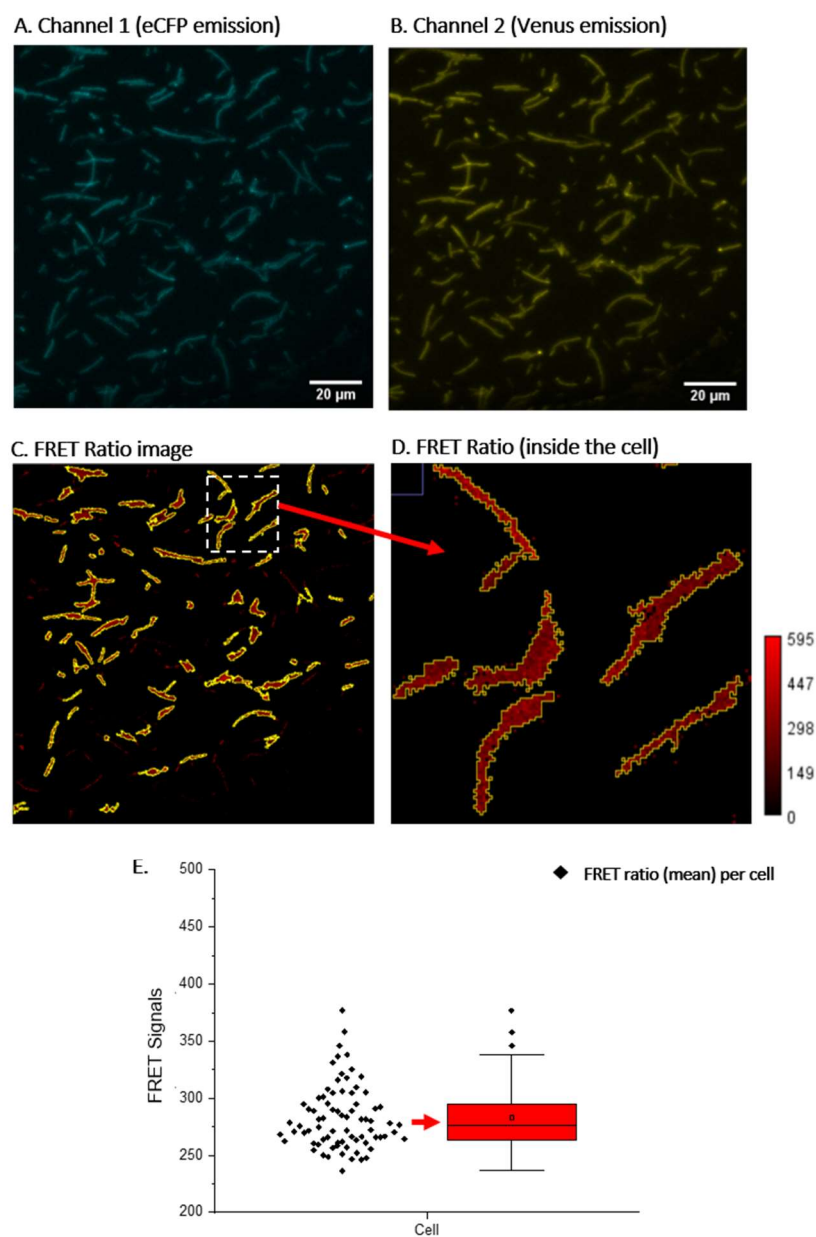


Fig.4.12. Representative images of *P. putida* KT2440T7 expressing eCFP (A) and Venus FP (B) in the absence of heavy metals. The region of interest (white square) was selected on Image C to show the pixel distribution of the emission ratio inside the host cells (red colour bar, Image D). A box plot (Figure E) shows the distribution range of the FRET signals from all cells on the image, with median value of 276, mean value of 282 ± 27.9 , min and max value of 236.5 and 337.95, respectively (Image E).

Figure 4.12 above shows representative images acquired from excitation of eCFP at 458 nm in the absence of heavy metals. The fluorescent region inside the cells is shown in images A and B, indicating the eCFP and Venus FP expression, and the FRET ratio is shown in Image C. The distribution inside the host cells is shown in Image D. The purpose of the white square was to magnify the cells so that the pixel distribution inside each cell can be shown clearly. It should be noted that the signals from all cells in one image were calculated and taken into

consideration for statistical analysis. The mean values of the FRET ratio distribution inside the cell were calculated and designated as the emission ratio of the host cells. Figure 4.12, E, shows the average value of the emission ratio from all cells on the image. Visualization of the host cells exposed to low and high concentrations of Pb^{2+} , Cd^{2+} , and Zn^{2+} is shown in Figures 4.13, 4.14, and 4.15, respectively. As cells were exposed to higher concentrations of metals, the FRET signal increased, indicating metal binding to CMT in the biosensor.

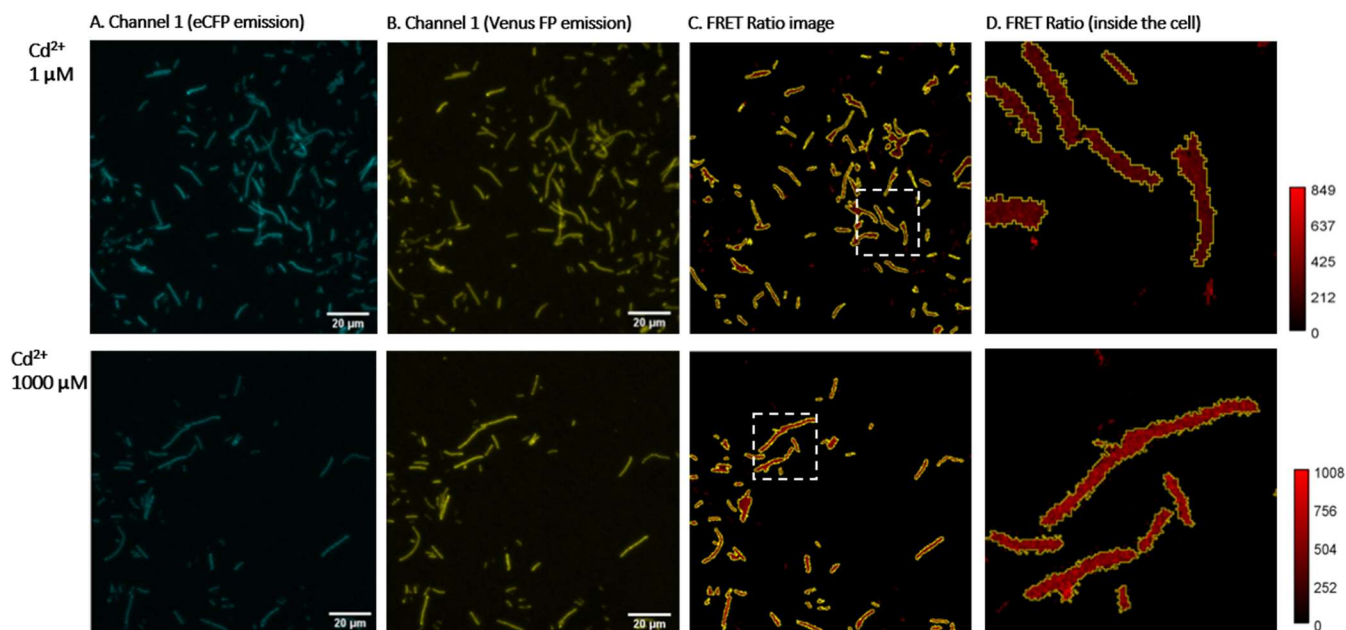


Figure 4.13 Representative images of *P. putida* KT2440T7 expressing eCFP (A) and Venus FP (B) after exposure to Cd^{2+} at 1 μM and 1000 μM . The FRET ratio image (C) was obtained from image processing using ImageJ (Fiji). The region of interest (white square) was selected on Image C to show the pixel distribution of the FRET ratio inside the host cells as shown in image D. Level of FRET signals (mean gray value) inside the cell is shown in the red colour bar.

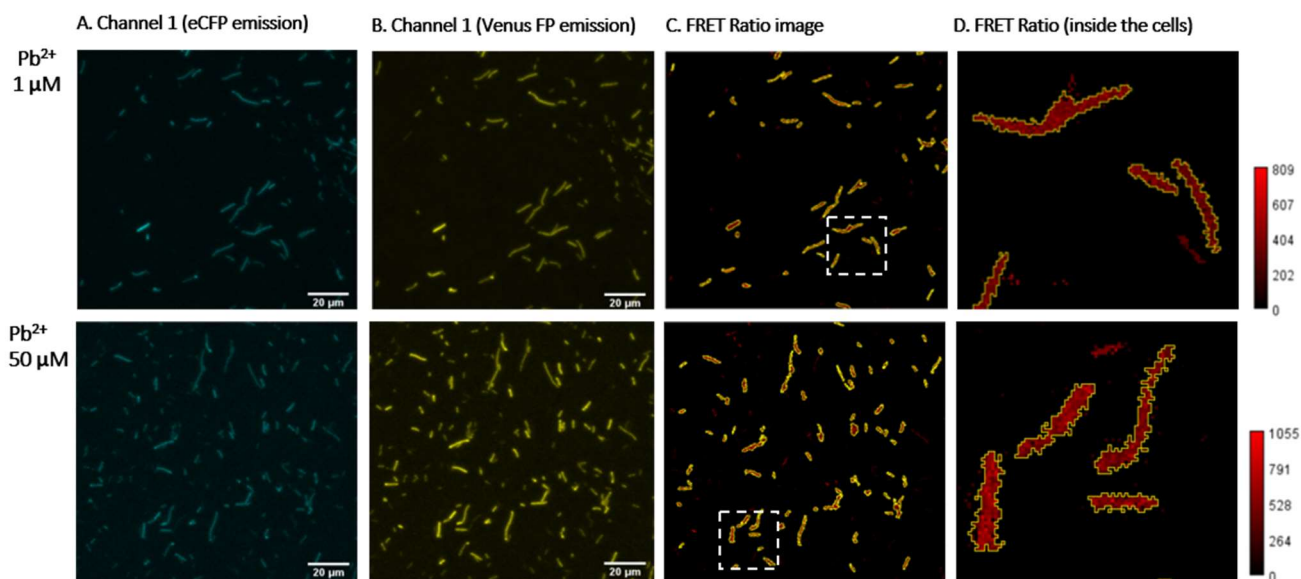


Figure 4.14 Representative images of *P. putida* KT2440T7 expressing eCFP (A) and Venus FP (B) after exposure to Pb^{2+} at 1 μM and 50 μM . The FRET ratio image (C) was obtained from image processing using ImageJ (Fiji). The region of interest (white square) was selected on Image C to show the pixel distribution of the FRET ratio inside the host cells as shown on image D. Level of FRET signals (mean gray value) inside the cell is shown in the red colour bar.

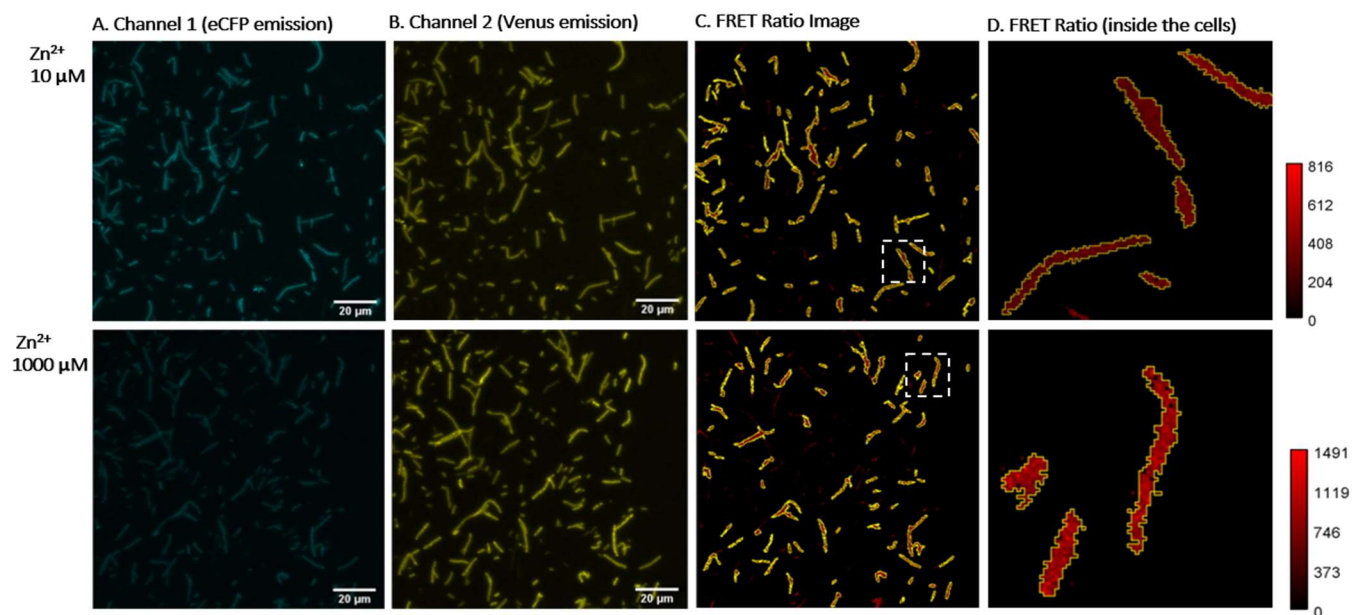


Figure 4.15 Representative images of *P. putida* KT2440T7 expressing eCFP (A) and Venus FP (B) after exposure to Zn^{2+} at 1 μM and 1000 μM . The FRET ratio image (C) was obtained from image processing using ImageJ (Fiji). The region of interest (white square) was selected on Image C to show the pixel distribution of the FRET ratio inside the host cells as shown on image D. Level of FRET signals (mean gray value) inside the cell is shown in the red colour bar.

Metal-induced FRET signals of cells in response to heavy metal concentrations is shown in Figure 4.16. Each box plot represents the distribution of signals from all cells in one image. The FRET signals in response to Cd^{2+} started to increase significantly from the cell's exposure to concentration of 10 μM , then a maximum signal was achieved due to exposure at 1000 μM . Pb^{2+} exhibits the lowest minimum concentration that can be detected starting from 0.1 μM , in which the FRET signal dropped significantly ($p < 0.05$) at 100 μM . The FRET signals in response to Zn^{2+} started to increase significantly from the cell's exposure to concentration of 100 μM , in which the signals increased until the exposure at 1000 μM .

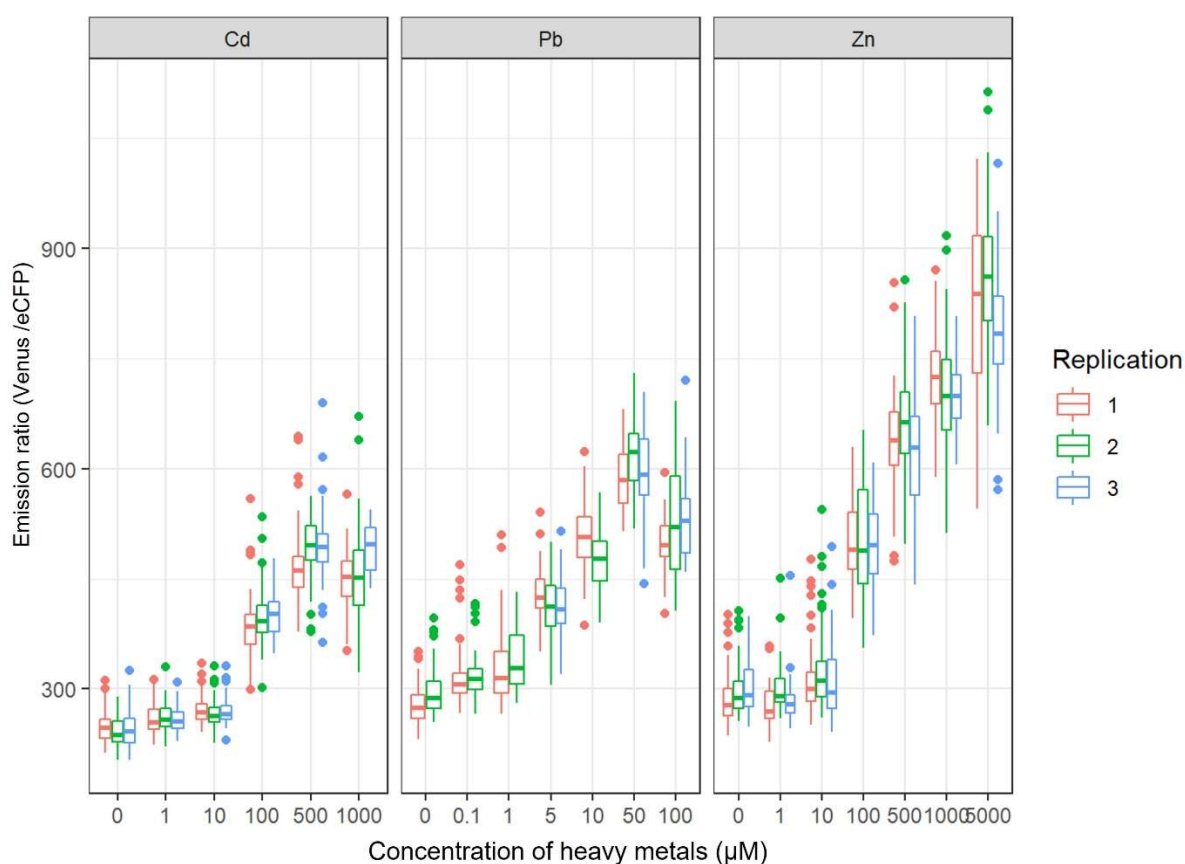


Figure 4.16 Metal-induced FRET signals inside *P. putida* in response to different concentrations of Cd^{2+} , Pb^{2+} , and Zn^{2+} . The box plot represents the emission ratio from all cells in one image. FRET measurement was carried out using confocal microscopy. This figure shows the lower and higher detection limit of the FRET biosensor inside *P. putida*, which were 10-1000 μM (Cd^{2+}), 0.1-50 μM (Pb^{2+}) and 100-5000 μM (Zn^{2+}).

Figure 4.16 shows *P.putida* cells bearing the FRET biosensor which were exposed to different concentrations of Cd^{2+} , Pb^{2+} , and Zn^{2+} . Confocal measurements were carried out in three replications from each heavy metal tested for each concentration. The box plot represents emission ratio signals from all cells in one image. Prior to the curve fitting, the FRET emission ratio (Y-axis) was normalised by subtracting the values of emission ratio in the absence of metal ($0 \mu\text{M}$).

The curve fitting was carried out by taking the mean value from each image (box plot) and running the models based on the cooperative and non-cooperative (simple binding affinity) binding equations. The statistical validation was performed by using the Akaike Information Criterion (AIC) test model. AIC works by evaluating the model's fit on the data set and adding a penalty term for the complexity of the model. The desired result was to find the lowest possible AIC indicating the best model fit. The statistical analysis showed that the AIC units were less than 2 for the model of non-cooperative binding equation. Therefore, the curves for all heavy metals tested were well fitted to this model and followed a rectangular hyperbolic curve (Figure 4.17).

The plot was fitted to a simple binding affinity model (Equation 1), assuming the metal binding on CMT was non-cooperative. Figure 4.17 shows that the curve fitting followed a rectangular hyperbolic curve, from which the apparent K_a and FRET maximum parameters were estimated.

Table 4.2 shows that the apparent K_a indicating the measurement range inside *P.putida* for Pb^{2+} was $8.26 \pm 1.09 \mu\text{M}$, which is 6-times lower than the value for Cd^{2+} ($68.35 \pm 11.73 \mu\text{M}$) and 24-times lower than the value for Zn^{2+} ($204.007 \pm 29.72 \mu\text{M}$). The apparent FRET maximum values indicate the maximum concentration that can be measured, which is 366.20 ± 15.88 for $50 \mu\text{M}$ of Pb^{2+} , 251.06 ± 9.12 for $1000 \mu\text{M}$ of Cd^{2+} , and 522.92 ± 16.44 for $5000 \mu\text{M}$ of Zn^{2+} . The maximum value to Zn^{2+} suggests that the concentration of this metal in the host cell was higher than Cd^{2+} and Pb^{2+} .

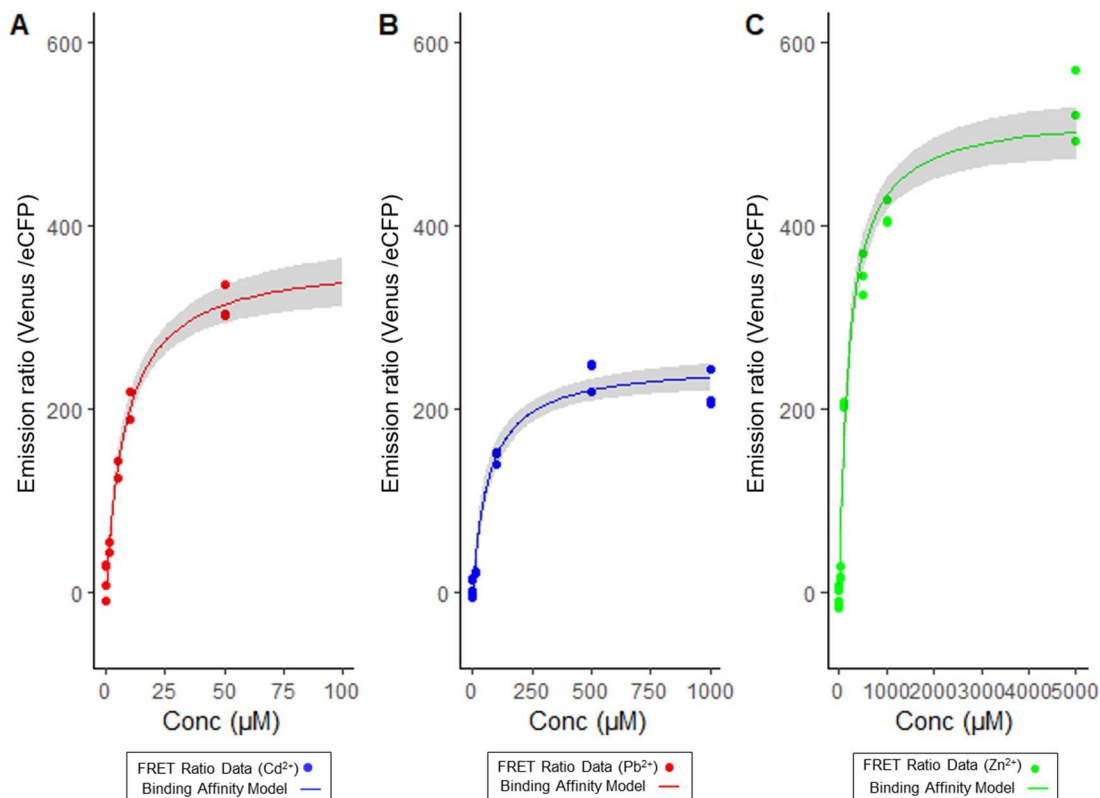


Figure 4.17 Changes in emission ratios inside *P. putida* KT2440T7 in response to Pb^{2+} (A), Cd^{2+} (B), and Zn^{2+} (C). Measurement was carried out using a confocal microscope. Dots represent the mean of the FRET ratio data obtained from the cells in one image, whereas rectangular hyperbolic lines represent the fitting curves based on a simple binding affinity model (Equation 1).

Table 4.2 Apparent K_a and FRET maximum parameters estimated from the curve fitting describing the binding sensitivity of the FRET biosensor to Pb, Cd, and Zn inside *P. putida* KT2440T7. FRET measurement was carried out using confocal microscopy.

Heavy metals	Parameters	Estimate \pm standard error
Cd	Ka (μ M)	68.35 ± 11.73
	Max.value	251.06 ± 9.12
Pb	Ka (μ M)	8.26 ± 1.09
	Max.value	366.20 ± 15.88
Zn	Ka (μ M)	204.007 ± 29.72
	Max.value	522.92 ± 16.44

4.5. Discussion

FRET biosensors for heavy metal sensing have been developed in a variety of host cells, including mammalian (Chiu and Yang, 2012), microalgae (Rajamani *et al.*, 2014) and fruit fly (*Drosophila melanogaster*) (Yang *et al.*, 2020). These studies have shown the capability of FRET biosensor to measure the response of host cells to heavy metals. In this research, the FRET biosensor was expressed inside a soil bacterium, *P. putida* and measured intracellular concentrations following exposure to Cd^{2+} , Pb^{2+} , and Zn^{2+} . The biosensor construction involved cloning the *eCFP-CMT-Venus* gene into the pEBP18 vector, compatible with protein production in the *P. putida* KT2440T7 strain (Troeschel *et al.*, 2012). The functionality of this vector was confirmed by the expression of the FRET biosensor controlled by the T7 promoter system.

4.5.1 Metal-induced FRET signals in *P. putida*

This research has demonstrated the use of confocal microscopy for FRET measurement. Laser at 458 nm can excite the donor (eCFP), resulting in energy transfer from eCFP to the acceptor (Venus FP). Changes in the emission ratio (Venus FP/eCFP) correspond to the concentration of heavy metals, confirming the metal sensing ability of the FRET biosensor in *P. putida* (Figure. 4.16). Using confocal microscopy enabled the visualization of metal-induced FRET signals in the context of a cellular physiological environment.

The FRET ratio signals revealed that the detection limit of the FRET biosensor inside *P. putida* was very low for Pb^{2+} ($8.26 \pm 1.09 \mu\text{M}$) compared to Cd^{2+} ($68.35 \pm 11.73 \mu\text{M}$), and Zn^{2+} ($204.007 \pm 29.72 \mu\text{M}$). The apparent FRET maximum due to Pb^{2+} was exhibited at $50 \mu\text{M}$, which was also the lowest compared to Cd^{2+} and Zn^{2+} . Based on these results, it can be inferred that *P. putida* responded to each metal in a different way. Pb^{2+} exhibited the lowest metal concentration in the cell compared to Zn^{2+} and Cd^{2+} showing that Pb^{2+} was unfavourable for the host cell. Reduction in FRET signal due to cells exposure at $100 \mu\text{M}$ indicated a very toxic level in which the cell cannot tolerate. Pb^{2+} has no biological function and once it enters the cytoplasm this metal could bind to essential proteins through coordination by cysteine, glutamic acid or histidine, to disrupt cellular function (Martinez-Finley *et al.*, 2012).

The minimum detection limit for Cd^{2+} ($10 \mu\text{M}$) and Zn^{2+} ($100 \mu\text{M}$) were higher than Pb^{2+} ($0.1 \mu\text{M}$). This can be explained through the role of metal efflux transporters in *P. putida* KT2440. Hynninen (2010) reported that the CBA transporter (CzcCBA1) and cadA P-type ATPase are responsible for transporting Cd^{2+} and Zn^{2+} from the periplasmic membrane before entering the cytoplasm. The efflux transporter can cover extracellular metal concentrations within the range

of 10 to 100 μM . Above these concentrations, some metals may escape from the transporter and enter the cytoplasm. Therefore, they can be sensed by the FRET biosensor and subjected to intracellular resistance mechanisms. These efflux transporters did not regulate the levels of Pb^{2+} and therefore lower exposure (0.1-1 μM) to Pb could cause this metal to pass through the cell membrane and be detected by the FRET biosensor. The efflux transporter specifically for Pb^{2+} in *P. putida* is still unclear but Leedj arv *et al* (2008) suggested the involvement P-type ATPase that could remove a small amount of Pb^{2+} . However, it seems that the native detoxification system cannot resist exposure to Pb^{2+} above 50 μM , causing a toxic impact on the cell.

Interestingly, the FRET signals increased significantly until exposure to 5000 μM of Zn^{2+} , indicating a high metal concentration inside the cell (Figure 4.16). Zinc is an essential metal required by the host cell in trace amounts for cellular metabolism. However, at high concentrations it can disrupt the homeostatic balance of the cell and cause toxicity (Rouch *et al*, 1995; Choudhary and Sar, 2009). Apparently, the *P. putida* cells were still capable of maintaining zinc homeostatic even when the external concentration reached 5000 μM . Some possible mechanisms of *P. putida* KT2440 to regulate high exposure to zinc are the intracellular redox mechanisms which can be activated due to extracellular concentration above 2500 μM Peng *et al*. (2018).

Compared to *E. coli*, FRET biosensors in *P. putida* exhibited higher apparent K_a and FRET maximum values, indicating that the host cell has the capability to withstand a broader range of metal concentrations. This is supported by C anovas *et al* (2003), who found many genes involved in metal homeostasis and tolerance in the chromosome of *P. putida* KT2440. Metal transporters on the cell membrane and intracellular resistance mechanisms to Pb^{2+} , Cd^{2+} and Zn^{2+} provide this host cell with the capability to maintain influx and efflux of metals, thus affecting the available metal concentrations for detection by the FRET biosensors.

4.5.2 Potential application of FRET biosensor in *P. putida*

The fact that *P. putida* KT2440 can survive in high metal concentrations (Leedj arv *et al*, 2008; Peng *et al*., 2018) makes this host cell very promising for biosensor application in a polluted environment. This has been shown in studies which have exploited this host cell for measuring heavy metal toxicity in environmental samples (Hynninen *et al*, 2010; Liu *et al*, 2012; Peng and Su, 2014). A biosensor that utilised *P. putida* KT2440 for Pb^{2+} , Cd^{2+} , and Zn^{2+} sensing relied on a transcription-inducible system (*czcI-lux* and *cadA1-lux*). The promoter activation of the efflux transporter gene fused with a lux gene was used to produce signals (Hynninen *et*

al, 2010). Their biosensor exhibited the detection limit of 0.90 μM for Pb^{2+} , 1.12 μM Cd^{2+} , and 0.16 μM , and 0.89 μM for Zn^{2+} . In contrast, the detection limits of the *P. putida* FRET biosensor developed in this study are 9-fold (Pb^{2+}), 68-fold (Cd^{2+}) and 200-fold (Zn^{2+}) higher than the *P. putida* KT2440 (*czc1-lux/cadA1-lux*).

The higher detection limit arises due to the CMT properties which bind larger amounts of metals than the regulatory protein (cadR) of the *cadA* gene in the inducible biosensor. CMT is a metallothionein containing 20 Cys residues which provide binding sites for seven metals (Sutherland, *et al*, 2012), whilst cadR is a regulator protein with only 3 Cys residues responsible for metal binding (Lee *et al*, 2001). The difference in detection range between these biosensors indicates that the FRET biosensor in *P. putida* is a more suitable candidate for application in a highly polluted environment.

The use of confocal microscopy for FRET measurement can potentially detect bioavailable heavy metals when living host cells are introduced directly into the polluted soil. FRET measurement using confocal microscopy has been widely used in the field of biomedical research (Sekar and Periasamy, 2003; Yang *et.al*, 2020); however, the application for monitoring of pollutants in environmental samples (e.g polluted soil) has not been found in literature. The main drawback is due to the common use of transcription-inducible biosensors in which the measurement of the signal was typically performed by using spectroscopy instruments. This approach involves mixing the soil samples with water followed by separation of filtrate which is considered as an indirect measurement. The FRET biosensor developed in *P.putida* offers a direct approach in which the host cell can be deployed into the soils and the changes in FRET signals can be measured *in-situ* using confocal microscopy.

The emission ratio images were calculated with subsequent metal concentrations to generate the standard curves describing the response of the host cell to heavy metal exposure. The standard curves can potentially be used to measure the range of bioavailable metal concentrations as the host cells are exposed to any metal-polluted environment. The FRET biosensors detect the number of metals from the surrounding environment that can pass through the cell membrane to enter the cytoplasm and potentially cause toxicity.

4.5.3 Future development of the FRET biosensor

The genome sequence of *P. putida* KT2440 has been well characterised (Nelson *et al.*, 2002; Belda *et al.*, 2016). Therefore, the FRET biosensor can potentially be developed by integrating the gene encoding eCFP-CMT-Venus into the chromosome in which the protein expression is controlled by a constitutive promoter. This will allow the expression of the FRET biosensor

without the need for IPTG induction. Chromosomal gene expression offers a more stable basis for FRET biosensor construction than plasmid-based approaches and eliminates the use of antibiotics for plasmid maintenance (Saleski *et al.*, 2021).

Properties of the host cell could be modified to improve the detection limit of the biosensor. This has been shown by Hynninen *et al* (2010), in which the disruption of metal efflux transporters in the host cell can improve the detection limit of an inducible biosensor by up to 45-fold. The activities of influx and efflux transporters on the cell membrane maintain the cellular metal concentration; thus removing the efflux transporter causes the metals to accumulate in the cell and influence the concentration of available metals for detection by the FRET biosensor.

FRET measurement using confocal microscopy can be affected by photobleaching which causes loss of signals. The use of antifade-containing oxyrase enzymes provides a protection in live-cell imaging and was proven to minimize the photobleaching effect. These enzymes were isolated from *E.coli* plasma membranes and have the ability to metabolize free radical oxygen to reduce photobleaching (Thurston *et al.*, 2000). Therefore, further development of the biosensor should consider integrating the gene encoding oxyrase into the genes of *P. putida* to enable the enzymes to be produced without affecting the intracellular function. This will reduce the effect of photobleaching without the addition of the antifade reagent.

4.6 Conclusion

The FRET biosensor (fusion of CMT between eCFP and Venus) has been developed inside *P. putida* KT2440T7. The expression was based on the pEBP18-CMT vector under the control of a T7 promoter. Changes in the emission spectra of eCFP and Venus FP were observed following the exposure of the cells to Pb^{2+} , Cd^{2+} , and Zn^{2+} , indicating the sensing ability of the FRET biosensor. FRET measurement using confocal microscopy was successfully performed, providing accurate information on metal-induced FRET signals at the cellular level. The analysis of the FRET ratio images revealed that the detection limit of the FRET biosensor inside *P. putida* was $8.26 \pm 1.09 \mu\text{M}$ for Pb^{2+} , $68.35 \pm 11.73 \mu\text{M}$ for Cd^{2+} , and $204.007 \pm 29.72 \mu\text{M}$ for Zn^{2+} .

The comparison of FRET signals between *E. coli* and *P. putida* showed that the FRET biosensor in *P. putida* measured higher metal concentrations, particularly to Cd^{2+} and Zn^{2+} . This was probably due to the role of metal transporters in the cell membrane that maintain metal homeostasis in *P. putida*, thereby influencing the amount of metal sensed by the FRET biosensor. The standard curves of metal-induced FRET signals to Pb^{2+} , Cd^{2+} , and Zn^{2+} have been produced to describe the response of *P. putida* to metal exposure. This can potentially be used to measure the concentration of bioavailable metals in a real polluted environment. Therefore, the next experiment focused on applying this biosensor to monitor changes in heavy metal bioavailability as a monitoring tool to support the remediation of metal-contaminated soil. This research has identified further development needs of the biosensor to increase the stability of FRET biosensor expression, improve the detection limit inside the host cell and reduce the photobleaching effect.

5. A FRET biosensor for measuring the bioavailability of heavy metals in biochar-amended soil

5.1. Introduction

Bioavailability is an important parameter to measure the extent and potential risk of heavy metal contamination in soils (Peijnenburg *et al.*, 2007). Soil pore water is considered to contain the most mobile heavy metals in the form of free ions, hence potentially causing toxicity to soil organisms (Giller, *et.al.*, 2009). However, bioavailable metals are present in many forms, so a single measurement from soil pore water is often insufficient.

Analytical protocols based on chemical extraction methods are commonly used to determine the proportions of metal fractions in soils, which are operationally defined as exchangeable, carbonate-bound, hydrous-oxide bound, organic matter-bound and residual (Maiz *et al.*, 2000). This approach relies on the exchange of metals in the soil with extractants such as salts or weak acids, but does not directly represent the biological relevance of the metals. A biosensor is therefore an attractive approach to assess the biological impact of heavy metal toxicity as it directly measures metals at the location where damage occurs, i.e. within the cell cytoplasm.

Microbes play an essential role in soil function and productivity but are more sensitive to heavy metal stress than soil animals or plants (Chaudri *et al.*, 2008; Giller, *et.al.*, 2009). Some studies of heavy metal toxicity focus on the changes in activities and diversity within microbial populations without considering the actual impact at the cellular level. Various bacteria-based biosensors have been widely developed for sensing different metals, but only a few have been applied to environmental samples (Gireesh-Babu *et al.*, 2012, Roda *et al.*, 2012, Maderova *et al.*, 2013, Yoon *et.al.*, 2016a,b). The main challenge relates to the signal interference due to the complex nature of soils. This issue could be overcome by optimizing the experimental method and conditions to obtain a reliable and accurate measurement of metal bioavailability.

Current strategies for biosensor application in soil mainly involve mixing the soil samples with water or minimal salt solution. The biosensor cells are then exposed to the resultant soil suspension or supernatant for signal measurements (Song *et al.*, 2014; Yoon *et al.*, 2016a,b). In this method, the soil samples are diluted 10-20 times and shaken to break down soil aggregates. The pre-treatment process of soils with high dilution and shaking alters the soil conditions and can potentially release bioavailable metals, resulting in an overestimated

measurement. Direct application of biosensors in a soil slurry may offer a more representative measurement of the actual metal bioavailability. This approach still requires further development in which the host cells should be separated from the soil matrix, followed by subsequent signal measurement (Maderova *et al*, 2013).

The previous study (Chapter 4) showed that the FRET signals in *P.putida* were proportional to the concentration of heavy metals that were available to enter the host cell and bound with CMT. In this chapter the host cell was exposed to heavy metal-contaminated soil to evaluate changes in bioavailable metals following the use of biochar and compost amendments as a remediation method. The results from the biosensor deployment were used to assess the performance of biochar and compost in reducing the bioavailability of the heavy metals in the soil.

5.2. Aim and objectives

The aim of the experiment described in this chapter was to evaluate the application of *P.putida* bearing the FRET biosensor as a tool to measure the bioavailability of heavy metals in the remediation metal-contaminated soil amended with biochar and compost.

The objectives of this study are:

1. To develop an assay in which the biosensor can measure bioavailable heavy metals at the water field capacity of the soil, based on measurement of the FRET signals in cells separated from the soil or by direct measurement (soil *in situ*).
2. To integrate the biosensor results with other soil parameters: pH, extractable metals (NH₄NO₃ extraction), soil microbial activity (soil respiration) and phospholipid fatty acid (PLFA) profiles using stable isotope probing, to assess the effectiveness of biochar as an amendment for the remediation of metal contaminated soil.

Hypotheses:

1. Bacterial cells expressing the FRET sensor in soil samples will sense different fractions of metals: 1) cells present in pore water, which detect soluble metals, and 2) cells attached to soil or compost particles, which detect metals associated with a solid phase that cannot be readily extracted.
2. The bioavailable concentrations of heavy metals in soil which has not been amended with biochar and/or compost are high.
3. The biosensor can detect a reduction in metal bioavailability, indicating a shift in toxicity due to biochar and compost amendment, which can be independently

confirmed by (i) a decrease in metal solubility, (ii) improved soil microbial activity indicated by a higher CO₂ mineralization rate, and (iii) changes in the structure of the soil microbial community.

5.3 Methods

5.3.1 Experiment of Soil amendment with biochar and compost

5.3.1.1 Pot experiment set up

The contaminated soil used in this experiment was obtained from Wemyss Mine, an abandoned mine located 15 km southeast of Aberystwyth in Wales. Soil was dried at 20 ± 5 °C for 1 week and sieved through a 2 cm stainless sieve. Square plastic pots (width 10 cm, depth 20 cm) were lined at the bottom with fiberglass to avoid soil loss through the drainage holes. The pots were filled with soil or soil supplemented with organic amendments (biochar, compost, or both), as follows:

1. Soil (S): 1.2 kg of contaminated soil
2. Soil and biochar (S+B): 1.164 kg soil and 36 g biochar (3 % w/w)
3. Soil and compost (S+C), 976 g of soil and 224 g of compost (18 % w/w)
4. Soil, compost, and biochar (S+C+B): 940 g of soil, 36 g of biochar (3% w/w) and 224 g of compost (18 % w/w)

Each treatment was replicated four times. Deionized water was added to each pot until water holding capacity was reached. The pots were allowed to equilibrate for 7 days at 22 °C in the dark. The pots were protected with insulation material (Celotex, 100mm GA4100) to prevent overheating in summer or freezing in winter. The pots were placed on a raised bed in the outdoor compound at Arthur Willis Research Centre (Figure 5.1) and left for 18 months (April 2019-October 2020) under ambient environmental conditions.

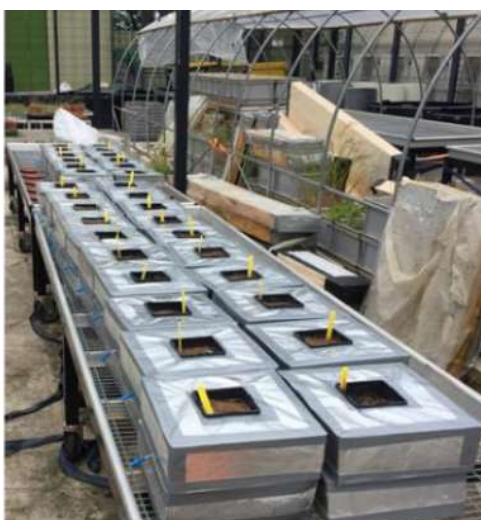


Fig. 5.1 Set up for outdoor pot experiment of soil amendment with biochar and compost (the experiment was prepared and carried out by Rosa Soria). The experiment was located at Arthur Willis Research Centre, Sheffield, UK.

The purpose of drying the soil was to obtain dry weight sample. The main reason for doing this step is because the mixing of soil with biochar and compost was carried out based on a dry weight basis. If the soil was wet, then mixing with biochar will not be accurate because some water in the soil can interfere with the weight measurement. Oven temperature of 40°C is considered not to severely affect the microorganisms in the soil. Few studies have reported that soil microorganisms can survive at temperature 40°C, this was shown by their capability to perform respiration in the soil. The respiration rate reduced at temperature above 40°C (Richardson, *et.al*, 2012; Liu, *et.al*, 2018). However, the drying process may affect the moisture content in the soil which was required by microbes. This was solved later by adding deionised water until water holding capacity was reached before starting the incubation.

5.3.1.2 Soil sampling and Analysis

Soil samples were collected after 18 months for physicochemical analysis (Table 5.1) and bioavailable metals measurement using the FRET Biosensor. Chemicals used for these analysis were Kanamycin (Thermofisher), IPTG, MOPS (3-(N-morpholino)propane sulfonic acid) (Sigma Aldrich), Pb(NO₃)₂, ProLong Live Antifade solution (1:100) (Thermofisher), NH₄NO₃ (Acros Organic), HNO₃ (Fisher Scientific), HCl (37%, Fisher Scientific), 13C-labelled glucose (Sigma Aldrich). Materials used were *P.putida* KT2440T7 bearing pEBP18-CMT, Biochar (WSP 550, UK Biochar Research Centre), 0.45 µm syringe filters (Fisherbrand™ Non-sterile PTFE Syringe Filter), 0.2 µm membrane (Whatman® Cyclopore® polycarbonate and polyester membranes, Merck), 10 mL syringe, 50 mL polyethylene centrifuge tubes, microscope slides, CoverWell™ Imaging Chambers (Grace Bio-Labs).

1. pH measurement

Soil samples were analysed for pH (Thermo Orion 5 star, FB68800 pH meter) and Electric Conductivity (JENWAY, 470 Cond meter) in a 1:2.5 (w/v) suspension of soil in deionised water (Beesley et al. 2010).

2. Total Heavy metals

Dried and sieved soils were placed in 15 mL glass tubes and digested with 5 mL of Aqua Regia (4:1, HCl:HNO₃) using HNO₃ (68%, Fisher Scientific) and HCl (37%, Fisher Scientific) for 4 hours at 120 °C in a heating block (Wawra et al. 2018). Following this, extracts were diluted to 25 mL with deionized water and filtered using 0.45 µm syringe filters (Fisherbrand™ Non-sterile PTFE Syringe Filter). All samples were analysed by ICP-MS (PerkinElmer, Sciex Elan DRCII).

3. Bioavailable heavy metals

Bioavailable heavy metals in soils were determined using NH_4NO_3 (1 M) according to Wawra et al. (2018). Briefly, 10 g of dried soil was weighed in flasks and filled up with 25 ml of 1 M- NH_4NO_3 solution. The flasks were shaken for 2 hours, let stand, and the soil solution was filtered. The filtrates were stabilized with 1% (v/v) of HNO_3 (65%) and the metal concentrations were determined by ICP-OES (Perkin Elmer Optima 7300).

4. Organic matter content

Organic matter in soil was determined using the $\text{K}_2\text{Cr}_2\text{O}_7$ titration method with FeSO_4 following the British Standard BS1377 (BS 2018).

5. Available ammonium

Ammonium (NH_4^+) was determined according to ISO, (1997), briefly, 2.0 g of soil was mixed with 20 mL of 2 M KCl solution for 1 hour at 120 rpm; the samples were filtered through 0.45 μm syringe filters (Fisherbrand™ Non-sterile PTFE Syringe Filter) and NH_4^+ determined with a continuous flow analyser (Skalar San+).

6. Available nitrate

Available nitrate was determined according to Miranda *et al.* (2001); 2.00 g of soil was mixed with 2M KCl solution and shaken for 30 min at 120 rpm in room temperature. The mixtures were filtered with 0.45 μm syringe filters. The filtrates were mixed with vanadium cocktail solution (1:1 ratio). This solution consisted of concentrated VCl_3 (400 mg VCl_3 in 50 mL 1M HCl), 2% sulphanilamide (2 g sulphanilamide in 100 mL of 5% HCl), 0.1% NEED (0.1 g N-ethylenediamine dihydrochloride in 100 mL water) and water in a volume ratio of 9.2: 139: 70: 1.15, respectively. The samples were incubated in the dark for 2 hours and measured at 540 nm using a UV-spectrophotometry (UV-2401PC, Shimadzu).

7. Available phosphate

Available phosphate was determined based on the Olsen method (Iatrou et al. 2014). Briefly, 2.00 g of soil was mixed with 40 mL of 0.5 N NaHCO_3 solution (pH 8.5) for 30 minutes at 120 rpm. The samples were filtered using 0.45 μm syringe filters and Phosphate was determined with the ascorbic acid method (Murphy and Riley 1962) at 880 nm by UV visible spectroscopy (UV-2401PC, Shimadzu).

Table 5.1 Physicochemical parameters of the biochar-amended soil experiment

Parameters	Methods
pH	pH meter
Electric conductivity (EC)	JENWAY, 470 conductivity meter
Organic matter content	BS1377-3:2018 (BS, 2018)
Available nitrate NO ₃ ⁻	Acidic Griess reaction (Miranda <i>et.al</i> , 2001)
Available phosphate PO ₄ ³⁻	Olsen method (Iatrou <i>et al.</i> , 2014)
Total heavy metals ¹	Aqua regia digestion followed by ICP-OES analysis
Bioavailable heavy metals ²	NH ₃ NO ₄ extraction

Notes

1: Assumed to be ‘total’ based on the complete digestion of the sample using the reagent indicated

2: Based on chemical extraction using the reagent indicated

Table 5.2 Soil samples used for biosensor test

Treatment	Pot Numbers
Soil (control)	20
	5
	24
	12
Soil + Biochar (3% w/w)	26
	27
	7
Soil + Compost (40% v/v)	8
	9
Soil + Biochar (3% w/w) + Compost (40% v/v)	4
	23
	31

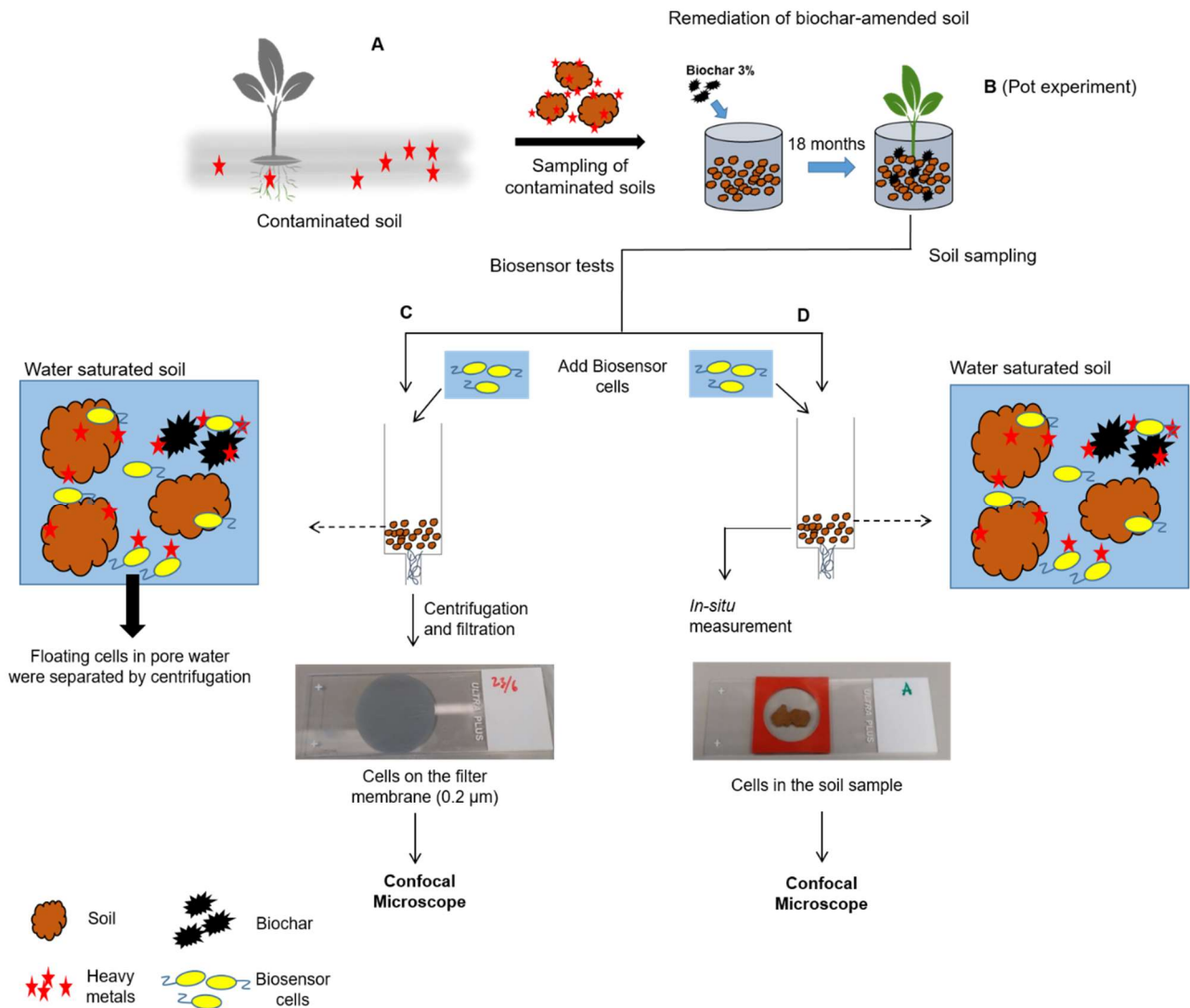


Fig. 5.2 Summary of FRET biosensor application to measure the bioavailability of heavy metals in soil remediation. Contaminated soil was sampled from an abandoned mine land in Wemyss (A). The contaminated soil was amended with biochar, compost, and mixture of biochar and compost in pot-scale experiment during 18-months incubation outdoors (B). Soil from the experimental pot was sampled for the analysis of metal bioavailability using the FRET biosensor. The biosensor cells were introduced directly into the soil samples at water holding capacity for sensing different fractions of metals: pore water (C) and metals associated with the solid phase (D). Cells present in pore water (C) were separated by centrifugation followed by filtration on a membrane for FRET signal measurement using a confocal microscope. *In-situ* measurement (D) was carried out as the cells were in contact with soil particles.

5.3.2. Biosensor Test

5.3.2.1 Preparation of Biosensor cells

P.putida KT2440T7 bearing pEBP18-CMT was recovered from a frozen glycerol stock. The cells were grown overnight in a selective LB liquid (10 µg/mL of Gentamicin and 20 µg/mL of Kanamycin) while shaking at 27°C. The overnight culture was transferred (10% v/v) into the same medium. Protein expression was induced by adding IPTG (0.125 mM final concentration). The cells were grown for 20 hours while shaking at 27°C for 20 hours.

Before harvesting the expression of fluorescent proteins (eCFP and Venus FP) was checked using the fluorescence microscope Nikon Eclipse LV 100. *P.putida* KT2440T7 expressing the FRET biosensor was harvested by centrifugation (3000 rpm for 10 minutes) and re-suspended with MOPS (3-(N-morpholino)propanesulfonic acid) medium (Sigma Aldrich) at pH 7. The final optical density (OD) was adjusted to 0.5, ready for soil application.

As part of quality assurance, the biosensor cells used over the experiment were grown in the same conditions (28°C, shaking at 120 rpm) including the same concentration of IPTG addition (final concentration of 1.25 mM according to Troeschel, *et.al*, 2012). This can help to maintain the expression level of the fluorescent protein pairs in all cells. The final OD of cells was maintained at 0.5 so that the cell numbers were expected to be the same for all experimental set up. The QC was performed by employing the negative control; the biosensor cells were exposed to MOPS buffer without the addition of heavy metals. The FRET ratio signals from these cells were expected to be lower than the cells exposed to the polluted soils.

The number of cells in the 0.6 ml was not measured during the experiment. The optical density (OD) was set at the value of 0.5 for all the experiments. The consistency of cell numbers was maintained by using the cells from the same batch culture with similar growing conditions. According to Yap and Trau (2019), the concentration of *E.coli* cells measured by spectrophotometer (600 nm) with the OD value of 0.5 may contain approximately $1 \times 10^9 - 1.5 \times 10^9$ cells/mL.

5.3.2.2 Initial test : soil exposure with cell separation

The initial application of the biosensor was carried out by introducing the host cells into the following soil samples at water holding capacity: 0.6 mL/gram (soil+biochar) and 0.8 mL/gram (soil+compost), followed by separating the host cells before the FRET measurement. A 5 gram dried and sieved soil sample was put into a 10 mL syringe in which the tip was covered by glass wool. A 3 mL volume of biosensor cells (OD 0.5) was added to 5 grams of soil sample

from the soil control and soil with biochar treatments. A 4 mL volume of biosensor cells was added to 5 grams of soil sample from the soil with compost treatment. The samples were incubated for period of time (1, 2, and 3 hours) at room temperature and put inside a 50 mL polyethylene tube for centrifugation (Figure 5.3). The difference in time incubation was used to determine the equilibrium between water, host cells and the soil samples as these could affect the number of cells that can be separated.

The water and cells were extracted from the samples by centrifuge at 1000 x g for 5 minutes. The water was collected and filtered through an 11 μm pore size filter paper (Whatman) to remove the soil particles. The filtrate was collected in a separate tube and filtered through a dark 0.2 μm membrane (Whatman® Cyclopore® polycarbonate and polyester membranes, Merck). ProLong Live Antifade reagent (Thermofisher) with a ratio of 1:100 was added to the host cells on the filter membrane. The filter membrane was placed on the microscope slide and covered with a coverslip. The FRET signal of the cells was measured using a confocal laser microscope (Zeiss LSM Airyscan). The settings on the confocal microscope were the same as when the cells were tested in heavy metal solutions (Chapter 4, section 4.3.7).

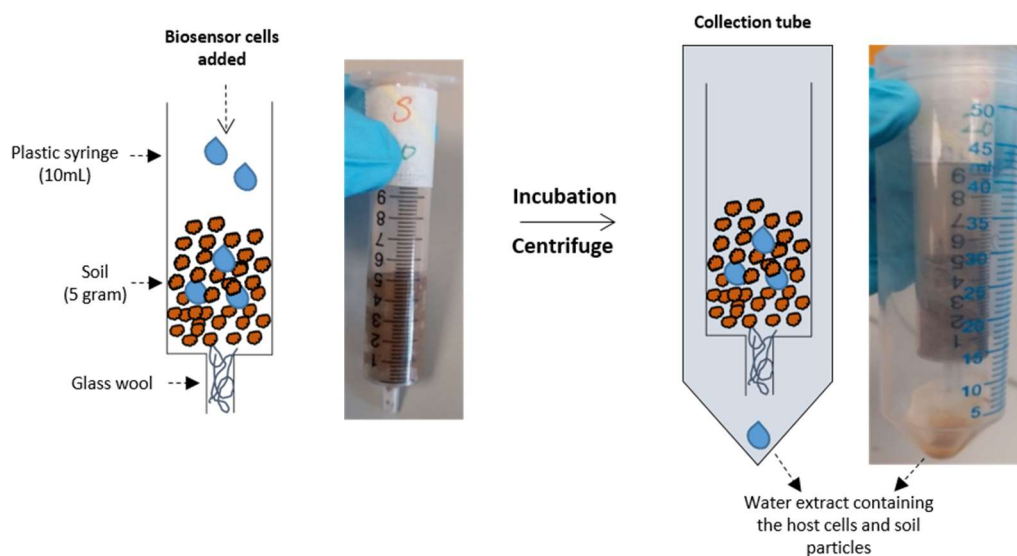


Figure 5.3 Experimental setup for the initial application of the biosensor. Biosensor cells were added to 5 grams of soil sample under various treatments until saturated in a syringe. The host cells were separated from the soil by centrifugation, followed by filtration and FRET measurement using a confocal microscope

5.3.3 Biosensor test: *In situ* soil measurement

In situ measurement was carried out by measuring the FRET signals directly under a microscope as the host cells were exposed to the soil samples. A 0.6 mL volume of biosensor cells (OD 0.5) was added to 1 gram samples from the pots of soil only (control) and soil with biochar treatments. A 0.8 ml volume of biosensor cells (OD 0.5) was added to 1 gram samples from the pots of soil with compost treatment. The mixture was incubated at room temperature for 3 hours.

Following the incubation, the soil sample was put on a microscope slide, ProLong Live Antifade solution (1:100) was added to the soil and covered with CoverWell™ Imaging Chambers (Grace Bio-Labs) (Figure 5.4). The FRET signal of the cells was measured by using a confocal laser microscope (Zeiss LSM Airyscan). The settings on the confocal microscope were the same as described in Chapter 4, Section 4.3.7



Figure 5.4. Biosensor assay for *in situ* measurement of bioavailable metals in soil samples. The soil sample containing biosensor cells was placed on a glass slide and covered with the imaging chamber. FRET signals of the host cells were measured using a confocal microscope.

The images of the FRET emission ratio in *P.putida* host cells were processed using ImageJ (Fiji) as described in Chapter 4, Section 4.3.7. Fluorescence emission from the soil particles may interfere with the fluorescence signals of the biosensor. Therefore, Channel 1 (eCFP emission) and Channel 2 (Venus FP emission) were merged and used to distinguish the fluorescence signals of the host cells from the background of the soil samples.

5.3.4 Estimation of bioavailable metal concentrations

The concentration of bioavailable metals in the host cell was determined from the standard curve of *P.putida* bearing FRET sensor in response to Pb^{2+} (Chapter 4, Figure 4.16-A). This metal was selected because it is highly toxic and constitutes a large fraction of the heavy metals in the Weymss soil. The *in vivo* binding test revealed that the biosensor exhibits a greater

response to Pb^{2+} than Cd^{2+} or Zn^{2+} (Chapter 4). The standard curve to Pb^{2+} fitted to a simple binding affinity model (Equation 1):

$$R = \frac{[M].FRET_{max}}{K_a + [M]} \quad (1)$$

where R is the FRET emission ratio of the biosensor, $FRET_{max}$ is the FRET ratio maximum (366) at a saturating metal concentration (50 μM), K_a is the half-maximum concentration of metal-binding affinity (8.26 μM), and M is the concentration of bioavailable metal in the system (μM).

The FRET emission ratio of cells in each pot was corrected using the mean value of cells in the absence of metals (control). The bioavailable metal concentration detected by each cell (M) was calculated using the variables in Equation 1. The FRET signals can be higher than the maximum (R_{max} : 366) for several reasons: 1) the R_{max} value from curve fitting is an average (with a measure of variance, so in a set of measurement some signals will be higher), and 2) the FRET sensor may respond differently at high metals concentration, due to a reduction in signals under these conditions.

5.3.5. *In situ* biochar test

As a control experiment, the host cells were exposed to biochar saturated with Pb, in which the FRET signals were measured directly using the confocal microscope. Biochar (WSP 550, UK Biochar Research Centre) was dried and ground to obtain particles less than 2 mm. A 20 mL volume of $Pb(NO_3)_2$ solution (1 mM) pH 6.8 was added to 200 mg of biochar in a 50 mL polyethylene. A 20 mL volume of deionised water was added to 200 mg of biochar as a negative control. The mixtures were incubated at room temperature for 18 hours while shaking at 120 rpm.

The mixtures were filtered using 11 μm pore size filter paper (Whatman) to separate metal-saturated biochar. A 0.12 ml volume of biosensor cells (OD 0.5) in MOPS media was added to 200 mg of metal-saturated biochar and incubated for 3 hours at room temperature. As a control the cells were also added to biochar without Pb^{2+} exposure. Following the incubation, the biochar samples were put on a microscope slide, ProLong Live Antifade solution (1:100) was added to the sample and covered with CoverWell™ Imaging Chambers (Grace Bio-Labs). The

FRET signal of the cells was measured using the confocal laser microscope (Zeiss LSM Airyscan).

The biochar samples were extracted with NH_4NO_3 . A 200 mg sample of biochar was added to 5 ml of NH_4NO_3 (1M, Acros Organic) and incubated overnight while shaking. The mixture was filtered using a 0.2 μm syringe filter to separate the biochar particles. The filtrates were acidified with 1%(v/v) of HNO_3 (Fisher) and the metal concentrations determined by ICP-OES.

Total heavy metals in the biochar samples were determined according to ISO standard 169:2013 (ISO, 2013). A 200 mg sample of biochar was placed in a glass tube and mixed with 5 ml of Aqua Regia (4:1, $\text{HCl}:\text{HNO}_3$) using HNO_3 (68%, Fisher Scientific) and HCl (37%, Fisher Scientific). The mixture was digested at 120 °C for 4 hours and allowed to cool at room temperature. The mixture was filtered using 0.2 μm pore size syringe filter to separate the biochar particles and brought to final volume of 10 mL with deionised water. The concentration of metals was determined by ICP-OES.

5.3.6 Statistical analysis

An ANOVA test was used to evaluate any significant differences of physicochemical parameters between soil treatments, followed by the Tukey HSD post-hoc test. The level of significance was set to 0.05.

For the image processing data, cells were identified as objects >2 pixels in size and the mean value for each cell extracted from the channel (FRET ratio image). The mean value for each cell in the FRET ratio image was copied and transferred into an excel file in csv. format for graphing and statistical analysis using R version 3.52 (R core Team 2018). A Violin plot was used to visualize the distribution of the FRET signals and their probability density. A normality test was performed to check whether the data was normally distributed for each experimental pot. If the data is not normally distributed, the differences in FRET signals among the treatment group were calculated using a non-parametric Kruskal-Wallis test, followed by pairwise comparison using the Wilcoxon signed-rank test. All significant levels were quoted at the 95% confidence level ($p < 0.05$).

5.3.7. Analysis of soil respiration and PLFAs

The effect of biochar as an amendment on microbial activity in metal-contaminated soil was assessed within a secondment undertaken at Boku University, Austria. The secondment was conducted in collaboration with another research student (Rosa Soria). The experiment involved investigation of respiration rate (CO₂ production) attributed to mineralisation of isotopically labelled substrates (glucose and cell biomass) and changes in microbial community composition, based on phospholipid fatty acid (PLFA) profiles, using stable isotope probing.

The main reasons for using the PLFAs in this experiment are: 1). Analysis of microbial lipids is simple and can be used as a biomarker that reflects the distinct and characteristic lipid composition of microbial families (Watzinger, 2015), 2.) Phospholipids represent the living microorganisms because the degradation of PLFAs is within minutes to hours with the half time of 2.7 days (faster than nucleic acid and proteins) (Kindler, *et.al*, 2009), and 3). Total PLFAs analysis can be used as a proxy for total microbial biomass simply by calculating the sum of PLFAs from all microorganisms detected (Wawra, *et.al*, 2018).

5.3.7.1 Soil preparation and set up of experiment

A 1 kg of the contaminated soil was mixed with 3% (w/w) of biochar WSP550 (Biochar Research Centre, UK) and placed in a plastic pot (wide x length x depth; 15 x 15 x 10 cm). Another 1 kg of soil without biochar addition was used as a control. Deionised water was added into the soils (biochar treatment and control) until 60% of water holding capacity was reached. Both samples were incubated at room temperature for one week.

Two chemical compounds were used in the experiment: ¹³C-labelled glucose (Sigma Aldrich, 99% ¹³C atom) as an easily biodegradable substrate and ¹³C-labelled *E.coli* DH5α strain bacteria biomass as a complex substrate. The bacteria biomass was prepared by cultivating the in M9 minimal media (Cold Spring Harbor Protocol, 2010) containing 1 g/L of ¹³C-labelled glucose 99.9% (Sigma Aldrich). The incubation was carried out in shaker (120 rpm) at 28°C for 24 hours. The culture was harvested by centrifugation (3000 rpm for 10 minutes) and freeze-dried.

a. Soil substrate-induced respiration

The objective of this experiment was to measure the activity (respiration process) of microorganisms in the soil following the biochar addition. The respiration was evaluated based on the ability of soil microbes to mineralize ¹³C-labelled glucose and ¹³C-labelled bacteria biomass as the substrates.

A 2 gram sample of soil from each biochar-amended soil and control experiment was put into 20.5 mL glass vial (5 mL). 100 μ L volume of substrate solution (equal to 500 μ g of solid substrate) was added into the soils. The experiment was carried out in five replicates. Following the substrate addition, the vials were closed with rubber septum and immediately flushed with synthetic air (no CO₂). The measurement of CO₂ inside each vial was carried out using EA-IRMS (Elemental Analysis-Isotopic Ratio Mass Spectrometry coupled with Delta V Advantage, Thermo Scientific, Germany) every 4 hours during 48 hours (for glucose substrate) and 96 hours (for biomass substrate).

b. PLFA

Extraction of PLFA was carried out from the soil samples after the CO₂ respiration measurement have been completed. The extraction procedures were performed according to Watzinger (2015), which consisted of four stages: lipid extraction, separation, methylation, and fatty acid measurement. 2 grams of soil samples from each vial were mixed with 1.7 ml citric buffer (0.085 M citric acid, 0.065 M tri-potassium citrate adjusted at pH 4), 2.1 ml chloroform, 3.2 ml methanol and 1.00 ml 19:0 PLFA methanol (15 nmol PLFA standard), followed by incubation overnight at room temperature. The mixture was centrifuged at 2000 g for 1 minute and the supernatant was collected for further processing. Lipids in the supernatant were separated using solid phase extraction columns (Isolute SI) filled with a 500 mg unbonded silica, 50 μ m in diameter and 60 Å pore size. The separated lipid was mixed with 1 ml of 0.2 M KOH in methanol for methylation and to transform the phospholipids into fatty acid methyl esters (FAMES).

The final samples were collected in GC-vials and stored in the dark in at -20 °C. Analyses of FAMES were carried out using a GC-c-IR-MS (gas chromatography— combustion— isotopic ratio mass spectrometry) with an HP5890 Series II (Agilent, Santa Clara, USA) connected to a Delta S via a Combustion II Interface (Finnigan, Bremen, Germany). The sample (4 μ M) was injected into the GC column at a temperature of 70 °C for 2 min, then subsequently increased stepwise to 160 (15 °C min⁻¹) and 280 °C (2.5 °C min⁻¹). 300, 200, 100, 50 μ M 13:0 FAME (Methyltridecanoate) and 19:0 FAME (Nonadecanoate) in isooctane were used as FAME standards. Isotopic ratios and areas were analysed to determine the total ¹³C-PLFA and related fatty acid compositions.

5.4. Results

5.4.1 Physicochemical parameters of soil samples

The pot experiment of soil amendment with biochar and compost was carried out by Rosa Soria a separate research project. Soil samples from her experiment were used to test the performance of the FRET Biosensor in measuring the bioavailable metals from a real environmental sample. Rosa also performed the physicochemical analysis of the soil samples (Table 5.1) and the data were used in this thesis (Figure 5.5) as a comparison with the results from FRET biosensor measurement.

The physicochemical properties of the soil samples (after 18 months of outdoor incubation) from selected experimental pots are summarised in Figure 5.5 and Figure 5.6. The data was provided by Rosa Soria (see Appendices 4 for the raw data) and shown here for comparison with the biosensor function. The pH of the contaminated soil was acid, within the range of pH 4.9-5.1. Treatment with biochar significantly increased ($p < 0.05$) the pH to pH 5.4-5.5. The addition of compost caused the pH to increase pH 7.0–7.2, which was not significantly different ($p > 0.05$) from the mixed biochar and compost treatment.

There was no significant difference ($p > 0.05$) in organic matter content and available phosphate between the control soil and biochar-treated soil. These parameters were increased significantly ($p < 0.05$) due to the addition of compost. No significant differences between treatments were observed for ammonium or nitrate ($p < 0.05$). But the results indicated that a higher concentration of nitrate was found in all treatments relative to the concentration of ammonium. This was supported by Bandara *et.al*, (2021) who mentioned that an increase in pH due to biochar application can stimulate nitrifiers microbes in acidic soil. A high degree of nitrification process resulted in a high level of nitrate production in the soil.

Ammonium and nitrate are common forms of nitrogen which that be taken up by organisms in soils. However, nitrate is the most available source of nitrogen for plants and microbes. Ammonium is more likely to bind with minerals and organic colloids in the soil, therefore becoming less available for cellular uptake (Marschner *et.al*, 1987, Florio *et.al*, 2015).

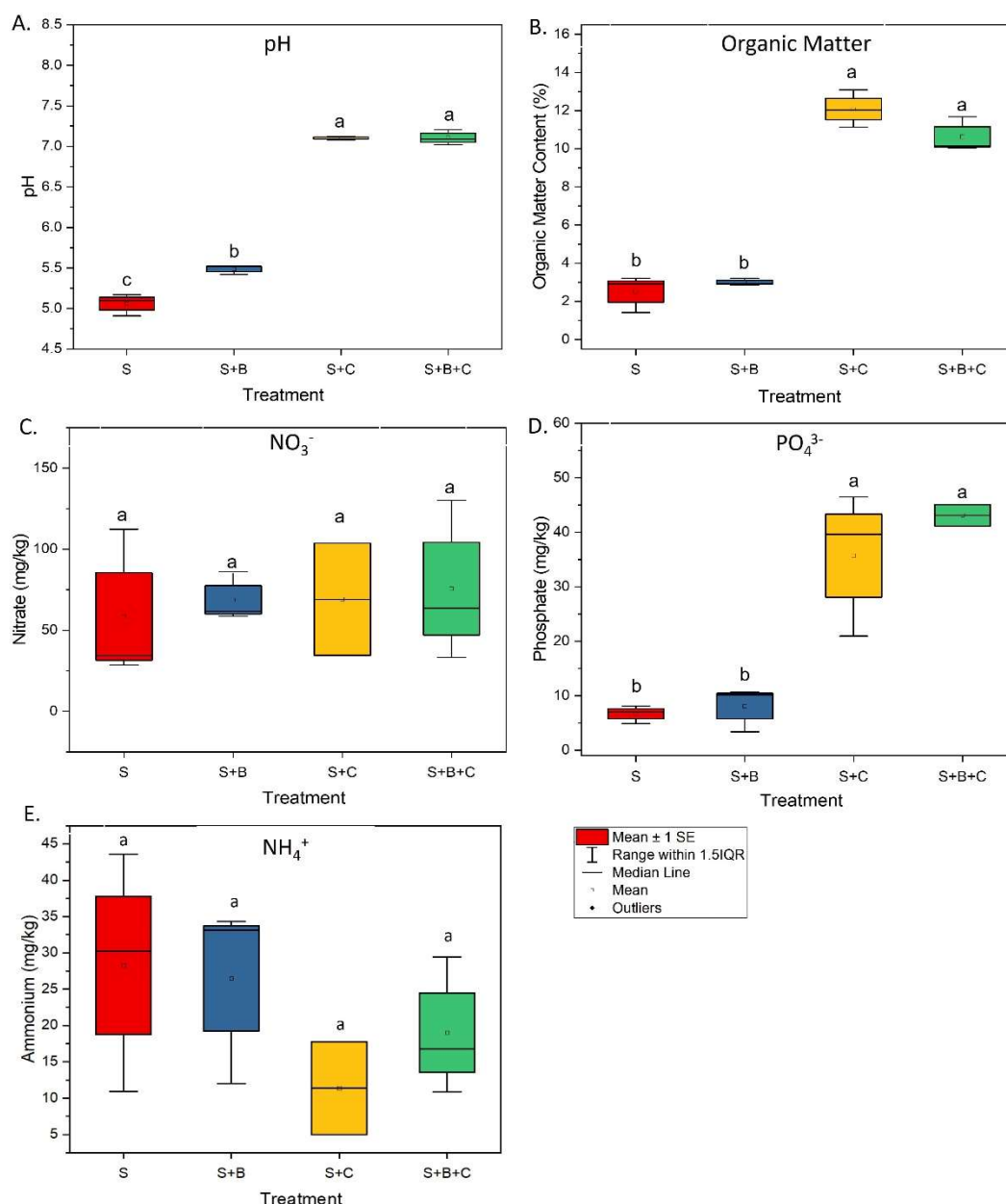


Figure 5.5 Box plot of physicochemical parameters of the soil samples showing the data mean, range, and median for pH (A), organic matter content (B), available nitrate (C), available phosphate (D), and available ammonium (E). Error bars represent the standard error with the number of sample (n)=3. The different letters indicate significant differences between the treatments ($p < 0.05$; one-way ANOVA, Tukey's honestly significant difference (HSD) post hoc test).

Pb and Zn were the major heavy metal contaminants (Figure 5.6). The average concentration of Pb was 3347 mg/kg and Zn was 2109 mg/kg. The total zinc was not significantly different ($p > 0.05$) in the biochar treatment but decreased significantly ($p < 0.05$) in the compost treatment. Total cadmium was very low, with an average concentration of 123 mg/kg in the contaminated soil. The total heavy metal concentration does not provide information on

bioavailability and therefore a chemical extraction using NH_4NO_3 was employed to determine metal solubility.

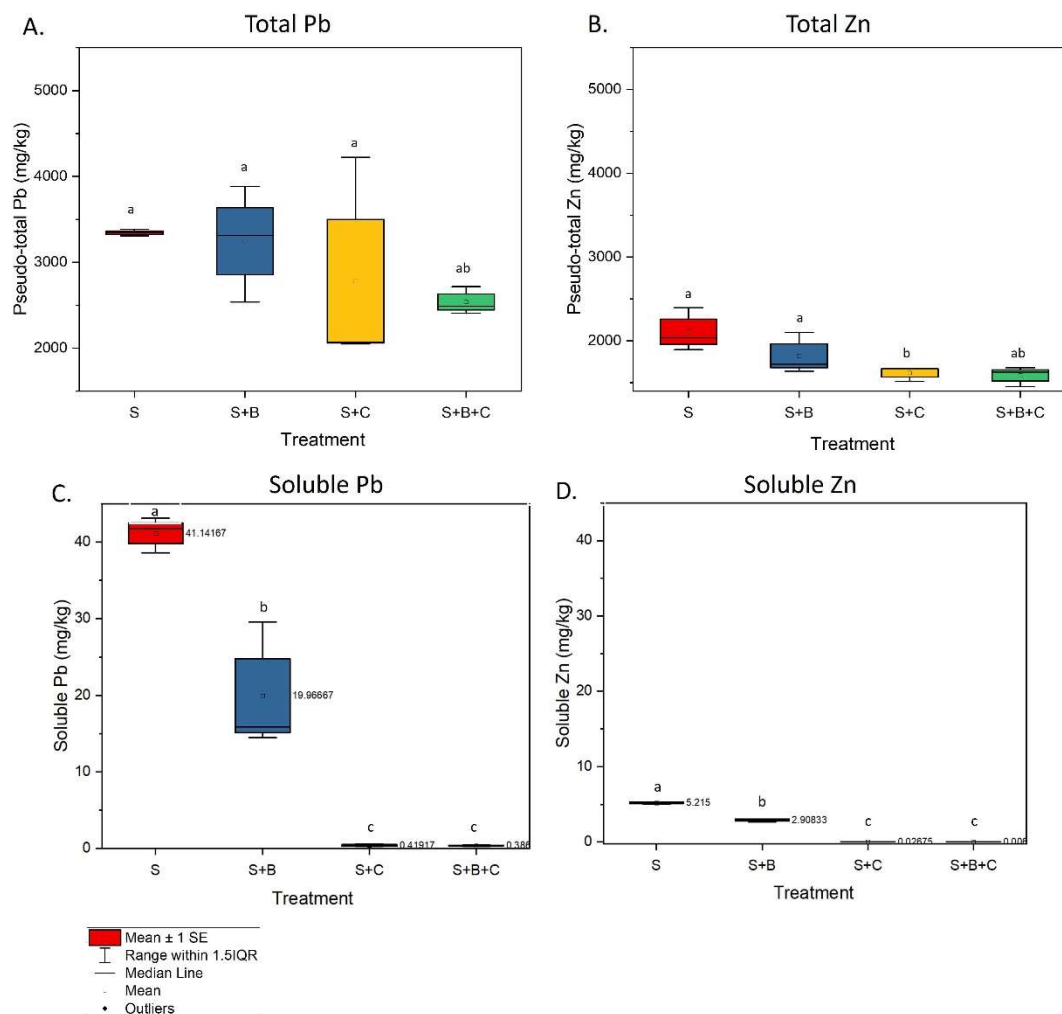


Figure 5.6 Box plot of physicochemical parameters of the soil samples showing the data mean, range and median for the concentration of total Pb (A), Zn (B), and concentration of soluble metals Pb(C) and Zn(D) measured by NH_4NO_3 extraction. Error bars represent the standard error with the number of sample ($n=3$). Different letters indicate significant differences between the treatments ($p < 0.05$; one-way ANOVA, Tukey's (HSD) post hoc test).

Soluble metals extracted by NH_4NO_3 were considered as bioavailable. Soils without amendment exhibited an average bioavailable Pb of 16.45 mg/L, which was reduced significantly ($p < 0.05$) to 7.98 mg/L with biochar treatment. Amendment with compost and a mixture of compost and biochar further reduced the bioavailable Pb to 0.16 mg/L and 0.154 mg/L, respectively, but they are not significantly different. Bioavailable Zn was approximately 70-80% lower than Pb. There was a significant reduction in Zn, from 2.08 mg/L in control soil to 1.16 mg/L in biochar treated soil. There was a further reduction in Zn to 0.01 mg/L and

0.002 mg/L, respectively, in the amendment with compost and a mixture of compost with biochar.

5.4.2. Biosensor function in soil-water extracts

The host cells that were incubated in the soil samples at time intervals were separated by centrifugation. Pore water containing the host cells and some soil particles accumulated at the bottom of the collection tube following the centrifugation (Figure 5.3). The results showed that the host cells can be extracted from soil samples after incubation for 2 hours. The purpose of centrifugation was to separate or extract the biosensor cells from the soil matrix. This only applies if the incubation of cells in the soil is less than 2 hours. Incubation more than 2 hours can cause the soil equilibrium to be reached so the cells are strongly adsorbed onto the soil matrix and become more difficult to be separated by centrifugation. No cells can be extracted after 3 hours of incubation, possibly because the equilibrium within the soil has been reached.

The FRET signal of the host cells separated from the soil samples are compared with cells in the absence of metal in Figure 5.7 below. Cells in the absence of metal exhibited a median FRET signal of 387, which increased to 662 in cells extracted from soil without amendment (S-Pot20). Cells extracted from biochar-amended soil samples (S+C-Pot 8) experienced a reduced FRET signal to 640 and further reduction to 425 and 369 in samples of compost and mixture of compost with biochar, respectively.

The FRET signals of host cells extracted from soil samples were not normally distributed. This can be seen most clearly with signals from soil with compost addition. Statistical tests revealed significant differences in the FRET signals (Kruskal-Wallis, $p < 0.01$; Chi-squared = 92.70) for all treatments, except for the comparison between soil and soil+biochar, as well as between soil+compost+biochar and cells in the absence of metals (Wilcoxon rank, $p > 0.05$) (Table 5.3).

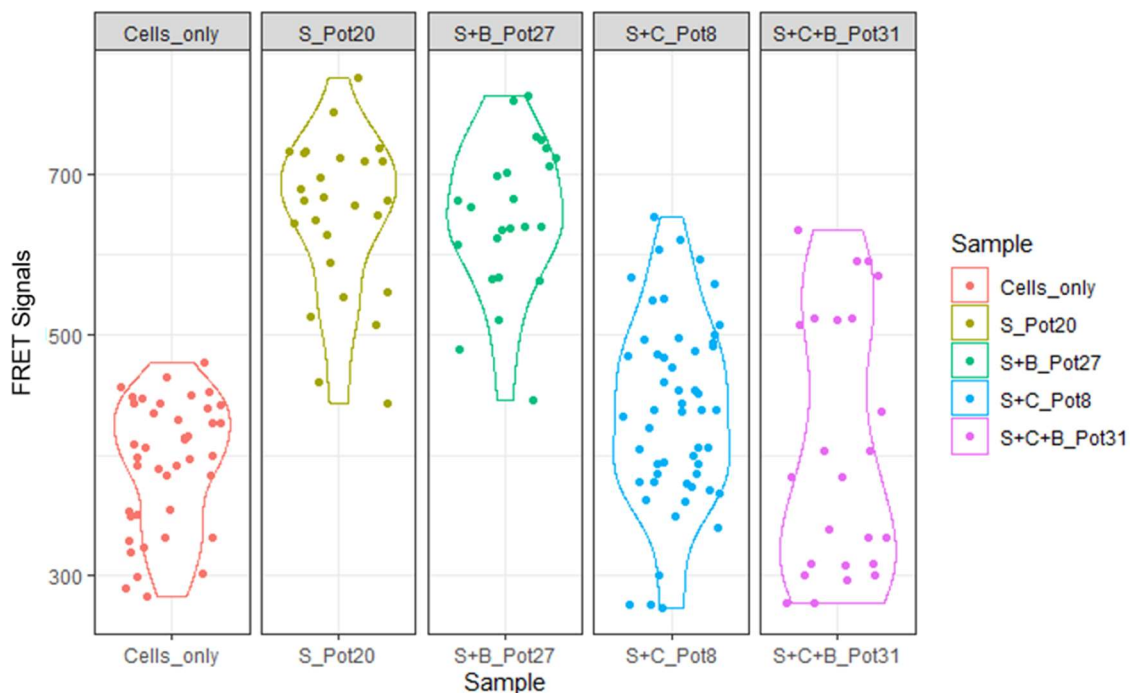


Figure 5.7 FRET signals in the host cells after exposure to soil (S_Pot20), soil+biochar (S+B_Pot 27), soil+compost, (S+C_Pot 8) and soil+compost+biochar (S+C+B_Pot31) samples. The host cells were separated from the samples and the FRET signals were measured on the cells attached to the filter membrane. The signals were compared to host cells in the absence of metals as a negative control. Each dot represents the emission ratio signal from a single cell.

Table 5.3. Summary of Pairwise comparison using Wilcoxon rank between soil treatments

Treatment	Cell_only	S_Pot20	S+B_Pot27	S+C_Pot 8
S_Pot20	p<0.001	-	-	-
S+B_Pot27	p<0.001	p= 0.84	-	-
S+C_Pot 8	p<0.01	p<0.001	p<0.001	-
S+C+B_Pot31	p= 0.83	p<0.001	p<0.001	p= 0.21

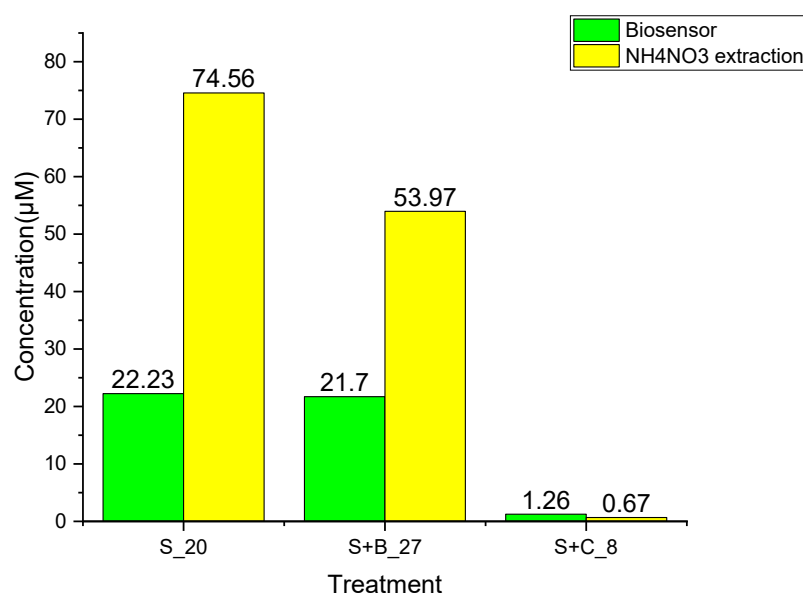


Figure 5.8 Comparison of bioavailable Pb^{2+} detected by the biosensor extracted from soil samples and soluble Pb (NH_4NO_3 extraction) from each treatment pot. Bioavailable Pb^{2+} was determined from the standard curve of the host cell in response to Pb^{2+} . The concentration of metal from NH_4NO_3 was converted into micromolar (μM) to obtain the similar unit with the biosensor measurement. Treatments: soil control without amendment (S_20), soil+biochar amendment (3%) (S+B_27) and soil+compost amendment (S+C_8).

The concentration of bioavailable Pb^{2+} was calculated based on the standard curve of the host cells in response to Pb^{2+} (see section 5.3.4 above) and the results were compared with bioavailable Pb obtained from the NH_4NO_3 extraction. The results show that bioavailable Pb^{2+} in soil without treatment was $22.23 \mu M$, which is slightly higher than soil with biochar ($21.7 \mu M$), but this was reduced to $1.26 \mu M$ in soil with compost treatment (Figure 5.8). A similar trend can be observed from the results of soluble Pb extracted by ammonium nitrate, in which the metal concentration reduced by up to 28% and 99% in soil amended with biochar and compost, respectively. Bioavailable Pb^{2+} detected by the biosensor was approximately 30% and 40% lower than the that in the ammonium nitrate extraction in the control soil and biochar-amended soil.

5.4.3. *In situ* soil measurement

The FRET signals were measured directly while the cells were exposed to the soils. The cover well chamber provided a stable environment for measuring the FRET signals under the microscope. The host cells expressing the FRET biosensor could be distinguished from the soil background by merging the images of Channel 1 (eCFP emission) and Channel 2 (Venus FP

emission) (Figure 5.9-C). This allowed image processing to measure the distribution of emission ratio signals inside the cells, as shown in images D and E.

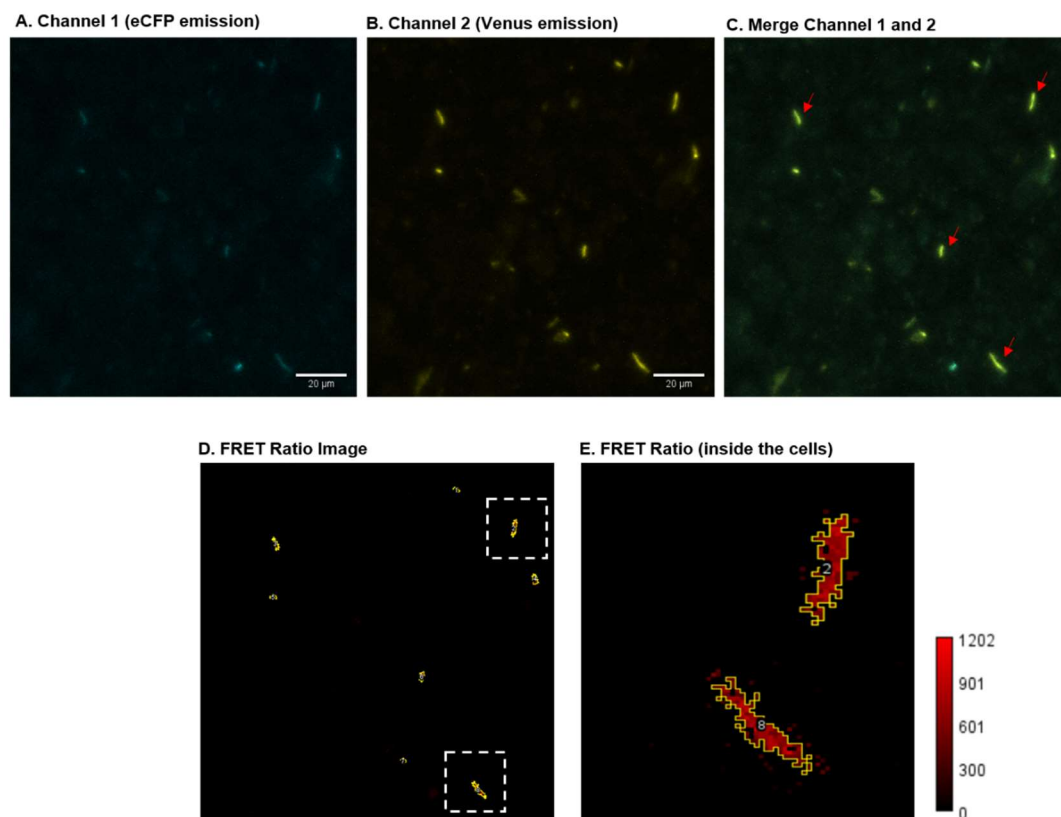


Figure 5.9 Representative images of *P.putida* KT2440T7 expressing the FRET biosensor after exposure to the contaminated soil samples. Emission signals of eCFP (A) and Venus FP (B) can be observed inside the cell. The merging of Channels 1 and 2 (C) allows observation of the host cells as indicated in the red arrows. The FRET ratio of the host cells was obtained from image processing using ImageJ (Fiji). The region of interest (white square) was selected on Image C to show the pixel distribution of the FRET signals inside the host cells (image D). Level of FRET signals (mean gray value) inside the cell is shown in the red colour bar.

Visualization of the host cells exposed to soil only, soil+biochar, and soil+compost treatment are shown in Figures 5.9 and 5.10, respectively. Some cells exposed to soil without amendment show higher emission ratio signals than soil treated with biochar and compost (see colour bar). This indicates that the FRET biosensor can detect the presence of bioavailable metals from the soil samples.

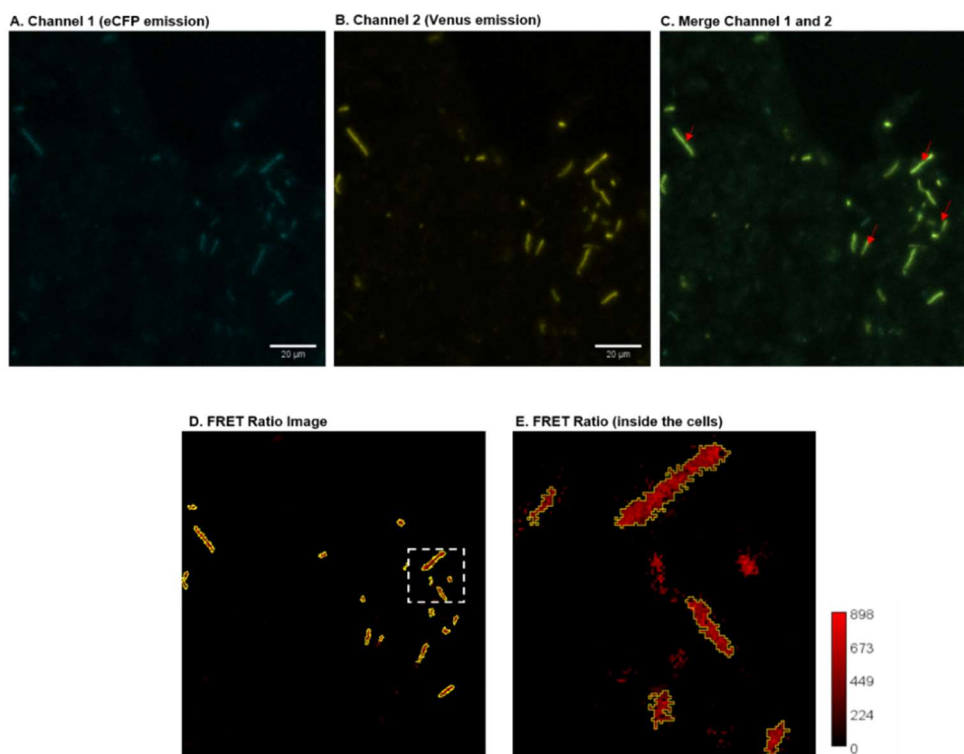


Figure 5.10 Representative images of *P. putida* KT2440T7 expressing the FRET biosensor after exposure to the biochar-amended soil. Emission signals of eCFP (A) and Venus FP (B) can be observed inside the cell. The merging of Channels 1 and 2 (C) allows observation of the host cells as indicated in the red arrows. The FRET ratio of the host cells was obtained from image processing using ImageJ (Fiji). The region of interest (white square) was selected on Image C to show the pixel distribution of the FRET signals inside the host cells (image D). Level of FRET signals (mean gray value) inside the cell is shown in the red colour bar.

The FRET signals in response to bioavailable metals in each soil treatment is shown in Figure 5.11. In the absence of metal, cells show a median FRET signal of 260 with limited variance between individual cells. When the cells were in contact with contaminated soil, the FRET signals were higher and the distribution of individual cells much greater, indicating heterogeneity in the samples. A Kruskal-Wallis test showed that all amended soils gave a higher signal than the cells without heavy metals ($p < 0.05$). The highest values were obtained from soil without amendment (median value of 581), decreasing in the order: soil+biochar (median value of 527), soil+compost (median value of 388) and soil+biochar+compost (median value of 364). All FRET signals in soil samples were much higher than in the cells without heavy metals. At the other extreme, in soil+biochar+compost samples, some cells had FRET signals similar to cells without heavy metals. Figure 5.11 shows that the FRET signals were reproducible, as indicated by the similar distribution pattern from each pot in the same treatment.

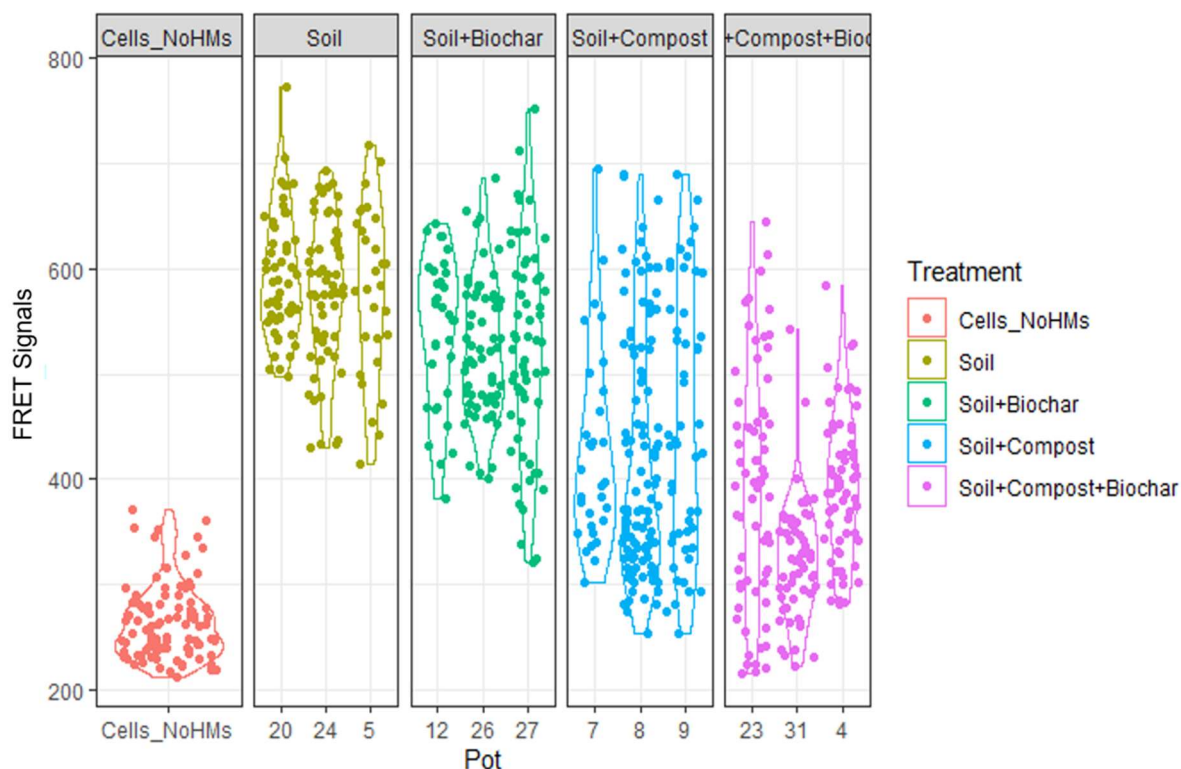


Figure 5.11. FRET signals in the host cells exposed to soil, soil+biochar, soil+compost, and soil+compost+biochar compared to the host cells without metal exposure. The FRET signals within host cells were measured directly from the soil samples using a confocal microscope. Each dot represents the emission ratio signals from a single cell. Signals from 50 cells were measured from soil in each pot to give a representative measurement. The distribution of the signal is shown as a violin plot.

The amount of bioavailable Pb^{2+} in soil samples was calculated from the standard curve based on the binding of Pb^{2+} with CMT inside *P.putida* cell (Figure 4.17, Chapter 4). The concentration of bioavailable Pb^{2+} in each experimental pot is shown in (Appendices V). A plot of average metal concentration from three pots for each treatment with corresponding mean FRET signals is shown in Figure 5.12. Soil without amendment contained the highest bioavailable metal concentration ($39.29 \pm 1.28 \mu M$), with a significant reduction ($p < 0.05$) in the treatment with biochar ($28.24 \pm 1.6 \mu M$), compost ($13.69 \pm 2.01 \mu M$) and the mixture of biochar with compost ($6.28 \pm 1.81 \mu M$). These results show that amendment with biochar and compost mixture was the most effective treatment in reducing the bioavailable heavy metal concentration.

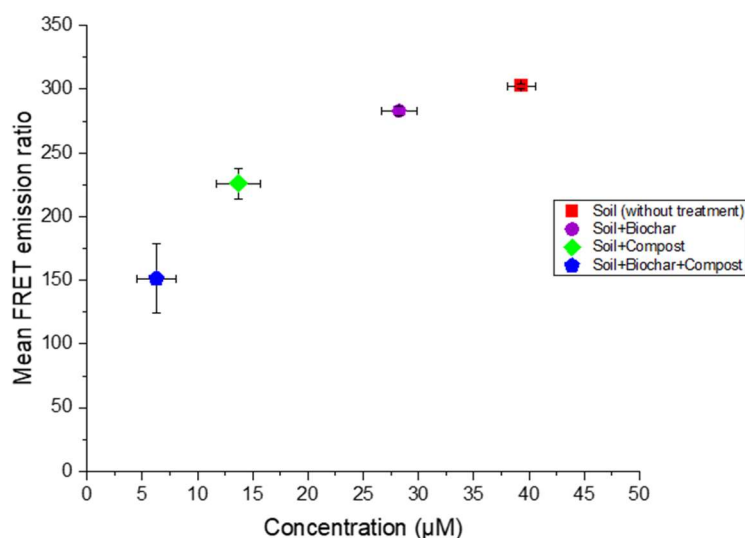


Figure 5.12 Bioavailable metal concentrations were obtained from the analysis of the FRET ratio inside the host cells. The concentration was calculated by subtracting the mean FRET value of the host cell (in the absence of metal). Each dot represents the mean concentration from 3 pots for each treatment. Different colors distinguish treatments between biochar, compost and a mixture of biochar and compost. Error bars represent standard error from concentration and mean FRET signals from all cells in each treatment.

5.4.4 Comparison of *in situ* biosensor measurement with soluble metal based on NH_4NO_3 extraction

Figure 5.13 compares the bioavailable metals measured by the biosensor (*in situ* measurement) and NH_4NO_3 extraction. Both analyses show that amendment with biochar can reduce the bioavailability of heavy metals and amendment with a mixture of biochar and compost enhances the reduction. However, the bioavailable metals measured by the NH_4NO_3 extraction

were overestimated. Data from the control soil shows that the average extractable metal was approximately 49% higher than the biosensor measurement. A similar trend was observed for the soil + biochar samples, which were 24% higher. In contrast, data from soils with compost and biochar + compost treatments show the bioavailable metal measured from NH_4NO_3 extraction was 94% and 88% lower, respectively, than that measured by the biosensor.

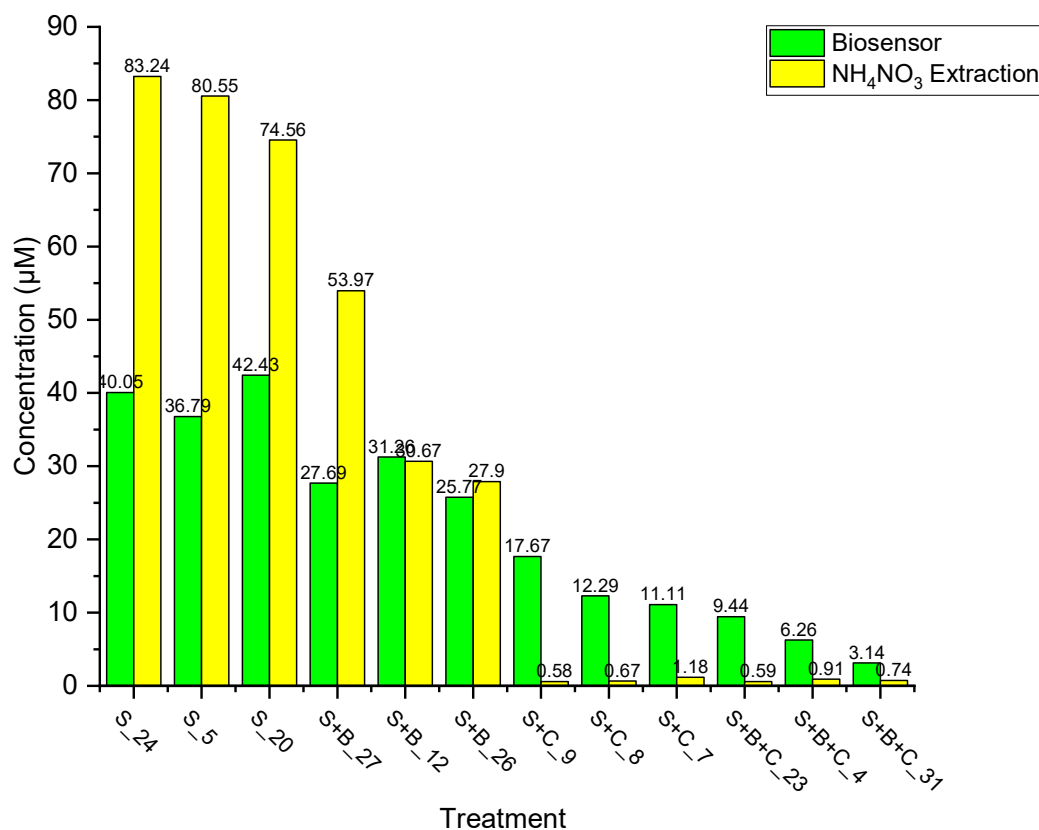


Figure 5.13 Plot of bioavailable metal concentrations from NH_4NO_3 extraction and biosensor measurement. Concentrations measured by the NH_4NO_3 extraction were converted into moles for comparison with the biosensor results. Treatments: soil control without amendment (S_24,5,20), soil+biochar amendment (3%) (S+B_27,26,9), soil+compost amendment (S+C_9,8,7) and soil+biochar+compost amendment (S+B+C_23,4,31).

5.4.5. *In situ* biochar test

The host cells were exposed to biochar saturated with Pb^{2+} so that the FRET signal response to Pb^{2+} accumulation on the biochar surface could be determined (Figure 5.14). In the absence of metal, cells show a median FRET signal of 294. The FRET signal increased significantly ($p < 0.05$) when the cells were in contact with metal-saturated biochar, in which the median FRET signal was 463. The cells exposed to biochar without metal saturation showed a median FRET signal of 343, which was significantly lower ($p < 0.05$) than metal-saturated biochar but significantly higher ($p < 0.05$) than cells in the absence of metal.

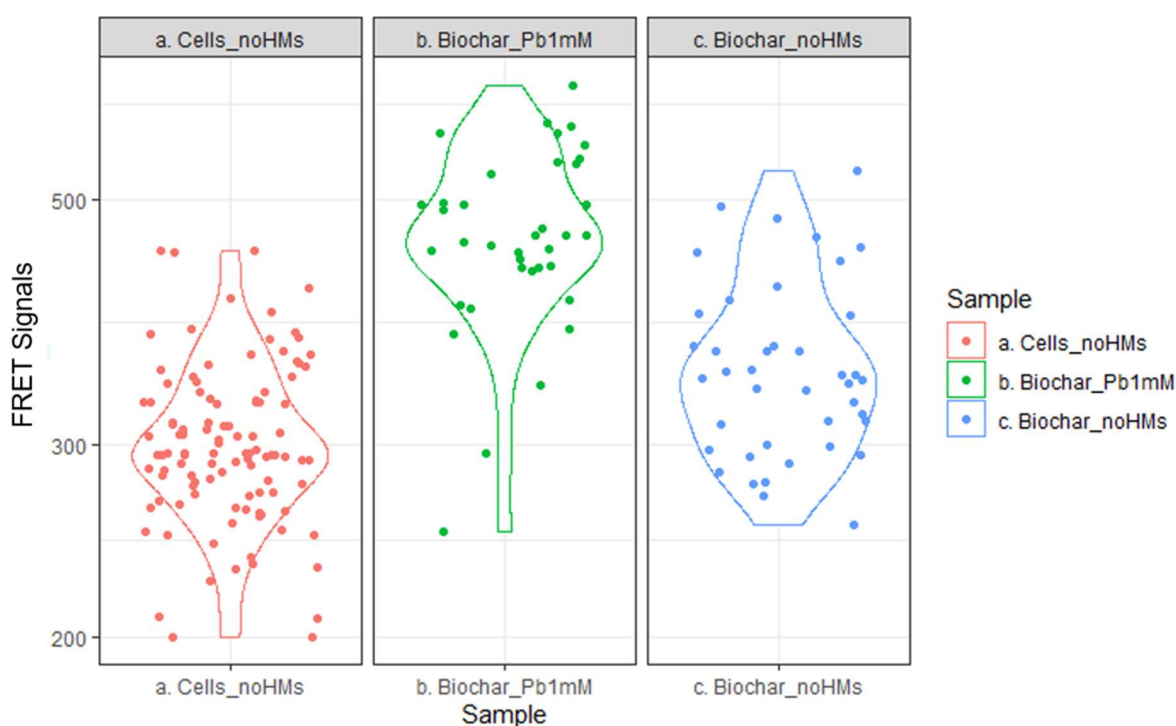


Figure 5.14 FRET signals in the absence of metal compared to cells exposed to biochar saturated with Pb^{2+} (1mM) and biochar without metal saturation. Each dot represents the emission ratio signal from a single cell. The FRET signals were statistically analysed using a Kruskal Wallis test followed by Pairwise comparison using Wilcoxon rank between each sample. The significance level was indicated by a p value < 0.05 .

Bioavailable Pb^{2+} sensed by the biosensor from metal-saturated biochar samples was $6.73 \mu M$, which is 6-times lower than metal in the biochar control (Figure 5.15). This shows that the biosensor detected bioavailable Pb^{2+} on the biochar surface. Soluble Pb^{2+} (NH_4NO_3 extraction) from metal-saturated biochar was 8-times higher than the biosensor measurement, showing that not all extractable metal was available to the biosensor. Total Pb^{2+} in the sample of metal-

saturated biochar was much higher than the biochar control and only a small portion was extractable or available to the biosensor cells.

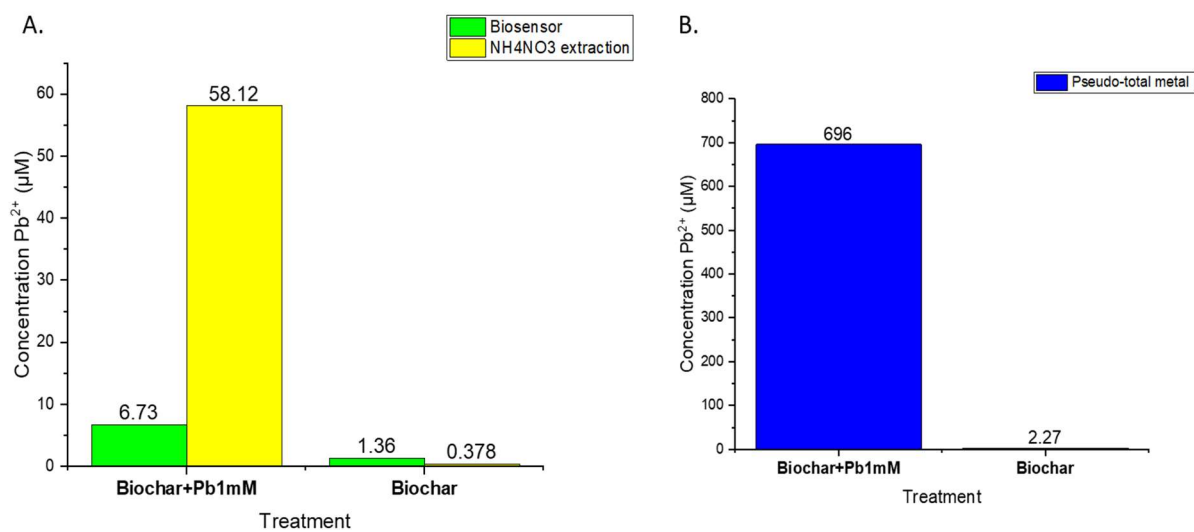


Fig.5.15 Plot of bioavailable Pb^{2+} concentration from biochar saturated with Pb^{2+} (1mM) and biochar control, determined by the FRET biosensor and NH_4NH_3 extraction (A). The total metal concentration from the biochar samples has a very high Pb in the biochar saturated with Pb^{2+} compared with the biochar only (B).

5.4.6. Measurement of soil respiration in biochar-amended soil

The production of carbon dioxide in biochar-amended soil was higher than soil without amendment for both substrates, indicating greater microbial activity in the biochar treatment (Figure 5.16 A and B). The respiration is represented as a rate to determine whether the CO₂ release occurs slower or faster than the control (without biochar treatment). There was a significant difference (ANOVA, $p < 0.05$) in CO₂ production between the two treatments. In the presence of glucose, the increase in CO₂ concentration was observed and distinguished between treatments starting from 240 minutes (4 hours) and 1440 minutes (24 hours) in the biomass substrate. The delta value indicates the enrichment of ¹³C in the evolved CO₂. Figure 5.16 C shows that utilisation of ¹³C-glucose in the biochar-amended soil occurred at a higher rate than the control soil at the beginning (up to 500 minutes), but this subsequently decreased. The utilisation of ¹³C from the biomass substrate occurred at a lower rate than the glucose substrate. Figure 5.16 D shows a high delta CO₂ before 1440 minutes, probably caused by the utilisation of left over ¹³C from glucose used to cultivate the biomass. The uptake of ¹³C from biomass substrate occurred faster in soil with biochar treatment compared to a control soil.

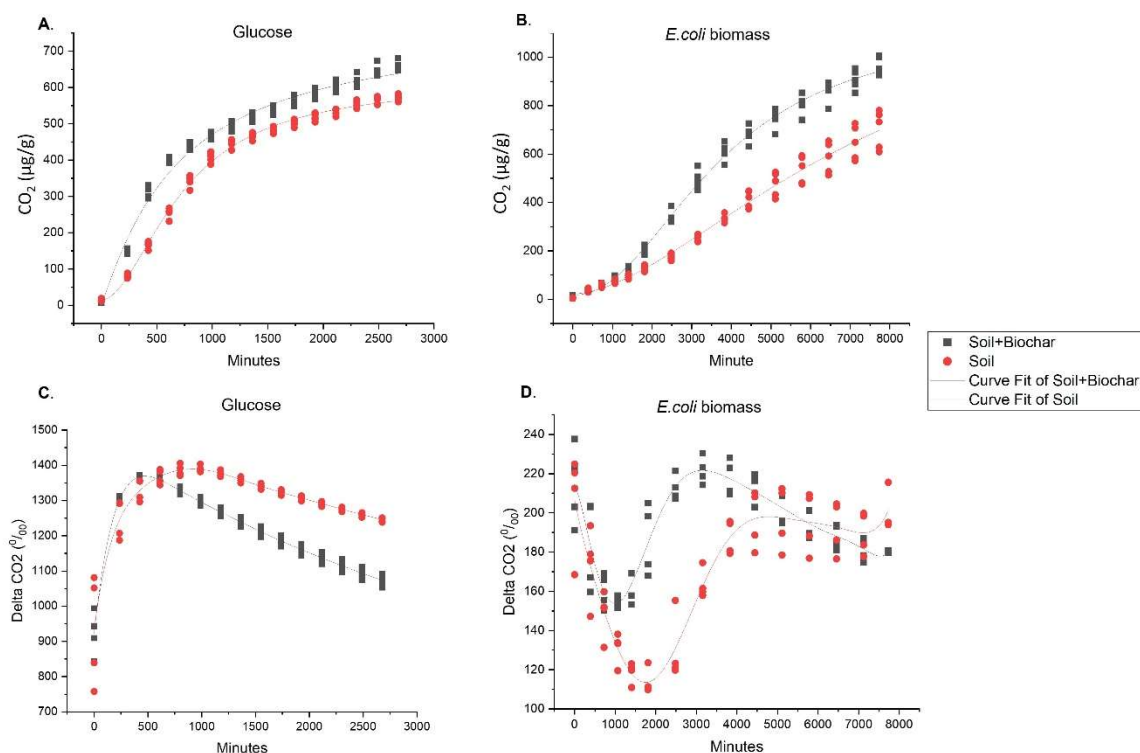


Figure 5.16 CO₂ production and Delta ¹³C-CO₂ from soil only and soil with biochar treatment utilising simple (¹³C glucose) and complex (¹³C labelled *E. coli* biomass) substrates. The CO₂ production data from glucose (A) and biomass (B) were fitted to a logistic curve, whereas delta CO₂ from glucose (C) and biomass (D) were fitted to polynomial curve. The number of samples from each treatment (n) = 4-5.

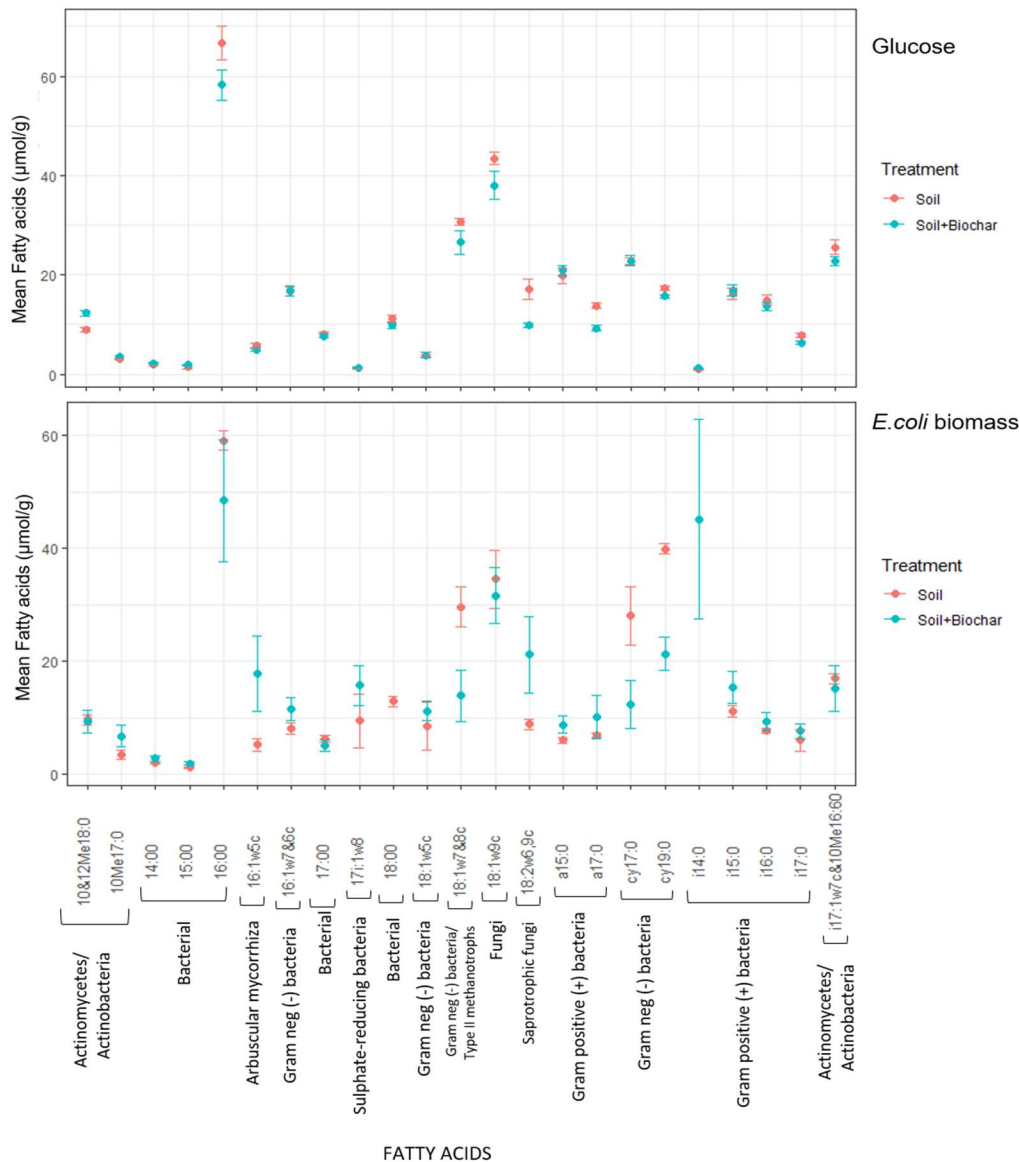


Figure 5.17 Mean fatty acids ($\mu\text{mol/g}$) measured in the experimental soil with biochar and control soil using the glucose and *E.coli* biomass substrates. The error bar represents the standard error from the mean value of fatty acid in each treatment ($n=4-5$).

Figure 5.17 describes the PLFAs of living microorganisms belonging to gram positive (+) and gram negative (-), and fungi in the soil experiments. The results show that the microbial composition of the contaminated soil was similar to the biochar-amended soil, however the abundance was different. The experiment with the glucose substrate exhibited a small difference in the amount of each fatty acid between the control soil and biochar-amended soil. In this case, the amount of bacteria 16:00, gram-negative 18:1w7&8c, saprotrophic fungi, and actinobacteria were higher in the soil without amendment. In contrast, the experiment with biomass substrate showed much higher fatty acids in the biochar-amended soil than the control soil. Treatment with biochar resulted in a higher presence of arbuscular mycorrhiza, gram

negative bacteria 16:1w7&6c, saprotrophic fungi, and all gram-positive bacteria. In the control soil, the group of gram negative bacteria cy17:0 and cy19:0 were more abundant.

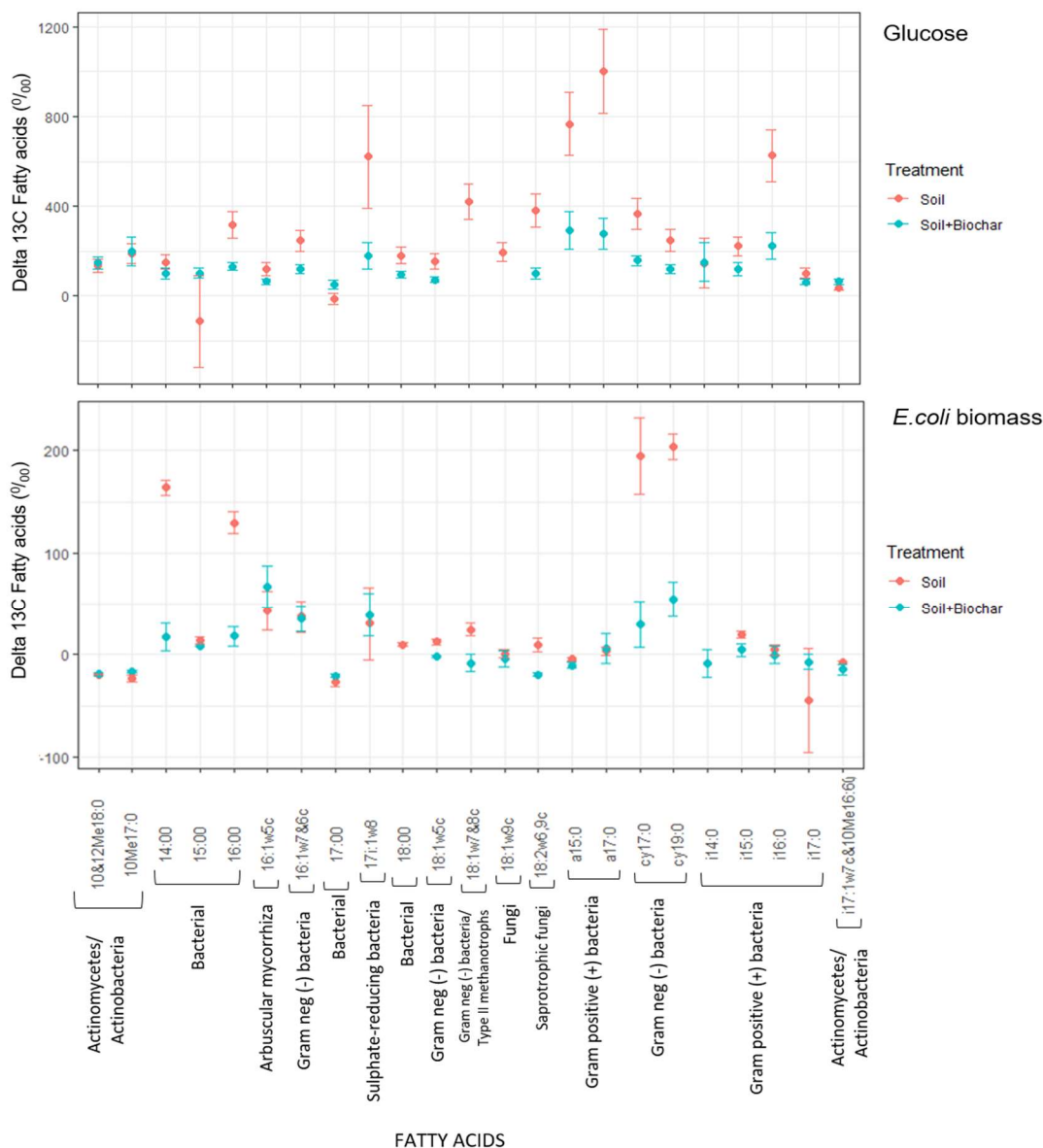


Figure 5.18 Uptake of ^{13}C -labelled substrate into single PLFAs in the experimental soil with biochar and control soil using the glucose and *E.coli* biomass substrates. The error bar represents the standard error from the mean value of ^{13}C incorporation into each fatty acid (n=4-5).

Figure 5.18 presents the uptake of ^{13}C -labelled substrates into the fatty acids. It seems some groups of microbes in the contaminated soil were more active in degrading the additional substrates compared to microbes in the biochar-amended soil. In the control soil there was higher incorporation of ^{13}C from the glucose substrate in the following groups of bacteria: 16:0, gram-negative bacteria, 16:1w7&6c, cy17:0, cy19:0, sulphate-reducing bacteria,

saprotrophic fungi, gram positive bacteria; a15:0, a17:0, and almost all gram positive bacteria. The experiment with the ^{13}C -labelled biomass substrate showed higher incorporation of ^{13}C into the fatty acids from the following groups: 14:00, 16:00, saprotrophic fungi, and gram negative bacteria 18:1w7&8c, cy17:0, cy19:0.

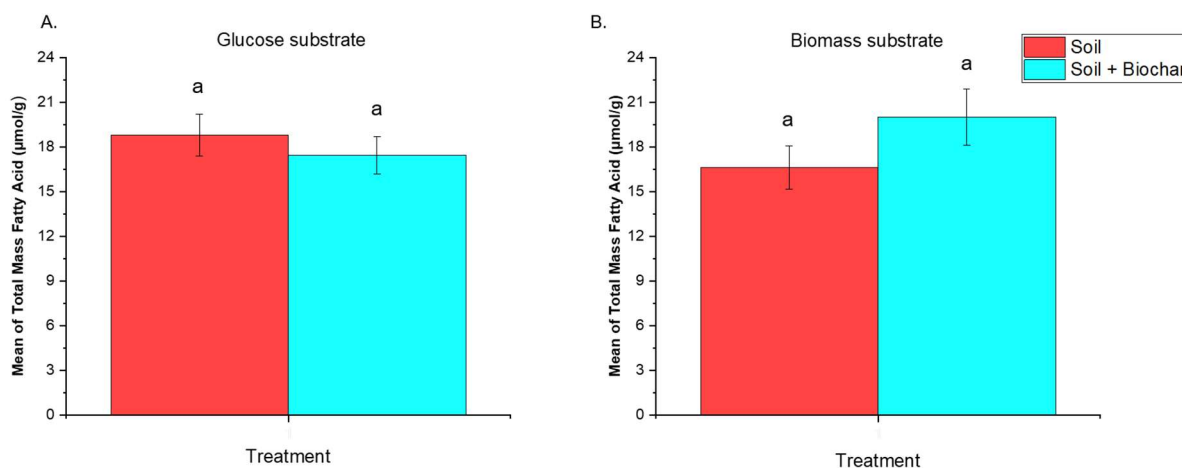


Figure 5.19 Mean of total microbial fatty acid in soil amended with biochar and soil only treated with glucose (A) and *E.coli* biomass (B) substrates. The bars show means with standard errors, n=4-5. The letters indicate the statistical differences between treatments (ANOVA, $p < 0.05$).

The PLFA data can be summed as total fatty acids and used as a proxy for microbial biomass (Figure 5.19). The experiment with the glucose substrate showed a slightly higher mean of total fatty acids from the contaminated soil than the biochar-amended soil, although they are not significantly different ($p > 0.05$). The experiment with the biomass substrate resulted in a higher total fatty acid content from the biochar-amended soil than the contaminated soil, although they are not significantly different ($p > 0.05$).

5.5. Discussion

The assessment of contaminated soil remediation has moved towards a risk-based approach by considering the bioavailability of contaminants. The traditional measurement of bioavailable metals using chemical extraction only distinguishes metal solubility or mobility in soil fractions which are not directly relevant from a biological view point (Kim *et al.*, 2015). A biosensor is an attractive approach for detecting bioavailable metals, to measure the associated risk to living organisms. Employing a soil microbe as the host cell for a biosensor is relevant because it can potentially be used as a proxy to monitor soil health and function. Therefore, this research applied the FRET biosensor inside a soil bacteria, *P.putida*, to quantify metal bioavailability in the remediation of biochar-amended metal-contaminated soil. The biosensor function was integrated with soil physicochemical parameters to assess the performance of biochar in reducing heavy metal toxicity in the soil.

Most biosensor studies have showed good performance of the sensor when tested with a metal solution under laboratory conditions. However, the functionality and application in direct contact with soils remains a challenge. The main drawbacks are the extreme soil conditions, such as low pH, limited nutrients, high mineral oxide content and toxic contaminants, which may suppress the host cell activities and cause signal interference (Cai *et al.*, 2018; Kim *et al.*, 2020). These issues were minimized by utilising the *P.putida* host cell coupled with the FRET measurement using confocal microscopy. This research has proven that the host cell can function well, regardless of the stress associated with abiotic factors in the contaminated soil, such as acidic pH and limited nutrient availability. The capability of *P.putida* KT2440 to survive under low pH conditions is mainly due to the role of the ABC transporter in the inner membrane and the cytochrome ubiquinol oxidase that maintains intracellular pH and redox status (Reva *et al.*, 2006).

5.5.1 Direct application of the FRET biosensor in the soil

The biosensor was applied directly in the soil at water holding capacity to simulate a real field condition. The initial attempt involved separating the host cells from soil samples, in which the biosensor can detect bioavailable metal in the pore water. The FRET signals indicated a small reduction in metal bioavailability in the biochar-amended soil sample and enhanced reduction in compost-amended soil and mixture of biochar and compost-amended soil samples (Figure 5.7). The results showed that the bioavailable Pb^{2+} according to the biosensor measurement was much lower than that obtained by NH_4NO_3 extraction, suggesting that not all soluble metals in pore water were available to the host cells.

The use of pore water samples to determine metal toxicity was also carried out by Beesley *et al.* (2014), in which the water samples were tested using a bacteria luminescence biosensor. They observed toxicity reduction in water extracted from an organic-amended soil compared with the contaminated soil without amendment. Metal ions in pore water are often considered as the most bioavailable (Giller *et al.*, 2009). However, the results from the current study suggest that bioavailable metal detected by the biosensor was not the same amount as the soluble metal extracted by ammonium nitrate. Yoon *et al.* (2016b) mentioned that most bioavailable metals in soils may exist as non-extractable forms associated with soil particles. Therefore, *in situ* biosensor measurement was carried out in the current study to measure the bioavailability of metals associated with the solid phase in the soil samples.

5.5.2 *In situ* measurement

FRET signals can be measured *in situ* as the host cells were in contact with soil samples. This approach was more direct, without involving the separation of cells for measurement. The results revealed a significant reduction in FRET signals from soil treated with biochar and greater reduction in signals from the soil treated with a mixture of biochar and compost. The FRET measurement showed a distribution of signals from individual cells, suggesting heterogeneity of metal concentrations in the soil samples. This finding was supported by other studies carried out using X-ray fluorescence spectroscopy, which found that hundred- and thousand-fold differences in metal concentrations can occur over micrometer distances in contaminated soils (Jacobson *et al.*, 2007; Schmid *et al.*, 2016). The heterogeneous distribution of metal contamination in soil is caused by the soil physicochemical properties, mainly pH, moisture and mineral aggregates (Qu *et al.*, 2019; Zeng *et al.*, 2021). As the metals were heterogeneously distributed at spatial scales relevant to exposure to biosensor cells, they may trigger various responses of the biosensor cells.

The various responses were enhanced in biochar- and compost-treated soil, in which some cells produced FRET signals similar to cells exposed to contaminated soil (without amendment), or cells in the absence of metals. Mixing with biochar and compost appeared to create locally low and high metal concentrations in the soil. Cells exposed to locally high metal concentration areas, where no biochar or compost was present produced high FRET signals (500-600). In contrast, cells exposed to low metal concentrations exhibited low FRET signals (250-350) (Figure 5.11). The control experiment revealed that cells exposed to biochar saturated with Pb^{2+} produced FRET signals within the range of 433 – 528, indicating that some metals bound on the biochar surface were bioavailable.

Despite the complexity of the soil samples, the FRET biosensor can determine the level of bioavailable metal which can be distinguished between each treatment. The results revealed that the concentration of bioavailable metal in the contaminated soil is reduced approximately 28% due to biochar amendment. The amendment with compost resulted in a greater reduction of 65%, and the mixture of biochar compost further reduced the bioavailable metal by up to 84% (Figure 5.12).

5.5.3 Comparison of bioavailable metal measured by the biosensor and NH_4NO_3 extraction

In contaminated soil and biochar-amended soil samples, the bioavailable Pb^{2+} based on NH_4NO_3 extraction was overestimated, with the metal concentrations approximately 2-fold higher than that measured by the biosensor (Figure 5.13). In contrast, the bioavailable Pb^{2+} measured by NH_4NO_3 extraction in compost-treated soil was lower than that from the biosensor analysis.

Employing a neutral salt (NH_4NO_3) solution is only sufficient to measure the bioavailable fraction of highly mobile metals (Gryschko *et al.*, 2005). This method is typically used to understand the correlation between a metal in soil pore water and its potential uptake by plants (Meers *et al.*, 2007). The extraction mechanism involves displacing the readily soluble metal fraction from exchangeable sites on solid phases in the soil into the soil solution mimicking the pore water. This mechanism is different for the biosensor, in which the metals must enter into the cell and bind with CMT to induce the FRET signals.

The different amounts of bioavailable metal measured by the biosensor and NH_4NO_3 extraction can also be influenced by the variation in pH and organic matter content, induced by the amendment (Figure 5.5 A&B). The low pH (4.9) in contaminated soil (without amendment) caused the metals to be more mobile and highly soluble. Hence they can be easily extracted by NH_4NO_3 . A slight increase in pH (5.5) due to biochar amendment resulted in a 40-50% reduction in soluble metal, but this is not the case with the biosensor, which only showed a 20% reduction in bioavailable metal. In compost-amended soil the increase of pH to pH 7-8 can decrease the mobility of metals, resulting in a reduction in soluble metal concentrations of up to 90%. In this case, the biosensor cells can still detect the presence of local metal accumulation which was not extractable by NH_4NO_3 .

The treatment with biochar, compost, and a combination of the two increased the soil pH. This can be attributed to the alkalinity of the biochar and compost used. Biochar contains mineral ash dominated by carbonates alkali which can release into the soils and increase the pH (Mensah and Frimpong 2018, Bandara *et al.* 2021). The compost was originated from garden waste which contained high level of basic cations. According to Walker, *et.al*, 2004, an increase in soil pH by compost was attributed to the release of NH₃ over the time, activities of microbes that can create reducing conditions, or due to displacement of hydroxyls from sesquioxide surfaces by organic anions.

Soil pH is the most significant factor influencing the bioavailability of heavy metals (Park, *et al*, 2010). This study suggested that the immobilisation of heavy metals by biochar was mainly controlled by pH (5.5 to 6). Heavy metals become more mobile at low pH compared to moderate acidic up to slightly alkaline soil pH. The addition of biochar increased soil pH due to dissociation from functional groups (carboxyl, phenolic, hydroxyl, and carbonyl) which enhance the binding affinity to metal cations, thus reducing heavy metals bioavailability (Park, *et al*, 2010). In case of compost, the increase in pH (7.0 – 7.5) was mainly due to a high production of NH₃ during decomposition. The increasing pH from compost improved the stability constant of metal-organic complexes thus reducing heavy metals bioavailability and mobility (Kim, *et al*, 2015). The reduction of Pb bioavailability and the pH increased in this experiment was supported by the fact that the amount of Pb sorption is a function of pH in which increases sharply at pH 5 and reached maximum at pH 8 (Park, *et al*, 2010; Beesley, *et al*, 2010).

Amendment with compost increased the organic matter content and phosphate in the contaminated soil (Figure 5.5). There was no significant change in organic matter from biochar treatment, but the change was significant due to compost treatment. Changes in soil organic matters following the compost addition were mainly due to decay of the easily degradable organic matters such as polysaccharides and to a certain extent microbial biomass (Leifeld *et. al.* 2002). The increase in phosphate concentration due to compost treatment is associated with the composition of compost which was originated from plant material. Phosphates in plant cell materials are present largely as organic P compounds such as phosphate ester. The release of Phosphate was correlated with organic matter decomposition due to microbial activities over time (Mkhabela and Warman 2005).

Other studies have reported that soil amendment with organic-rich materials can significantly increase the soluble organic matter to which free ions can complex and result in a low soluble

metal fraction (Bernal *et al*, 2007; Wasilkowski *et al*, 2014). In the current research the combination of high organic matter content and neutral pH may lead to Pb^{2+} complexation with an organic ligand. According to some studies (Smith *et al*, 2009; Kim *et al*, 2019) this complex is relatively stable in soil. The low concentration of extractable metal in Figure 5.11 confirms this and therefore Pb^{2+} associated with organic matter was considered to be non-extractable Pb^{2+} , and potentially detected by the biosensor cells. Maderova *et al* (2011) suggested that bioavailable heavy metals in soil may be present as non-extractable forms, which can induce a response in biosensors. Metal associated with the solid phase may become bioavailable and have a toxic effect on soil microorganisms. A possible mechanism is that the active surface charge on bacteria cell walls can potentially displace metals from the soil sorption sites, resulting in increased bioavailability (Wu *et al*, 2006; Maderova *et al*, 2013). The cell wall of *P.putida* was probably capable of removing more Pb^{2+} from the exchange site, making it available to enter the cell. Some studies have reported that *P.putida* contains extracellular polymeric substances enabling the adsorption of metal (Ueshima *et al*, 2008), which can potentially be applied for the bioremediation of metal-polluted environments (Khashei *et al*, 2018).

P.putida has developed multiple defense strategies to protect the cell from bioavailable heavy metals. Extracellular Polymeric Substance (EPS) is an effective strategy for metal detoxification and is known as the first barrier mechanism before entering the metals into the cell. The surface of EPS on the *P.putida* cell membrane contains functional groups such as carboxylic and sulfhydryl sites (Yu, *et.al*, 2020). Heavy metals such as Cd and Pb can bind onto these sites forming a metal complexation and adsorption on the cell envelopes. EPS production also mediates cell-to-cell and cell-to-surface attachment leading to biofilm formation. This will improve the survival ability of the cells in a highly polluted environment (Abee *et.al*, 2011).

Figure 5.13 shows that the number of metals detected by the biosensor is not necessarily the same amount as metals extracted by the ammonium nitrate. Heavy metals reported by the FRET biosensors are considered bioavailable because these metals can cross the cell membrane from the medium the organism inhabits. Once the transfer occurred, the metals can be transformed, stored, or toxic within the organism. Heavy metals extracted by ammonium nitrate are not always bioavailable and can be considered as bio accessible. According to Semple, *et.al*, 2002, bio accessible metals can be reached by organisms, however, this often depends on given place, spatial range, and time. These metals might cross the cell membrane if the organism gain access

to them. Some conditions that can cause bio accessible metals to become bioavailable are the release of metal from adsorption sites due to physical removal, or movement of organisms leading to direct contact with the metals.

5.5.4 Improvement of soil microbial activities in biochar-amended soil

The biosensor has shown that soil amendment with biochar can reduce the heavy metal bioavailability, with a decrease in metal toxicity. This was supported in the soil respiration experiment and represented by CO₂ production from ¹³C-labelled substrates. This parameter appeared to be sensitive and responsive to the changing environmental conditions in the contaminated created by the addition of biochar. The reduction in metal bioavailability increased the base soil respiration, indicating an improvement in the soil biological processes (Friedlová, 2010).

Based on PLFA measurements, the fatty acid composition was different between treatments. However, some microbes (gram-positive bacteria i14:0, i15:0, i17:0, saprotrophic fungi, and arbuscular mycorrhiza 16:1w5c) were present more in biochar-amended soil supplied with the complex substrate (Figure 5.17). This trend is very similar to the results from other studies (Kelly *et al*, 2003; Wasilkowski *et al*, 2014) which have reported an increased level of fatty acids originating from gram-positive (15:0) and mycorrhizal fungi (16:1w5c). Gram-positive bacteria were more dominant than gram-negative bacteria in the remediated soil. Interestingly, a small increase in arbuscular mycorrhiza was observed following the addition of biochar, despite the absence of plant rhizosphere in this experiment. This supports the idea that biochar can provide favourable conditions for the growth of mycorrhizal fungi, which may enhance nutrient and moisture uptake by plants (Yuan *et al*, 2011; Millar and Bennett, 2016). The group of gram-negative bacteria (cy17:0, cy19:0) were predominance in the contaminated soil without amendment. A similar result was also found by Wasilkowski *et al* (2014), suggesting that these gram-negative bacteria have some tolerance to heavy metals. The results from the current study indicate that these groups can actively metabolize ¹³C from the complex substrate in an environment with high concentrations of bioavailable metal.

The presence of fungi such as arbuscular mycorrhizal and saprotrophic fungi in the soil samples indicated that treatment with biochar can provide a habitable environment for these microorganisms. Arbuscular mycorrhizal is important for soil restoration because it can carry out symbiosis with plants providing nutrients for plant roots and improving plant growth (Barea and Jeffries, 1995). It has been reported that arbuscular mycorrhiza can colonize plant

rhizosphere in soil contaminated with heavy metals (Cd, Zn, and Pb) (Vogel-Mikus, *et.al*, 2005). These fungi contribute to the remediation of contaminated soil mainly by protecting plants against the toxic effects of metals. This can be done in several mechanisms; binding heavy metals into roots so the translocation into shoot tissues can be restricted, and reduce shoot metal concentration, improving nutrient supplies by immobilising minerals such as phosphorous so it can be accessed by plants (Khan, *et.al*, 2014). Arbuscular mycorrhizal has the ability for immobilisation of heavy metals by secreting polyphosphate in which later can precipitate with metals. The formation of precipitating polyphosphate can increase metal adsorption to fungal cell walls and reduce metal bioavailability in the soil (Javaid, 2011).

Overall, the total microbial fatty acids are not statistically different between treatments. This is probably caused by several factors, such as a short incubation time of 2-3 days compared to the pot experiment (18 months) and a heterogeneous distribution of ^{13}C in the substrate in the soil sample. The analysis of PLFAs is a sensitive indicator for monitoring the changes in the microbial community. This method is preferred over total microbial isolation. However, the main limitation of PLFA analysis is the low taxonomic resolution (Watzinger, 2015). In this case, a study of the microbial community using a metagenomics approach is preferred.

This research has shown that the FRET biosensor can be used as a monitoring tool to complement chemical analysis using basic soil parameters and soil biological processes. Direct measurement of the FRET signal *in situ* can be used to represent the actual impact of metal toxicity on soil microorganisms. The application of this biosensor is relatively easy and quick. Some studies have tried to recover biosensor cells from the soil matrix, by using a density gradient medium followed by centrifugation (Hurdebise *et al.*, 2015). Zhang *et al.* (2011) reported the separation of functionalized biosensor cells with magnetic nanoparticles (Fe_3O_4) from soil samples under a magnetic field. These methods require complex preparation. Moreover, the use of chemicals (e.g. a gradient medium or Fe_3O_4) can completely alter the soil environment of the microbes, which may affect the production of the signals. *In situ* measurement using the FRET biosensor does not require laborious and time-consuming soil preparation or recovery of cells from the soil matrix. The measurement can be carried out with the minimum destruction or modification of soil samples, thereby mimicking the response of soil microbes as they exist in the field environment.

5.6. Conclusion

P.putida KT2440T7 bearing the FRET biosensor was exposed to soil samples contaminated with heavy metals and the same samples amended with biochar and compost, and was shown to be capable of measuring the bioavailability of heavy metals in the different media. *In situ* measurement of the FRET biosensor using a confocal microscope enables direct application with less disruption of the soil matrix.

The analysis of NH_4NO_3 -extractable metal did not necessarily represent the actual amount of metal available to soil microbes. The biosensor detected non-extractable Pb^{2+} , which is more likely related to metal associated with the solid phase. Although the extractable metal represents the most bioavailable fraction, the non-extractable metals should also be considered as they may provide a contribution to metal bioavailability with inherent biological relevance.

The biosensor can detect high metal bioavailability in control (unamended) soil and a reduction in metal bioavailability in biochar-amended soil. The most efficient treatment in reducing metal bioavailability was amendment with a mixture of biochar and compost, indicating a decrease in metal toxicity. This research has shown that the biosensor is an important tool to assess metal bioavailability and can be used to complement chemical analysis to evaluate the effectiveness of soil remediation performance.

There remains a need to explore the relationship between biosensor measurement with a more comprehensive analysis of changes in soil microbes, such as gained from a metagenomic or meta-transcriptomic approach. Future work requires the robustness of the biosensor application in various types of contaminated soils to be tested with different remediation methods. This will help to validate the biosensor performance in a range of applications.

6. Synthesis, future research, and conclusion

6.1 Synthesis

Heavy metal contamination may cause a toxic impact to soil organisms depending on the level of bioavailability. Anawar *et al.* (2015) reported that the remediation of contaminated soil with biochar can reduce heavy metal bioavailability through immobilization of metals on its surface. The interpretation of bioavailable metals still utilises chemical extractions to distinguish the mobility of metals in soil fractions (Kim *et al.*, 2015). However, the analysis of bioavailability must take into account the biological response to assess the risk of toxicity. To address this, the application of bacteria biosensors for sensing of heavy metals is an attractive approach and has received increasing attention. Numerous research on bacteria biosensors rely on the transcription-inducible reporter system which provides a non-direct measurement of heavy metal bioavailability (Table 2.1, Chapter 2). Nevertheless, the research is still mainly at a proof-of-concept stage, focusing on the genetic construction of the biosensor rather than optimizing application strategies for real environmental samples.

Therefore, a FRET biosensor in *P.putida* was developed and designed to mimic the response of soil microbes to heavy metals. This study employed the biosensor to measure the bioavailability of heavy metals in biochar- and compost-amended soil. The biosensor function was integrated with soil chemical parameters and microbial activity to evaluate the remediation performance of biochar in reducing heavy metal toxicity in metal-contaminated soil. This is the first application of a FRET biosensor for sensing heavy metal bioavailability in real contaminated environmental samples.

6.1.1 Development of the FRET biosensor

The FRET biosensor components consist of a CMT fused between eCFP and Venus FP (Figure 2.9, Chapter 2). Its construction exploited chicken metallothionein (CMT) as the sensing domain because CMT has been well characterised and can simulate the metal binding of the FRET biosensor in the cytoplasm (Rajamani *et al.*, 2014). In chapter 3, the FRET biosensor was successfully constructed and tested *in vitro* to prove the concept of FRET using a spectrofluorimeter. The sensing capability was indicated by a decreased eCFP signal and an increased Venus FP signal due to metal binding with CMT. The FRET ratio (Venus/eCFP signal) corresponds to metal concentrations in which the biosensor was exposed. The K_a parameter revealed the sensitivity of the FRET biosensor to be in the order: $Pb^{2+} > Cd^{2+} > Zn^{2+}$.

The FRET biosensor was expressed in *E.coli* BL21 Rosetta 2(DE3) and showed its capability to measure Pb^{2+} , Cd^{2+} , and Zn^{2+} inside the cell. The results showed a lower metal binding inside the cell than in metal solution (*in vitro*) (Figure 3.17, Chapter 3), indicating the difference in metal concentrations. This can be attributed to the metal regulations on the cell membrane, which affect the amount of metal sensed by the FRET biosensor. The FRET signals provided information that binding of metals with the active sites of CMT inside the cell can be interpreted as a direct response to the bioavailable heavy metals.

6.1.2 FRET biosensor in *P.putida*

The FRET biosensor constructed in Chapter III was expressed inside *P.putida* KT2440T7. This bacterium was chosen because it is typically found in contaminated soil, providing a robust host cell for environmental application. Moreover, the KT2440T7 strain is a safe host cell for genetic manipulation to express a recombinant protein under the T7 promoter system (Troeschel *et al.*, 2012). In chapter 4, the use of confocal microscopy to measure bioavailable metals at the resolution of the cells was demonstrated. This approach enabled the visualization of metal-induced FRET signals inside the host cell.

The analysis of FRET signals in *P.putida* indicated that Pb^{2+} was more toxic than Cd^{2+} and Zn^{2+} . Parameters of apparent K_a and FRET maximum suggest that metal binding in *P.putida* was higher than *E.coli* which can be observed clearly from the exposure to elevated concentrations of Cd^{2+} and Zn^{2+} (above 100 μM) (Figure 4.9, Chapter 4). This indicates that *P.putida* can function at high metal exposure, which is probably due to the role of the metal efflux transporter as the first defense mechanism (Hynninen, 2010).

Standard curves were produced as the measurement range of bioavailable Pb^{2+} , Cd^{2+} , and Zn^{2+} which will be useful when the host cells are exposed to a metal-contaminated soil (Figure 4.17, Chapter 4). FRET signals above the maximum value indicated a toxic concentration which is damaging for the cells. The ability of the FRET biosensor in *P.putida* to measure bioavailable metals in a real contaminated soil was investigated in Chapter V.

6.1.3 Application of FRET biosensor in soil remediation

In chapter V a strategy was developed to implement the FRET biosensor as a representative measurement of actual metal bioavailability in the remediation of heavy metal-contaminated soil using biochar and compost as amendments to reduce metal bioavailability. This was done by introducing the *P.putida* cells bearing FRET biosensors into soil at water holding capacity and

directly measured the FRET signals using the confocal microscopy *in situ*, as the cells were in contact with the soil samples (Figure 5.2, Chapter 5).

The biosensor was able to measure the reduction in metal bioavailability in the contaminated soil due to biochar and compost amendment. Using the standard curve, the bioavailable Pb^{2+} concentration ($39.29 \pm 1.28 \mu\text{M}$) in contaminated soil without amendment indicated a near toxic level for the host cell (Figure 5.12, Chapter 5). The soil became less toxic due to biochar amendment, resulting in a decrease of bioavailable metal to $28.24 \pm 1.6 \mu\text{M}$. The level of bioavailable metal was further reduced to $13.69 \pm 2.01 \mu\text{M}$ and $6.28 \pm 1.81 \mu\text{M}$ due to amendment with compost and mixture of compost and biochar, respectively. It was concluded that a mixture of biochar and compost amendment provided the most effective remediation treatment in reducing heavy metal bioavailability in this specific soil.

The FRET biosensor showed a reduction in heavy metal bioavailability, suggesting a shift of toxicity in the biochar- and compost-amended soil. This was supported by an increase in the bulk soil pH and organic matter content with these amendments (Figure 5.5, Chapter 5), which was presumed to contribute to the reduced metal solubility (Figure 5.6, Chapter 5), and an improvement in soil respiration (Figure 5.16, Chapter 5). The bioavailable Pb^{2+} detected by the FRET biosensor was not the same as soluble Pb^{2+} extracted by NH_4NO_3 . This was not surprising as the biosensor measured biologically-relevant metals, whilst ammonium nitrate relied on utilising neutral salt to displace ion metal from the exchangeable site into the soil pore water (Gryschko *et al.*, 2005). Apparently, the biosensor measured bioavailable metal associated with the solid-phase, which cannot be readily extracted. This was supported by Maderova *et al* (2011), who identified solid-phase forms of metals that can be sensed by bacteria biosensors. The high pH and organic matter content in the compost-amended soil was suspected to have resulted in a Pb-organic matter complex that could be available to the host cell. Based on this, the application of biosensors is important to measure non-extractable metals that are potentially bioavailable.

This study has demonstrated that the biosensor can be used as a reliable tool, complementing chemical-based methods for soil toxicity assessment. The functionality of *P.putida* as a host cell showed a robust measurement of bioavailable metal in harsh soil conditions, such as low pH, limited nutrient availability and high metal concentrations. Compared to other biosensor applications described in the literature, the application of the FRET biosensor in this study is relatively simple with minimal destruction or modification of soil samples. Quantitative

information on bioavailability from biosensors is essential and could contribute to the assessment of remediation performance for heavy metal-contaminated soil.

6.2 Future research

Further studies are required to obtain more comprehensive information on the relationship between the reduction in bioavailable metals and changes in microbial communities and function. Metagenomics analysis will provide more accurate information than PLFA regarding the species of microbes that can survive in the contaminated soil and the shift of communities due to amendment effects. Meta transcriptomic study reveals the expression of genes responsible for metal resistance mechanisms in soil (Lehembre *et al.*, 2013). These mechanisms can potentially be exploited as a sensing domain of the FRET biosensor.

The performance of the FRET biosensor in this study still needs to be validated for application in different soil types, contaminant sources and remediation methods. The contaminated soil used in the current research was originally from an abandoned mine containing a high concentration of Pb. Various metal contamination sources include metal waste disposal, fossil fuel combustion and agricultural practices (He *et al.*, 2015). Metal contamination from these activities may behave differently than in soils impacted by mining activity, leading to various toxicity levels. Different soil properties, such as texture, porosity and moisture, will mainly influence the distribution of heavy metals in soils. In addition to biochar amendment, soil washing and phytoremediation are frequently used methods for the remediation of metal-contaminated soil (Wuana and Okieimen, 2011). Testing the biosensor with various soil samples will provide information on the robustness of the sensor and thus its application can potentially be expanded to assess the performance of different remediation methods.

The construction of the FRET biosensor in this study offers flexibility and is relatively easy to modify for different applications. As the genomic sequence of *P.putida* KT2440 has been well characterised (Nelson *et al.*, 2002; Belda *et al.*, 2016), the properties of the host cell and FRET biosensor components could be modified to meet specific purposes.

More stable production of FRET biosensors could be achieved by integrating the gene encodes eCFP-CMT-Venus FP into the chromosome and expressed constitutively. This will avoid additional use of inducers and antibiotics during cells preparation. Cloning a gene that encodes oxyrase enzymes in the genome of *P.putida* is an attractive approach because the production of these enzymes could metabolize free radical oxygen arising from photobleaching (Thurston, *et*

al, 2000). This can potentially minimise the impact of photobleaching without the addition of an antifade reagent.

Integrating the FRET biosensor gene construct into the chromosomal expression system may face some challenges such as finding a suitable cloning technique, metabolic burden for the cell, and production of high background fluorescence signals. The selection of cloning technique is important to maintain the orientation of the FRET construct (eCFP-CMT-Venus) and the accuracy of DNA insertion in the target promoter. Unlike the T7 promoter system which requires IPTG induction, a promoter that can express the FRET biosensor constitutively is required for protein expression from the chromosome gene construct. The constitutive promoter should allow for high protein synthesis and at the same time can maintain a stable protein expression.

The chromosomal expression means the target FRET biosensor protein is expressed as the cells grow and multiply. This may cause an additional metabolic burden to the host cells. Therefore, an improvement of media composition and incubation parameters (pH, oxygen, and temperature) should be considered to maintain the nutrient requirement and optimal conditions during cell growth.

Another challenge may arise from an overproduction of FRET biosensors resulting in high background signals. A high level of eCFP and Venus Fluorescent proteins could increase the signal-to-noise ratio. This may interfere with the ratio calculation of these two donor-acceptor proteins. If this case happens, another approach for FRET measurement should be implemented such as acceptor photobleaching or fluorescence lifetime imaging (Bajar, *et.al*, 2016).

Expression of oxyrase in *P.putida* is possible because the enzymes are originated from the plasma membrane of *E.coli*, so the genetic sequence and protein expression systems have been well studied (Thurston *et.al*, 2000). Some challenges that need to be considered mainly come from genetic modification. Oxyrase works by removing dissolved oxygen outside the cell, whereas the protein expression will occur in the cytoplasm. Therefore, the sequence of oxyrase should be modified by adding gene encodes anchor protein. This will enable the oxyrase to be transported to the outer cell membrane. Another modification might use the genetic system in which the enzymes can be released out of the cell. A high level of oxyrase expression may influence the available oxygen for the host cell. If limited oxygen concentration occurs, cellular processes such as respiration could be inhibited and affect biosensor performance. Therefore, the promoter system should be selected carefully to avoid the high expression level of oxyrase.

The sensitivity and selectivity of the FRET biosensor towards heavy metals can be modified by using different sensing domains. Other types of metallothionein from prokaryotes and eukaryotes

with different metal binding affinities to a group or specific metal have been well characterised. Ngu and Stillman (2006) have identified arsenic binding to mammalian metallothionein. Exploitation of this metallothionein may lead to the application of a FRET biosensor for measuring the bioavailability of arsenic in soils. Bacterial metallothionein from *P.aeruginosa* has been known to bind a broader range of toxic heavy metals, including copper, zinc, cadmium, and mercury (Pietrosimone, 2014). This can potentially be used as a component of a FRET biosensor for application in soil contaminated with a mixture of heavy metals.

6.3 Conclusion

A FRET biosensor that measures bioavailable metals in contaminated soil was developed by exploiting the combination of CMT as a binding site for metals and FRET pairs (eCFP and Venus FP) as reporter proteins. This research has described the construction of the FRET biosensor and expressed the protein in *E.coli* for initial testing and further in *P.putida* as a relevant host cell for application to heavy metal-contaminated soil. The biosensor can function in measuring Pb^{2+} , Cd^{2+} , and Zn^{2+} inside both host cells, indicated by the changes in metal-induced FRET signals.

The FRET biosensor in *P.putida* has been successfully applied directly to measure bioavailable metals in contaminated soil using confocal microscopy. This provided information on the status of metal toxicity at the cellular level. Results from the biosensor showed that a reduction of metal bioavailability occurred in biochar-amended soil. The reduction was enhanced due to amendment with a mixture of biochar and compost, indicating the most effective treatment.

This research has also demonstrated that the decrease of metal bioavailability deduced from the biosensor measurement was in supported with changes in metal bioavailability based on measurement of soil chemical properties, soluble metals using NH_4NO_3 extraction and soil respiration. It has shown that the biosensor can be used as a tool to complement these parameters. The application of this biosensor is relatively easy and quick compared to analytical methods using chemical extractions. Therefore, the integration of this biosensor in soil remediation assessment is strongly recommended. This will help to provide information on risks associated with bioavailable metals so the performance of remediation strategies to improve soil restoration can be assessed precisely.

7. References

- Abee, T., Kovacs, A.T., Kuipers, O.P., and van der Veen, S. (2011). Biofilm formation and dispersal in Gram-positive bacteria. *Current Opinion in Biotechnology*. 22:172–179. <http://dx.doi.org/10.1016/j.copbio.2010.10.016>
- Abraham, B. G., Santala, V., Tkachenko, N. V., & Karp, M. (2014). Fluorescent protein-based FRET sensor for intracellular monitoring of redox status in bacteria at single cell level. *Analytical and Bioanalytical Chemistry*, **406**(28), 7195-7204. DOI: 10.1007/s00216-014-8165-1.
- Abuknesha, R.A., al-Mazeedi, H.M. & Price, R.G. (1992) Reduction of the rate of fluorescence decay of FITC- and carboxyfluorescein- stained cells by anti-FITC antibodies. *Histochem. Journal*. 24, 73–77
- Ahmad, M., Anjum, N. A., Asif, A., & Ahmad, A. (2020). Real-time monitoring of glutathione in living cells using genetically encoded FRET-based ratiometric nanosensor. *Scientific Reports*, **10**(1), 1-9. DOI: 10.1038/s41598-020-57654-y.
- Ahmad, M., Rajapaksha, A. U., Lim, J. E., Zhang, M., Bolan, N., Mohan, D., ... & Ok, Y. S. (2014). Biochar as a sorbent for contaminant management in soil and water: a review. *Chemosphere*, 99, 19-33. DOI: 10.1016/j.chemosphere.2013.10.071.
- Amari, T., Ghnaya, T. & Abdelly, C. (2017). Nickel, cadmium and lead phytotoxicity and potential of halophytic plants in heavy metal extraction, *South African Journal of Botany SAAB*, **111**, 99–110. DOI: 10.1016/j.sajb.2017.03.011.
- Ameen, S., Ahmad, M., Mohsin, M., Qureshi, M. I., Ibrahim, M. M., Abdin, M. Z., & Ahmad, A. (2016). Designing, construction and characterization of genetically encoded FRET-based nanosensor for real time monitoring of lysine flux in living cells. *Journal of Nanobiotechnology*, **14**(1), 1-11. DOI: 10.1186/s12951-016-0204-y.
- Anawar, H. M., Akter, F., Solaiman, Z. M., & Strezov, V. (2015). Biochar: an emerging panacea for remediation of soil contaminants from mining, industry and sewage wastes. *Pedosphere*, **25**(5), 654-665. DOI: 10.1016/S1002-0160(15)30046-1.
- Andrews, G. K., Fernando, L. P., Moore, K. L., Dalton, T. P., & Sobieski, R. J. (1996). Avian metallothioneins: structure, regulation and evolution. *The Journal of Nutrition*, **126**(suppl_4), 1317S-1323S. DOI: 10.1093/jn/126.suppl_4.1317S.
- Arora, N. K., Khare, E., Singh, S., & Maheshwari, D. K. (2010). Effect of Al and heavy metals on enzymes of nitrogen metabolism of fast and slow growing rhizobia under explanta conditions. *World Journal of Microbiology and Biotechnology*, **26**(5), 811-816. DOI: 10.1007/s11274-009-0237-6.

- Assunção, A. G., Gjetting, S. K., Hansen, M., Fuglsang, A. T., & Schulz, A. (2020). Live Imaging of Phosphate Levels in Arabidopsis Root Cells Expressing a FRET-Based Phosphate Sensor. *Plants*, **9**(10), 1310. DOI: 10.3390/plants9101310.
- Bae, J. W., Seo, H. B., Shimshon, B., & Bock, G. M. (2020). An optical detection module-based biosensor using fortified bacterial beads for soil toxicity assessment. *Analytical and Bioanalytical Chemistry*, **412**(14), 3373-3381. DOI: 10.1007/s00216-020-02469-z.
- Bagdasarian, M. A., Lurz, R., Rückert, B., Franklin, F. C. H., Bagdasarian, M. M., Frey, J., & Timmis, K. N. (1981). Specific-purpose plasmid cloning vectors II. Broad host range, high copy number, RSF 1010-derived vectors, and a host-vector system for gene cloning in *Pseudomonas*. *Gene*, **16**(1-3), 237-247. DOI: [https://doi.org/10.1016/0378-1119\(81\)90080-9](https://doi.org/10.1016/0378-1119(81)90080-9)
- Bajar, B. T., Wang, E. S., Zhang, S., Lin, M. Z., & Chu, J. (2016). A guide to fluorescent protein FRET pairs. *Sensors*, **16**(9), 1488. DOI: 10.3390/s16091488.
- Bandara, T., Herath, I., Kumarathilaka, P., Hseu, Z.Y., Ok, Y.S. and Vithanage, M. (2017). Efficacy of woody biomass and biochar for alleviating heavy metal bioavailability in serpentine soil. *Environmental Geochemistry and Health*, **39**(2), pp.391-401. DOI: 10.1007/s10653-016-9842-0.
- Bandara, T., Franks, A., Xu, J., Chathurika, J.B.A.J., and Tang, C., 2021. Biochar aging alters the bioavailability of cadmium and microbial activity in acid contaminated soils. *Journal of Hazardous Materials*, 420, 126666.
- Barea, J.M. and Jeffries, P. (1995) Arbuscular mycorrhizas in Sustainable Soil-Plant Systems. In: Varma, A. and Hock, B., Eds., *Mycorrhiza*, Springer, Berlin, Heidelberg, 521-560. http://dx.doi.org/10.1007/978-3-662-08897-5_23
- Beesley, L., Inneh, O. S., Norton, G. J., Moreno-Jimenez, E., Pardo, T., Clemente, R., & Dawson, J. J. (2014). Assessing the influence of compost and biochar amendments on the mobility and toxicity of metals and arsenic in a naturally contaminated mine soil. *Environmental Pollution*, **186**, 195-202. DOI: 10.1016/j.envpol.2013.11.026.
- Beesley, L., Moreno-Jiménez, E., Gomez-Eyles, J. L., Harris, E., Robinson, B., & Sizmur, T. (2011). A review of biochars' potential role in the remediation, revegetation and restoration of contaminated soils. *Environmental Pollution*, **159**(12), 3269-3282. DOI: 10.1016/j.envpol.2011.07.023.
- Belda, E., Van Heck, R. G., José Lopez-Sanchez, M., Cruveiller, S., Barbe, V., Fraser, C., ... & Médigue, C. (2016). The revisited genome of *Pseudomonas putida* KT2440 enlightens its value as a robust metabolic chassis. *Environmental Microbiology*, **18**(10), 3403-3424. DOI: 10.1111/1462-2920.13230.
- Bereza-Malcolm, L. T., Mann, G., & Franks, A. E. (2015). Environmental sensing of heavy metals through whole cell microbial biosensors: a synthetic biology approach. *ACS Synthetic Biology*, **4**(5), 535-546. DOI: 10.1021/sb500286r.

- Bereza-Malcolm, L., Aracic, S., & Franks, A. E. (2016). Development and application of a synthetically-derived lead biosensor construct for use in gram-negative bacteria. *Sensors*, **16**(12), 2174. DOI: 10.3390/s16122174.
- Bernal, M. P., Clemente, R., & Walker, D. J. (2007). The role of organic amendments in the bioremediation of heavy metal-polluted soils. *Environmental research at the leading edge*, 1-57.
- Bernas, T., Zarebski, M., Cook, P.R., and Dobrucki, J.W. (2004) Minimizing photobleaching during confocal microscopy of fluorescent probes bound to chromatin: role of anoxia and photon flux. *Journal of Microscopy*, **215**, 281-296.
- Binet, M. R., & Poole, R. K. (2000). Cd (II), Pb (II) and Zn (II) ions regulate expression of the metal-transporting P-type ATPase ZntA in Escherichia coli. *FEBS letters*, **473**(1), 67-70. DOI: 10.1016/S0014-5793(00)01509-X.
- Branco, R., Cristóvão, A. & Morais, P. V. (2013). ‘Highly Sensitive, Highly Specific Whole-Cell Bioreporters for the Detection of Chromate in Environmental Samples’, *PLoS ONE*, **8**(1), 13–17. DOI: 10.1371/journal.pone.0054005.
- Brocklehurst, K. R., Hobman, J. L., Lawley, B., Blank, L., Marshall, S. J., Brown, N. L., & Morby, A. P. (1999). ZntR is a Zn (II)-responsive MerR-like transcriptional regulator of zntA in Escherichia coli. *Molecular Microbiology*, **31**(3), 893-902. DOI: <https://doi.org/10.1046/j.1365-2958.1999.01229.x>.
- Bruins, M. R., Kapil, S. & Oehme, F. W. (2000). Microbial resistance to metals in the environment’, *Ecotoxicology and Environmental Safety*, **45**(3), 198–207. DOI: 10.1006/eesa.1999.1860.
- Cai, P., Liu, X., Ji, D., Yang, S., Walker, S. L., Wu, Y., ... & Huang, Q. (2018). Impact of soil clay minerals on growth, biofilm formation, and virulence gene expression of Escherichia coli O157: H7. *Environmental Pollution*, **243**, 953-960. DOI: 10.1016/j.envpol.2018.09.032.
- Cangelosi, V., Ruckthong, L. & Pecoraro, V. (2017). 10. Lead (II) Binding in Natural and Artificial Proteins. In A. Sigel, H. Sigel & R. Sigel (Ed.), *Lead: Its Effects on Environment and Health* (pp. 271-318). Berlin, Boston: De Gruyter. DOI: 10.1515/9783110434330-010.
- Cánovas, D., Cases, I., & De Lorenzo, V. (2003). Heavy metal tolerance and metal homeostasis in Pseudomonas putida as revealed by complete genome analysis. *Environmental Microbiology*, **5**(12), 1242-1256. DOI: 10.1046/j.1462-2920.2003.00463.x.
- Cardoso, E. J. B. N., Vasconcellos, R. L. F., Bini, D., Miyauchi, M. Y. H., Santos, C. A. D., Alves, P. R. L., ... & Nogueira, M. A. (2013). Soil health: looking for suitable indicators. What should be considered to assess the effects of use and management on soil health?. *Scientia Agricola*, **70**, 274-289. DOI: 10.1590/S0103-90162013000400009.
- Carter, K. P., Young, A. M., & Palmer, A. E. (2014). Fluorescent sensors for measuring metal ions in living systems. *Chemical Reviews*, **114**(8), 4564-4601. DOI: 10.1021/cr400546e.

- Castillo, J., Gáspár, S., Leth, S., Niculescu, M., Mortari, A., Bontidean, I., ... & Csöregi, E. (2004). Biosensors for life quality: Design, development and applications. *Sensors and Actuators B: Chemical*, **102**(2), 179-194. DOI: 10.1016/j.snb.2004.04.084.
- Chatterjee, S., Lee, J. B., Valappil, N. V., Luo, D., & Menon, V. M. (2011). Investigating the distance limit of a metal nanoparticle based spectroscopic ruler. *Biomedical Optics Express*, **2**(6), 1727-1733. DOI: 10.1364/BOE.2.001727.
- Chaudri, A., McGrath, S., Gibbs, P., Chambers, B., Carlton-Smith, C., Bacon, J., ... & Aitken, M. (2008). Population size of indigenous *Rhizobium leguminosarum* biovar *trifolii* in long-term field experiments with sewage sludge cake, metal-amended liquid sludge or metal salts: effects of zinc, copper and cadmium. *Soil Biology and Biochemistry*, **40**(7), 1670-1680. DOI: 10.1016/j.soilbio.2008.01.026.
- Chen, P. R., Wasinger, E. C., Zhao, J., Van Der Lelie, D., Chen, L. X., & He, C. (2007). Spectroscopic insights into lead (II) coordination by the selective lead (II)-binding protein PbrR691. *Journal of the American Chemical Society*, **129**(41), 12350-12351. DOI: 10.1021/ja0733890.
- Cheng, H., & Hu, Y. (2010). Lead (Pb) isotopic fingerprinting and its applications in lead pollution studies in China: a review. *Environmental pollution*, **158**(5), 1134-1146. DOI: 10.1016/j.envpol.2009.12.028.
- Chibuike, G. U., & Obiora, S. C. (2014). Heavy metal polluted soils: effect on plants and bioremediation methods. *Applied and Environmental Soil Science*, **2014**, 752708. DOI: 10.1155/2014/752708.
- Chiu, T. Y., & Yang, D. M. (2012). Intracellular Pb²⁺ content monitoring using a protein-based Pb²⁺ indicator. *Toxicological Sciences*, **126**(2), 436-445. DOI: 10.1093/toxsci/kfs007.
- Chiu, T. Y., Chen, P. H., Chang, C. L., & Yang, D. M. (2013). Live-cell dynamic sensing of Cd²⁺ with a FRET-based indicator. *PLoS One*, **8**(6), e65853. DOI: 10.1371/journal.pone.0065853.
- Choudhary, S., & Sar, P. (2009). Characterization of a metal resistant *Pseudomonas* sp. isolated from uranium mine for its potential in heavy metal (Ni²⁺, Co²⁺, Cu²⁺, and Cd²⁺) sequestration. *Bioresource Technology*, **100**(9), 2482-2492. DOI: 10.1016/j.biortech.2008.12.015.
- Cobbett, C., & Goldsbrough, P. (2002). Phytochelatins and metallothioneins: roles in heavy metal detoxification and homeostasis. *Annual Review of Plant Biology*, **53**(1), 159-182. DOI: 10.1146/annurev.arplant.53.100301.135154.
- Cold Spring Harbor Protocol (2010). *M9 minimal medium (standard)*. doi:10.1101/pdb.rec12295. Access at <http://cshprotocols.cshlp.org/content/2010/8/pdb.rec12295.short>. Access date: 30th Dec 2021, 16:14

- Cui, J., Kaandorp, J. A., & Lloyd, C. M. (2008). Simulating in vitro transcriptional response of zinc homeostasis system in *Escherichia coli*. *BMC Systems Biology*, **2**(1), 1-14. DOI: 10.1186/1752-0509-2-89.
- Cui, Z., Luan, X., Jiang, H., Li, Q., Xu, G., Sun, C., ... & Huang, W. E. (2018). Application of a bacterial whole cell biosensor for the rapid detection of cytotoxicity in heavy metal contaminated seawater. *Chemosphere*, **200**, 322-329. DOI: 10.1016/j.chemosphere.2018.02.097.
- Day, R.N., and Davidson, M.W. (2012) Fluorescent proteins for FRET microscopy: Monitoring protein interactions in living cells. *Bioessays*. 2012 May;34(5):341-50. doi: 10.1002/bies.201100098.
- Dean J.R. (2010). Heavy Metal Bioavailability and Bioaccessibility in Soil. In: Cummings S. (eds) Bioremediation. *Methods in Molecular Biology (Methods and Protocols)*, **599**, 15–36, Humana Press, United States. DOI: 10.1007/978-1-60761-439-5_2.
- Dhalaria, R., Kumar, D., Kumar, H., Nepovimova, E., Kuča, K., Torequl Islam, M., & Verma, R. (2020). Arbuscular mycorrhizal fungi as potential agents in ameliorating heavy metal stress in plants. *Agronomy*, **10**(6), 815. DOI: 10.3390/agronomy10060815.
- Diep, P., Mahadevan, R., & Yakunin, A. F. (2018). Heavy metal removal by bioaccumulation using genetically engineered microorganisms. *Frontiers in Bioengineering and Biotechnology*, **6**, 157. DOI: 10.3389/fbioe.2018.00157.
- Ding, Z., Wu, J., You, A., Huang, B., & Cao, C. (2017). Effects of heavy metals on soil microbial community structure and diversity in the rice (*Oryza sativa* L. subsp. Japonica, Food Crops Institute of Jiangsu Academy of Agricultural Sciences) rhizosphere. *Soil Science and Plant Nutrition*, **63**(1), 75-83. DOI: 10.1080/00380768.2016.1247385.
- Elcin, E., & Öktem, H. A. (2020). Inorganic cadmium detection using a fluorescent whole-cell bacterial bioreporter. *Analytical Letters*, **53**(17), 2715-2733. DOI: 10.1080/00032719.2020.1755867.
- EPA 1992. Behavior of Metals in Soils. *Ground Water Issue*. EPA/540/S-92/018 October 1992
- Espinosa-Urgel, M., Kolter, R., & Ramos, J. L. (2002). Root colonization by *Pseudomonas putida*: love at first sight. *Microbiology*, **148**(2), 341-343. DOI: 10.1099/00221287-148-2-341.
- Fehr, M., Frommer, W. B., & Lalonde, S. (2002). Visualization of maltose uptake in living yeast cells by fluorescent nanosensors. *Proceedings of the National Academy of Sciences*, **99**(15), 9846-9851. DOI: 10.1073/pnas.142089199.
- Fernández, M., Niqui-Arroyo, J. L., Conde, S., Ramos, J. L., & Duque, E. (2012). Enhanced tolerance to naphthalene and enhanced rhizoremediation performance for *Pseudomonas putida* KT2440 via the NAH7 catabolic plasmid. *Applied and Environmental Microbiology*, **78**(15), 5104-5110. DOI: 10.1128/AEM.00619-12.

- Florio, A., Felici, B., Migliore, M., Teresa, M., Abate, D., and Benedetti, A., 2015. Nitrogen losses , uptake and abundance of ammonia oxidizers in soil under mineral and organo-mineral fertilization regimes. *Society of Chemical Industry*, 96, 2440– 2450.
- Friedlova, M. (2010). The influence of heavy metals on soil biological and chemical properties. *Soil and Water Research*, 5(1), 21-27. DOI: 10.17221/11/2009-SWR.
- Gadd, G. M. (2010). Metals, minerals and microbes: geomicrobiology and bioremediation. *Microbiology*, 156(3), 609-643. DOI: 10.1099/mic.0.037143-0.
- Gehrig, P. M., You, C., Dallinger, R., Gruber, C., Brouwer, M., Kägi, J. H., & Hunziker, P. E. (2000). Electrospray ionization mass spectrometry of zinc, cadmium, and copper metallothioneins: evidence for metal-binding cooperativity. *Protein Science*, 9(2), 395-402. DOI: 10.1110/ps.9.2.395.
- Giller, K. E., Witter, E., & McGrath, S. P. (2009). Heavy metals and soil microbes. *Soil Biology and Biochemistry*, 41(10), 2031-2037. DOI: 10.1016/j.soilbio.2009.04.026.
- Gong, T., Liu, R., Che, Y., Xu, X., Zhao, F., Yu, H., ... & Yang, C. (2016). Engineering *Pseudomonas putida* KT 2440 for simultaneous degradation of carbofuran and chlorpyrifos. *Microbial Biotechnology*, 9(6), 792-800. DOI: 10.1111/1751-7915.12381.
- Graumann, K., & Premstaller, A. (2006). Manufacturing of recombinant therapeutic proteins in microbial systems. *Biotechnology Journal: Healthcare Nutrition Technology*, 1(2), 164-186. DOI: 10.1002/biot.200500051.
- Gryschko, R., Kuhnle, R., Terytze, K., Breuer, J., & Stahr, K. (2005). Research articles soil extraction of readily soluble heavy metals and as with 1 M NH₄NO₃-solution. *J. Soils Sediments*, 5(2), 101-106. DOI: 10.1065/jss2004.10.119.
- Guo, G., Zhou, Q., & Ma, L. Q. (2006). Availability and assessment of fixing additives for the in situ remediation of heavy metal contaminated soils: a review. *Environmental Monitoring and Assessment*, 116(1), 513-528. DOI: 10.1007/s10661-006-7668-4.
- Gupta, P., Diwan, B. (2017) Bacterial Exopolysaccharide mediated heavy metal removal: A Review on biosynthesis, mechanism, and remediation strategies. *Biotechnology Reports*. 13, 58-71, <https://doi.org/10.1016/j.btre.2016.12.006>
- Harms, H., Wells, M.C., & Van der Meer, J.R. (2006). Whole-cell living biosensors—are they ready for environmental application?. *Appl Microbiol Biotechnol*, 70, 273–280. DOI: 10.1007/s00253-006-0319-4.
- Harmsen, J. (2007). Measuring Bioavailability: From a Scientific Approach to Standard Methods. *Journal of Environmental Quality*, 36, 1420–1428. DOI: 10.2134/jeq2006.0492.
- Harris, J. (2009). Soil microbial communities and restoration ecology: facilitators or followers?. *Science*, 325(5940), 573-574. DOI: 10.1126/science.1172975.

- Hartley, J. L., Temple, G. F., & Brasch, M. A. (2000). DNA cloning using in vitro site-specific recombination. *Genome Research*, **10**(11), 1788-1795. DOI: 10.1101/gr.143000.
- He, W., Yuan, S., Zhong, W. H., Siddikee, M. A., & Dai, C. C. (2016). Application of genetically engineered microbial whole-cell biosensors for combined chemosensing. *Applied Microbiology and Biotechnology*, **100**(3), 1109-1119. DOI: 10.1007/s00253-015-7160-6.
- Hochreiter, B., Pardo-Garcia, A., & Schmid, J. A. (2015). Fluorescent proteins as genetically encoded FRET biosensors in life sciences. *Sensors*, **15**(10), 26281-26314. DOI: 10.3390/s151026281.
- Hoorman, J. J. (2011). The role of soil bacteria. *Ohio State University Extension*. Columbus, pp. 1-4. DOI: 10.2323/jgam.7.128.
- Hurdebise, Q., Tarayre, C., Fischer, C., Colinet, G., Hiligsmann, S., & Delvigne, F. (2015). Determination of zinc, cadmium and lead bioavailability in contaminated soils at the single-cell level by a combination of whole-cell biosensors and flow cytometry. *Sensors*, **15**(4), 8981-8999. DOI: 10.3390/s150408981.
- Hynninen, A. (2010). *Zinc, cadmium and lead resistance mechanisms in bacteria and their contribution to biosensing*. Doctoral dissertation, University of Helsinki, Faculty of Agriculture and Forestry, Department of Food and Environmental Sciences, Division of Microbiology. Available at: <http://urn.fi/URN:ISBN:978-952-10-6263-6>.
- Hynninen, A., Tönismann, K., & Virta, M. (2010). Improving the sensitivity of bacterial bioreporters for heavy metals. *Bioengineered Bugs*, **1**(2), 132-138. DOI: 10.4161/bbug.1.2.10902.
- Ibraheem, A., Yap, H., Ding, Y., & Campbell, R. E. (2011). A bacteria colony-based screen for optimal linker combinations in genetically encoded biosensors. *BMC Biotechnology*, **11**(1), 1-13. DOI: 10.1186/1472-6750-11-105.
- Ivask, A., François, M., Kahru, A., Dubourguier, H. C., Virta, M., & Douay, F. (2004). Recombinant luminescent bacterial sensors for the measurement of bioavailability of cadmium and lead in soils polluted by metal smelters. *Chemosphere*, **55**(2), 147-156. DOI: 10.1016/j.chemosphere.2003.10.064.
- Ivask, A., Rõlova, T., & Kahru, A. (2009). A suite of recombinant luminescent bacterial strains for the quantification of bioavailable heavy metals and toxicity testing. *BMC Biotechnology*, **9**(1), 41. DOI: 10.1186/1472-6750-9-41.
- Ivask, A., Virta, M., & Kahru, A. (2002). Construction and use of specific luminescent recombinant bacterial sensors for the assessment of bioavailable fraction of cadmium, zinc, mercury and chromium in the soil. *Soil Biology and Biochemistry*, **34**(10), 1439-1447. DOI: 10.1016/S0038-0717(02)00088-3.

- Jacobson, A. R., Dousset, S., Andreux, F., & Baveye, P. C. (2007). Electron microprobe and synchrotron X-ray fluorescence mapping of the heterogeneous distribution of copper in high-copper vineyard soils. *Environmental Science & Technology*, **41**(18), 6343-6349. DOI: 10.1021/es070707m.
- Javaid, A. (2011) Importance of Arbuscular Mycorrhizal Fungi in Phytoremediation of Heavy Metal Contaminated Soils. In: Khan, M.S., Ed., *Biomanagement of Metal-Contaminated Soils*, Springer, Berlin, Heidelberg, 125-141.
- Jeffery, S.; Abalos, D.; Prodana, M.; Bastos, A.C.; Van Groenigen, J.W.; Hungate, B.A.; Verheijen, F. Biochar boosts tropical but not temperate crop yields. *Environ. Res. Lett.* 2017, 12. <https://doi.org/10.1088/1748-9326/aa67bd>
- Jia, X., Bu, R., Zhao, T., & Wu, K. (2019). Sensitive and specific whole-cell biosensor for arsenic detection. *Applied and Environmental Microbiology*, **85**(11), e00694-19. DOI: 10.1128/AEM.00694-19.
- Jung, .M.C Heavy Metal Concentrations in Soils and Factors Affecting Metal Uptake by Plants in the Vicinity of a Korean Cu-W Mine. *Sensor (Basel)*. 8, 2413-2423. doi: 10.3390/s8042413
- Kalies, S., Kuetemeyer, K., and Heisterkamp, A. Mechanisms of high-order photobleaching and its relationship to intracellular ablation. *Biomedical Optics Express*. 2, 4.
- Kabata-Pendias, A., & Pendias, H. (2001). Trace elements in soils and plants CRC Press Inc. 2nd edition, *Boca Raton*, FL, USA.
- Kaper, T., Lager, I., Looger, L. L., Chermak, D., & Frommer, W. B. (2008). Fluorescence resonance energy transfer sensors for quantitative monitoring of pentose and disaccharide accumulation in bacteria. *Biotechnology for Biofuels*, **1**(1), 1-10. DOI: 10.1186/1754-6834-1-11.
- Kelly, J. J., Häggblom, M. M., & Tate, R. L. (2003). Effects of heavy metal contamination and remediation on soil microbial communities in the vicinity of a zinc smelter as indicated by analysis of microbial community phospholipid fatty acid profiles. *Biology and Fertility of Soils*, **38**(2), 65-71. DOI: 10.1007/s00374-003-0642-1.
- Khalili, M., Soleyman, M.R., Baazm, M., and Beyer, C. (2015) High-level expression and purification of soluble bioactive recombinant human heparin-binding epidermal growth factor in *Escherichia coli*. *Cell Biology International*. 39, 858-864. doi: 10.1002/cbin.10454
- Khan, A., Sharif, M., Ali, A., Shah, S.N.M., Mian, I.A., Wahid, F., Jan, B., Adnan., Nawaz, S., and Ali, N. (2014) Potential of Arbuscular Mycorrhiza Fungi in Phytoremediation of Heavy Metals and Effect on Yield of Wheat Crop. *American Journal of Plant Sciences*, **5**, 1578-1586. <http://dx.doi.org/10.4236/ajps.2014.511171>
- Khashei, S., Etemadifar, Z., & Rahmani, H. R. (2018). Immobilization of *Pseudomonas putida* PT in resistant matrices to environmental stresses: a strategy for continuous removal of heavy metals under extreme conditions. *Annals of Microbiology*, **68**(12), 931-942. DOI: 10.1007/s13213-018-1402-7.

- Kim, H., Jang, G., & Yoon, Y. (2020). Specific heavy metal/metalloid sensors: current state and perspectives. *Applied Microbiology and Biotechnology*, **104**(3), 907-914. DOI: 10.1007/s00253-019-10261-y.
- Kim, R. Y., Yoon, J. K., Kim, T. S., Yang, J. E., Owens, G., & Kim, K. R. (2015). Bioavailability of heavy metals in soils: definitions and practical implementation—a critical review. *Environmental Geochemistry and Health*, **37**(6), 1041-1061. DOI: 10.1007/s10653-015-9695-y.
- Kindler, R., Miltner, A., Thullner, M., Richnow, H.-H., Kästner, M., 2009. Fate of bacterial biomass derived fatty acids in soil and their contribution to soil organic matter. *Organic Geochemistry*. 40, 29-37. <http://dx.doi.org/10.1016/j.orggeochem.2008.09.005>
- Kremers, G. J., Goedhart, J., van Munster, E. B., & Gadella, T. W. (2006). Cyan and yellow super fluorescent proteins with improved brightness, protein folding, and FRET Förster radius. *Biochemistry*, **45**(21), 6570-6580. DOI: 10.1021/bi0516273.
- Landy, A. (1989). Dynamic, structural, and regulatory aspects of λ site-specific recombination. *Annual Review of Biochemistry*, **58**(1), 913-941. DOI: 10.1146/annurev.bi.58.070189.004405.
- LaRossa, R. A., Smulski, D. R., & Van Dyk, T. K. (1995). Interaction of lead nitrate and cadmium chloride with Escherichia coli K-12 and Salmonella typhimurium global regulatory mutants. *Journal of Industrial Microbiology and Biotechnology*, **14**(3-4), 252-258. DOI: 10.1007/Bf01569936.
- Li, P. S., Peng, Z. W., Su, J., & Tao, H. C. (2014). Construction and optimization of a Pseudomonas putida whole-cell bioreporter for detection of bioavailable copper. *Biotechnology Letters*, **36**(4), 761-766. DOI: 10.1007/s10529-013-1420-2.
- Liu, T., Yang, L., Hu, Z., Xue, J., Lu, Y., Chen, X., Griffiths, B., Whalen, J.K., and Liu, M. (2020). Biochar exerts negative effects on soil fauna across multiple trophic levels in a cultivated acidic soil. *Biology and Fertility of Soils*, 56:597–606. <https://doi.org/10.1007/s00374-020-01436-1>
- Liu, Y., He, N., Wen, X., Xu, L., Sun, X., Yu, G., Liang, L., Schipper, L.A. (2018). The optimum temperature of soil microbial respiration: Patterns and controls. *Soil Biology and Biochemistry*. 121. 35-42.
- Lee, S. W., Glickmann, E., & Cooksey, D. A. (2001). Chromosomal locus for cadmium resistance in Pseudomonas putida consisting of a cadmium-transporting ATPase and a MerR family response regulator. *Applied and Environmental Microbiology*, **67**(4), 1437-1444. DOI: 10.1128/AEM.67.4.1437-1444.2001.
- Leedjarv, A., Ivask, A., & Virta, M. (2008). Interplay of different transporters in the mediation of divalent heavy metal resistance in Pseudomonas putida KT2440. *Journal of Bacteriology*, **190**(8), 2680–2689. DOI: 10.1128/JB.01494-07.

- Lehmann, J. (2007). A handful of carbon. *Nature*, **447**(7141), 143-144. DOI: 10.1038/447143a.
- Leica-Teledyne Photometrics (2021). *What is spinning disk confocal microscopy*. Available at: <https://www.photometrics.com/learn/spinning-disk-confocal-microscopy/what-is-spinning-disk-confocal-microscopy>
- Liu, P., Huang, Q., & Chen, W. (2012). Construction and application of a zinc-specific biosensor for assessing the immobilization and bioavailability of zinc in different soils. *Environmental Pollution*, **164**, 66-72. DOI: 10.1016/j.envpol.2012.01.023.
- Lorenz, K.; Lal, R. Carbon Sequestration in Agricultural Ecosystems. *Springer International Publishing*: Cham, Switzerland, 2018.
- Ma, Y., Oliveira, R. S., Freitas, H., & Zhang, C. (2016). Biochemical and molecular mechanisms of plant-microbe-metal interactions: relevance for phytoremediation. *Frontiers in Plant Science*, **7**, 918. DOI: 10.3389/fpls.2016.00918.
- Maderova, L., Watson, M., & Paton, G. I. (2011). Bioavailability and toxicity of copper in soils: Integrating chemical approaches with responses of microbial biosensors. *Soil Biology and Biochemistry*, **43**(6), 1162-1168. DOI: 10.1016/j.soilbio.2011.02.004.
- Magrisso, S., Erel, Y., & Belkin, S. (2008). Microbial reporters of metal bioavailability. *Microbial Biotechnology*, **1**(4), 320-330. DOI: 10.1111/j.1751-7915.2008.00022.x.
- Mahar, A., Ping, W. A. N. G., Ronghua, L. I., & ZHANG, Z. (2015). Immobilization of lead and cadmium in contaminated soil using amendments: a review. *Pedosphere*, **25**(4), 555-568. DOI: 10.1016/S1002-0160(15)30036-9.
- Maiz, I., Arambarri, I., Garcia, R., & Millan, E. (2000). Evaluation of heavy metal availability in polluted soils by two sequential extraction procedures using factor analysis. *Environmental Pollution*, **110**(1), 3-9. DOI: 10.1016/S0269-7491(99)00287-0.
- Malhotra, A. (2009) Tagging for protein expression. *Methods Enzymol.*, **463**, pp. 239-258 [https://doi.org/10.1016/S0076-6879\(09\)63016-0](https://doi.org/10.1016/S0076-6879(09)63016-0)
- Marschner, H., Römheld, V., and Cakmak, I., 1987. Root-induced changes of nutrient availability in the rhizosphere. *Journal of Plant Nutrition*, **10** (9–16), 1175–1184
- Martin-Betancor, K., Rodea-Palomares, I., Muñoz-Martín, M. A., Leganes, F., & Fernandez-Pinas, F. (2015). Construction of a self-luminescent cyanobacterial bioreporter that detects a broad range of bioavailable heavy metals in aquatic environments. *Frontiers in Microbiology*, **6**, 186. DOI: 10.3389/fmicb.2015.00186.
- Martinez-Finley, E. J., Chakraborty, S., Fretham, S., & Aschner, M. (2012). Admit one: how essential and nonessential metals gain entrance into the cell. *Metallomics: Integrated Biometal Science*, **4**(7), 593–605. DOI: 10.1039/c2mt00185c.

- McGowen, S. L., Basta, N. T., & Brown, G. O. (2001). Use of diammonium phosphate to reduce heavy metal solubility and transport in smelter-contaminated soil. *Journal of Environmental Quality*, **30**(2), 493-500. DOI: 10.2134/jeq2001.302493x.
- Medynska-Juraszek, A., Bednik, M., & Chohura, P. (2020). Assessing the Influence of Compost and Biochar Amendments on the Mobility and Uptake of Heavy Metals by Green Leafy Vegetables Agnieszka. *Environmental Research and Public Health*. **17**, 7861, DOI: 10.3390/ijerph17217861.
- Meers, E., Samson, R., Tack, F. M. G., Ruttens, A., Vandegheuchte, M., Vangronsveld, J., & Verloo, M. G. (2007). Phytoavailability assessment of heavy metals in soils by single extractions and accumulation by *Phaseolus vulgaris*. *Environmental and Experimental Botany*, **60**(3), 385-396. DOI: 10.1016/j.envexpbot.2006.12.010.
- Mensah, A.K. and Frimpong, K.A., 2018. Biochar and/or Compost Applications Improve Soil Properties, Growth, and Yield of Maize Grown in Acidic Rainforest and Coastal Savannah Soils in Ghana. *International Journal of Agronomy*.8. <https://doi.org/10.1155/2018/6837404>
- Misra, V., Tiwari, A., Shukla, B., & Seth, C. S. (2009). Effects of soil amendments on the bioavailability of heavy metals from zinc mine tailings. *Environmental Monitoring and Assessment*, **155**(1), 467-475. DOI: 10.1007/s10661-008-0449-5.
- Miyawaki, A., Llopis, J., Heim, R., McCaffery, M., Adams, J.A., Ikura, M., & Tsien, R.Y. (1997). Fluorescent indicators for Ca²⁺ based on green fluorescent proteins and calmodulin. *Nature*, **388**, 882–887. DOI: 10.1038/42264.
- Mkhabela, M.S. and Warman, P.R., 2005. The influence of municipal solid waste compost on yield, soil phosphorus availability and uptake by two vegetable crops grown in a Pugwash sandy loam soil in Nova Scotia. *Agriculture, Ecosystems & Environment*, **106** (1), 57–67.
- Moebius-Clune, B.N., Moebius-Clune, D.J., Gugino, B.K., Idowu, O.J., Schindelbeck, R.R., Ristow, A.J., Van Es, H.M., Thies, J.E., Shayler, H.A., McBride, M.B., Kurtz, K.S.M., Wolfe, D.W., & Abawi, G.S. (2016). *Comprehensive Assessment of Soil Health – The Cornell Framework*, Edition 3.2, Cornell University, Geneva, NY. Available at: bit.ly/SoilHealthTrainingManual.
- Nakazawa, T. (2002) Travels of a *Pseudomonas*, from Japan around the world. *Environmental Microbiology*. **12**, 782-786.
- National Research Council. (2003). *Bioavailability of contaminants in soils and sediments: processes, tools, and applications*. National Academies Press. Washington, D.C.
- Natural Resources Conservation Services (2012). Soil Health. Retrieved online via <https://www.nrcs.usda.gov/wps/portal/nrcs/main/soils/health/> [last accessed: 28/08/2021].
- Nelson, K. E., Weinel, C., Paulsen, I. T., Dodson, R. J., Hilbert, H., Martins dos Santos, V. A. P., ... & Fraser, C. M. (2002). Complete genome sequence and comparative analysis of the metabolically versatile *Pseudomonas putida* KT2440. *Environmental Microbiology*, **4**(12), 799-808. DOI: 10.1046/j.1462-2920.2002.00366.x.

- Neyrolles, O., Mintz, E., and Catty P. (2013) Zinc and copper toxicity in host defense against pathogens: *Mycobacterium tuberculosis* as a model example of an emerging paradigm. *Front. Cell. Infect. Microbiol.* 3, 89. <https://doi.org/10.3389/fcimb.2013.00089>
- NJDEP (New Jersey Department of Environmental Protection) (1996). Site Remediation & Waste Management Program, Guidance document: Soil Cleanup Criteria. Available at: <https://www.nj.gov/dep/srp/guidance/scc/0> [last accessed: 28/08/2021].
- Olaniran, A. O., Balgobind, A., & Pillay, B. (2013). Bioavailability of heavy metals in soil: impact on microbial biodegradation of organic compounds and possible improvement strategies. *International Journal of Molecular Sciences*, **14**(5), 10197-10228. DOI: 10.3390/ijms140510197.
- Ovečka, M., & Takáč, T. (2014). Managing heavy metal toxicity stress in plants: biological and biotechnological tools. *Biotechnology Advances*, **32**(1), 73-86. DOI: 10.1016/j.biotechadv.2013.11.011.
- Pace, C. N., Vajdos, F., Fee, L., Grimsley, G., & Gray, T. (1995). How to measure and predict the molar absorption coefficient of a protein. *Protein Science*, **4**(11), 2411-2423. DOI: 10.1002/pro.5560041120.
- Park, J.H., Lamb, D., Paneerselvam, P., Choppala, G., Bolan, N., and Chung, J.-W., 2010. Role of organic amendments on enhanced bioremediation of heavy metal(loid) contaminated soils. *Journal of Hazardous Materials*, 185, 549–574.
- Park, J. H., Choppala, G. K., Bolan, N. S., Chung, J. W., & Chuasavathi, T. (2011). Biochar reduces the bioavailability and phytotoxicity of heavy metals. *Plant and Soil*, **348**(1), 439-451. DOI: 10.1007/s11104-011-0948-y.
- Patzer, S. I., & Hantke, K. (1998). The ZnuABC high-affinity zinc uptake system and its regulator Zur in *Escherichia coli*. *Molecular Microbiology*, **28**(6), 1199-1210. DOI: 10.1046/j.1365-2958.1998.00883.x.
- Peijnenburg, W. J., Zablotskaja, M., & Vijver, M. G. (2007). Monitoring metals in terrestrial environments within a bioavailability framework and a focus on soil extraction. *Ecotoxicology and Environmental Safety*, **67**(2), 163-179. DOI: 10.1016/j.ecoenv.2007.02.008.
- Peng, J., Miao, L., Chen, X., & Liu, P. (2018). Comparative transcriptome analysis of *Pseudomonas putida* KT2440 revealed its response mechanisms to elevated levels of zinc stress. *Frontiers in Microbiology*, **9**, 1669. DOI: 10.3389/fmicb.2018.01669.
- Penumetcha, P., Lau, K., Zhu, X., Davis, K., Eckdahl, T.T., and Campbell, A.M. (2010) Improving the Lac system for synthetic biology. *Bios.* 81 (1), 7-15. <https://doi.org/10.1893/011.081.0104>
- Periasamy, A. (2001). *Methods in Cellular Imaging*. Oxford University Press, Oxford, New York. 434 pp

- Qin, W., Liu, X., Yu, X., Chu, X., Tian, J., & Wu, N. (2017). Identification of cadmium resistance and adsorption gene from *Escherichia coli* BL21 (DE3). *Rsc Advances*, **7**(81), 51460-51465. DOI: 10.1039/c7ra10656d.
- Qu, C., Chen, W., Hu, X., Cai, P., Chen, C., Yu, X. Y., & Huang, Q. (2019). Heavy metal behaviour at mineral-organo interfaces: Mechanisms, modelling and influence factors. *Environment International*, **131** (1), 104995. DOI: 10.1016/j.envint.2019.104995.
- Ramos-Gonzales, M.I., Campos, M.J., and Ramos, J.L. (2005) Analysis of *Pseudomonas putida* KT2440 Gene Expression in the Maize Rhizosphere: In Vitro Expression Technology Capture and Identification of Root-Activated Promoters. *Journal of Bacteriology*. **187**, 12, 4033-4041. doi:10.1128/JB.187.12.4033–4041.2005
- Rajamani, S., Torres, M., Falcao, V., Ewalt Gray, J., Coury, D. A., Colepiccolo, P., & Sayre, R. (2014). Noninvasive evaluation of heavy metal uptake and storage in microralgae using a fluorescence resonance energy transfer-based heavy metal biosensor. *Plant Physiology*, **164**(2), 1059-1067. DOI: 10.1104/pp.113.229765.
- Ravikumar, S., Ganesh, I., Yoo, I. K., & Hong, S. H. (2012). Construction of a bacterial biosensor for zinc and copper and its application to the development of multifunctional heavy metal adsorption bacteria. *Process Biochemistry*, **47**(5), 758-765. DOI: 10.1016/j.procbio.2012.02.007.
- Renella, G., & Giagnoni, L. (2016). Light dazzles from the black box: whole-cell biosensors are ready to inform on fundamental soil biological processes. *Chemical and Biological Technologies in Agriculture*, **3**(1), 1-15. DOI: 10.1186/s40538-016-0059-3.
- Reva, O. N., Weinel, C., Weinel, M., Böhm, K., Stjepandic, D., Hoheisel, J. D., & Tümmler, B. (2006). Functional genomics of stress response in *Pseudomonas putida* KT2440. *Journal of Bacteriology*, **188**(11), 4079-4092. DOI: 10.1128/JB.00101-06.
- Richardson, J., Chatterjee, A., and Jenerette, G.D (2012) Optimum temperatures for soil respiration along a semi-arid elevation gradient in southern California. *Soil Biology and Biochemistry*. **46**, pp. 89-95
- Rieuwerts, J.S., Thornton, I., Farago, M.E., and Ashmore, M.R. (1998) Factors influencing metal bioavailability in soils: preliminary investigations for the development of a critical loads approach for metals. *Chemical Speciation and Bioavailability*, **10** (2). DOI: 10.3184/095422998782775835
- Riley, R. G. & Zachara, J. M. (1992). *Chemical contaminants on DOE lands and selection of contaminant mixtures for subsurface science research*. US Department of Energy, Office of Energy Research, Subsurface Science Program. Washington, D.C., USA.
- Rizza, A., Walia, A., Lanquar, V., Frommer, W. B., & Jones, A. M. (2017). In vivo gibberellin gradients visualized in rapidly elongating tissues. *Nature Plants*, **3**(10), 803-813. DOI: 10.1038/s41477-017-0021-9.

- Romero-Isart, N., & Vašák, M. (2002). Advances in the structure and chemistry of metallothioneins. *Journal of Inorganic Biochemistry*, **88**(3-4), 388-396. DOI: 10.1016/S0162-0134(01)00347-6.
- Rosano, G.L., & Ceccarelli, E.A. (2014). Recombinant protein expression in Escherichia coli: advances and challenges. *Frontiers in Microbiology*, **5**, 172. DOI: 10.3389/fmicb.2014.00172.
- Sanderson, M.J., Smith, I., Parker, I., and Bootman, M.D. (2014) Fluorescence Microscopy. *Cold Spring Harb Protoc.* ; 10. doi:10.1101/pdb.top071795.
- Sahuquillo, A., Rigol, A., & Rauret, G. (2003). Overview of the use of leaching/extraction tests for risk assessment of trace metals in contaminated soils and sediments. *TrAC Trends in Analytical Chemistry*, **22**(3), 152-159. DOI: 10.1016/S0165-9936(03)00303-0.
- Saleski, T. E., Chung, M. T., Carruthers, D. N., Khasbaatar, A., Kurabayashi, K., & Lin, X. N. (2021). Optimized gene expression from bacterial chromosome by high-throughput integration and screening. *Science Advances*, **7**(7), eabe1767. DOI: 10.1126/sciadv.abe1767.
- Saydam, N., Adams, T. K., Steiner, F., Schaffner, W., & Freedman, J. H. (2002). Regulation of metallothionein transcription by the metal-responsive transcription factor MTF-1: identification of signal transduction cascades that control metal-inducible transcription. *Journal of Biological Chemistry*, **277**(23), 20438-20445. DOI: 10.1074/jbc.M110631200.
- Schmid, G., Zeitvogel, F., Hao, L., Ingino, P., Adaktylou, I., Eickhoff, M., & Obst, M. (2016). Submicron-scale heterogeneities in nickel sorption of various cell–mineral aggregates formed by Fe (II)-oxidizing bacteria. *Environmental Science & Technology*, **50**(1), 114-125.
- Semple, K.T., Doick, K.K., Jones, K.C., Burauel, P., Craven, A., and Harms, H. (2004). Defining Bioavailability and Bioaccessibility of Contaminated Soil and Sediment is Complicated. *Environmental Science & Technology*. 15, 229A
- Shakya, M., Lo, C. C., & Chain, P. S. (2019). Advances and challenges in metatranscriptomic analysis. *Frontiers in Genetics*, **10**, 904. DOI: 10.3389/fgene.2019.00904.
- Sharma, M. R., & Raju, N. S. (2013). Correlation of heavy metal contamination with soil properties of industrial areas of Mysore, Karnataka, India by cluster analysis. *International Research Journal of Environment Sciences*, **2**(10), 22-27. Available at: <http://www.isca.me/IJENS/Archive/v2/i10/4.ISCA-IRJEvS-2013-166.pdf>.
- Shim, T., Yoo, J., Ryu, C., Park, Y. K., & Jung, J. (2015). Effect of steam activation of biochar produced from a giant Miscanthus on copper sorption and toxicity. *Bioresource Technology*, **197**, 85-90. DOI: 10.1016/j.biortech.2015.08.055.
- Silver, S., & Phung, L. T. (2005). A bacterial view of the periodic table: genes and proteins for toxic inorganic ions. *Journal of Industrial Microbiology and Biotechnology*, **32**(11-12), 587-605. DOI: 10.1007/s10295-005-0019-6.

- Smejkalova, M., Mikanova, O., & Boruvka, L. J. P. S. (2003). Effects of heavy metal concentrations on biological activity of soil micro-organisms. *Plant Soil and Environment*, **49**(7), 321-326. Available at: http://www.cazv.cz/2003/pse7_03/5-smejkalova.pdf.
- Soleja, N., Jairajpuri, M. A., Queen, A., & Mohsin, M. (2019). Genetically encoded FRET-based optical sensor for Hg²⁺ detection and intracellular imaging in living cells. *Journal of Industrial Microbiology and Biotechnology*, **46**(12), 1669-1683.
- Song, Y., Jiang, B., Tian, S., Tang, H., Liu, Z., Li, C., ... & Li, G. (2014). A whole-cell bioreporter approach for the genotoxicity assessment of bioavailability of toxic compounds in contaminated soil in China. *Environmental Pollution*, **195**, 178-184. DOI: 10.1016/j.envpol.2014.08.024.
- Soria, R. I., Rolfe, S. A., Betancourth, M. P., & Thornton, S. F. (2020). The relationship between properties of plant-based biochars and sorption of Cd (II), Pb (II) and Zn (II) in soil model systems. *Heliyon*, **6**(11), e05388. DOI: 10.1016/j.heliyon.2020.e05388.
- Structural Genomics Consortium. (2008). Protein production and purification. *Nature Methods*, **5**(2), 135. <https://doi.org/10.1038/nmeth.f.202>.
- Studier, F. W., & Moffatt, B. A. (1986). Use of bacteriophage T7 RNA polymerase to direct selective high-level expression of cloned genes. *Journal of Molecular Biology*, **189**(1), 113-130. DOI: 10.1016/0022-2836(86)90385-2.
- Sutherland, D. E., Summers, K. L., & Stillman, M. J. (2012). Noncooperative metalation of metallothionein 1A and its isolated domains with zinc. *Biochemistry*, **51**(33), 6690-6700. DOI: 10.1021/bi3004523.
- Suzuki, K. T., & Maitani, T. (1981). Metal-dependent properties of metallothionein. Replacement in vitro of zinc in zinc-thionein with copper. *Biochemical Journal*, **199**(2), 289-295. DOI: 10.1042/bj1990289.
- Tang, J., Zhu, W., Kookana, R., & Katayama, A. (2013). Characteristics of biochar and its application in remediation of contaminated soil. *Journal of Bioscience and Bioengineering*, **116**(6), 653-659. DOI: 10.1016/j.jbiosc.2013.05.035.
- Tanhuanpaa, K., Virtanen, J. & Somerharju, P. (2000) Fluorescence imaging of pyrene-labeled lipids in living cells. *Biochim. Biophys. Acta*, **1497**, 308–320.
- Thévenot, D. R., Toth, K., Durst, R. A., & Wilson, G. S. (2001). Electrochemical biosensors: recommended definitions and classification. *Biosensors and Bioelectronics*, **16**(1-2), 121-131. DOI: 10.1016/S0956-5663(01)00115-4.
- Thurston, M., Maida, D., & Gannon, C. (2000). Oxyrase cell-membrane preparations simplify cultivation of anaerobic bacteria. *Laboratory Medicine*, **31**(9), 509-512. DOI: 10.1309/48HU-6NRF-6ARX-K2U8.
- Troeschel, S. C., Thies, S., Link, O., Real, C. I., Knops, K., Wilhelm, S., ... & Jaeger, K. E. (2012). Novel broad host range shuttle vectors for expression in Escherichia coli, Bacillus

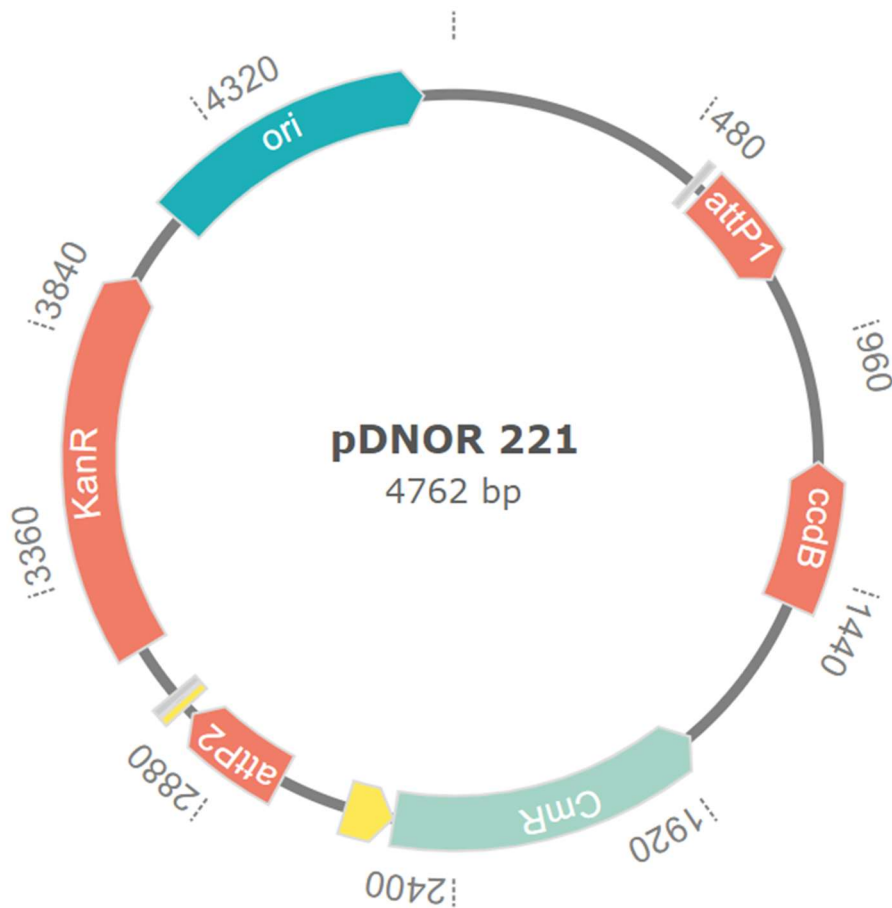
- subtilis and *Pseudomonas putida*. *Journal of Biotechnology*, **161**(2), 71-79. DOI: 10.1016/j.jbiotec.2012.02.020.
- Trott, D., Dawson, J.J.C., Killham, K.S., Miah, M.R.U., Wilson, M.J., and Paton, G.I. (2006). Comparative evaluation of a bioluminescent bacterial assay in terrestrial ecotoxicity testing. *Journal of Environmental Monitoring*, **9**, 44-50.
- Tsien, R. Y. (1998). The green fluorescent protein. *Annual review of biochemistry*, **67**(1), 509-544. DOI: 10.1146/annurev.biochem.67.1.509.
- Turdean, G. L. (2011). Design and development of biosensors for the detection of heavy metal toxicity. *International Journal of Electrochemistry*, **2011**, 343125. DOI: 10.4061/2011/343125.
- Ueshima, M., Ginn, B. R., Haack, E. A., Szymanowski, J. E., & Fein, J. B. (2008). Cd adsorption onto *Pseudomonas putida* in the presence and absence of extracellular polymeric substances. *Geochimica et Cosmochimica Acta*, **72**(24), 5885-5895. DOI: 10.1016/j.gca.2008.09.014.
- United States Environmental Protection Agency (1996). *Report: recent Developments for In Situ Treatment of Metals contaminated Soils*. Office of Solid Waste and Emergency Response. Available at: https://www.epa.gov/sites/default/files/2015-08/documents/recent_dev_metals_542-r-97-004.pdf.
- United States Environmental Protection Agency (2002). Supplemental guidance for developing soil screening levels for superfund sites. Office of Solid Waste and Emergency Response, Washington, D.C. Available at: <http://www.epa.gov/superfund/health/conmedia/soil/index.htm>.
- VanEngelenburg, S. B., & Palmer, A. E. (2008). Fluorescent biosensors of protein function. *Current Opinion in Chemical Biology*, **12**(1), 60-65. DOI: 10.1016/j.cbpa.2008.01.020.
- Vik, E. A., Bardos, P., Brogan, J., Edwards, D., Gondi, F., Henrysson, T., ... & Papassiopi, N. (2001). Towards a framework for selecting remediation technologies for contaminated sites. *Land Contamination and Reclamation*, **9**(1), 119-127. Available at: https://www.researchgate.net/profile/Ferenc-Gondi/publication/228590582_Towards_a_framework_for_selecting_remediation_technologies_for_contaminated_sites/links/0deec52722f8427559000000/Towards-a-framework-for-selecting-remediation-technologies-for-contaminated-sites.pdf.
- Vogel-Mikuš, K., Drobne, D. and Regvar, M. (2005) Zn, Cd and Pb Accumulation and Arbuscular Mycorrhizal Colonisation of Pennycress *Thlaspi praecox* Wulf. (Brassicaceae) from the Vicinity of a Lead Mine and Smelter in Slovenia. *Environmental Pollution*, **133**, 233-242. <http://dx.doi.org/10.1016/j.envpol.2004.06.021>
- Waadt, R., Hitomi, K., Nishimura, N., Hitomi, C., Adams, S. R., Getzoff, E. D., & Schroeder, J. I. (2014). FRET-based reporters for the direct visualization of abscisic acid concentration changes and distribution in *Arabidopsis*. *Elife*, **3**, e01739. DOI: 10.7554/eLife.01739.

- Walker, D.J., Clemente, R., and Bernal, M.P., 2004. Contrasting effects of manure and compost on soil pH, heavy metal availability and growth of *Chenopodium album* L. in a soil contaminated by pyritic mine waste. *Chemosphere*, 57 (3), 215–224
- Wang, A. S., Angle, J. S., Chaney, R. L., Delorme, T. A., & Reeves, R. D. (2006). Soil pH effects on uptake of Cd and Zn by *Thlaspi caerulescens*. *Plant and Soil*, **281**(1), 325-337. DOI: 10.1007/s11104-005-4642-9.
- Watzinger, A. (2015). Microbial phospholipid biomarkers and stable isotope methods help reveal soil functions. *Soil Biology and Biochemistry*, **86**, 98-107. DOI: 10.1016/j.soilbio.2015.03.019.
- Wawra, A., Friesl-Hanl, W., Jager, A., Puschenreiter, M., Soja, G., Reichenauer, T., and Watzinger, A. (2018). Investigations of microbial degradation of polycyclic aromatic hydrocarbons based on ¹³C-labeled phenanthrene in a soil co-contaminated with trace elements using a plant assisted approach. *Environmental Science and Pollution Research*. 25:6364–6377. <https://doi.org/10.1007/s11356-017-0941-y>
- Weiss, D.J., Mason, T.F.D., Zhao, F.J., Kirk, G.J.D., Coles, B.J. and Horstwood, M.S.A. (2005). Isotopic discrimination of zinc in higher plants. *New Phytologist*, **165**, 703-710. DOI: 10.1111/j.1469-8137.2004.01307.x.
- Wuana, R. A., & Okieimen, F. E. (2011). Heavy metals in contaminated soils: a review of sources, chemistry, risks and best available strategies for remediation. *International Scholarly Research Notices*, **2011**, 402647, DOI: 10.5402/2011/402647.
- Xie, Y., Fan, J., Zhu, W., Amombo, E., Lou, Y., Chen, L., & Fu, J. (2016). Effect of heavy metals pollution on soil microbial diversity and bermudagrass genetic variation. *Frontiers in Plant Science*, **7**, 755. DOI: 10.3389/fpls.2016.00755.
- Xu, T., Close, D. M., Sayler, G. S., & Ripp, S. (2013). Genetically modified whole-cell bioreporters for environmental assessment. *Ecological Indicators*, **28**, 125-141. DOI: 10.1016/j.ecolind.2012.01.020.
- Yang, D. M., Fu, T. F., Lin, C. S., Chiu, T. Y., Huang, C. C., Huang, H. Y., ... & Chang, Y. F. (2020). High-performance FRET biosensors for single-cell and in vivo lead detection. *Biosensors and Bioelectronics*, **168**, 112571. DOI: 10.1016/j.bios.2020.112571.
- Yi, L., Hong, Y., Wang, D., & Zhu, Y. (2007). Determination of free heavy metal ion concentrations in soils around a cadmium rich zinc deposit. *Geochemical Journal*, 41(4), 235-240. DOI: 10.2343/geochemj.41.235.
- Yoon, Y., Kim, S., Chae, Y., Jeong, S. W., & An, Y. J. (2016a). Evaluation of bioavailable arsenic and remediation performance using a whole-cell bioreporter. *Science of the Total Environment*, **547**, 125-131. DOI: 10.1016/j.scitotenv.2015.12.141.

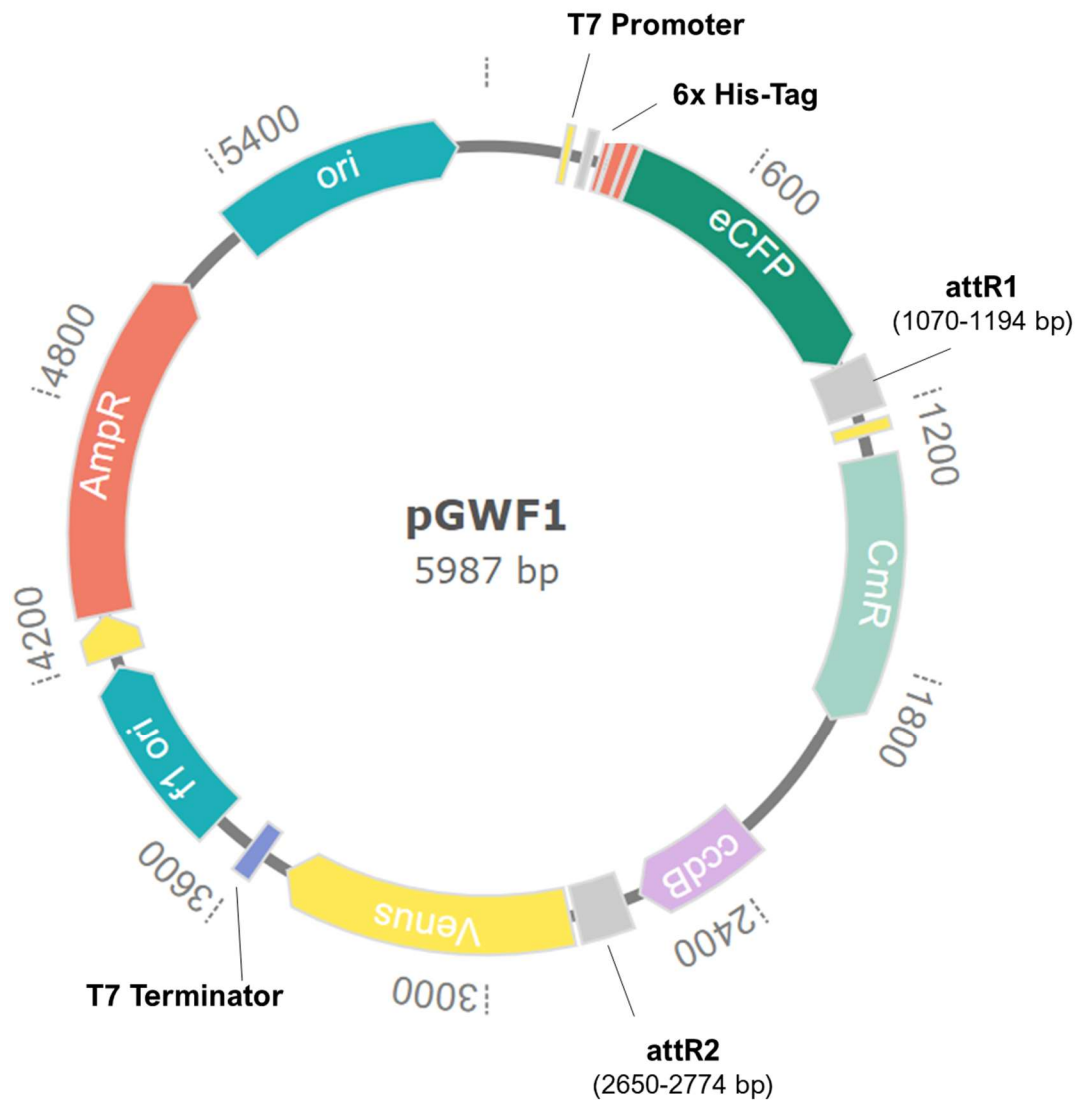
- Yoon, Y., Kim, S., Chae, Y., Kang, Y., Lee, Y., Jeong, S. W., & An, Y. J. (2016b). Use of tunable whole-cell bioreporters to assess bioavailable cadmium and remediation performance in soils. *PLoS One*, **11**(5), e0154506. DOI: 10.1371/journal.pone.0154506.
- Yu, Q., Mishra, B., and Fein, J.B (2020). Role of bacterial cell surface sulfhydryl sites in cadmium detoxification by *Pseudomonas putida*. *Journal of Hazardous Materials*. 391, 122209. <https://doi.org/10.1016/j.jhazmat.2020.122209>
- Yuan, J. H., Xu, R. K., & Zhang, H. (2011). The forms of alkalis in the biochar produced from crop residues at different temperatures. *Bioresource Technology*, **102**(3), 3488-3497. DOI: 10.1016/j.biortech.2010.11.018.
- Yun, S. W., & Yu, C. (2015). Immobilization of Cd, Zn, and Pb from soil treated by limestone with variation of pH using a column test. *Journal of Chemistry*, **2015**. 641415. DOI: 10.1155/2015/641415.
- Zaccolo, M. (2004). Use of chimeric fluorescent proteins and fluorescence resonance energy transfer to monitor cellular responses. *Circulation Research*, **94**(7), 866-873. DOI: 10.1161/01.RES.0000123825.83803.CD.
- Žemberyová, M., Barteková, J., Závadská, M., & Šišoláková, M. (2007). Determination of bioavailable fractions of Zn, Cu, Ni, Pb and Cd in soils and sludges by atomic absorption spectrometry. *Talanta*, **71**(4), 1661-1668. DOI: 10.1016/j.talanta.2006.07.055.
- Zeng, N., Wu, Y., Chen, W., Huang, Q., & Cai, P. (2021). Whole-Cell Microbial Bioreporter for Soil Contaminants Detection. *Frontiers in Bioengineering and Biotechnology*, **9**, 622994. DOI: 10.3389/fbioe.2021.622994.
- Zhang, D., Fakhrullin, R. F., Özmen, M., Wang, H., Wang, J., Paunov, V. N., ... & Huang, W. E. (2011). Functionalization of whole-cell bacterial reporters with magnetic nanoparticles. *Microbial Biotechnology*, **4**(1), 89-97. DOI: 10.1111/j.1751-7915.2010.00228.x.
- Zhu, X., Chen, B., Zhu, L., & Xing, B. (2017). Effects and mechanisms of biochar-microbe interactions in soil improvement and pollution remediation: a review. *Environmental Pollution*, **227**, 98-115. DOI: 10.1016/j.envpol.2017.04.032.
- Zuo, Z., Gong, T., Che, Y., Liu, R., Xu, P., Jiang, H., ... & Yang, C. (2015). Engineering *Pseudomonas putida* KT2440 for simultaneous degradation of organophosphates and pyrethroids and its application in bioremediation of soil. *Biodegradation*, **26**(3), 223-233. DOI: 10.1007/s10532-015-9729-2.

8. Appendices

1. Vectors for Gateway Recombination



- a. Map of pDONR as the donor vector containing *attP1* and *attP2* sites for LR cloning. CmR is a chloramphenicol resistance gene, KanR is a kanamycin resistance gene, ori is a gene responsible for plasmid replication in *E.coli* cells. *ccdB* is gene that targets DNA gyrase in *E.coli*. The *ccdB* positive-selection marker acts by killing the background of cells with no cloned DNA, only cells containing a recombinant DNA giving rise to viable clones.



- b.** Map of pGWF1 as the destination vector containing *attR1* and *attR2* sites for BP cloning of CMT into between eCFP and Venus gene. CmR is a chloramphenicol resistance gene, AmpR is an ampicillin resistance gene, ori is a gene responsible for plasmid replication in *E.coli* cells. *ccdB* is gene that targets DNA gyrase in *E.coli*. The *ccdB* positive-selection marker acts by killing the background of cells with no cloned DNA, only cells containing a recombinant DNA giving rise to viable clones.

2. Buffer composition for 6xHis-tag purification (indicated as a final concentration)

Composition	NPI-10	NPI-20	NPI-500
NaH ₂ PO ₄	50 mM	50 mM	50 mM
NaCl	300 mM	300 mM	300 mM
Imidazole	10 mM	20 mM	500 mM
NaOH	Adjust pH to 8		

3. Composition of SDS Page reagents

Coomassie Brilliant Blue R-250 stain solution

Components	Quantity (100 mL)	Final concentration
Coomassie Brilliant Blue R-250	0.05 g	0.05%
Methanol	50 mL	50% (v/v)
Glacial acetic acid	10 mL	10% (v/v)
Deionised H ₂ O	to 100 mL	

Destain solution

Components	Quantity (100 mL)	Final concentration
Methanol	30 mL	30% (v/v)
Glacial acetic acid	10 mL	1% (v/v)
Deionised H ₂ O	to 100 mL	

SDS Gel loading buffer (5X)

Components	Quantity (100 mL)	Final concentration
Tris 0.5 M pH 6.8	25 mL	125 mM
Glycerol	50 mL	50% (v/v)
SDS	4 g	8 % (w/v)
Bromphenol blue	5 mg	0.1 % (w/v)
Deionised H ₂ O	to 100 mL	

Tris-glycine electrophoresis buffer (1L, 10x stock)

Components	Quantity (100 mL)	Concentration
Tris base	30.3 g	250 mM
Glycine	144 g	1.9 m

SDS	10 g	1% (w/v)
Deionised H ₂ O	to 1 L	

4. Physicochemical properties of soil samples from selected experimental pots after 18 months of outdoor incubation (data was provided by Rosa Soria)

Parameters	Unit	Soil			Soil + Biochar			Soil+Compost			Soil+Biochar+Compost			Method
		20	5	24	12	26	27	8	7	9	23	31	4	
pH	-	5.17	4.91	5.1	5.52	5.52	5.42	7.08	7.12	7.11	7.21	7.02	7.09	FB68800 pH meter
Electric Conductivity (EC)	μS	63	5.07	58.9	60.1	68.7	79.9	249	206	242	208	262	250	JENWAY, 470 conductivity meter
Organic Matter Content	%	1.41	3.21	2.91	3.21	2.87	2.91	13.08	11.14	12.02	10.05	10.14	11.68	BS1377-3:2018 (BS, 2018)
Available Nitrate NO₃⁻	mg/kg	112.29	34.34	28.61	86.10	58.54	61.66	103.69	34.53	N.A	33.23	63.65	130.09	Acidic Griess reaction (Miranda et.al, 2001)
Available Phosphate PO₄³⁻	mg/kg	7.04	8.12	4.87	10.18	3.37	10.70	20.93	39.64	46.53	45.07	41.15	39.90	Olsen method (Iatrou et al., 2014)
Total Heavy Metals														
Cd	mg/kg	138.65	122.64	108.44	126.95	114.94	16.58	110.36	104.75	176.66	93.60	16.82	126.43	
Pb	mg/kg	3381.77	3308.99	3350.41	2538.31	3311.90	3884.21	2050.49	4222.46	2067.64	2405.89	2716.60	2489.63	
Zn	mg/kg	2396.50	1893.99	2036.68	1721.89	2102.36	1636.24	1666.44	1668.01	1516.22	1627.11	1455.91	1678.51	
Mg	mg/kg	24167.28	20644.26	20847.02	18623.24	21151.79	20824.94	20557.98	21031.36	21678.23	20306.84	21497.75	21486.39	
Bioavailable Heavy metals														
		NH ₃ NO ₄ extraction												
Cd	mg/L	0.006	0.006	<0.0027	0.006	<0.0027	<0.0027	<0.0027	<0.0027	<0.0027	<0.0027	<0.0027	<0.0027	
Pb	mg/L	15.44	16.69	17.24	6.35	5.78	11.83	0.139	0.244	0.120	0.123	0.153	0.188	
Zn	mg/L	2.135	2.103	2.02	1.07	1.19	1.23	0.008	<0.0059	0.024	0.008	<0.0059	<0.0059	
Mg	mg/L	128.44	130.21	112.13	138.36	117.98	120.09	169.36	130.32	117.77	166.65	163.95	125.505	

5. Bioavailable Pb²⁺ measured in pot experiments by the FRET biosensor inside *P.putida* KT2440T7 host cells

Pot Number	Treatment	Bioavailable Pb ²⁺ (μM)
20	Soil	42.43
5	Soil	36.79
24	Soil	40.05
12	Soil+Biochar	31.26
26	Soil+Biochar	25.77
27	Soil+Biochar	27.69
8	Soil+Compost	12.29
7	Soil+Compost	11.11
9	Soil+Compost	17.67
23	Soil+Biochar+Compost	9.44
31	Soil+Biochar+Compost	3.14
4	Soil+Biochar+Compost	6.26

